DEVELOPMENT OF PROTECTION ALGORITHMS FOR COMPENSATED POWER NETWORK

Ph.D. THESIS

by

ASHOK MANORI

DEPARTMENT OF ELECTRICAL ENGINEERING
INDIAN INSTITUTE OF TECHNOLOGY ROORKEE
ROORKEE – 247 667 (INDIA)

May, 2016

DEVELOPMENT OF PROTECTION ALGORITHMS FOR COMPENSATED POWER NETWORK

A THESIS

Submitted in partial fulfilment of the requirements for the award of the degree

of

DOCTOR OF PHILOSOPHY

in

ELECTRICAL ENGINEERING

by

ASHOK MANORI

DEPARTMENT OF ELECTRICAL ENGINEERING
INDIAN INSTITUTE OF TECHNOLOGY ROORKEE
ROORKEE – 247 667 (INDIA)

MAY, 2016

INDIAN INSTITUTE OF TECHNOLOGY ROORKEE
ROORKEE

CANDIDATE'S DECLARATION

I hereby certify that the work which is being presented in the thesis entitled "**DEVELOPMENT OF PROTECTION ALGORITHMS FOR COMPENSATED POWER NETWORK**" in partial fulfilment of the requirements for the award of the Degree of Doctor of Philosophy and submitted in the Department of Electrical Engineering of Indian Institute of Technology Roorkee, Roorkee is an authentic record of my own work carried out during a period from **July, 2011 to May, 2016** under the supervision of Dr. Manoj Tripathy, Associate Professor, Department of Electrical Engineering, Indian Institute of Technology Roorkee, Roorkee and Prof. Hari Om Gupta, Director, Jaypee Institute of Information Technology Noida, Noida.

The matter presented in this thesis has not been submitted by me for the award of any other degree of this or any other Institution.

(Ashok Manori)

This is to certify that the above statement made by the candidate is correct to the best of our knowledge.

(Manoj Tripathy)
Supervisor

(H. O. Gupta)
Supervisor

Date:

ABSTRACT

Flexible Alternating Current Transmission System (FACTS) controllers can be connected throughout the complete length of transmission line. Moreover the preferred location is at the middle of the line because voltage sag is maximum at that point. Particularly shunt FACTS controllers are preferably connected in the middle as they provide voltage support to the line. When FACTS controllers are connected at the sending or receiving end substations the protection of transmission line becomes somewhat easier because measurements can be taken locally without any considerable time delay. If the FACTS controller is places at the middle of transmission line the protection of transmission line becomes a challenging task for protection engineers. In such condition transmission line has two sections first one before the FACTS device which is uncompensated portion whose impedance is linear and second one after the device which is being compensated and it's having variable impedance (non-linear). Therefore, ultimate challenge for protection engineers is to protect such a line which impedance is not linear throughout the whole length. To protect transmission line having midpoint compensation, first requirement is to know the section of line in which fault occur. After identifying fault section, an adaptive protection algorithm is needed to protect the complete line. In this work, fault section is identified by a combined wavelet-SVM based technique which takes very less time to analyze the pattern and select the faulty section. Wavelet transform decomposes all the frequency bands present in fault signal and SVM analyze the frequency patterns for different fault sections. Any transmission line fault signal has various frequency signals up-to 80 kHz. Relay which is placed at the bus receive all the frequency signals including fundamental frequency signal through current transformer. Any fault signal occurred before or after the FACTS device has different frequency spectrum because of the filtering by FACTS device itself. FACTS device filters the particular frequency band from the fault signal according to its inductance or capacitance value at that time (or according to its compensation level). In case of fix compensation inductance or capacitance value inserted by FACTS device is constant therefore it can be claimed that particular frequency signal will be missing if fault occurred in section-II. Although in case of variable compensation like TCSC or SVC, impedance inserted by the device is not constant so it cannot be say surely that which frequency band will be missing in frequency spectrum. So to make transmission line protection system reliable it is needed to find fault section clearly. For this purpose, a high pass filter is

installed at the FACTS device location which surely filters the high frequency signals generated in section two in case of fault. In case of fault in section one wavelet transform provides detail about high frequency components while section two fault has no or less detail about high frequency signals. One drawback of the wavelet transform is to its sensitivity for noise signals. Therefore to make relay performance less prone to noise signal a SVM classifier is added to make protection algorithm more adaptive. SVM has quality to draw an optimal hyper plane to classify two classes therefore it can classify the wavelet signals optimally for section one or two faults. Further SVM parameters are optimized by Genetic Algorithm to make classifier an optimal classifier. Results are compared with the RBFNN based classifier.

Presence of TCSC in the middle of transmission line creates major protection issues particularly in distance protection. First section of line has linear impedance trajectory can be easily protected by the convention mho relay algorithm. After TCSC point impedance of line is a shifted trajectory. In capacitive mode of operation it shifts into downward direction and in inductive mode of operation it shifts toward upward direction and in both the cases amount of shift depends upon the level of compensation. Therefore requirement of the transmission line protection system is such that it should be adaptive with the shifted impedance trajectory of the second portion of transmission line. Another challenge in protection of transmission line having TCSC is that, TCSC itself protected by MOV varistor which is a non-linear resistor. When fault current exceeds a certain limit overvoltage across TCSC capacitor become too high so, to protect TCSC from overvoltage, MOV discharge excessive energy through itself. In this case the equivalent impedance of TCSC with MOV is not linear and measured fault impedance has uncertain error. It is the requirement of the power engineer to place TCSC safely in the transmission line even in fault condition such that as soon as fault cleared it should function on the line accordingly to reduce economic losses. Therefore, in any short duration fault or transient condition, TCSC remain in the line and inserts its own impedance. To make transmission line protection system adaptive it is required to calculate TCSC impedance and with respect to this impedance it is required to make transmission line protection system adjustable. TCSC equivalent impedance depends on firing angle of thyristors therefore; it can be calculated by measuring a single variable. MOV setting is kept such that it operates in highly severe condition and it bypass high amount of current. In this case TCSC and MOV equivalent impedance comes into picture.

Similarly, the presence of shunt FACTS device such as SVC and STATCOM also creates some major protection issues when placed at the middle of transmission line. Certainly the preferred location for shunt FACTS device is at the middle because at this point voltage sag is maximum. Shunt devices provide voltage support at the point of connection by injecting a quadrature current into the line. Shunt devices does not affect the performance of relay for any fault before the point of connection. For any fault after the point of connection it introduces certain error in fault impedance calculation according to current injected by the device. Shunt devices inject both the leading or lagging current at the point of common coupling depending on the system requirement hence creates under and over reaching problems. Therefore to make transmission line protection system adaptable with the action of shunt FACTS device it is required to calculate the error introduced by the device. A compensation unit has been inserted in the conventional Mho relay which calculates error in terms of current injected by the shunt device into the transmission line.

Fault zone identification in compensated transmission line is constrained by several factors like fault resistance, loading conditions and mainly by the level of compensation at the time of fault. For a secure transmission line protection system, it is needed to deal with all above mentioned factors when deciding the faulty zone. In uncompensated transmission line, some fault zone identification techniques are proposed which make transmission line protection system adaptable with loading conditions and different values of fault resistance. In these zone identification techniques, fault impedance coordinates have been calculated for different types of faults and power system operating conditions. Decision is taken by training any intelligence tool like SVM to decide the particular fault zone. These techniques are adaptive to changing loading conditions and various values of fault resistance. In case of compensated transmission line, inductive portion of transmission line is also variable and can upwelling in any direction depending on the mode of operation of the compensator. Fault impedance coordinates of different zones for these lines are overlapping over the imaginary axis at the intersection of zones. Even the learning of intelligent tool by these coordinates cannot solve the problem completely because for two different fault locations same coordinates may exist. So, to solve zone identification problem in compensated transmission line, work is needed to be done on the both sides; first on fault impedance coordinates and second on intelligent tool. In this work impedance inserted by compensator into the transmission line is estimated and modified impedance coordinates of fault impedance is calculated for the learning of intelligence tool.

Due to several advantageous features SVM is used for fault zone identification in compensated transmission line. Results are compared with the RBFNN based classifier.

ACKNOWLEDGEMENT

I express my deepest sense of gratitude towards my supervisors Dr. Manoj Tripathy, Associate Professor, Department of Electrical Engineering and Dr. H O Gupta, Professor, JPIIT Noida, Noida for their patience, inspiring guidance, constant encouragement, moral support, and keen interest in minute details of the work.

My deepest gratitude and sincere thanks to Dr. R. P. Maheshwari and Dr. Barjeev Tyagi, Associate Professor, Department of Electrical Engineering, Indian Institute of Technology Roorkee, Roorkee without whose encouragement and support my PhD would not have been possible. I am thankful to Dr. B. Das, Chairmen SRC, Department of Electrical Engineering, Indian Institute of Technology Roorkee, Roorkee and Prof. S. P. Srivastava, Professor and Head, Department of Electrical Engineering, Indian Institute of Technology Roorkee, Roorkee and Prof R. C. Mittal Department of Mathematics, Indian Institute of Technology Roorkee, Roorkee for their invaluable direction, encouragement and support, and above all the noblest treatment extended by them during the course of my studies at IIT Roorkee.

I am grateful to Dr. C. P. Gupta Associate Professor, Department of Electrical Engineering, Indian Institute of Technology Roorkee, Roorkee and Dr. Mukhtiar Singh, Associate Professor, Department of Electrical Engineering, Delhi Technological Institute, New Delhi for his moral support, encouragement and suggestions for my research work.

I am also grateful to the Ministry of Human Resources and Development, Government of India, AICTE, New Delhi for sponsoring me for doctoral research work.

I express my sincere thanks to all seniors especially to Dr. Amit Kumar Chauhan and Dr. Bhargav Vyas for supporting me during the whole period. I extend my sincere thanks to my colleagues Mr. Shailendra Bhaskar, Mr. K S Sajan, Mr. Anubhav Agrawal, Mr. Nagendra Gautam for sharing and supporting me during my research work. I am also thankful to Mr. Jitendra, Kumar Mr. Om Hari Gupta and Mr. Sukanta Halder for their help and involvement in my research work. I am thankful to Mr. Kaushal Kumar, Mr. Ravi Kumar and Mr. Jatin Patel, for supporting me during my research work.

I express my sense of gratitude to Mr. Amir Ahmed, Caretaker, Workshop, Mr. Mohan Singh and Mr. Rishab Verma, Office Staff, Department of Electrical Engineering, Indian Institute of Technology Roorkee, Roorkee for their co-operation and assistance. I also express

my thanks to Mr. Mansa Ram and Mr. Rishipal, Hostel Staff, Azad Bhawan, and all the Mess Workers, Azad mess, for their consistent help at hostel level.

I am also very grateful to my B.Tech & M.Tech group friends Mr. Ashutosh Trivedi, Mr. Akshi K. Singh, Mr. Ankit Chauhan, Mr. Pushker Singh, Mr. Ashish Pangaria, Mr. Deepak Nayak, Mr. Abahs Kanungo, Mr. Prashant Thapliyal, Mr. Shobhit Srivastav, Mr.Chandan Choubey, Mr Amit Bhole, Mr. Siddharth Mehla, Mr. Shanker P S, Mr. K Trinad, Mr. Vikram Saini, Mr. Deepak Joshi, Mr. Ramakoti for their help and co-operation during my study.

I owe a debt of gratitude to my parents, my sisters, Mrs. Anita Dhyani, Mrs. Manju Maletha and my brother Mr. Deepak Manori, and brother-in-law Mr. Mohan Dhyani and Mr. Vinod Maletha for their consistent encouragement, moral support, patience and care. I am also thankful to my in-Laws, my brother and sister-in-laws for their support and care. I have no words to express the appreciation for my wife who stood by me at every moment, kept encouraging me in low moments and supported me technically and morally during my work.

Last but not the least; I am thankful to the almighty who gave me the strength and health for completing the work.

(Ashok Manori)

CONTENTS

LIST OF FIGURES

LIST OF TABLES

LIST OF ACRONYMS

3PC	Triple Processor Card
AI	Artificial Intelligence
ANFIS	Adaptive Neuro-Fuzzy Inference System
ANN	Artificial Neural Network
AORD	Alpha Order
ASC	Advance Series Compensation
BP	Back Propagation
BPNN	Back-Propagation Neural Networks
CAPS-ON	Number of On Capacitor
CCVT	Coupled Capacitor Voltage Transformer
CDPR	Current Differential Pilot Relay
ChNN	Chebyshev Neural Network
CRC	Conventional Relay Curve
CSC	Controllable Series Compensation
CSW	Capacitor Switch Signal
DFT	Discrete Fourier Transform
DSO	Digital Storage Oscilloscope
DSP	Digital Signal Processor
DT	Decision Tree
DUTT	Direct Under-Reaching Transfer Trip
ELM	Extreme Learning Machine
EMTDC	Electromagnetic Transients including Direct Current
FACTS	Flexible AC Transmission Systems
FCII	Fault Component Integrated Impedance
FFNN	Feed Forward Neural Network
FFT	Fast Furrier Transform
FLS	Fuzzy Logic System
FSC	Fixed Series Capacitor
GTO	Gate Turn Off
HF	High Frequency

HIF	High Impedance Fault
HOS	Higher Order Statistics
HPF	High Pass Filter
HST	Hyperbolic S-Transform
ICA	Independent Component Analysis Invariance Technique
IRC	Inter Rack Communication Card
KB	Block/ Deblock signal
KVL	Kirchhoff's Voltage Law
LG	Line-to-Ground
LLG	Line-to-Line-to-Ground
LM	Levenberg-Marquardt
MLP	Multi-Layer Perceptron
MLPNN	Multi-layer Perceptron Neural Networks
MOV	Metal Oxide Varistor
MRA	Multi Resolution Analysis
NN	Neural Networks
PCC	Point of Common Coupling
PLL	Phase Lock Loop
PMU	Phasor Measurement Unit
PNN	Probabilistic Neural Network
PRC	Proposed Relay Curve
PSCAD	Power System Computer Aided Design
PUTT	Permissive Under-reaching Transfer Trip
PWM	Pulse Width Modulation
RBFNN	Radial Basis Function Neural Network
RPC	Risc Processor Card
RRRV	Rate of Rise of Recovery Voltage
RTDS	Real Time Digital Simulator
SC	Series Capacitor
SSFC	Sub-Synchronous Frequency Component
SSSC	Static Synchronous Series Compensator
ST	S-Transform

STATCOM	Static Synchronous Compensator
SVC	Static Var Compensator
SVM	Support Vector Machine
TCR	Thyristor Controlled Reactor
TCSC	Thyristor Control Series Capacitor
TDNN	Time Delay Neural Networks
TLSE	Total Least Square Estimation
TLS-ESPRIT	Total Least Square- Estimation of Signal Parameters via the Rotational
TNA	Transient Network Analyzer
TRV	Transient Recovery Voltage
UHV	Ultra High Voltage
UPFC	Unified Power Flow Controller
VAR	Volt Ampere Reactive
VSC	Voltage Source Convertor
VSI	Voltage Source Invertor
WAMS	Wide Area measurement System
WIF	Workstation Interface Card
WT	Wavelet Transform

LIST OF SYMBOLS

'A'	Bus A
a	Scaling parameter
A1-4	Approximation coefficient
a1, a2	Firing pulses
b	Translation parameter
c	Center of activation function
C	Error penalty
Cs	Series capacitor
d	Euclidean distance
D	Training data
D1-4	Detailed coefficient
F	Sampling frequency
G	Gain
h	Hidden layer neurons
I	Current (rms)
i	Instantaneous current
I0	Zero sequence current
I1	Positive sequence current
I2	Negative sequence current
I_{Cmax}	Maximum capacitive current
I_f	Fault current
I_F	Fundamental component of inductor current
I_{Lmax}	Maximum inductive current
$I_{Ls}(t)$	Inductor current
I_r	Receiving end current
I_s	Source current
l	Fault location
Ls	Series inductor
N	Number of samples in SVM
R_f	Fault resistance

R_M	MOV resistance
V	Voltage
$V0$	Zero sequence voltage
$V1$	Positive sequence voltage
$V2$	Negative sequence voltage
V_m	Peak of driving line voltage
V_r	Receiving end voltage
V_s	Sending end voltage
w	Output weight
x	Input vector
X_C	Series capacitor reactance
X_{comp}	Compensated reactance
X_{Cs}	Fixed capacitor reactance
y	Output of RBFNN
Z	Fault impedance
$Z0$	Zero sequence impedance
$Z1$	Positive sequence impedance
$Z2$	Negative sequence impedance
Z_c	Surge impedance
Z_{comp}	Compensated impedance
Z_{net}	Net fault impedance
Z_{set}	Zone-1 set impedance
α	Firing angle
α_{Clim}	Firing angle limit in capacitive mode
α_{Llim}	Firing angle limit in inductive mode
γ	Propagation constant
ξ	Damping ratio
σ	Gaussian width
$\phi_i(x)$	Hidden layer output
$\psi(t)$	Mother wavelet
Ω	Ohms
ω_c	Characteristics frequency

CHAPTER 1
INTRODUCTION

To utilize the full capacity of transmission line for transmission of electric power over a power network, Flexible Alternating Current Transmission Systems (FACTS) are installed in the transmission line at different locations. Presence of FACTS system changes the transmission parameters and hence adversely affects the transmission line protection system by creating problems viz. reaching problem, zone setting, inversion and over-voltage issues. Therefore, there is a great need to identify the wider impact of different FACTS devices on the existing transmission line protection system and simultaneously the remedies of the problems. This chapter presents overview of compensated power network and survey of present and past developments in the field of protection of transmission lines having FACTS devices.

1.1 Overview

Day-by-day demand for electric power is continuously increasing due to vast industrialization and immense domestic use. Transmission lines of the existing power systems are supplying power close to their stability and thermal limits, which may lead to an unstable power system. Increase in wire density and requirement of extra costly towers is the main drawback of extending the existing power transmission system by constructing parallel lines. The extra construction may also best impeded by environmental issues. In the recent years, FACTS devices have been popular worldwide for increasing the power transfer by providing the optimum utilization of the system capability by pushing power system to their stability and thermal limits [1]–[4]. FACTS devices may be installed in the existing transmission line in series, shunt and composite manner according to the requirement [5]–[7]. FACTS device can be fixed at different location in the transmission line viz. at the terminals of line, at mid-point of line or some other locations. Optimum placement of series and shunt devices in the transmission line has been discussed in literature [8], [9]. Transmission lines are protected by techniques such as non-unit protection like overcurrent protection and distance protection, and unit protection like pilot wire protection. Distance protection is the most common protection scheme of long transmission line which measures the positive sequence impedance of transmission line and compares it with a set value, if it is less than the set value the relay operates. In distance protected transmission line, generally three protection zones are assigned

[10]–[12]. Insecurity is the common issue in distance protection which occurs due to uncertain fault resistance and variable compensation in transmission line. The FACTS devices affect the distance protection scheme during faulty or transient conditions because it is based on the voltage and current response at the relay point.

Controllable or Fixed Series Capacitors (FSC) are widely used in transmission line to obtain maximum transmission capability [13]. Series compensation introduces several problems like voltage and current inversion, over voltage, phase estimation, sub-synchronous frequencies and reaching problems (distance measurements). Mho distance relay is extensively used for the protection of compensated and uncompensated EHV (Extra High Voltage) transmission lines due to its directional discrimination capability. However the presence of Thyristor Controlled Series Capacitor (TCSC) in transmission line badly affects the operation of Mho distance relay specially the reaching characteristic of the relay. In case of capacitive compensation Mho relay shows over-reaching effect and in case of inductive compensation it shows under-reaching effect [14]–[16]. TCSC is commonly installed at the end of transmission line with generating stations and relays. If any fault occurs near the relays, the apparent impedance become capacitive and current or voltage phase changes by 180 degree which is sensed by the relay as a reverse fault. Another important series device is Static Synchronous Series Compensator (SSSC) which affects reaching as well as directionality of Mho relay. SSSC in the fault loop increases resistance and reactance of apparent impedance and its impact is worsen in capacitive mode of operation [17].

Shunt FACTS devices are widely used in transmission line. They maintain constant line voltage at the point of connection in transmission line by injecting current at this point. Which are preferably connected in the middle of the line because voltage sag is high at that mid-point. The most popular shunt FACTS devices are Static Var Compensator (SVC) and Static Synchronous Compensator (STATCOM). Shunt FACTS devices operate in capacitive or inductive mode and accordingly it supply or absorb reactive power into the connecting bus respectively. The distance relay shows under-reaching or over-reaching affects relative to the direction of current injection into the transmission line [18], [19].

Composite device like Unified Power Flow Controller (UPFC) is a combination of both series and shunt device and can affect the transmission line parameters in both the way, which create serious protection issues such as under-reaching and over-reaching. UPFC has the

unique ability to exchange reactive as well active power with the power system at the point of coupling so it equally affects the resistive and inductive portion of apparent impedance [20].

So, there is a need to make a flexible transmission line transmission line protection system which can adapt all the changes pop in transmission line by the FACTS devices. Protection engineers and researchers have done pleasing effort to analyze the effect of entire FACTS devices on transmission line protection system and suggested a lot of techniques to sort out the issues. Next sections of this chapter give the idea of the inclusive protection techniques for transmission line having series, composite and shunt devices respectively. The orientation of this chapter is towards the study which analyses the impact of entire FACTS devices on the transmission line protection system and almost review all the articles which provides the protection techniques for compensated transmission line.

1.2 Impact of Different FACTS Devices on Transmission Line Protection

In power transmission system there are mainly two types of compensation devices: (i) series devices e.g. Fixed Series Capacitor (FSC), TCSC and SSSC; (ii) shunt devices e.g. SVC and STATCOM. Impact of both types of devices is summarized as follows:

1.2.1 Impact of Series Devices

Mainly the impact of three types of series compensator devices on transmission line protection is discussed in literature viz. (i) FSC, (ii) TCSC and (iii) SSSC. FSC diminishes a particular amount of inductance from transmission line, hence creates over-reaching and directional issues. TCSC is a parallel combination of a capacitor and Thyristor Controlled Reactor (TCR) and the whole combination is protected by MOV (Metal Oxide Varistor) and a spark gap. TCSC affects the reaching characteristic of Mho relay [14], [21]–[26], fault direction misclassification (current and voltage inversion) [16], [27]–[30] and shows overvoltage issues [15], [31]–[38]. SSSC is a Voltage Source Invertor (VSI) based device and inserts a controlled series voltage in transmission line hence affects the security [17], [39]–[47] and directionality [44]–[46] of the relay.

1.2.1.1 Impact of FSC and TCSC on Line Protection

Series compensation devices are connected in series with the transmission line which affects the line parameters directly. During fault conditions, series capacitor suffers from the overvoltage that occurs across the FSC/ TCSC. The overvoltage protection to FSC/ TCSC is

provided by connecting a MOV across them which is again protected by spark gap. A circuit breaker is also installed across the FSC/ TCSC module to bypass it if a severe fault occurs. Initially which were protected by a non-linear resistor which was unable to damp transients below protective level [48]. Non-linear resistors were replaced by varistors which provide instantaneous reinsertion of capacitors during external faults [26], [49], [50]. An elementary single phase TCSC is shown in Fig. 1.1 (a). It consists of a fixed capacitor (C_S), shunted through a reactor of inductance L_S in series with a bidirectional thyristor switch. Current in the reactor can be controlled from maximum value to zero by the method of firing angle delay control. Complete range of α for capacitive and inductive compensation which is measured from the peak of reference voltage is shown in Fig. 1.1 (b). In Fig. 1.1 (b) α_{Llim} and α_{Clim} are the limiting value of firing angle in inductive mode and capacitive mode respectively.

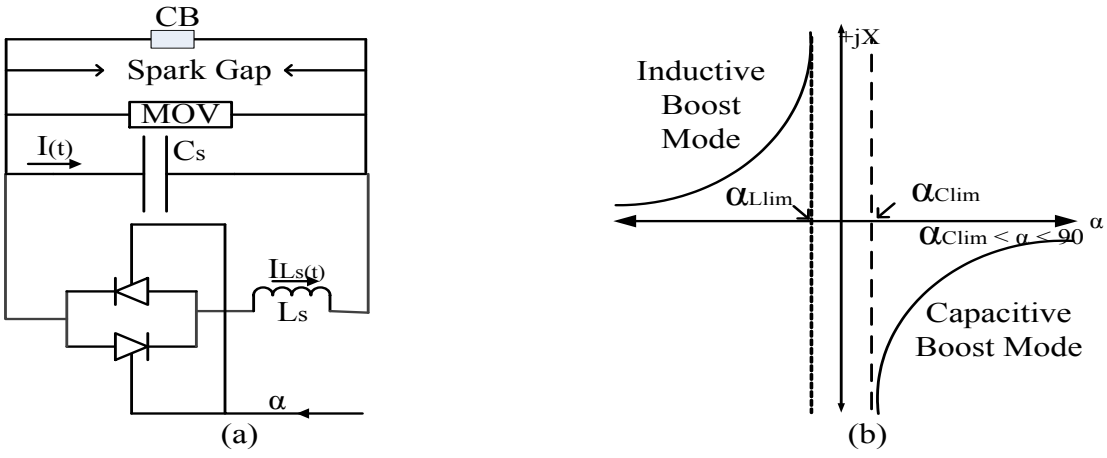

Fig. 1.1 TCSC (a) Symbolic circuit (b) Complete firing angle range [1-3]

In general, TCSC works in four different following modes of operation and depending on MOV conduction it shows reaching problems:

(i) *Capacitive Boost Mode ($\alpha_{Clim} < \alpha < \pi / 2$)* - In capacitor boost mode, TCSC behaves like continuously controllable capacitive reactance.

(ii) *Inductive Boost Mode ($0 < \alpha < \alpha_{Llim}$)* - In inductive boost mode, TCSC behaves like continuously controllable inductive reactance.

(iii) *Blocking Mode ($\alpha = \pi/2$)* - In blocking mode, thyristors are turned off and TCSC behaves like a FSC.

(iv) *Bypass Mode (α = 0)* - In bypass mode, thyristors are fully conductive and TCSC behaves like a parallel capacitor inductor module and whose resultant impact is inductive.

1.2.1.1.1 Reaching Problems

In TCSC transmission line, reach measurement by distance relay depends upon the status of the TCSC impedance which is varying in nature. The varying nature of impedance inserted by TCSC in the line creates under-reaching and over-reaching at the relay point in inductive and capacitive compensation respectively and that is a challenge to the protection engineer. Due to this variable impedance, there is no clear boundary between zone-1 and zone-2 hence overlapping area exists at the boundary as shown in Fig. 1.2. Due to this overlapping area, fault in zone-1 can extend up to zone-2, while zone-2 faults may fall within zone-1 according to the mode of operation of TCSC. This creates severe problem of zone identification in case of fault in transmission line having TCSC [14], [21]–[26].

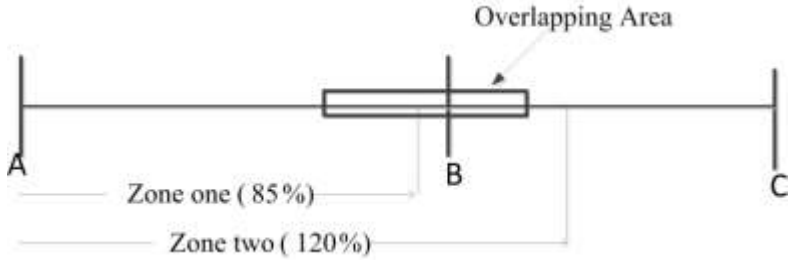

Fig. 1.2 Typical representation of overlapping area between zone-1 and zone-2

1.2.1.1.2 Inversion Problems

(i) *Voltage Inversion*

In distance protection, voltage inversion is a change of 180 degrees in the voltage phase angle at relay bus from the actual fault voltage. For elements responding to phase quantities, voltage inversion can occur for a fault near a series capacitor if the impedance from the relay to the fault is capacitive rather than inductive. If a fault occur in transmission line on right side of series device as shown in Fig. 1.3 and inductive reactance of fault point to relay point in X_{Lf}, if capacitive reactance of series capacitor X_C is greater than the X_{Lf} then voltage inversion take place at relay bus. Voltage inversion may affect directional and distance elements [16], [27]–[30].

(ii) *Current Inversion*

A current inversion occurs on a series-compensated line when, for any fault in zone-1, the equivalent system at one side of the fault is capacitive and the equivalent system at the other side of the fault is inductive. In this case, from Fig. 1.3, if equivalent impedance left to the fault point is capacitive i.e. $X_C > X_S + X_{Lf}$; then the current inversion takes place [16], [27]–[30].

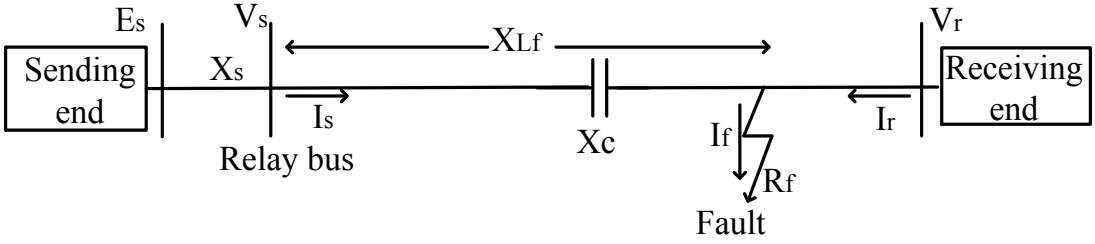

Fig. 1.3 Single line diagram for voltage and current inversion

1.2.1.1.3 Causes of Over-voltage across Series Compensator

Severe over-voltage generates across the terminals of FSC and TCSC during some conditions. Following are the roots of overvoltage across FSC and TCSC discussed in the literature.

(i) Series capacitor voltage on heavy load or fault conditions has significant impact on closing and opening of transmission lines [32], [36], [37].

(ii) When series compensation is employed, the upper limit of compensation level is set, beyond which self-excited oscillations may be induced in the system resulting in load rejection for the particular system. Severe temporary over-voltages occur during load rejection at the remote end of a long transmission line which initially carries substantial power.

(iii) If the fault is beyond the remote series capacitor, severe circuit breaker voltages may occur although voltages across the capacitors are not high.

(iv) During fault the transient recovery voltage (TRV) of the circuit breakers increases due to series capacitor [15], [31], [33]–[35], [38].

1.2.1.2 Impact of SSSC on Transmission Line Protection

SSSC also affects the reaching characteristics of distance protection and shows voltage inversion problem in the line which is similar to TCSC [44]. A few publications have been

shortsighted in literature which analyzes the impact of SSSC on transmission line protection system. The impact of SSSC on transmission line transmission line protection system can be summarized as follows [17], [40]–[43], [45], [46].

(i) SSSC can be installed at the substation or at the middle of the line as midpoint compensator. SSSC affects the transmission line protection system depending upon its location. SSSC does not affect the line transmission line protection system if not present in the fault loop.

(ii) SSSC is connected in series with the transmission line and works in capacitive and inductive mode of operation so it shows both over-reaching and under-reaching effects at relay end.

(iii) SSSC share both the active and reactive power in transmission line so it affects resistance as well as reactance of apparent impedance in transmission line.

(iv) Capacitive mode of SSSC mainly affects the apparent resistance while inductive mode largely affects the apparent reactance of transmission line.

(v) A. Kazemi *et al.* in 2008 [39] presents the impact of Voltage Transformer (VT) location w.r.t. SSSC and it is concluded that for least impact of SSSC on distance protection, VT in front of SSSC is the preferred location [43].

(vi) A. Kazemi *et al.* in 2009 [47] gives comparison of the impact of SSSC and STATCOM on distance trip characteristics with respect to installation point of view. It was shown that for line end installation the impact of SSSC is more than STATCOM while for mid-point installation STATCOM impact is more than SSSC.

1.2.2 Impact of Shunt Devices

Presence of shunt FACTS device significantly affects the performance of transmission line protection system and creates security and reliability issues. It maintains constant line voltage at the point of connection in transmission line by injecting current at that point. It is preferably connected in the middle of the line because voltage sag is high at that point. Shunt FACTS devices supply or absorb current into the connecting bus. The distance relay shows under reaching or overreaching effects relative to the direction of current injection into the transmission line. It was found that mid-point FACTS compensation could affect the distance relays concerning impedance measurement, phase selection and operating times leading to under-reaching and over-reaching of Mho relay.

1.2.2.1 Reaching Problems

Basic principle of distance protection is to measure impedance between relay point and the fault point, if it is less than the set value then the relay trips. In the normal loading conditions with STATCOM, resistance values are more and reactance values are less when compared to the resistance and reactance values without STATCOM. If the shunt device is connected in the middle of the transmission line and fault occurs on right half of the line, relay operating parameters changes and accordingly the relay will mal-operates. Single line diagram of shunt FACTS device in a transmission network in case of any line fault is shown in Fig. 1.4.

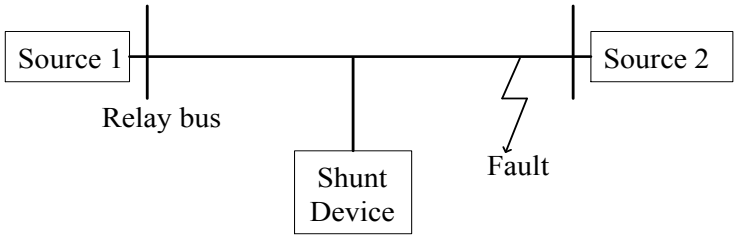

Fig. 1.4 Single line diagram of shunt device in transmission line

Due to presence of shunt device in the path between relay bus and fault point, the measured impedance by Mho relay changes significantly depending upon the action of the shunt device explained below for different action [18], [19], [51]–[65].

(i) Over-reaching

Shunt device absorbs reactive power from the transmission system in inductive mode of operation hence the net impedance reduces and Mho relay exhibits over-reaching effect. SVC in normal operating mode show comparatively moderate over-reaching difficulties than STATCOM. In case of light loads, line voltage increases due to Ferranti effect and the STATCOM works in inductive mode of operation to reduce over-voltage. It takes current from the connecting bus and hence absorbs reactive power from the system. The change in transmission line impedance by the STATCOM in both operating modes is a function of current injected by the device.

(ii) Under-reaching

In case of heavy loads, line voltage drops below the reference value and the shunt device SVC/STATCOM works in capacitive mode of operation. It supplies current into the connecting bus and hence injects reactive power into the system thus increasing the resistance

and the reactance value of fault impedance. In this case net impedance of transmission line increases and distance relay shows under-reaching effects [66].

(iii) High Operating Time

Mho relay responds within the time after the fault occurs until steady state value of the line impedance is found and for Mho relay usually the operating time is less than 1 cycle. In case of fault, shunt device takes 5 to 7 cycles to settle down in steady state condition. So the operating time of Mho relay increases significantly high.

(iv) Miss Phase selection

In case of mid-point shunt compensation if any unsymmetrical fault occurs in the transmission line, the faulty phase experiences severe under voltage effect as compared to healthy phase. Shunt FACTS device supplies even equal compensation for all the phases and healthy phase voltage increases due to this overcompensation. Due to this overcompensation healthy phase may experience high line current and the overcurrent relay may result it as a fault [19], [67].

1.3 Protections of Series Compensated Network: A Review

Following are the different remedial algorithms which suggest the protection of series compensated (FSC and TCSC) transmission line.

1.3.1 Artificial Neural Network (ANN) based Algorithms

ANN has the ability to classify highly nonlinear input patterns by adjusting the weight and biases of the neurons. Multilayer Neural Networks (NN) are suggested to improve the accuracy of fault detection in various power system components [24],[68]–[82][83]–[85]. Back Propagation (BP) algorithms and Radial Basis Network (RBN) were seemed to be an option in the differentiation of abnormal conditions from healthy condition in series compensated line. Different parameters of a compensated transmission network like instantaneous voltage or current or both, firing angle or various frequency signals presents in fault current filtered by Wavelet Transform/ Fast Fourier Transform (WT/ FFT), were selected as the feature of input vector in neural network. Back-Propagation Neural Networks (BPNN) is easy to implement and frequently used for fault detection with classification accuracy achieved up to 99.9%. Although, it suffers from local conversion and gives false results [73], [75], [76], [80]. Q Y Xuan *et al.* in 1993 proposed a BPNN topology which take voltage from Capacitor Voltage Transformer (CVT) as input vector to classify faulty condition in Controllable Series

Compensation (CSC) transmission system [80]. Same authors improved the technique in [75], [76], by providing a complete protection algorithm which give complete idea about fault location, detection and classification. BPNN with Total Least Square Estimation (TLSE) of voltage and current by rotational invariance technique was proposed in ref. [73] for protection of line having TCSC. Feed Forward Neural Network (FFNN) has an application on determining on line voltage across the series capacitor which was used to calculate actual relay voltage at bus [24], [70]; same algorithm was improved in ref. [74] by introducing a memory element in neural network called Time Delay Neural Network (TDNN) which has ability to predict temporal patterns. Multi-layer Perceptron Neural Networks (MLPNN) with Levenberg-Marquardt (LM) training algorithm was employed for fault classification and location in TCSC line [72]. Radial Basis Feed-Forward Neural Networks (RBFNN) are generally faster and less number of parameters are required to train, in literature RBFNN has been used for fault detection, classification and location with the maximum of 99.9 % accuracy [71], [77]. Composite ANN techniques have the facility of better feature extraction from the all possible inputs which produce fast and accurate results. A.Y. Abdelaziz *et al.* used superimposed voltage and current traveling wave along with ANN for identifying fault type and faulty phase [69]. Bhargav Vyas *et al.* proposed composite Wavelet Transform (WT) and Chebyshev Neural Network (ChNN) algorithm for fault classification and zone identification in mid-point TCSC transmission line and got high classification accuracy above 99.0 % with the advantageous features of ChNN [78], [86].

A complete generalized, summarized algorithm for ANN and ANN/WT/FFT based composite protection algorithm for series compensated network is shown in Fig. 1.5. In this algorithm relaying signal like voltage, current and firing angle are measured at the relay bus. Measured relaying signal sampled at a desired frequency and arranged in some window size to generate patterns. Several patterns are generated for all possible power system operating conditions as input to ANN/ ANN-WT/ ANN-FFT based relay. Different ANN based relay can be used to classify fault type, phase, direction and location by analyzing the same input patterns.

Table 1.1 shows the year wise development in neural network based techniques for protection of series compensated transmission line. It is concluded that BPNN is easy to implement and frequently used for fault detection with classification accuracy achieved up to 100%, although it suffers from local conversion and gives false result. In case of BPNN/

MLPNN/ TDNN the structure of NN always differs and it is very difficult to obtain optimal number of hidden layer and neurons. Generally it depends on the input feature, required output and the non-linearity of the relaying signal. The RBFNN as compared to BPNN are generally faster and are less number of parameters required to train. In most of the algorithms, rated system voltage is chosen to be 400 kV or 500 kV. Whereas in newly Ultra High Voltage (UHV) transmission system has been installed above 1000 kV in which transients are severe and needed to be analyzed with respect to ANN. A versatile ANN structure can be achieved through training it by using a large number of patterns having almost all types of features and applying some optimization techniques. It can be observed that for less numbers of testing patterns, NN can show dummy increase in percentage accuracy.

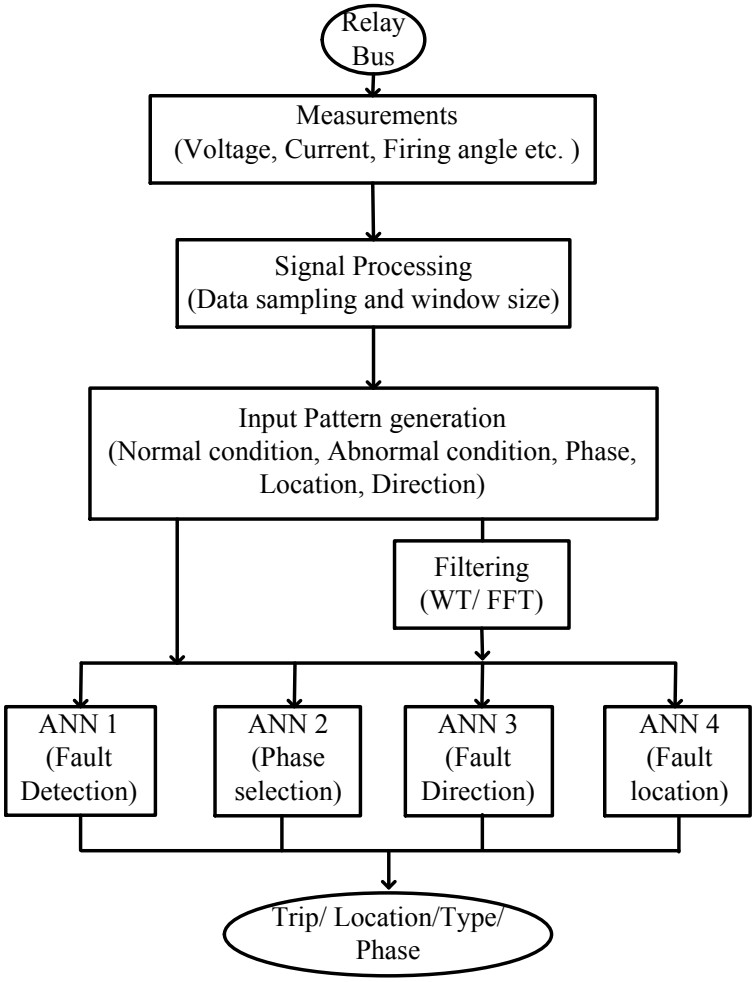

Fig. 1.5 Flow chart of ANN based protection algorithm for series compensated transmission line

Table 1.1 Comparative study of ANN based algorithm for protection of series compensated line

Publishing Year/ref	Methods /Types	System Specification (voltage/length)	Sampling rate/time	Sample Window length	Patterns	Accuracy (max) %	Output
1993[80]	MLP- BPNN	500 kV/240 miles	1.4 ms	8	27	100	Fault detection
1996[76]	MLBPNN	500 kV/380 km	960 sample/s	4	5000	100	Fault detection/ classification/ location
1998[79]	Neuro- Fuzzy			½ cycle			Fault detection/ classification
2005[69]	Traveling Wave/BPNN	500 kV/100 miles	16 sample/cycle	¼ cycle	70	100	Fault classification/ phase selection
2007[77]	RBFNN	500 kV/380 km	720 sample/s	4	2000	95.99	Detection/classification/location/ direction
2009[72]	MLPNN-BPNN	500 kV/160 miles	960 sample/s	¼ cycle	7650	95.6	Fault classification/ location
2011[73]	Total Least Square/BPNN	230 kV	512 sample/cycle	½ cycle	54	100	Detection/ classification
2012[74]	TDNN	500 kV/400 km	16 sample/cycle		768	100	Fault classification
2012[87]	ANFIS	400 kV/300 km			500	99.90	Fault location in SSSC line
2014[78]	ChNN/ WT/SVM	400 kV/300 km	4 kHz	½ cycle	32400	99.39	Fault classification

1.3.2 Support Vector Machine (SVM) based Algorithms

The SVM is a machine learning technique used for statistical classification and regression analysis. SVM constructs a number of hyper planes in a high dimensional space to separate data points which belongs to different classes. ANN based relaying technique need lot of training and testing before implementation, so it takes more time on training and can suffer from multiple local minima too. Due to better classification, features selection capability and fast convergence rate of SVM, it has ability to obtaining healthy and faulty condition, fault phase selection and fault location in series compensated line [88], [89]. SVM along with WT used as effective tool to classify fault phases and zone in TCSC line. WT decomposed the current signal into various frequency components and SVM analyzed various frequency features to identify healthy and faulty conditions [90], [91]. Drawback of WT-SVM technique was a delay inserted by WT therefore the technique was improved by Z. Moravej *et al.* in 2012 by replacing WT by S-transform [89]. An optimum SVM optimized by GA was proposed in 2012 to classify all types of line faults in TCSC transmission line and it was shown that optimization through GA, improves the performance of SVM [92]. A composite SVM based generalized protection algorithm for protection of series compensated transmission line is shown in Fig. 1.6. In this algorithm SVM classifier takes either sampled relaying signal or filtered signal as input patterns to detect and classify fault, fault phase selection and fault location estimation.

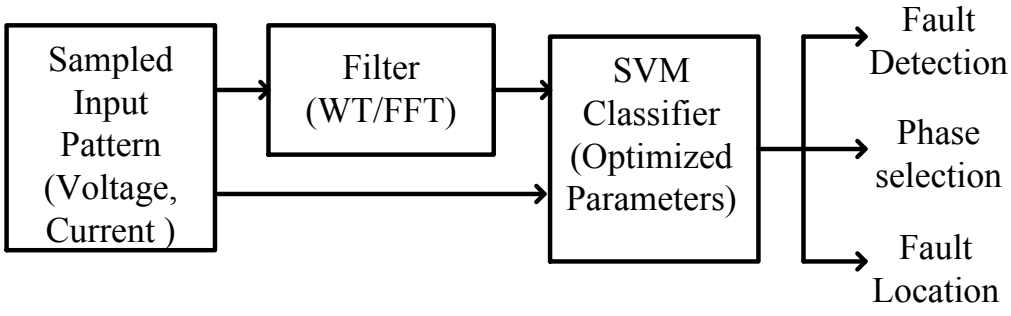

Fig. 1.6 Generalized SVM based protection algorithm for series compensated transmission line

Table 1.2 shows the yearly development in SVM based methods for protection of series compensated transmission line. From the Table 1.2, it is found that Gaussian radial basis kernel function is extensively used for fault detection and classification and accuracy is achieved up to 100% with lesser average time (1/2 cycle) than ANN based relays.

Table 1.2 Comparative study of SVM based algorithm for protection of series compensated line

Publish Year/ref	Method used	Kernel Function	Sampling Frequency	Window Length	Training Pattern	%Testing Accuracy	Output
2007[93]	SVM	Polynomial Gaussian	1 kHz	½ cycle	500	95.09	Fault Classification/ Section Identification
2008[90]	SVM/WT	Gaussian	4 kHz	-	25200	93.917	Fault Detection
2010[94]	SVM	Gaussian	-	1 cycle	25200	98.0	Fault Classification
2011[95]	SVM	Polynomial	-	½ cycle	672	100	Detection/ Classification
2012[92]	SVM /GA	Gaussian	1-4 kHz	4-80 samples	4400	99.93	Fault Classification
2012[89]	SVM/S-transform	Gaussian	2.5 kHz	-	1870	100	Fault detection/ classification/ Location
2012[91]	SVM/WT	Gaussian	4 kHz	½ cycle	2400	99.81	Fault Detection
2014[78]	SVM/ANN	Gaussian	4 kHz	½ cycle	32400	99.39	Fault classification

1.3.3 Wavelet Transform (WT) based Algorithms

Due to high speed and ability of time-frequency localization of signals, WT become a good tool for transmission line protection system. WT-MRA (Multi Resolution Analysis) decomposes the fault current into bands of various frequencies. P.K. Dash *et al.* found an application of Discrete Wavelet Transform (DWT) to separate out faulty phase and faulty section in mid-point series compensated line. Based upon the different wavelet energy presented in healthy and fault signals decision was taken [96]. Use of Wavelet Packet (WP) in place of DWT was done in ref. [97] for boundary protection of SC (Series Compensated) line, which is having more signal information than DWT. Similar boundary protection work was done using db4 as mother wavelet by Ashraf I. Megahed *et al.* in 2006 and they extended the work further for fault classification in SC line using Haar as mother wavelet [98]. V. J. Pandya and S. A. Kanitkar found the application of WT in Current Differential Pilot Relay (CDPR) Protection of SC line. They measured line current at both ends and analyzed the patterns of spikes for internal and external fault [99]. High Impedance Fault (HIF) distorted the voltage wave form measure by Coupled Capacitive Voltage Transformer (CCVT) and DWT analyzed the voltage patterns in case of HIF and generated trip decision [100]. Fault detection in SC line using DWT was improved by using Independent Component Analysis (ICA) in addition with DWT. ICA was used in pre-procession to reduce the burden of unnecessary data input for DWT [101]. Discrete Fourier Transform (DFT) has decomposed the fundamental phasor of voltage and current to calculate absolute value of all three phase impedances to classify fault in SC line [102].

Detailed coefficient (D_n) contains the information of particular frequency signal presents in the current. Pattern of D_n from level 1 to 9 for different wavelet series like db, Haar etc. were analyzed to detect the type of fault and fault zone as shown in Fig. 1.7.

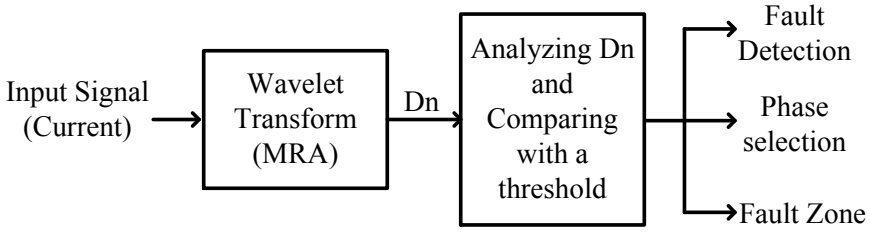

Fig. 1.7 WT based protection algorithm for series compensated transmission line

Table 1.3 Comparative study of WT based algorithm for protection of series compensated line

Publish year/ref	Authors	System Specification (voltage/frequency /length)	Wavelet/series used	Level	Frequency/ Sampling rate	Output
2004[97]	Z Chen *et al.*	500 kV/50 Hz/480 km	Wavelet Packer Transform	2	-	Fault Zone detection
2006[98]	A I Megahad *et al.*	500 kV/50 Hz/400 km	Haar/ db4	1-6	1-3 kHz	Fault zone/classification
2007[99]	V J Panda *et al.*	400 kV/50 Hz/300 km	Db4/db6	6	20 kHz	Fault zone/classification
2009[100]	E S T Eldin *et al.*	500 kV/50 Hz/150 km	Db4/Clark Transform	1	200 kHz	High Impedance fault detection
2011[101]	H C Dubey *et al.*	230 kV/50 Hz/300 km	Db4/haar/ICA	2	-	Fault detection
2014[78]	B Vyas *et al.*	400 kV/50 Hz/300 km	Wavelet Packet Transform	2	4 kHz	Fault classification

In fault clearing process it was required to extract actuating frequency component from voltage and current as quickly as possible. WT has an advantage of less discrimination time so it is widely used in protection of compensated/uncompensated line.

In WT based methods, selection the mother wavelet is very important task to achieve higher accuracy and reliability in case of series compensated line protection. Table 1.3 shows the year wise growth in wavelet transform based techniques for protection of series compensated transmission line and it is concluded that Daubechies wavelets (db) and Haar wavelets are widely used for the resolution of fault current and voltage signals.

1.3.4 Fuzzy based Protection Algorithms

Fuzzy logic has the ability to classify various input features into different categories based on some mathematical relations. A. K. Pradhan *et al.* in 2004 [103] proposed a Fuzzy Logic System (FLS) based approach to classify fault and healthy condition in series compensated line. Higher Order Statistics (HOS) was used for appropriate feature extraction from current signal which reduced the effect of noise and provided the accuracy of 100%. FLS along with WT classified the faulty phase and fault zone in mid-point series compensated line [104]. A composite fuzzy and ANN based protection technique for TCSC transmission line was suggested by S.R. Samantaray *et al.* in 2005 [105], sequence component of voltage and current, firing angle were taken as input to obtain exact fault location.

1.3.5 Adaptive Distance Algorithms

Adaptive distance protection has been popular for the protection of series compensated transmission line. Series compensator along with its protective circuit inserts non-linear voltage hence non-linear impedance into the transmission line. Adaptive distance algorithm estimates the non-linear quantity and adaptively protects the transmission line. Broadly the adaptive distance algorithms can be classified as follows:

1.3.5.1 Voltage Compensation based Relay

Series compensation device adds a voltage in the line during healthy and faulty conditions. In case of fault, this voltage does not allow the line voltage to fall much and creates error at the relay end which uses line voltage to calculate fault impedance. It is needed to calculate the voltage across series device during fault to sort out the error.

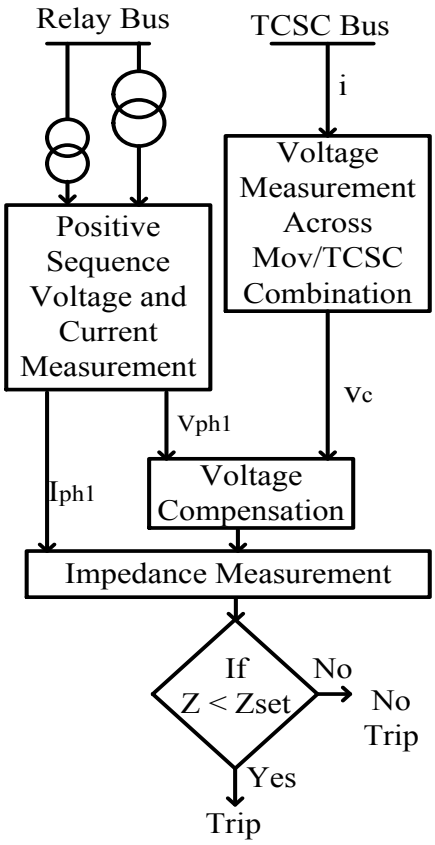

Fig. 1.8 Voltage compensation algorithm

Adaptive distance relays were developed in past to protect Advanced Series Compensated (ASC) line successfully [72-85][106]. Some of the adaptive relays compensated the error by calculating the voltage inserted by ASC into the line. Voltage compensation based adaptive relays online calculated the instantaneous value of series voltage across ASC or SC in terms of current flowing through it [72-78]. Computed voltage was simultaneously subtracted from the relay voltage which gives accurate relay voltage and line was successfully protected up-to 80 % for first zone [107]–[110]. Ricardo Dutra *et al.* in 2004 proposed a hybrid protection algorithm which was applicable for both EHV and SC line. Proposed algorithm was the combination of main distance protection scheme, fast tripping algorithm for phase to phase fault and phase to ground fault the main outcome of this algorithm was fast operation of relay for all types of fault [111]. A satisfactory Mho relay algorithm was suggested in ref. [112] which used residual current for the compensation of error inserted by SC in line. A combination of several distance relay algorithms were used for protection of ASC line. Relays were set for particular compensation degree of ASC therefore they had certain limitations for other degree

of compensation [113]. A generalized voltage compensation based protection algorithm is shown in Fig. 1.8.

1.3.5.2 Impedance Computation based Relay

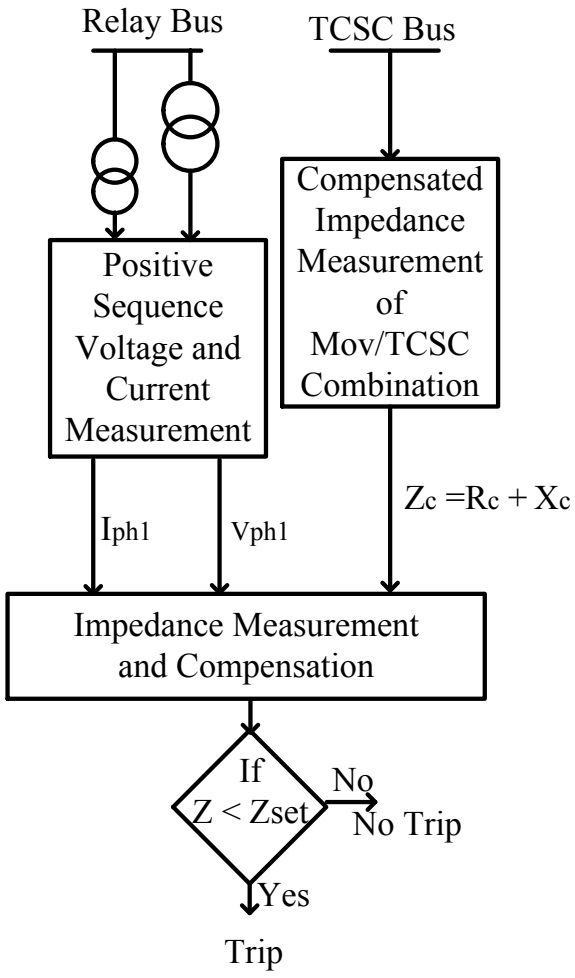

Fig. 1.9 Impedance compensation algorithm

Series device is protected by MOV which acts as a nonlinear resistor. In case of fault, device with its transmission line protection system adds dynamic impedance in the transmission line and changes the impedance measured by distance relay resulting in reaching mal-operation. Some other type of adaptive relays directly measured the impedance inserted by ASC into the line [79-85][114]. P K Dash *et al.* in 2001 proposed a simplified model of TCSC and fault impedance was calculated with the relative position of TCSC w.r.t. relay bus and it was concluded that Mho relay impedance calculation was modified when fault loop includes TCSC [115]. Vijay H. Makwana and Bhavesh R. Bhalja in 2011-12 suggested an adaptive distance relay algorithm for parallel series compensated transmission line which was

independent of mutual coupling parameters. SC impedance was calculated using robust non-linear equations [116], [117].

Fault Component Integrated Impedance (FCII) measured the capacitive impedance of line in cased of healthy condition or external fault condition and in case of internal fault FCII reflects the line impedance which was less than previous cases (healthy condition or external fault) [118], [119]. In ref. [120], [121] an advanced simplified linear model of SC/MOV has been proposed. The scheme was independently protected the line during inter phase fault and SCs parameters were not required for the adaptive protection. Combined impedance compensation algorithm is shown in Fig. 1.9.

1.3.6 Directional Relaying based Algorithms

In inversion problems voltage and current signals are inverted by 180 degree and relay misclassifies fault direction. Voltage or current inversion creates serious directional issues and it became difficult to discriminate between forward and reverse fault [16], [21], [29], [30], [122]. P Jena and A K Pradhan proposed a technique in which direction of fault in voltage inversion was defined by sign of the angle difference of fault and pre-fault positive-sequence current phasor and in current inversion case fault direction was discriminated by change in magnitude of positive-sequence voltage at the relay location and phase change in positive-sequence current provides the solution [123]. Suggested technique was improved in refs. [28], [124] by introducing a voting based directional discrimination method for transmission line having TCSC. In voting scheme, three different positive sequence based phase comparator decides the direction of fault occurred in transmission line. Similar technique was extended for double circuit transmission line with series compensation and an additional negative sequence phased comparator was added to decide fault direction by voting method [27].

1.3.7 Fault Zone/ Section/ Location in Series Compensated Transmission Line

Series compensator inserts nonlinear impedance into the transmission line which creates error in reach measurement of distance protection. A deterministic method to calculate the value of nonlinear impedance has been proposed by Damier Novosel *et al.* and a FFNN had been implemented to calculate the nonlinear voltage across the series capacitor in terms of line current. Proposed techniques allowed online adjustment to reach measurement of distance relay and fault location in SC line, however the method was simple but constrained by accuracy [24]. M. M. Saha *et al.* proposed an improved technique and they calculated fundamental frequency

equivalent of series capacitor and MOV instead of calculating voltage drop across it, the technique improved accuracy to some extent but did not discussed about the time taken by the algorithm [125]. Fault section in ASC line was found by measuring the differences in transient current associated or not associated with ASC [126]. Measurement of voltage across SC and MOV is constrained by measurement error and depends on device parameters. C. S. Yu *et al.* suggested a synchronized phasor measurement technique in which three phase voltages and currents were measured at sending and receiving end to estimate the fault location. The technique was independent of series device and highly accurate up to 99.5 % [127].

A combined DWT and ANN based fault location algorithm for series compensated line is suggested by W J Cheong. In that algorithm DWT extracted detailed coefficients of three phase voltages and currents at relay end and different ANNs classified the fault sections and fault locations. Proposed composite technique got high accuracy above 99.0 % [128], [129]. P K Dash *et al.* proposed a RBFNN based distance protection to assessment of fault location with error less than 1.0 %. Firing angle of TCSC thyristor was taken as an additional input along with voltage, current and frequency to take care of nonlinearity introduced by SC and MOV [71]. Use of Extreme Learning Machine (ELM) enhances the speed of FFNN and it also has better interpolation and approximation capability. ELM combined with DWT improved fault location assessment in series compensated line [130], [131].

A combined DWT and SVM techniques detects weather the fault occur before the TCSC installation point of after the point. It was found that signal content in current for fault occurring before and after the installation point is different. DWT extract the feature and SVM is to decide the fault zone [90]. WT has a limitation of creating some delay for processing which may be considerable therefore to overcome this problem S-transform (ST) was proposed. Hyperbolic ST (HST) having high-resolution invertible time-frequency with SVM has been proposed in [89] to locate fault in SC line.

An adaptive differential protection technique has been used for the protection of transmission line[132]. Fault location in SC line protected by differential relay was suggested by M.M. Saha *et al.* in 2010. Fault current was measured at both the end and voltage at relay end only. Two subroutines were used to identify the exact hypothetical fault occurred before and after the SC [133]. Travelling wave was helpful in fault location estimation technique in which fault distance from measurement point was measured by time taken by travelling wave generated during fault. Fast Fourier Transform (FFT) detects the harmonic content present in

fault and correspondingly removes the error [134]. Mahdi Ghazizadeh Ahsaee and Javad Sadeh in 2011 proposed a SCs parameter free fault location method which calculate exact fault location by calculating wave propagation time. The problem was transformed into an optimization one to estimate propagation time and fault resistance [135]. Fault location and identification is a challenging task in double circuit compensated transmission line because line current may rise abruptly in the healthy line too. Measurement of voltage and current at both the ends of parallel line can help in estimating fault location [136]. A method for identification of fault circuit in parallel compensated or uncompensated transmission line was proposed by M. M. Saha *et al.* in 2014. In that method, a factor was defined by the ratio of summation of differential current in both lines to decide whether the fault occurred in line one or other, but the method has limitation if both lines were faulty [137]. Ning Kang *et al.* in 2015 calculated the equivalent impedance inserted by series capacitor in parallel transmission line with taking mutual coupling and shunt capacitance into account. Distributed line equivalent was taken into account to write Kirchhoff's Voltage Law (KVL) equation to calculate voltage difference at the terminals of series compensator [138].

Application of Phasor Measurement Unit (PMU) in series compensated transmission line can be important in locating faults without need of line parameters and SC specifications [139]. Ali H. Al-Mohammed and M. A. Abido proposed a similar PMU based technique which measures pre-fault voltage and current at both the terminals of SC and line terminals to estimate exact fault location [140]. The scheme is improved by A. Y. Abdelaziz *et al.* in 2013 and proposed a generalized fault location scheme for compensated as well uncompensated lines. Symmetrical components of voltage and currents were calculated at both ends and distributed line parameters were used for calculation of per unit fault distance from relay bus [141]. Accurate phasor approximation of voltage and current are essential input for fault location estimation in series compensated line. Due to the interaction of line inductance and series capacitor, Sub-Synchronous Frequency Components (SSFCs) were generated in fault current and voltage which badly affect the phasor assessment based fault location technique [142]. R. Rubeena *et al.* proposed a technique which scans whole fault data to filter out SSFCs and decking dc components from voltage and current signals to measure correct phasor [143].

1.3.7.1 Fault Location Estimation by Two End Measurement Method

For uncompensated line (no series device), any fault, between sending and receiving end, the per unit fault length from sending end was given by equation (1.1) [141].

$$l = \frac{1}{\gamma L_e} tanh^{-1}\left[\frac{\cosh(\gamma L_e)V_r - Z_c \sinh(\gamma L_e) I_r - V_s}{\sinh(\gamma L_e)V_r - Z_c \cosh(\gamma L_e) - Z_r I_s}\right] \quad (1.1)$$

Where V_s, I_s are sending end voltage and current respectively, V_r, I_r are receiving end voltage and current respectively, Z_c is surge impedance, γ is propagation constant and L_e is the total length.

In case of series compensation, the transmission line is divided into two sections, section between 's' to 'c1' and section 'c2' to 'r'. Voltage across series device V_{c1} and V_{c2} is calculated by synchronizing measurement of current through the device and fault location can be calculated in two different sections from equation (1.1). The proposed algorithm used distributed parameters of the transmission line and utilized the synchronized measurements of voltages and currents at both ends of the line as shown in Fig. 1.10.

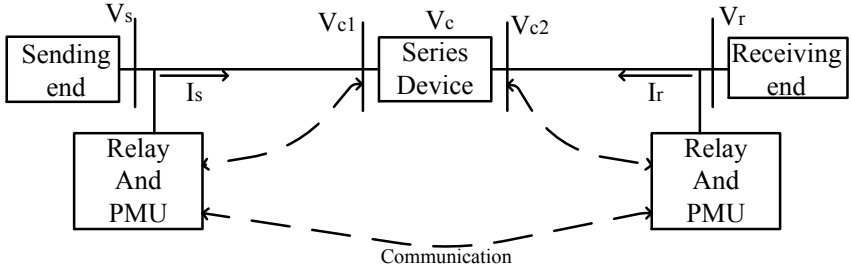

Fig. 1.10 PMU based fault location

Vyas B.*et al.* presented a comparative study of all fault location techniques for series compensated line. They classified the fault location algorithms based upon the number of measurement points viz. single, double, and multi end and concluded that single end measurement schemes has advantages of less data, simple and economical, but due to higher accuracy in two and multi end algorithms they are more popular [144].

1.3.8 Overvoltage Protection of Series Compensators

D. D. Wilson discussed about the significant voltage that occur across the circuit breaker when the fault is interrupting. It was shown in Transient Network Analyzer (TNA) that severs overvoltage may occur across circuit breaker if resistors are not inserted during opening of the

contacts [33]. V. Madzarevic *et al.* investigated that overvoltage in healthy line may exceeds above 2.0 pu due to subsequent bypassing of series capacitor in other line by spark-over of protective gap [37]. Over voltage transients in series compensated transmission line may occur due to reduction of load. It is shown in ref. [36] that the magnitude of transients overvoltage depends on the level of compensation and both are proportional to each other. F. Iliceto *et al.* in 1991 investigated that series capacitor protected by MOVs cases higher Transient Recovery Voltage (TRV) than spark gap. The magnitude of TRV was found to be more for higher short circuit current as occurred in three phase fault [38]. Sherif Omar Faried and Saleh Aboreshaid proposed a stochastic evaluation method to calculate maximum TRV across a circuit breaker protecting SCs. Maximum TRV was measured assuming the probability of different factors which affect power system and it was found that the probability of maximum TRV was least [31]. TRV and Rate of Rise of Recovery Voltage (RRRV) depends on various parameters like length of transmission line, SC, fault conditions, arc and power system oscillations. Sensitivity of TRV and RRRV on these parameters was mentioned by A. Parvizi *et al.* and they revealed that TRV amplitude increases with fault distance and RRRV was high at the beginning of the line [34]. Maximum value of TRV in double circuit transmission line was investigated by Zutao Xiang and it was found that TRV magnitude was higher in transmission line having series capacitor and forced bypassing of series capacitor with triggering gap can decrease the value of TRV [15].

Based upon the experimental studies following actions have been suggested to protect series compensator from overvoltage (TRV) [15], [33].

(i) Installation of fast protective device across the series device for bypassing.

(ii) Force triggering of protective gap or by lowering the breakdown voltage of gap.

(iii) Impedance has to be inserting in series or an arrester in parallel with the circuit breaker to reduce the peak of TRV.

(iv) Maximum compensation has to be set up-to permissible limit. Lower value of compensation generates lower overvoltage.

1.3.9 SSSC Impact and Protection Schemes

SSSC is a Voltage Source Invertor (VSI) based controllable device which inserts variable impedance in series with the transmission line. SSSC injects a variable voltage Es in

the transmission line according to the control strategy which depends on loading conditions of power system as shown in Fig. 1.11.

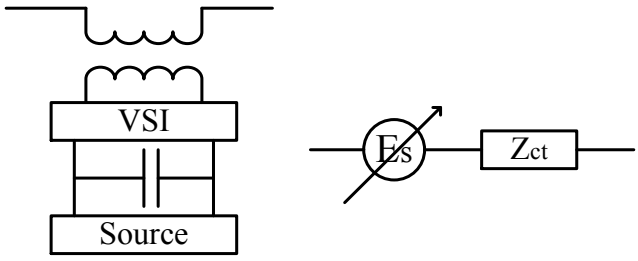

Fig. 1.11 Equivalent circuit of SSSC

S Jamali, A Kazemi and H Shateri examined the impact of SSSC and its installation point on distance relay tripping characteristics. They investigated that SSSC only affected the relay performance when it fall into the fault loop. It was dignified that in case SSSC not falling into fault loop and fault resistance was zero, measured fault impedance was actual. Inactive SSSC inserts a constant inductance of coupling transformer and shifts the tripping characteristic upward by a constant margin. In active mode of SSSC, adaptive tripping characteristics have been drawn for per unit injected voltage from 0 to 0.15 pu in leading and lagging mode of operations. It was concluded that in leading mode the quadrature trip characteristics shift downward in clockwise manner and in lagging mode the characteristic shifts towards upward direction [41], [42], [47]. Same authors suggested that in case of one end installation of SSSC, best position for installing voltage transformer was in front of SSSC [39], [43]. M. Khederzadeh *et al.* simulated a full 48-pulse GTO-SSSC model and found that in capacitive mode of SSSC apparent resistance affected mostly and in inductive mode apparent reactance affected mostly. They also concluded that apparent impedance mainly affected by zero sequence voltage injected by SSSC [17]. S Jamali, A Kazemi and H Shateri proposed an adaptive quadrilateral distance relay characteristic for protection for line having SSSC. They evaluated the measured impedance at the relaying point in the presence of SSSC and suggested ideal distance tripping characteristics. Proposed tripping curves were fully adaptive with the controlling parameters and installing location of SSSC [145]–[148].

Additionally, ANN based zone-1 protection for transmission line having SSSC as series compensator device was suggested by H. Rastegar *et al.* in 2006, [149]. In this technique, resistance and reactance of up to 85 % of transmission line with large variations in power system operating parameters were taken as training parameters. ANN makes the relay adaptive

for trapezoidal trip boundaries of distance relay. Parallel computation based Adaptive Neuro-Fuzzy Inference System (ANFIS) for fault location in transmission line having SSSC has been suggested by E Mohagheghi *et al.* in 2012 [87], in this scheme, apparent impedance was calculated for various faults created at several locations and simultaneously SSSC equivalent impedance was calculated to train the neuro-fuzzy system to find out the accurate fault location.

1.3.10 Modern Trend and Scope

Presently a lot of fixed capacitor installations are taking place into the transmission network. Compensation level can vary from 15 to 70 percent of total line inductance. To remove the effect of fixed series installations, distance protection is made slow enough to first remove capacitor from the line through protective gap and circuit breaker, and proper distance relay operation is restored [11]. These lines are protected by over-reaching schemes and first zone of protected line is stretched up-to 120 percent of the line to remove security issues completely. A carrier signal transmits from other end to relay bus which decides that the fault is internal. TCSC has limited installation compare to fixed capacitor and protection of mid-point TCSC line is still a challenging issue for protection engineers. Some important lines are protected by carrier current protection schemes as unit protection in which security problems does not occur but this protection, highly constraints by economical issue. Adaptive distance algorithms and composite AI techniques are highly appreciated for the protection. SSSC mounts as a part of UPFC and generally comes under the protection of transmission line having UPFC.

1.4 Protection Schemes for Transmission Line having Shunt Devices

In the normal loading conditions, resistance values were found more and reactance values were less in the presence of STATCOM. STATCOM was modeled as a constant current source which injected reactive power into the system and used to control voltage at the point of connection [18], [51], [63], [150]. Kazmi, Jamali and Shateri had done to find out the impact of SVC and STATCOM on distance relay and suggested the apparent impedance calculation with respect to SVC and STATCOM. SVC and STATCOM were modeled as impedance connected in shunt with the line. They analyzed that these devices affected the apparent impedance only if present in fault loop even in the case of zero fault resistance [54]–[58], [65]. If the shunt device is connected in the middle of the transmission line and fault occurs on right half of the line,

relay operating parameters changes and accordingly mal-operates [59], [61], [64], [151]. T S Sidhu *et al.* in 2005 vastly analyzed the impact of shunt FACTS devices on distance relay and they found that channel aided distance relay was suitable for the protection even this scheme had certain limitations in over-reaching phenomena [53]. Fadhel A. Albasri *et al.* in 2007 took the work forward and provided the detailed impact of shunt FACTS devices specially STATCOM w.r.t. phase selection, delayed response, under-reaching, over-reaching, transients, fault resistance and influence of location of fault and relay. They conclude that Direct Under-Reach Transfer Trip (DUTT) scheme was best suited for protection [19], [67].

In case of system faults, Voltage Source Convertor (VSC) based shunt device like STATCOM rapidly supplies dynamic VARs for voltage support [62], resulting in overcurrent and mal-functioning of STATCOM after system fault when VARs are required. Emergency pulse width modulation technique has been suggested by Subhashish Bhattacharya *et al.* in 2006 to prevent above mentioned problem. In this technique, VSC uses self-implemented PWM (Pulse width modulation) switching to control its phase current within limit and enable STATCOM to remain online during and after fault when it is required [152]. Kazmi, Jamali and Shateri gave a method for apparent impedance calculation in presence of STATCOM and suggested an adaptive quadrilateral distance relay characteristic with taking wide variations in power systems operating conditions which did not change with the operation of STATCOM [153], [154]. Robust protection of shunt compensated transmission line was done by calculating the error introduced by these devices into the Mho relay in terms of current injected by these devices into the line and the error was subtracted from the measured impedance [155]–[158]. Setting principles of distance relay for zone-1, 2 and 3 in case of under-reaching and over-reaching w.r.t. STATCOM are suggested in ref. [159] which made distance relay adaptive if STATCOM operate in a limit. Jung-Uk Lim *et al.* in 2008 proposed a differential current protection scheme for mid-point shunt compensated transmission line. Under this scheme the whole line was scanned in three segments to check whether the disturbance occurred was fault or the action of shunt device [160]. Application of ANN on protection of transmission line having STATCOM was presented by A. M. Ibrahim *et al.* in 2011. Transient value of voltage and current was taken as input vector and total least square rotational invariance technique in conjunction with ANN was found to be very accurate for detection of fault [73].

1.4.1 Adaptive Relay Setting

For any fault in transmission line, if fault resistance is zero and shunt device does not fall into the fault loop, the calculated apparent impedance shows the actual value of fault impedance and no modification is needed in protection algorithm. If shunt device falls in fault loop, it affects the trip boundaries according to controlling parameters of the device. In this case distance protection should be adaptive according to operation of shunt device. In literature [152]–[155], [157], [159], [161], apparent impedance calculation in case of fault in shunt compensated transmission line has been suggested as follows:

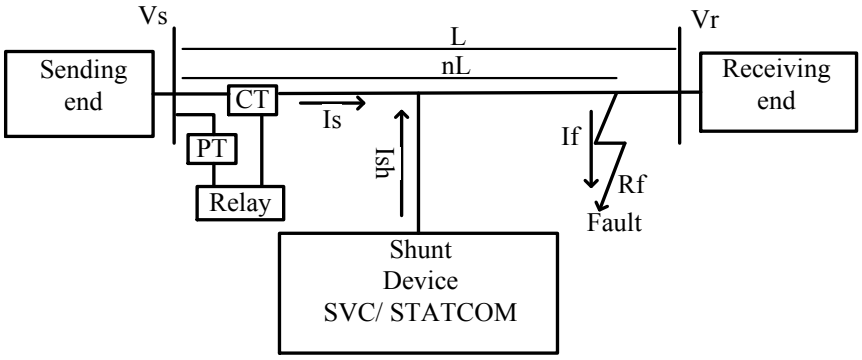

Fig. 1.12 Apparent impedance calculation

As shown in Fig. 1.12 for any LG fault at 'n' per unit length of line, the sending end voltage V_s can be given as:

$$V_s = nI_s Z_1 + nI_{0s}\left(Z_0 - Z_1\right) + I_{sh}(n-0.5)Z_1 + R_f I_f, \tag{1.2}$$

Measured impedance

$$Z = nZ_1 + \left(n - 0.5\right) Z_1\left(\frac{I_{sh}}{I_s}\right) + R_f\left(\frac{I_f}{I_s}\right) \tag{1.3}$$

First portion of equation (1.3) is the actual fault impedance and second portion is the error introduced by the shunt FACTS and third portion is due to fault resistance. Adaptive protection can be achieved by measuring the error introduced by the shunt device.

1.4.2 ANN based Techniques for Protection of Shunt FACTS Devices

In literature, ANN based approach using TLS-ESPRIT (Total Least Square- Estimation of Signal Parameters via the Rotational Invariance Technique) algorithm has been used to detect and classify fault in transmission line having STATCOM. Proposed technique has two hidden layers and back propagation algorithm used for network training. Half cycle pre fault

and full cycle post fault data of three phase voltage and currents for various power system operating conditions are taken as input to ANN and testing and validation accuracy was found to be 100 % [73].

1.4.3 Mitigation Trends for Reaching Effects

Literature suggested that, SVC did not show any considerable over-reaching effects as severe as shown by STATCOM. Following were the major remedial steps to reduce the over-reaching effects shown by STATCOM [19], [67], [156], [162].

(a) By reducing the reach setting of zone-1phase element.
(b) By allowing the adjacent line transmission line protection system to react for external faults.
(c) A blocking signal can be sent from remote end relay to zone-1 relay if remote end relay senses a reverse fault.

Following conclusive remedial steps has been taken to reduce the under-reaching effects shown by shunt FACTS device.

(a) Relays are operated with different channel added schemes to secure no under-reaching during fault in shunt compensated line.
(b) Direct under-reaching transfer trip (DUTT)
(c) Permissive under-reaching transfer trip (PUTT)

DUTT scheme performs well for any internal fault except its limitations on high fault resistance.

1.4.4 Fault Location in Line having Shunt FACTS Devices

M. Ghazizadeh-Ahsaee *et al.* in 2011[163] proposed a novel optimization technique to locate fault in shunt compensated transmission line without using the shunt device parameters. Distributed-parameter transmission line with synchronized measurement of voltage and current at both ends was used for algorithm. That technique converts fault location calculation into an optimization problem under some constraints of line fault. The algorithm was tested for several fault location and calculated error was of the order of 10^{-2}.

Table 1.4 Yearly advancement in protection of transmission line having shunt FACTS

Year	Authors	Device	System Descriptions (Ratings/ Length)	Techniques Used	Outcome/ Remediation of
2006	S Bhattacharya *et al.*	STATCOM	138 kV, 150 MVAR	Emergency PWM	Overcurrent protection of VSC
2007	F A Albasri *et al.*	SVC/ STATCOM	230 kV,110 MVAR /300 km	Channel aided Distance protection	Under-reach/ Over-reach
2008	S R Samantaray	UPFC/ TCSC	230 kV /300 km	Decision Tree	Fault zone identification and classification
2008	J U Lim *et al.*	STATCOM /UPFC	154 kV, 100 MVA	Differential current protection	Secure protection
2009	S Jamali *et al.*	STATCOM	400 kV/ 300 km	Adaptive distance protection	Adaptive trip boundaries
2009	Seethalakshmi *et al.*	UPFC	345 kV	Adaptive distance protection (ADP)/ GRNN	Under-reach/ Over-reach
2010	W H Zhang *et al.*	STATCOM	500 kV, 100 MVA /200 km	Apparent impedance calculation (Adaptive distance protection)	Zone protection
2011	Z Xi *et al.*	STATCOM	500 kV, 100 MVAR	Instantaneous phase lock loop (IPLL)	Overcurrent protection of VSC
2011	A M Abrahim *et al.*	STATCOM/ TCSC	230 kV	ANN/TLS- ESPRIT	Fault Detection, classification
2012	A R Singh *et al.*	SVC/ STATCOM	-	Adaptive distance protection	Robust Distance protection

Table 1.4 gives year wise summarized idea about the protection trends in the transmission line having composite and shunt devices. Adaptive distance protection has certain advantages over the other protection techniques suggested for the purpose. Apparent impedance of transmission line in the presence of compensating device is calculated in terms of current or voltage injected by the device in the line and distance relay trip characteristic has been strategized for a large variation in fault resistance and power factor (leading to lagging). Learning algorithms viz. ANN, DT and ELM are required to adapt variable quadrature trip characteristics of distance relay.

1.5 Author's Contribution

The aim of the present research work is to develop

- A detailed literature survey of the impact of series and shunt FACTS devices on protection of transmission line and the various schemes developed for the protection of compensated line has been carried out.
- A universal fault section algorithm has been developed for mid-point compensated (series/shunt) transmission line, tested with different transmission voltage and various Power system operating conditions.
- An advanced adaptive compensated Mho relay has been developed for the protection of TCSC transmission line which is fully compatible with all possible operating modes of TCSC and its protective circuit.
- An adaptive and robust Mho relay has been developed for the protection of shunt compensated transmission line having SVC or STATCOM at the middle of line.
- AI based first zone setting of compensated (series/shunt) transmission line algorithm has been developed successfully. Proposed algorithm mitigated the effect of compensation, fault resistance and heavy or light loading conditions effectively.
- Finally, proposed protection algorithm for series and shunt compensated transmission line has been validated in RTDS/RSCAD environment.

1.6 Organization of Thesis

The thesis has been organized in the following chapters:

Chapter 1: This chapter introduced about the advantages of FACTS devices in high power transmission along with the adverse impact on protection of transmission line. Literature survey

of the impact of series and shunt devices on protection of transmission line has been discussed and numerous protection methods presented in several chapters till the present time has been deliberated.

Chapter 2: This chapter presents a universal fault section identification algorithm for mid-point compensated transmission line. Fault section identification is an important task for protection of mid-point compensated transmission line. A novel technique has been presented for both types viz. series as well as shunt compensated line.

Chapter 3: This chapter presents an adaptive distance relay algorithm for protection of series compensated transmission line having fixed capacitor/ TCSC at mid-point of transmission line. Impedance of series compensator is measured and simultaneously subtracted from the gross fault impedance to achieve adaptive relaying.

Chapter 4: This chapter presents an adaptive zone setting for series compensated transmission line. Zone setting of distance relay is constrained by fault resistance and wide loading conditions. An AI based adaptive zone setting algorithm is developed which take care of all the operating conditions and accurately classify fault zone.

Chapter 5: This chapter presents an adaptive distance relay algorithm for protection of shunt compensated transmission line having SVC/ STATCOM at mid-point of transmission line. Impedance of shunt compensator is measured in terms of current induced by the compensator and simultaneously subtracted from the gross fault impedance to achieve adaptive relaying.

Chapter 6: This chapter presents an adaptive zone setting for shunt compensated transmission line. Zone setting of distance relay is constrained by fault resistance and wide loading conditions. An AI based adaptive zone setting algorithm is developed which take care of all the operating conditions and accurately classify fault zone.

Chapter 7: This chapter presents the validation results of adaptive protection of mid-point compensated transmission line in RTDS/ RSCAD environment.

Chapter 8: This chapter presents the summary of the entire thesis and concludes all the chapters. Advantages, achievements and limitations of the work have been discussed in this chapter. This chapter also gives the idea of future work which can been done in the area of protection of compensated transmission line.

CHAPTER 2
FAULT SECTION IDENTIFICATION

This chapter presents a universal fault section identification algorithm for the protection of transmission line having Flexible Alternating Current Transmission System (FACTS) in the middle of line. A High Pass Filter (HPF) is installed at the Point of Common Coupling (PCC) along with compensator to filter high frequency signals generated during fault in line section (section-II) after compensator. For any fault in section-II, high frequency components are missing at relay bus due to filtering at PCC. Wavelet Transform (WT) explores the different frequency signals present in fault current, which are analyzed by an optimal adaptive classifier (SVM/ RBFNN) to identify the faulty section. Compensated transmission networks having TCSC, SVC or STATCOM in the middle of line, have been considered in PSCAD/EMTDC software to simulate different operating conditions of transmission network. A WT- SVM/RBFNN based algorithm programed in MATLAB which classifies the fault sections.

2.1 Introduction

Protection of transmission line becomes a challenging task for protection engineers if FACTS controller is placed at the middle of transmission line [14], [19]. In this condition transmission line has two sections, first one before the FACTS device which is uncompensated portion whose impedance is fixed and second one after the device which is being compensated and having variable impedance. Therefore, ultimate challenge for protection engineer is to protect such a line where impedance is not linear throughout the whole length. To protect transmission line having midpoint compensation, first requirement is to identify the fault section of line. After identifying fault section, an adaptive protection algorithm is needed to protect the complete line.

Impact of series and shunt compensators on protection of transmission line with respect to security and reliability issues are explained in ref. [14], [19], which clearly indicates that FACTS devices created severe reaching problems if a fault occurs in right side (section-II) of compensator. Various fault distance estimation techniques have been suggested which calculates the series compensator voltage in terms of current flowing through it by using artificial neural network (ANN) [164]. WT based boundary protection classifies the internal and external fault in series compensated transmission line [98]. WT based techniques analyze

the signals which are different for internal and external faults, but the reliability of the technique is compromised for various operating conditions of compensator [86], [96]. A combined S-Transform and Logistic Model Tree based technique has been presented by Zahra Moravej *et al.* but the results are not discussed for varying compensation level of TCSC [165]. Support Vector Machine (SVM) has been used as a powerful tool for locating fault in transmission line[166]. SVM classifier analyzes the harmonic content present in the fault current to identify internal (within the zone) and external fault (outside zone) [93]. SVM combined with WT has proved to be effective tool in fault section identification in series compensated transmission line [90]. Performance of distance protection of shunt compensated transmission line having SVC and STATCOM is improved by adjusting the over-reaching and under-reaching permissive limit of relay [67]. An accurate fault location estimation technique in transmission line having STATCOM is presented in ref. [163], which uses synchronized measurement of voltage and current at both ends of line. However, no universal algorithm was reported for the section identification in case of either series or shunt compensated line. Proposed technique has clear advantages over the previously proposed techniques that it does not depends on the system parameters and comprehensively accepted for any type of mid-point compensated transmission line.

2.2 Test System Components

A 200 MVA, (230 and 400) kV, 50 Hz, 320 km long double fed transmission test system are used to test WT-RBFNN based section identification algorithm in compensated transmission line. Source data has been given in Appendix-A Table A.1. Two transmission voltage levels (230 kV and 400 kV) have been incorporated for the implementation of universal fault section identification algorithm. Per km sequence impedances of 230 kV and 400 kV transmission line in ohms are: ($Z1$ = 0.0362 + j0.508, $Z2$ = 0.0362 + j0.508, $Z0$ = 0.365 + j1.33) and ($Z1$ = 0.0242 + j0.378, $Z2$ = 0.0242 + j0.378, $Z0$ = 0.184 + j0.98) respectively [158], [167]. FACTS device is connected at the middle of transmission line at the point of common coupling (PCC). A second order HPF is also connected at the PCC to filter high frequency above 1 kHz. Section identification algorithm is tested on both types of line having series (TCSC) and shunt compensators (SVC/ STATCOM). Mid-point compensator divides the transmission line into two sections, first one before the compensator and another after the compensator. Protection schemes for both the section must be different for any fault occurs in any of the section. Brief

about the mid-point series and shunt compensated line with filter is given in following subsections:

2.2.1 TCSC Transmission System

TCSC is connected along with HPF at the PCC as shown in Fig. 2.1(a). Two different voltages level 230 kV and 400 kV are selected for the testing of the section identification algorithm. A Current Transformer (CT) is connected at the relay bus which parameters are given in Appendix-B Table B.1. Per phase maximum TCSC capacitor rating is 110 Ω with compensation varies from 15 % to 70 %. Thyristors nominal current rating is 2.5 kA and 2.2 kA and blocking voltage is 5.5 kV and 10 kV for 230 kV and 400 kV lines respectively. In PSCAD, 3-phase TCSC is used to generate data. A single phase TCSC installed on one phase is shown in Fig. 2.1(b), three similar single-phase TCSC has been used for each phase.

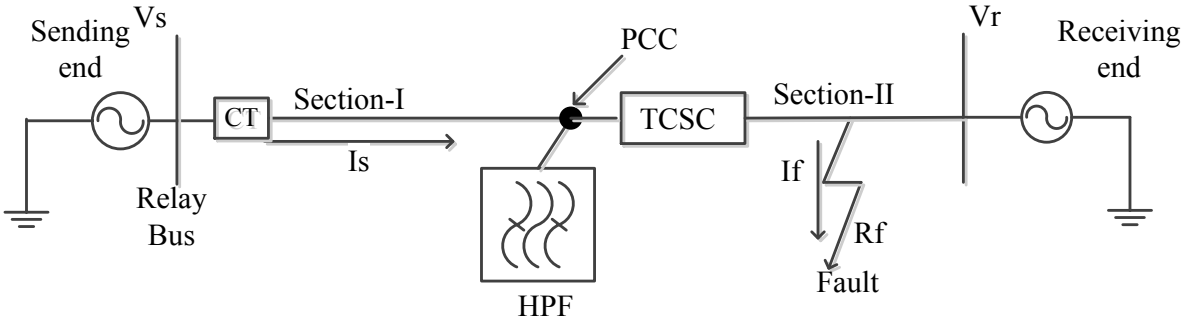

(a)

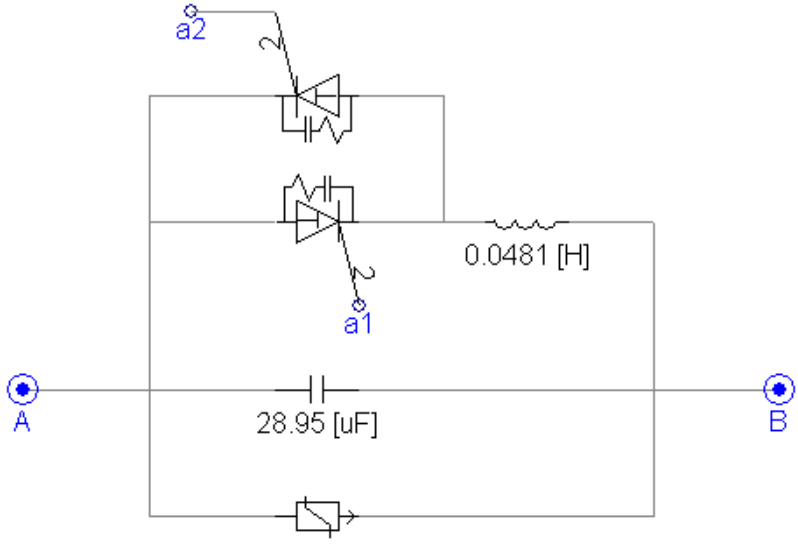

(b)

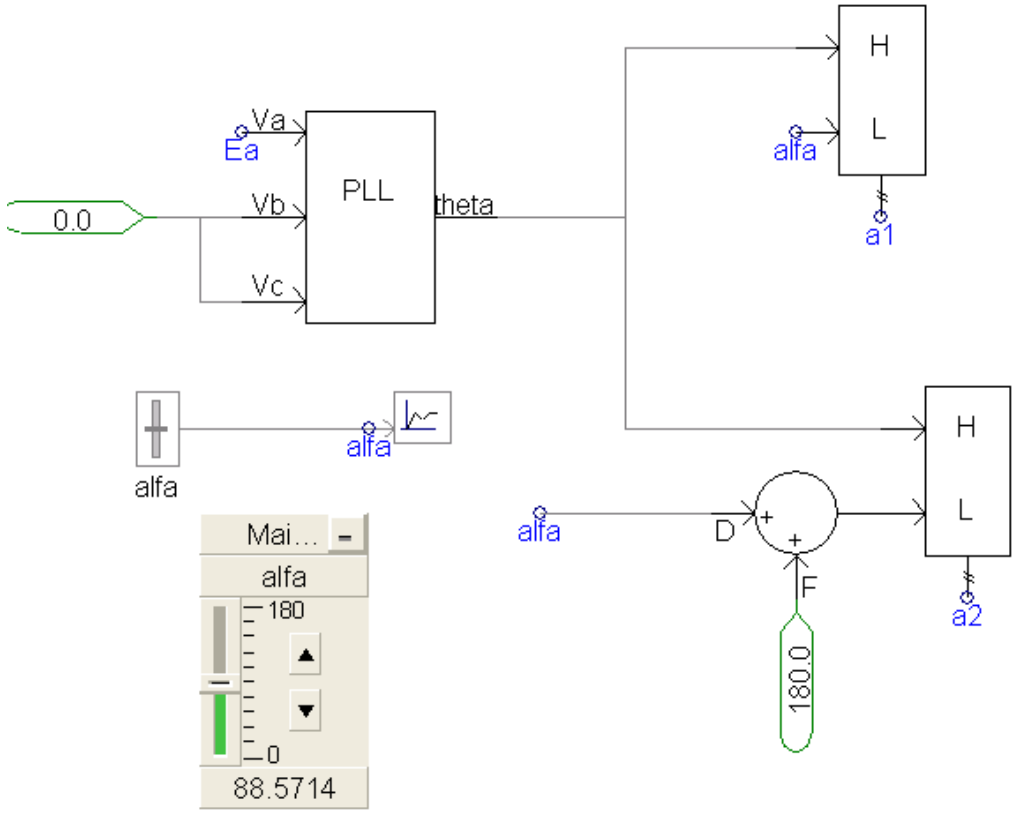

(c)

Fig. 2.1 (a) Transmission line having TCSC (b) Per phase TCSC module in PSCAD/EMTDC (c) Per phase control for TCSC

Capacitor values are calculated for different compensation levels. For particular value of series capacitance, firing angle of thyristor is kept near 85°-90° for full capacitive compensation. Phase Locked Loop (PLL) generates a ramp signal theta that varies between 0° and 360°, synchronized or locked in phase, to the input voltage E_a as shown in Fig. 2.1(c). Interpolated firing pulses (a1 and a2) are generated which are 180° phased shifted from each other and fed to antiparallel thyristors respectively. All types of shunt faults are created both side of the PCC at several locations in the transmission line. A protective Metal oxide varistor (MOV) with bypass switch also placed across TCSC to bypass excessive energy during fault. The detail explanation about the MOV is mentioned in next chapter subsection 3.2.1.

2.2.2 SVC/ STATCOM Transmission System

Shunt devices like SVC or STATCOM are connected in the middle of transmission line at the PCC [1], [2]. Difference between SVC and STATCOM working is that, SVC works as a variable current source and STATCOM works as the constant current source with respect to

line voltage. Fig. 2.2(a) shows mid-point compensated transmission line with equivalent of SVC having capacitive rating 167 MVAr and inductive rating 100 MVAr and STATCOM with power rating of ±100 MVAr. SVC and STATCOM models used in PSCAD/EMTDC have been shown in Fig. 2.2(b) and Fig. 2.2(c) respectively.

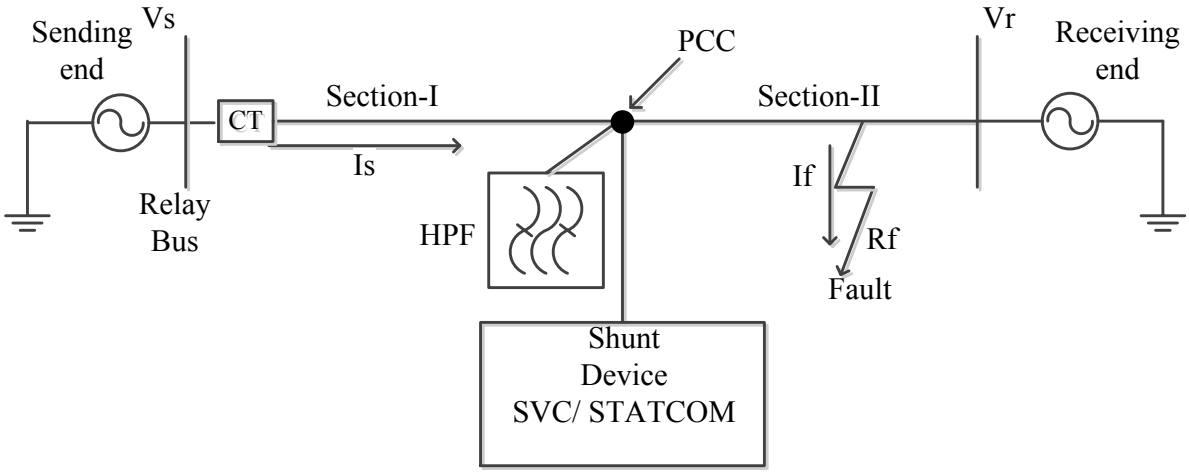

(a)

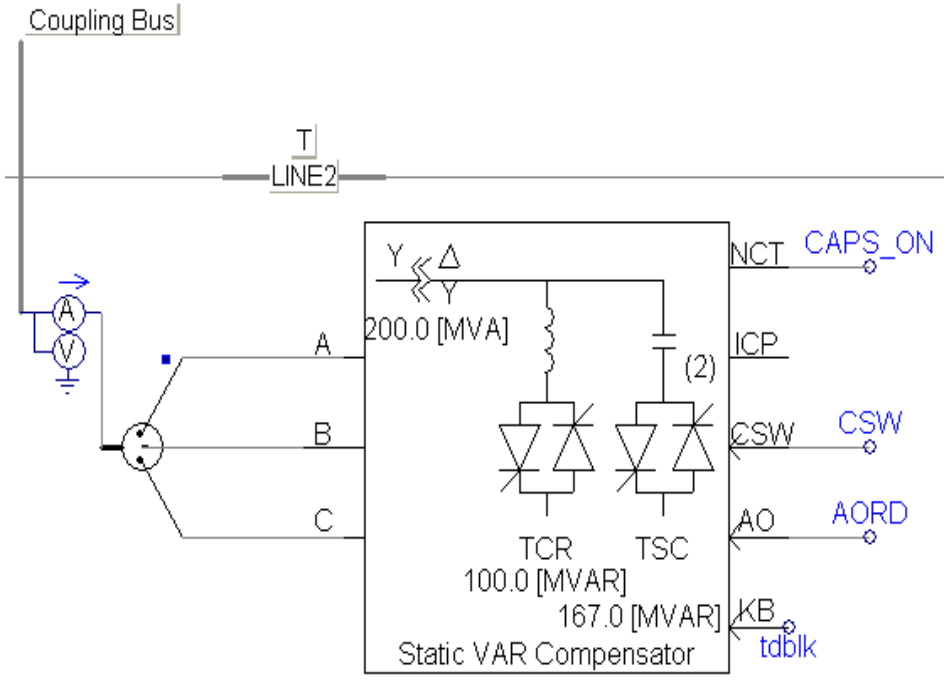

(b)

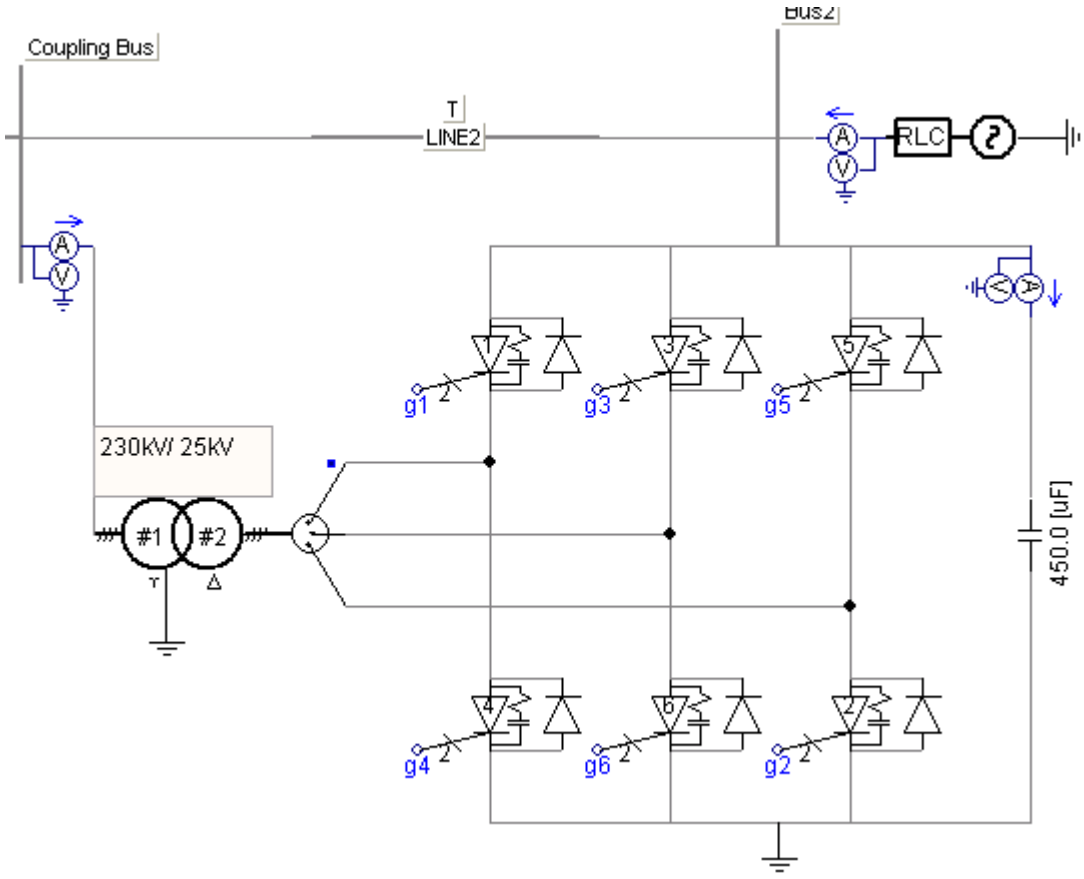

(c)

Fig. 2.2 (a) Transmission line having SVC or STATCOM (b) SVC module in PSCAD/EMTDC (c) 6-pulse STATCOM Module in PSCAD/EMTDC

In Fig. 2.2(b) SVC has maximum two number of TSC (thyristor switched capacitor) blocks, which share equal capacitive reactive power and the number of TSC blocks is controlled through *CAPS_ON*. TCR (thyristor controlled reactor) is a single unit which is controlled through thyristor firing angle order (*AORD*). In the proposed work, 6-pulse STATCOM with Pulse Width Modulation (PWM) control is used to boost voltage level at mid-point. PWM frequency is selected 33 times higher than the base frequency which reduces all dominating harmonics. In Fig. 2.2(c) the PSCAD/EMTDC model of working transmission system with 6-pulse STATCOM is shown. Detailed descriptions of the controlling of SVC and STATCOM have been mentioned in chapter-5 section 5.3.

2.2.3 High Pass Filter (HPF)

A second order HPF is also designed for the cutoff frequency of 1 kHz. Fault current contains high frequency signals from 1 kHz to 80 kHz [168]. HPF filter out all the high

frequency signals at the PCC generated due to fault in section-II. Filtered High Frequency (HF) signals are shown in Fig. 2.3.

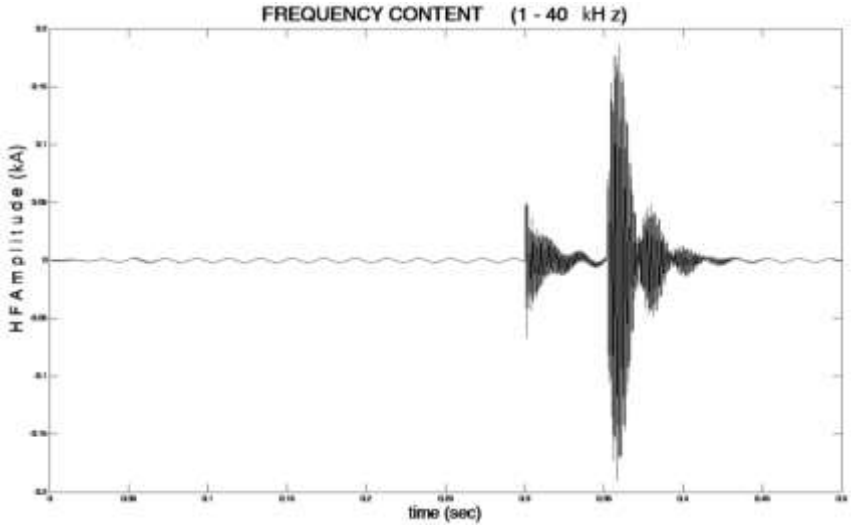

Fig. 2.3 High frequency content present in fault current

Designed HPF is represented by equation (2.1), X(s) and Y(s) are the input and output to the filter respectively. Fig. 2.4 shows the bode plot of the filter which shows that all high frequency signals above 1 kHz have been passed and rest of the signals (below 1 kHz) are blocked by the filter.

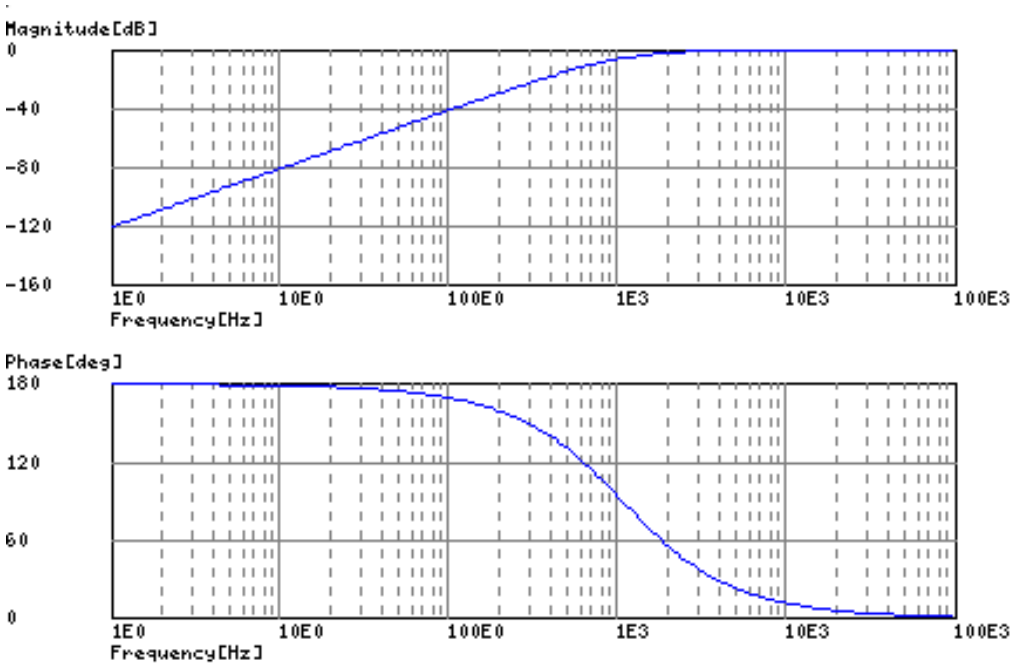

Fig. 2.4 Bode plot of HPF filter

$$\frac{Y(s)}{X(s)} = \frac{G\left(\frac{s}{\omega_c}\right)^2}{1+2\xi\left(\frac{s}{\omega_c}\right)+\left(\frac{s}{\omega_c}\right)^2} \quad (2.1)$$

Where, G = Gain, 1

ω_c = Characteristics frequency, 1 kHz

ξ = Damping ratio, 0.98

s = Laplace operator

Quality factor, Q = 0.49

2.3 Signal Processing

In the proposed section identification technique line current signal is received at the sending end relay bus which is explored with WT further the signal is analyzed with adaptive techniques like RBNN and SVM respectively. Detail about all the signal processing techniques have been given as follows:

2.3.1 Wavelet Transform

WT is a powerful wave analyzing tool introduced by Jean Morlet in 1982. WT provides the time localization of frequency components presents in a signal. Wavelets is a family of functions constructed from translations and expansions of a function called the mother wavelet '$\psi(t)$' whose average value is always zero and can be given by equation (2.2).

$$\psi_{a,b}(t) = \frac{1}{\sqrt{2^a}}\ \psi\left(\frac{t- b*2^a}{2^a}\right) \quad \text{Where, } a \text{ , b } \varepsilon \text{ R, } a \neq 0 \quad (2.2)$$

In Discrete Wavelet Transform (DWT) the mother wavelet is scaled by two that is provided by (2.3), where $x(t)$ is the signal to be analyzed. All the wavelet functions used in the transformation are derived from the mother wavelet through translation and scaling.

$$\psi_{a,b}(t) = \frac{1}{\sqrt{2^a}} \int_{-\infty}^{+\infty} x(t)\,\psi\left(\frac{t- b*2^a}{2^a}\right) dt \quad (2.3)$$

The parameter 'a' is the scaling parameter and it measures the degree of compression. The parameter 'b' is the translation parameter which determines the time location of the wavelet.

There are many types of mother wavelets such as Haar, Daubichies (dB), Coiflet (coif), Biorthogonal (bior), Reverse Biorthogonal (rbio) and Symmlet (sym) wavelets etc. The choice

of mother wavelet plays a significant role in detecting and localizing different types of fault transients. The choice also depends on a particular application. For short and fast transient disturbances, which generally occur in transmission line during fault, db4 is better [98]. The resolution of the signal, which is a measure of the amount of detail information in the signal, is determined by the filtering operations, and the scale is determined by up-sampling and down-sampling (subsampling) operations. One of the most important properties of DWT is Multi-Resolution Analysis (MRA) in which input signal resolve into thinner frequency band and each resolution is twice the previous one. Brief about the MRA technique is given in next sub-section.

2.3.1.1 Multi-Resolution Analysis

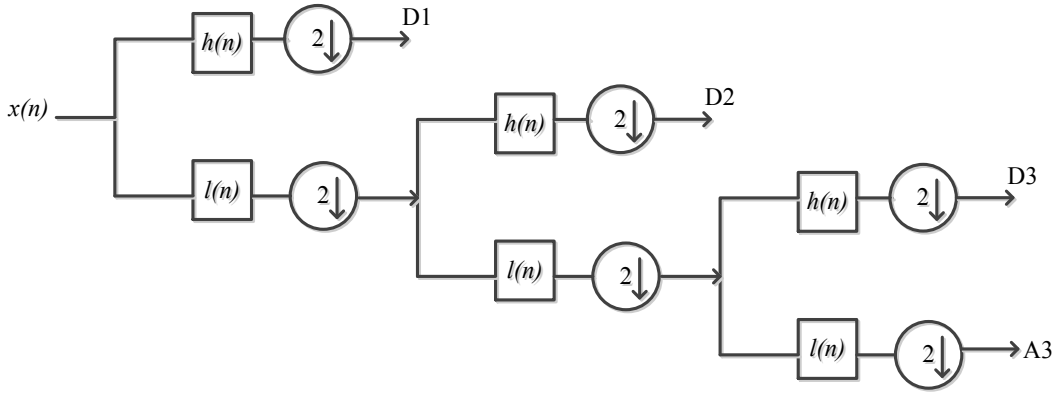

Fig. 2.5 Wavelet Multi-Resolution analysis [101].

MRA is a very useful implementation of DWT. In this analysis original sampled signal *x(n)* is passed through a high pass filter *h(n)* and a low pass filter *l(n)* as shown in Fig. 2.5 [169]. Then the outputs from both the filters are decimated by 2 to obtain the detail coefficients (*D1*) and the approximation coefficients (*A1*) at level one. The approximation coefficient is sent to the second stage to repeat the procedure for next level. Finally, the signal is decomposed at the expected level. In the case shown in Fig. 2.5, if the original sampling frequency of signal is *F*, the signal information captured by *D1* is a higher frequency band in between *F/4* and *F/2* at level 1. *D2* captures lower frequency band information in between F/8 and F/4 at level 2. *D3* captures the information between *F/16* and *F/8* and *A3* retains the rest of the information of original signal between 0 and *F/16*. In this study detailed coefficients *D1* to *D4*, at level one to four respectively are used for fault detection and classification algorithm [170].

2.3.2 Radial Basis Function Neural Network (RBFNN)

RBFNN is a feed-forward neural network which is trained by supervised learning algorithm. It has become a very dominant tool to many technical problems because of its collective approximation capability and fast learning speed. It is typically configured as three layers with a single hidden layer of units whose activation function is selected from a class of functions called basis functions. The numbers of nodes in input layer are same as the dimension of input vector. All the hidden layer nodes are directly connected to input layers nodes. The hidden layer basis function has a parameter center which can be represented by a vector of size same as input vector. The inputs to the hidden layer are the linear combinations of scalar weights and input vector $x = [x_1, x_2 \ldots x_n]^T$ where 'n' is number of input. Thus the input vector 'x' becomes the input to each neuron in the hidden layer. The incoming input vectors are mapped by the radial basis function in each hidden nodes. Each hidden node represents a single RBF and computes a Gaussian kernel function of 'x'. Gaussian kernel function is considered as activation function, as suggested in [171]. The radial distance 'd_i' between the input vector 'x' and the center of the basis function 'c_i' is computed for each unit 'i' in the hidden layer as using the Euclidean distance given by equation (2.4).

$$d_i = || x_i - c_i || \tag{2.4}$$

$\phi_i (x)$ is the hidden layer output of the i^{th} hidden node which can be given by equation (2.5) [172] as:

$$\phi_i(x) = \exp\left[-\frac{1}{2} \sum_{j=1}^{n} \frac{x_j - c_i^2}{\sigma_i^2} \right] \tag{2.5}$$

Where, c_i and σ_i denotes the center and width of the i^{th} hidden node respectively.

The output layer produces a vector $y = [y_1, y_2 \ldots y_m]$ for 'm' outputs by linear combination of the outputs of hidden nodes to produce the final output, which is given by equation (2.6).

$$y = \sum_{i=1}^{h} w_i \phi_i(x) \tag{2.6}$$

Where w_i denotes the hidden-to-output weight corresponding to the i^{th} hidden node and 'h' is the number of hidden nodes. In pattern classification applications the output of the radial basis function is limited to the interval (0, 1) by the sigmoidal function given by equation (2.7).

$$O_m(x)=\frac{1}{1+\exp[-y_i\ (x)]} \tag{2.7}$$

The structure of multi neurons three layered radial basis function neural network is shown in Fig. 2.6.

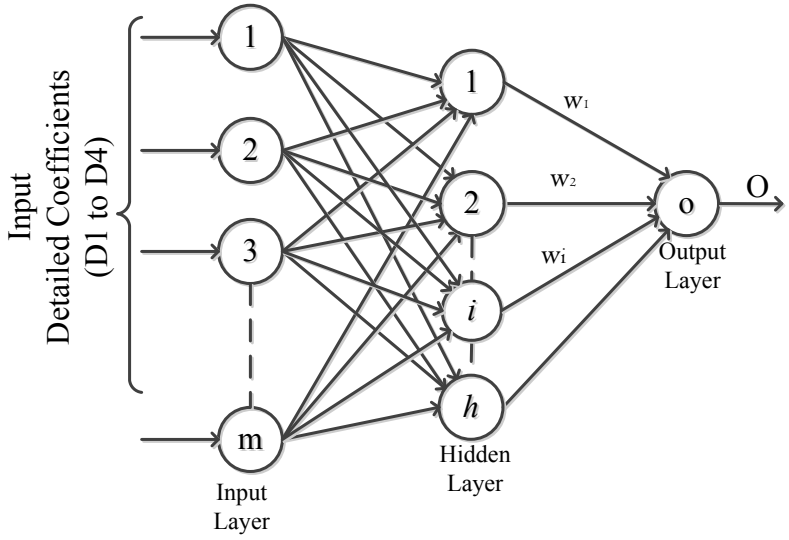

Fig. 2.6 Typical RBFNN structure

Generally, the Gaussian RBFNN training is performed as following:

i. *Pattern selection* – MRA detailed coefficients D1 to D4 at level four are selected as input pattern for RBFNN. Input patterns are sampled at 800 samples per cycle of 20ms. Patterns are given to neural network on the moving window scale of $1/16^{th}$, $1/8^{th}$ and $1/4^{th}$ cycle samples.

ii. *Data classification* – Total number of input patterns are 16500, out of which 70 % patterns are used for training and remaining patterns are used for testing and validation.

iii. Network selection – Neural network input neurons depends on the window size of input samples, which is tested on 50, 100 and 200 input neurons. Hidden layer neurons are optimized to reduce the training burden and one output neuron decides the classes.

iv. *Clusters selection* – Number of data clusters are taken as variable and minimize for the minimum permissible error in output.

v. Determine the optimal parameters of radial basis functions, i.e., Gaussian center and width or smoothing factor. Centers of the Gaussian function are determines by *K-means* clustering method [173]. Width of the Gaussian function for each hidden layer neuron is given by:

$\sigma = \frac{d_{max}}{\sqrt{2h}}$, where d_{max} is maximum distance between centers and 'h' is number of hidden layer neurons.

vi. Determine the output weight 'W' is given by:

$W = (\phi^T\phi)^{-1}\phi^T$ t, where 't' is target output which is chosen '0' for section-I fault and '1' for section-II fault.

vii. A threshold is applied at output layer which clearly set the output at 0 or 1.

2.3.3 Support Vector Machine

The SVM is a machine learning technique used for statistical classification and regression analysis. In classification task usually training and testing of data instances takes place. SVM constructs a number of hyper planes in a high dimensional space to separate data points which belongs to different classes. All the instances in the training set contains one target called 'level' and several attributed called 'features'. Hyper plane are obtained so that the maximum separating margin between the classes is achieved. A linear hyper plane is shown in Fig. 2.7, which separates two different classes denoted by stars and holes [174], [175].

Given a set of n dimensional training data $D = \{x_i, y_i\}$, i= 1, 2… N. N is the number of samples corresponding to class 1 and class 2, and $y_i \in \{-1, 1\}$, $x_i \in R^N$. Points x_i lie on the hyper plane $f(x) = 0$ which can separate the data in two classes. The hyper plane can be given by equation (2.8) [174], [175]:

$$f(x) = w^T x + \beta = 0 \tag{2.8}$$

Where, w is normal to the hyper plane and $|\beta|/||w||$ is perpendicular distance from the hyper plane to the origin. The optimal separating hyper plane shown in Fig. 2.7 can be defined as:

$f(x_i) \geq 1$ if $y_i = 1$ (class 1) and $f(x_i) \leq -1$ if $y_i = -1$ (class 2). These conditions can be combined in one set of inequalities as given by equation (2.9):

$$y_i f(x_i) - 1 \geq 0, \text{ or } y_i(w^T x_i + \beta) - 1 \geq 0, \text{ For i= 1, 2… } N \tag{2.9}$$

Computing the optimal hyper plane can be written as following optimization problem given by equation (2.10).

$$\text{Min } \left(\frac{1}{2}||w||^2 + C\sum_{i=1}^{N}\psi_i\right) \quad (2.10)$$

Where ψ_i is a measure of the degree of misclassification and C is error penalty. In the proposed algorithm, Radial Basis Function (RBF) has been considered as kernel function because it is advantageous in non-separable classification problem due to its ability of nonlinear input mapping. Performance of different kernel function based upon testing accuracy at data set of different location is shown in which suggests that RBF kernel is best suited for the required classification. RBF kernel required only one parameter, γ (γ = 1/2σ2, σ is kernel width), to adjust. SVM has been optimized for different value of 'C' and 'γ', typically selected value of C is 80 and γ is 0.0011.

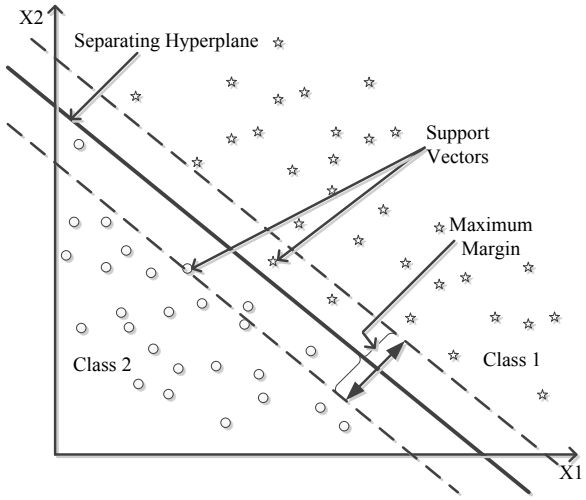

Fig. 2.7 A maximum margin hyper-plane separating two classes [93].

2.4 Proposed Section Identification Algorithm

Transmission line fault signal has various frequency signals up-to 80 kHz [168]. Any fault signal occurred before or after the FACTS device has different frequency spectrum because of the filtering by FACTS device itself. FACTS device filters the particular frequency band from the fault signal according to its inductance or capacitance value at that time (or according to its compensation level). In case of fix compensation, inductance or capacitance value inserted by FACTS device is constant therefore it can be claimed that particular frequency signals will be missing if fault occurred in section-II. But, in case of variable

compensation like TCSC or SVC, impedance inserted by the device is not constant so it is difficult to identify that which frequency band will be missing in frequency spectrum. Therefore to make transmission line protection system more reliable, it is necessary to find fault section clearly. For this purpose, a HPF is installed at the FACTS device location which surely filters the high frequency signals generated in section-II in case of fault. In case of fault in section-I, WT provides detail information about high frequency components whereas fault in section-II has less or no high frequency signals present.

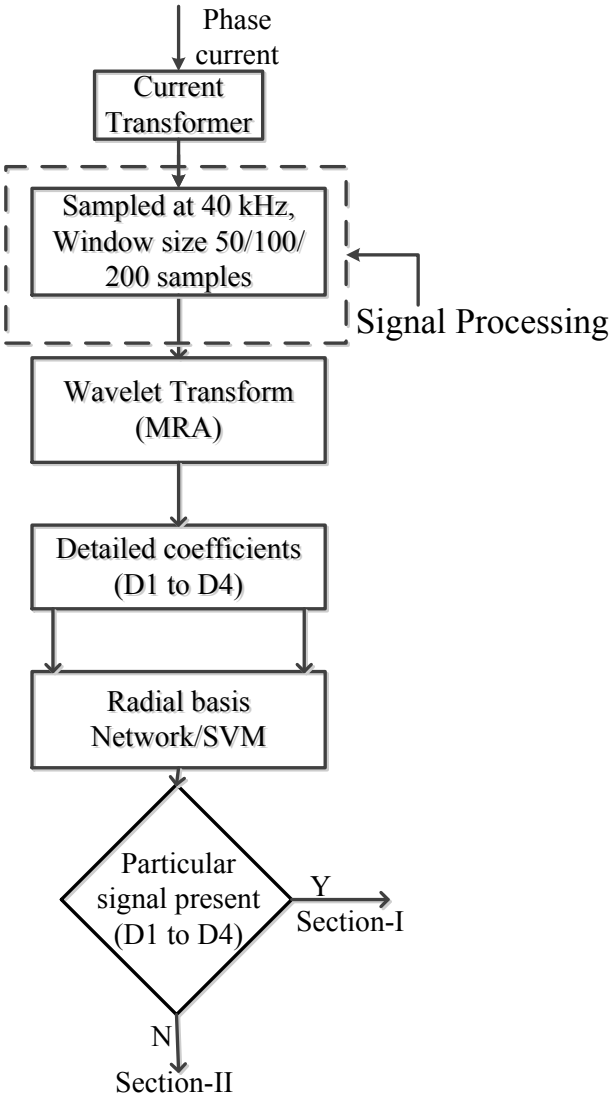

Fig. 2.8 Proposed fault section identification algorithm

One drawback of the WT is to its sensitivity for noise signals. Therefore to make relay performance less prone to noise signal a RBFNN/ SVM classifier is added to make section

identification algorithm more adaptive. RBFNN/ SVM has quality to classify two classes therefore it can classify the wavelet signals optimally for section-I or II faults.

Complete fault section algorithm is shown in Fig. 2.8. Current Transformer (CT) measures the input current at the relay bus. Parameters of CT are given in Appendix-B Table B.1. Wavelet based relay individually monitors all the three phase currents in healthy and faulty conditions. Sampling frequency is selected as 40 kHz and HPF cut-off frequency is 1 kHz, therefore, MRA decomposition has been selected up-to level four to analyze signals in between 1.25 kHz to 40 kHz. DWT decomposes the input current into the different frequency band (detailed coefficients D1 to D4) by MRA techniques. The output detailed coefficients are given as input to a RBFNN/SVM which decides whether the particular frequency signal is present or not in the fault current. If high frequency signals are present in the fault current, the section identification algorithm decides the fault occurred in the section-I, or, if they are absent, it decides as section-II.

2.5 Results and Discussion

To test the reliability and security of the proposed universal fault section algorithm for mid-point compensated transmission line, several power system operating conditions are considered. Several line faults are created on the both sides of compensator in the line and patterns are extracted by WT-MRA technique. Algorithm is tested for series as well as shunt mid-point compensated transmission line. Installation of HPF at the PCC removes the uncertainty in the filtering of high frequencies through compensator itself which improves the reliability of the algorithm. To advise the universality of the proposed algorithm, two different system voltages are taken as 230 kV and 400 kV, and both series and shunt compensated transmission lines are considered. Fig. 2.9 shows the MRA frequency patterns (D1 to D4) during faults conditions for section-I and section-II in the line having TCSC in Fig. 2.9 (a) and Fig. 2.9 (b) respectively. Results taken for 230 kV and 400 kV systems with 50 % compensation, illustrated in Fig. 2.9 and Fig. 2.10 respectively.

Similar results are taken for shunt compensated transmission line having SVC. Fig. 2.11 and Fig. 2.12 indicate the MRA decomposition results for 230 kV and 400 kV systems respectively for transmission line having SVC. Results are also taken for line with STATCOM shown in Fig. 2.13 and Fig. 2.14, respectively.

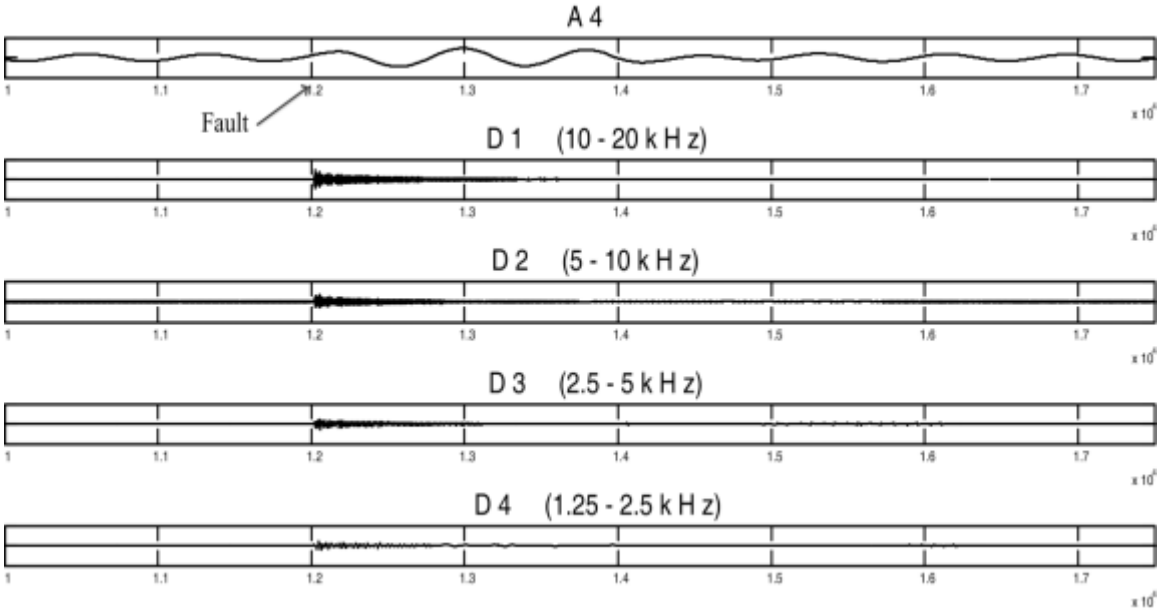

(a)

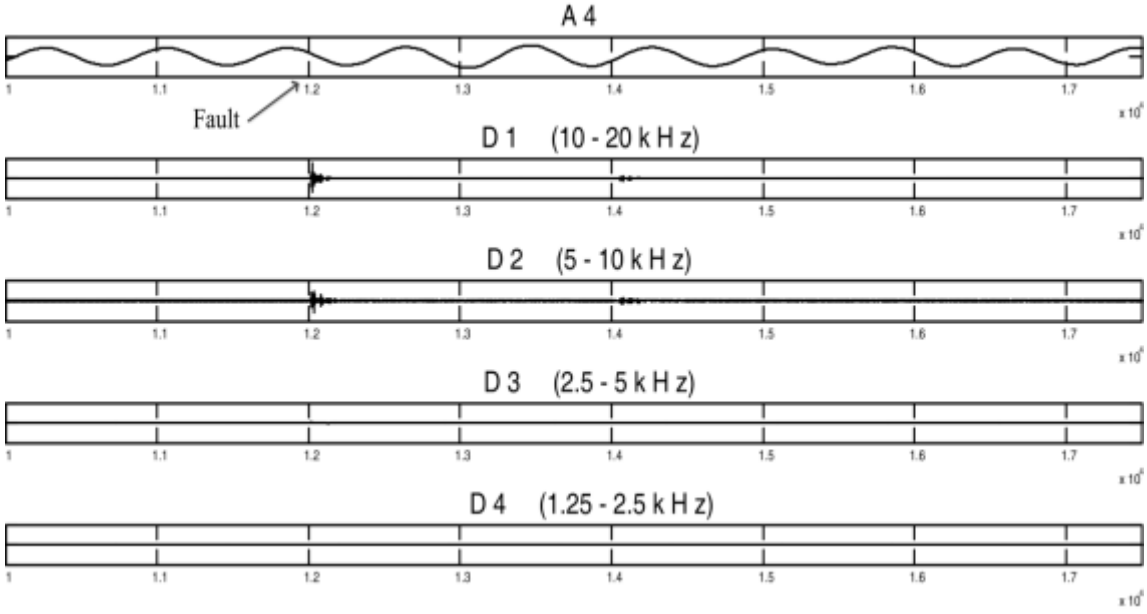

(b)

Fig. 2.9 MRA frequency patterns D1 to D4 for 230 kV systems and faults in section (a) I (b) II of TCSC line

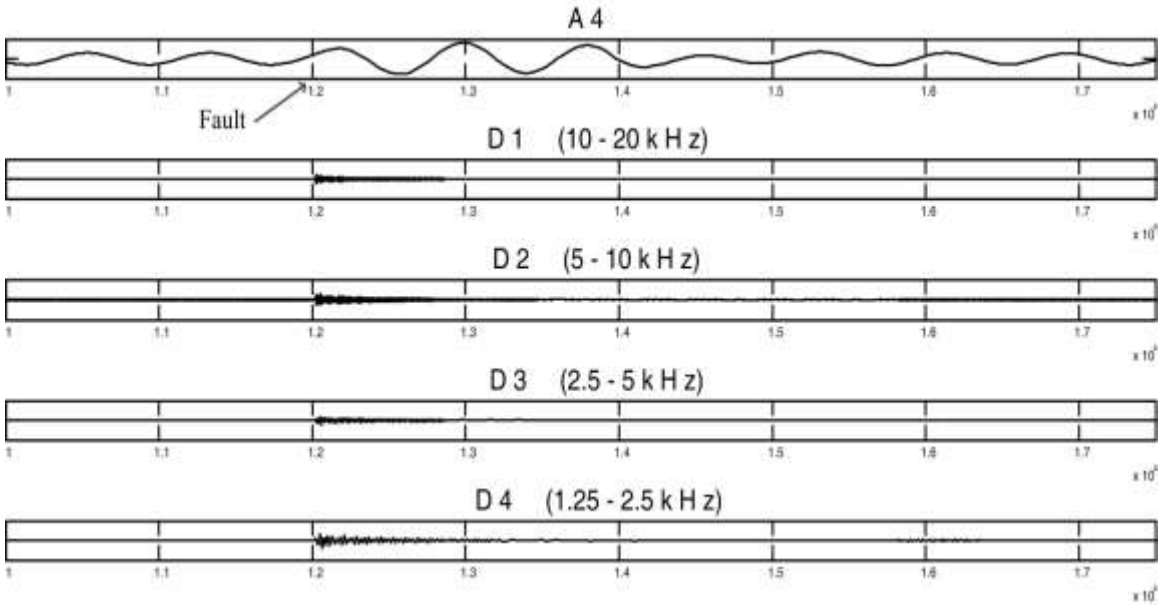

(a)

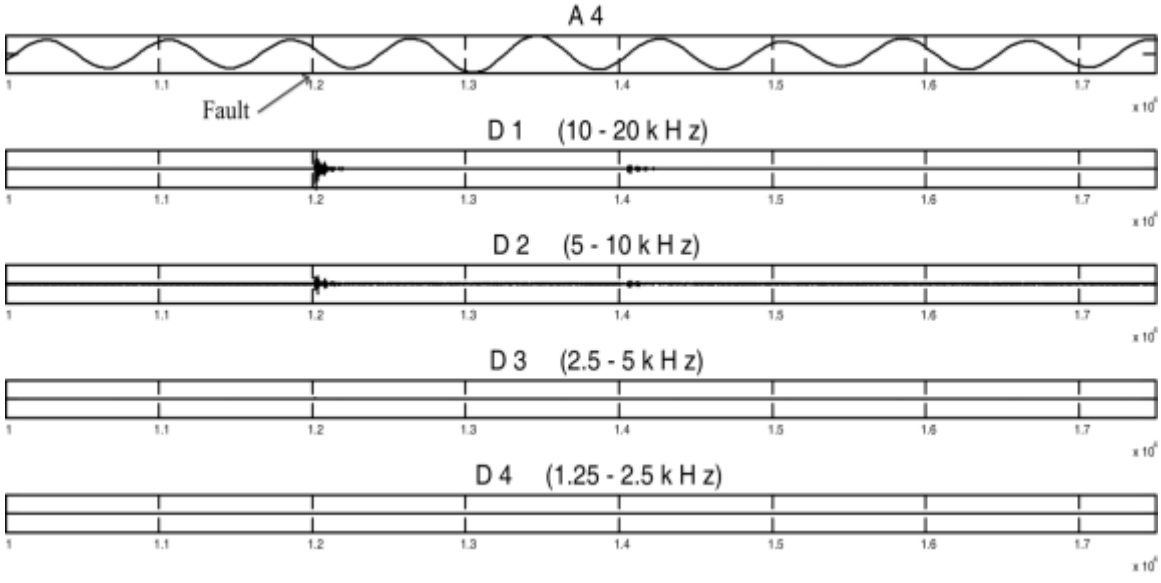

(b)

Fig. 2.10 MRA frequency patterns D1 to D4 for 400 kV systems and faults in section (a) one (b) two of TCSC line

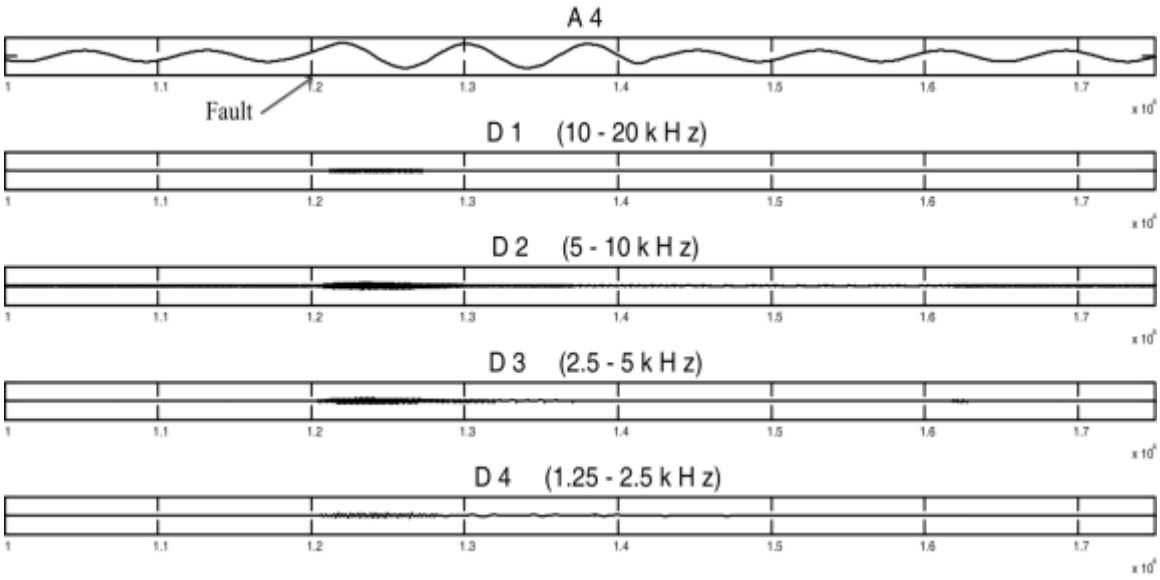

(a)

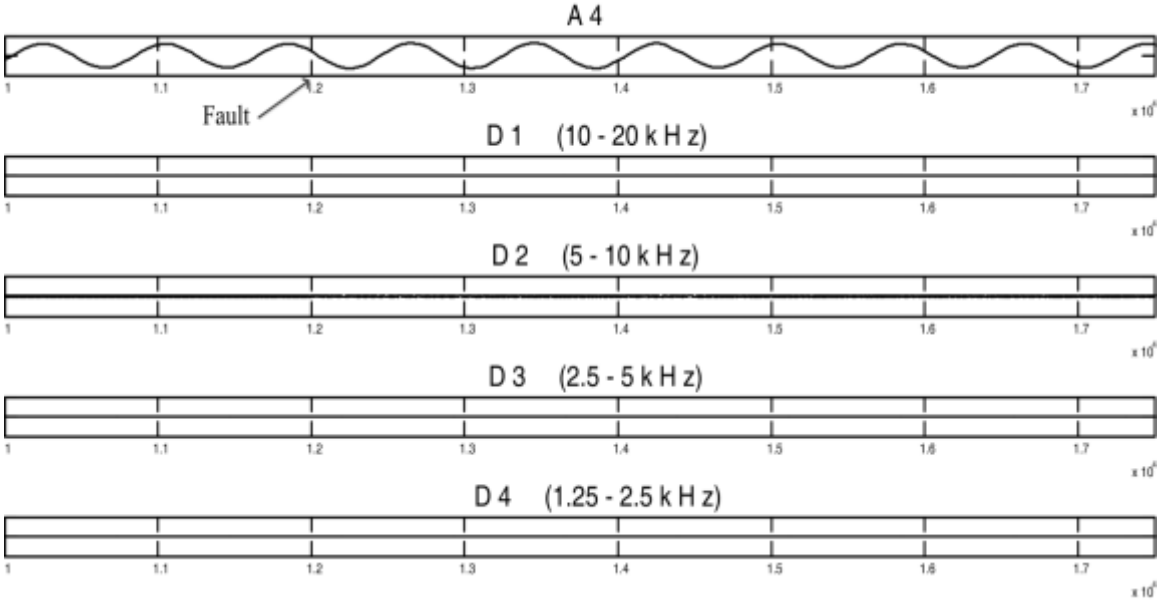

(b)

Fig. 2.11 MRA frequency patterns D1 to D4 for 230 kV systems and faults in section (a) I (b) II of SVC line

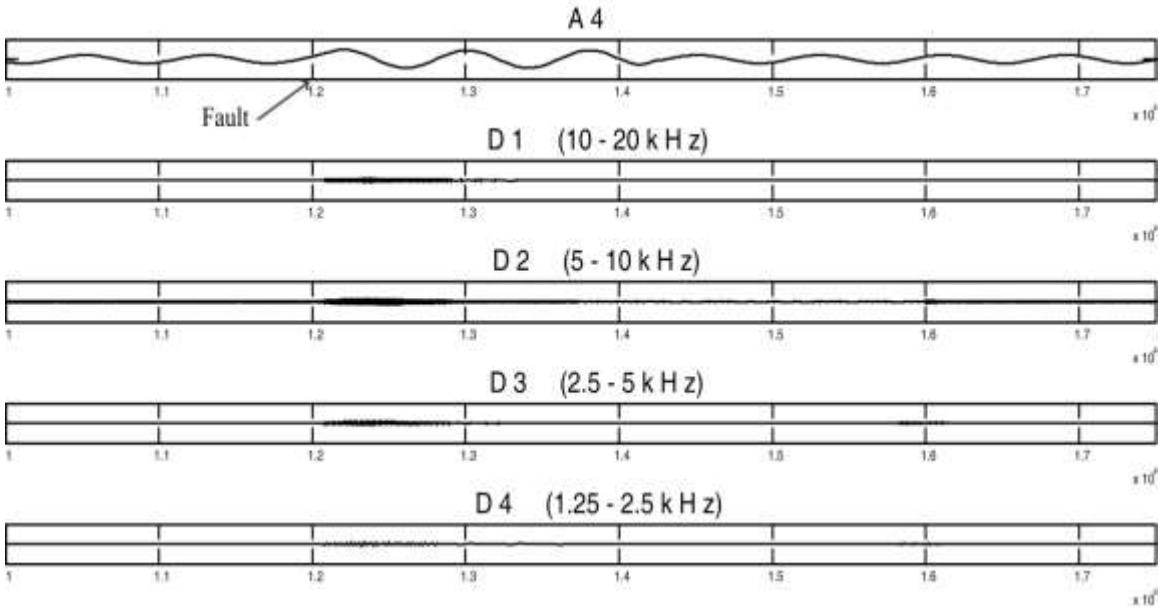

(a)

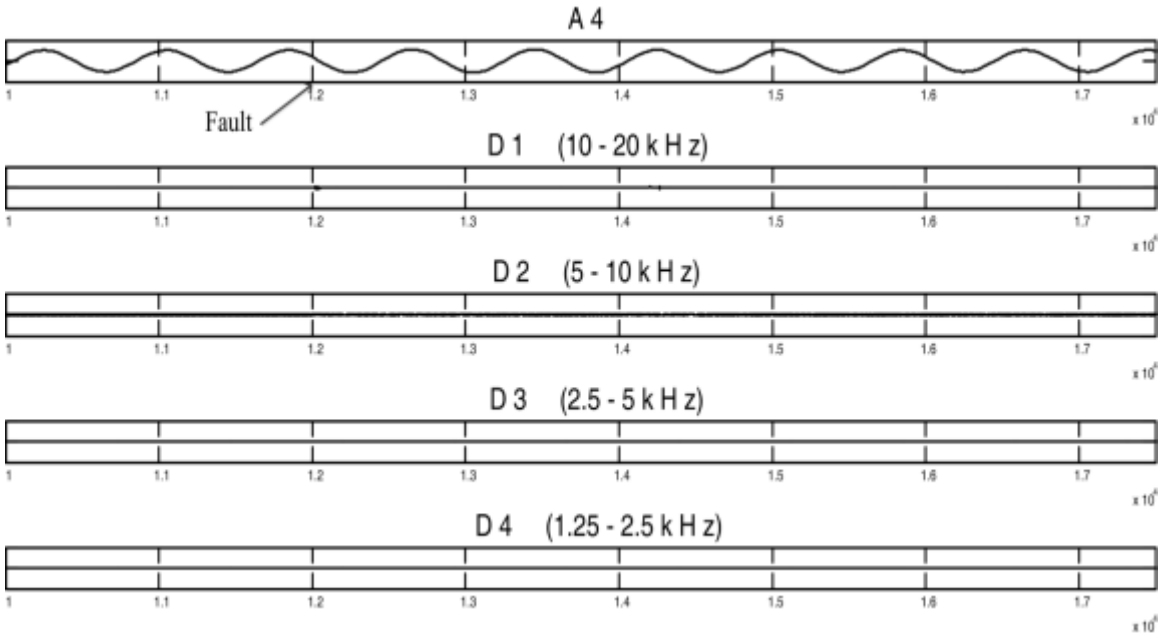

(b)

Fig. 2.12 MRA frequency patterns D1 to D4 for 400 kV line having SVC and fault in section (a) I (b) II of SVC line

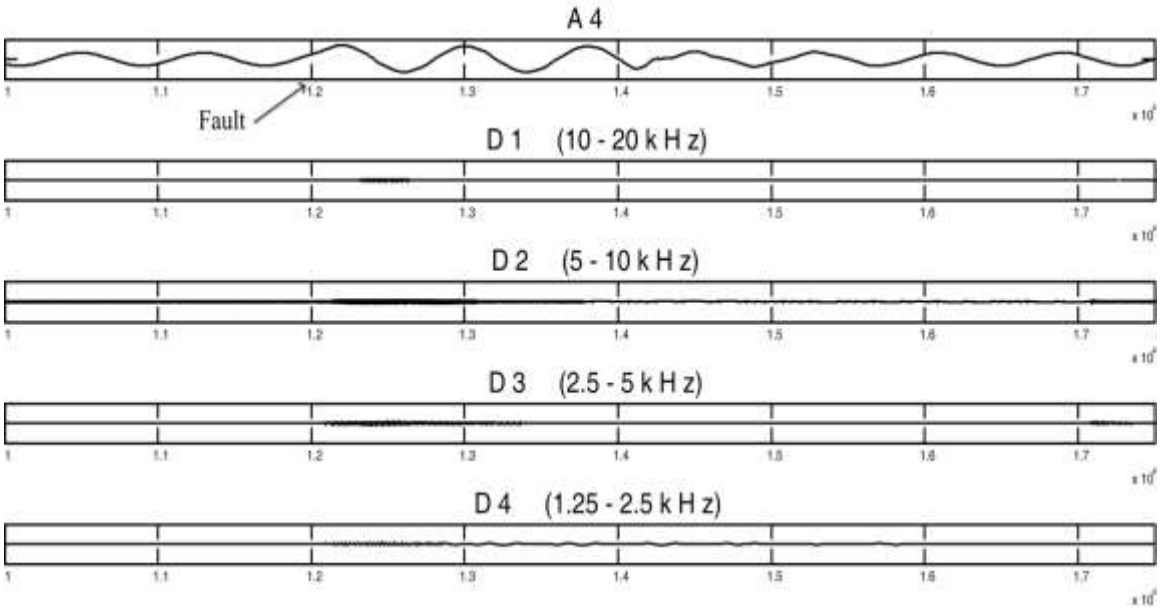

(a)

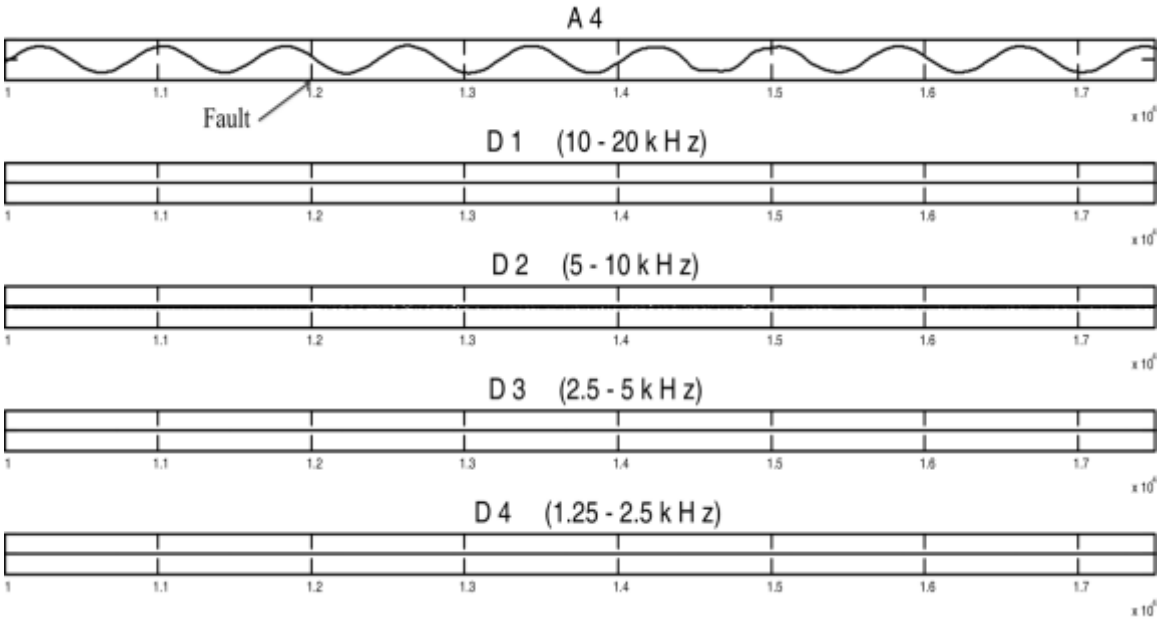

(b)

Fig. 2.13 MRA frequency patterns D1 to D4 for 230 kV line having STATCOM fault in section (a) I (b) II

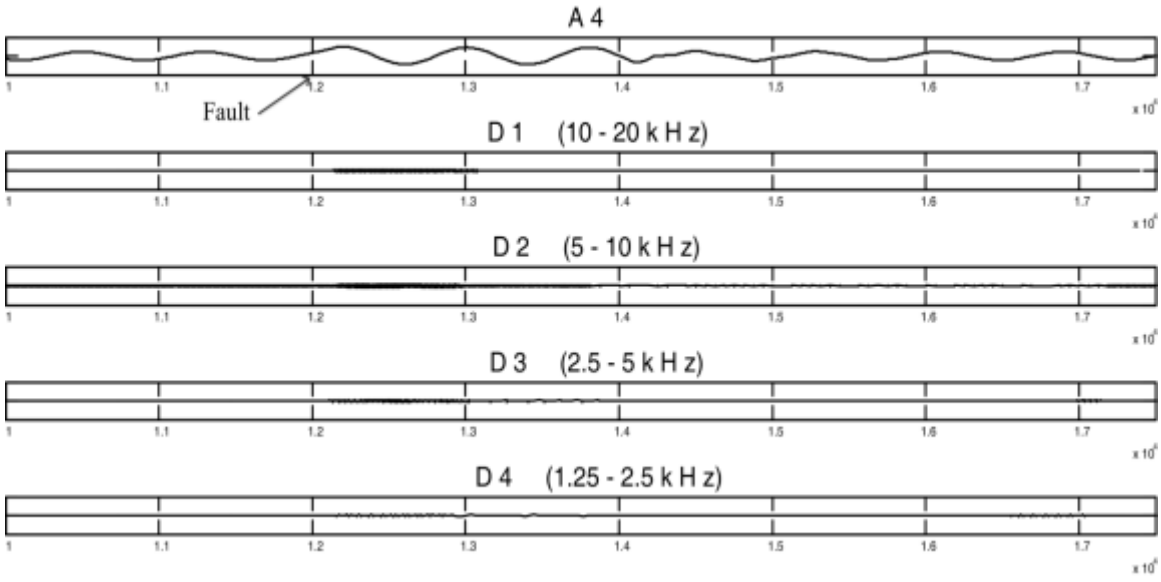

(a)

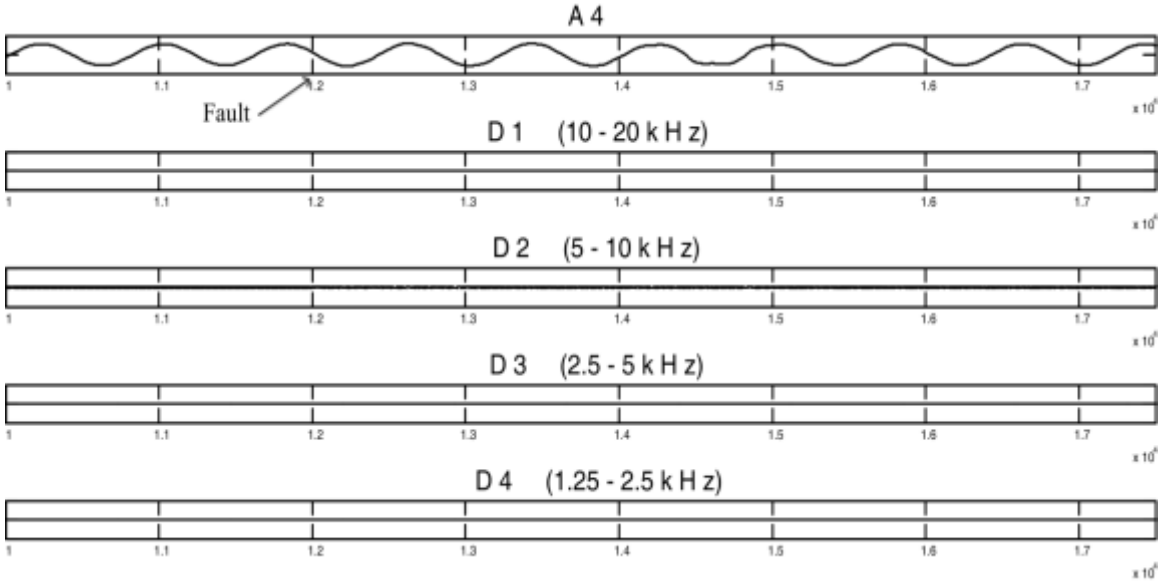

(b)

Fig. 2.14 MRA frequency patterns D1 to D4 for 400 kV line having STATCOM fault in section (a) I (b) II

It is clear from Fig. 2.9 to Fig. 2.14 that the magnitude of the high frequency components generated due to fault in section-I is higher than section-II. Regardless the system voltage, HPF filter out the high frequency components at the PCC and high frequencies amplitude are either missing or less in section-II faults. Radial basis network is trained by detailed coefficients to decide whether the fault in section-I or section-II. Magnitude of all the detailed coefficients from *D1* to *D4* in section-II is clearly less than the section-I; therefore out

of four patterns (*D1* to *D4*) any pattern can be used as input for SVM/ RBFNN. To provide the required training and testing data sets, various faults are created at several locations throughout the complete length of transmission line. The details of all the training combination are given in Table 2.1 as follows:

Table 2.1 Generated training conditions for RBFNN classifier

S. No.	**Operating fault conditions**	**Operating Values**
1	Fault resistance	0.1, 10, 50, 100 and 150Ω
2	Fault inception angle	0, 45, 60, 90 and 180^o
3	Load angle	10, 20, 30, 40 and 50^o
4	Fault type	AG, BG, CG, AB, BC, CA, ABG, BCG, CAG, and ABC
5	Voltage level	230 and 400 kV
6	Compensation level	TCSC- 3, SVC- 3, STATCOM- 1
7	Fault location	60, 120,150, 170, 240 and 300 km

Thus, total training data points generated at each location are 5*5*5*10*2*7= 17500 and total numbers of locations of fault taken for data generation are six so total numbers of training data patterns are 17500*6=105000. All the patterns are generated with TCSC, SVC and STATCOM test systems individually. The details of testing patterns for evaluating the classifier performance are given in Table 2.2.

Table 2.2 Generated testing conditions for RBFNN

S. No.	**Operating fault conditions**	**Operating values**
1	Fault resistance	0, 60, 100 and 160 Ω
2	Fault inception angle	20, 80, 120 and 150^o
3	Load angle	5, 35 and 45^o
4	Fault type	AG, AB, ABG, ABC and ABCG
5	Voltage Level	230 and 400 kV
6	Fault Location	50, 100, 225 and 275 km

2.5.1 Effect of Noise

In the proposed algorithm, per phase line current is measured at the receiving end which is associated with the 230 kV or 400 kV voltages. The most severe noise present in the transmission line is corona noise, which significantly affect the current or voltage signal. Corona effect is more severe at higher voltage level. Also the corona noise depends on weather conditions and it deteriorates in foul weather. Proposed algorithm has been checked for worst possible condition, if corona occurs in the 400 kV line in foul weather condition. In this condition corona generates the noise voltage up to 360 mV. For this condition Signal-to-Noise Ratio (SNR) is worse and the value can be calculated as: $SNR_{dB} = 20\log\left[\frac{A_{signal}}{A_{noise}}\right]$ where, A is amplitude and the SNR value found to be 120. SNRs are calculated for all weather conditions and possible noise voltage given in Table 2.3. One such case is shown in Fig. 2.15 with and without noise, respectively.

Table 2.3 SNR in transmission line in 400 kV line

Fair weather		**Foul weather**	
Noise voltage (mV)	**SNR**	**Noise voltage (mV)**	**SNR**
15	148	142	128
17	147	163	127
24	144	208	125
32	141	360	120

It is clear from the Fig. 2.15(a) and (b), that, there is no significant change in the MRA signals for worst noise case. It concludes that the large possible noise does not affect the MRA patterns hence the proposed universal fault section identification algorithm is immune to the noise. Further, this SNR has been added in all the 400 kV line patterns assuming that the worst condition is possible in all the cases and trained and tested with RBFNN/SVM which nullifies the possibility of any mal-operation.

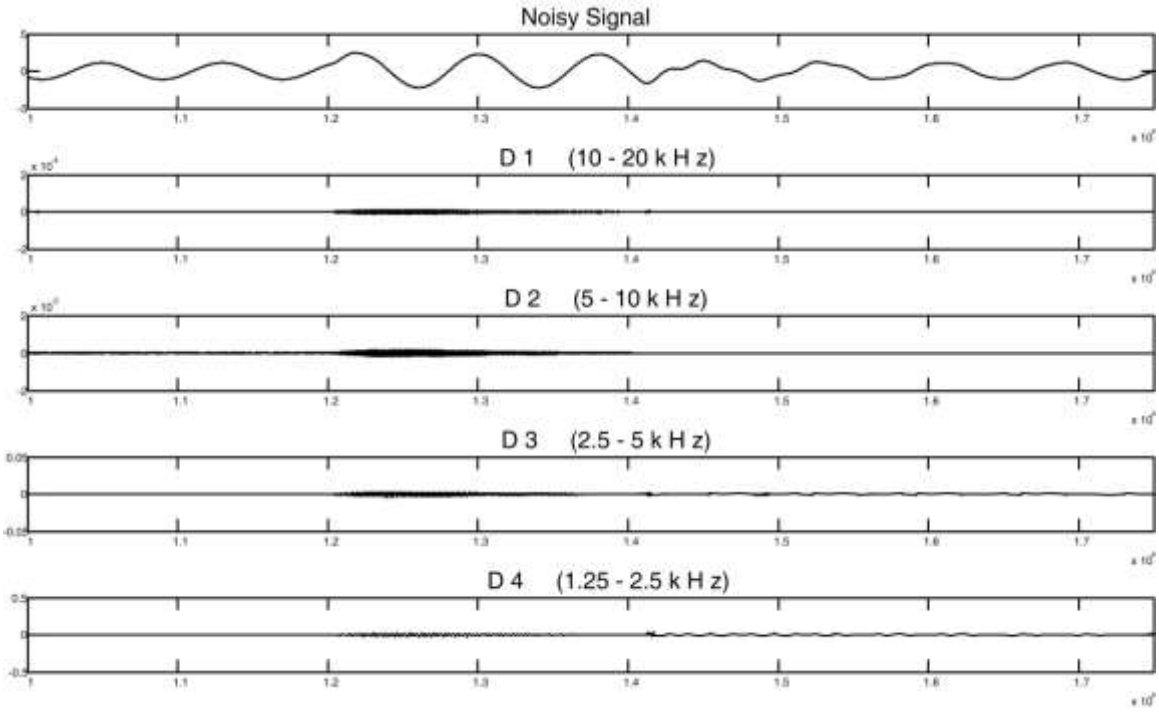

(a)

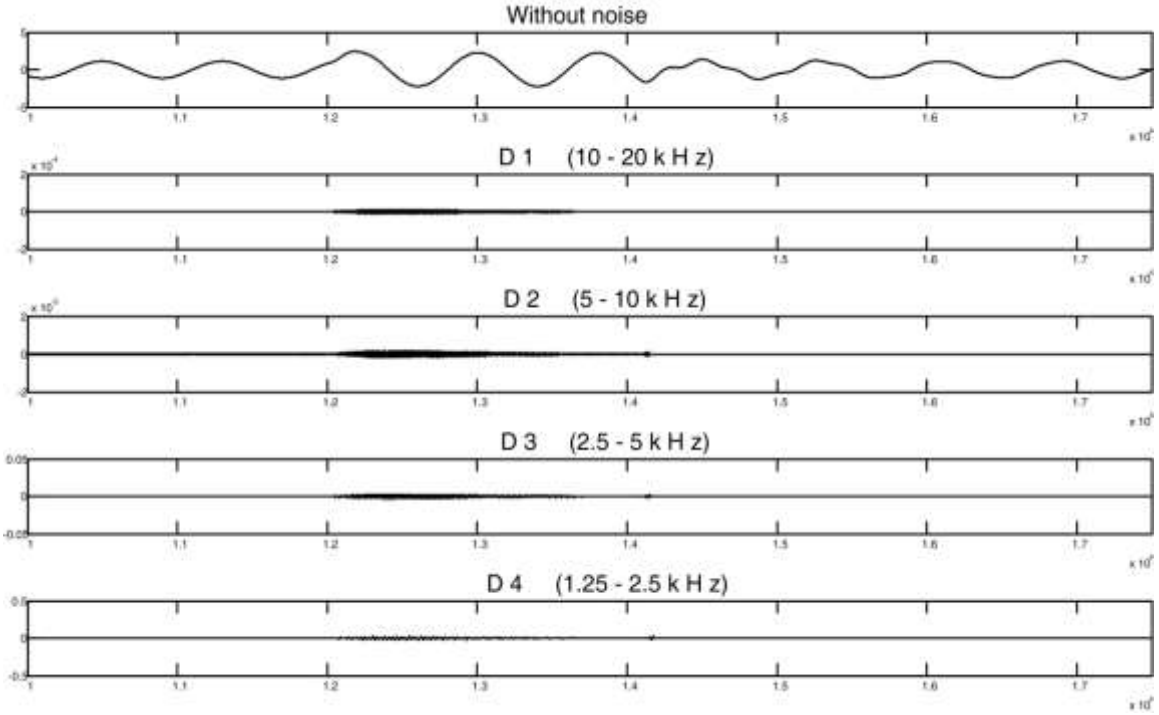

(b)

Fig. 2.15 MRA decompsition of fault current (a) With noise (SNR=120) (b) without noise

2.5.2 Performance Comparison and Accuracy

System frequency is 50 Hz and sampling frequency is chosen as 40 kHz such that per cycle samples are 800. RBFNN is tested for $1/16^{th}$, $1/8^{th}$ and $1/4^{th}$ cycle data with different

number of samples per cycle. Chosen sampling rate is best suited for the purpose and does not impose any memory burden or enormous error to the neural network. RBFNN is tested with all the detailed coefficients (*D1* to *D4*) and number of neurons in hidden layer kept as variable to adjust root mean square error within 0.01.

Performance of designed neural network with different window size as 50, 100 and 200 is shown in Table 2.4. It is concluded from Table 2.4 that the structure of neural network is optimum with detailed coefficient *D2*, with window size 100 sample i.e., the proposed algorithm is very fast and detect fault section within $1/8^{th}$ cycle time.

Table 2.4 RBFNN performance with detailed coefficients

Window Size	**Number of hidden layer neurons**			
	With D1	**With D2**	**With D3**	**With D4**
50	1538	1028	1087	874
100	408	**34**	49	76
200	59	54	42	53

Performance of neural network with *D2* is compared with *D1* and error is calculated with some input vector instances for window size 100 and 200 as shown in Fig. 2.16 (a) and Fig. 2.16 (b) respectively. Error trajectory amplitude with *D2* is found to be less than *D1* and it is concluded that with 100 samples window, error curve is smoother than 200 samples as shown in Fig. 2.16.

Final RBFN network is structured as 100 input neurons, 34 hidden layer neurons and one output. For section-I fault numerical '1' and for section-II faults numerical '0' is assigned. Sigmoidal function with a threshold of 0.5 at output layer adjusts the output value either at '1' or at '0'. Optimize neural network is tested with selected patterns and it is found that the neural network is nearly 99.9 % accurate as shown in Fig. 2.17.

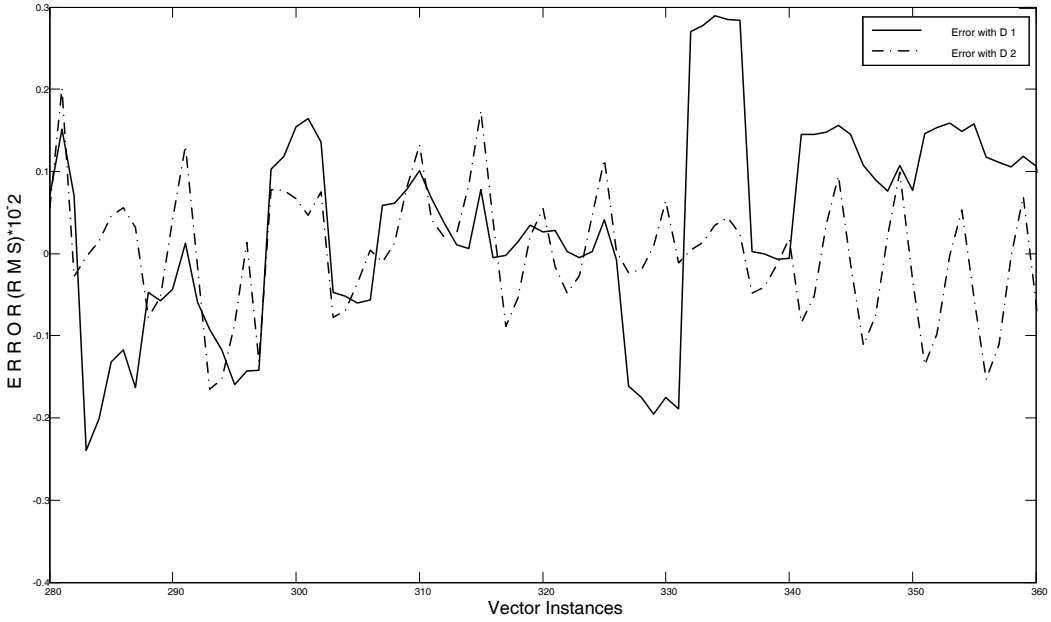

(a)

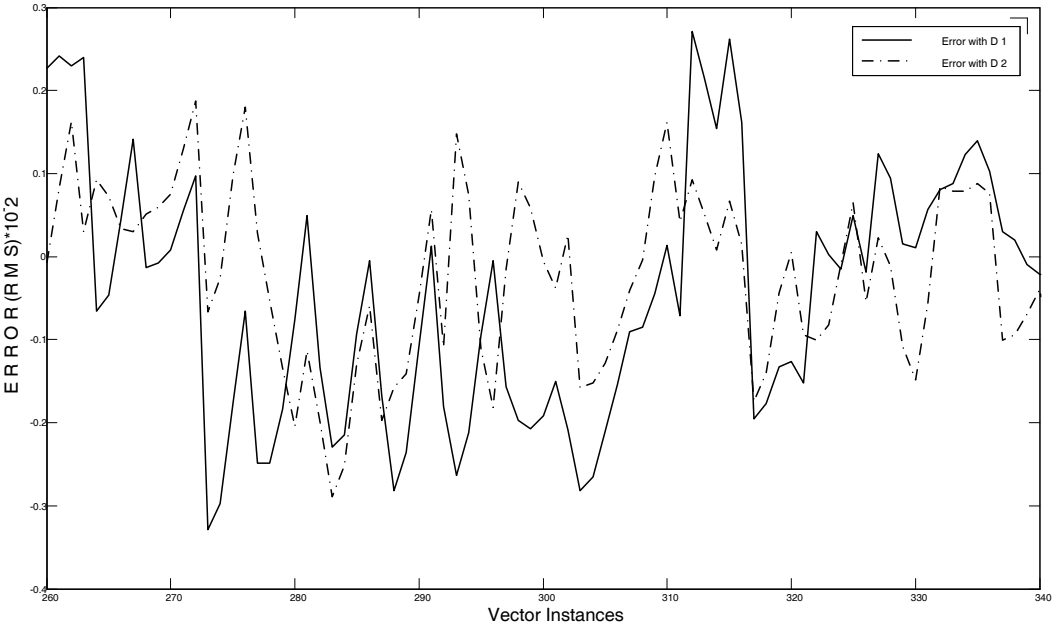

(b)

Fig. 2.16 Error curves (a) Window size 100 (b) Window size 200

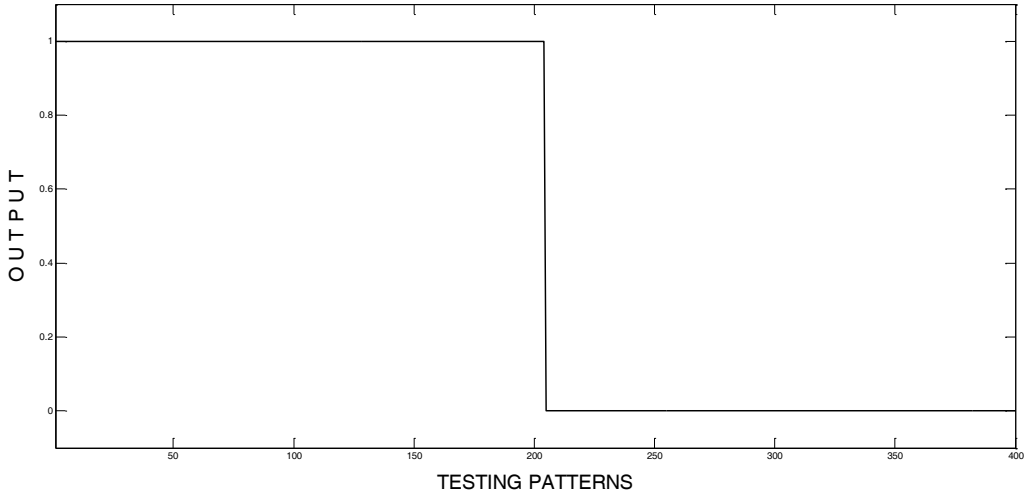

Fig. 2.17 Final output of RBFNN

From Table 2.2 total number of testing patterns at particular location can be calculated as 4*4*3*5*2 = 480. Testing patterns are generated in transmission line with all the compensator i.e. TCSC, SVC and STATCOM, therefore total testing patters at a location are 1440. After randomizing all the testing patterns 1000 patterns are taken to check the accuracy of SVM/ RBFNN which is given in Table 2.5.

Table 2.5 Classifier performance at different locations

S. No.	Testing location (km)	Accuracy		Training Time (sec)	
		RBFNN	SVM	RBFNN	SVM
1	50	100	100	125	38
2	100	99.8	99.9		
3	225	99.7	99.9		
4	275	99.9	100		

Possibility of misclassification of fault section in mid-point compensated transmission line gradually decreases at different stages. Application of HPF at mid-point creates a major difference in section-I and section-II fault patterns. In the next stage, WT-MRA confined the various frequency features for analysis on which the decision can be taken. In last stage, RBFNN/SVM learned all the conditions adaptively classify the fault section with the possibility of minimum error.

2.6 Summary

Fault section identification is the primary step for the protection of mid-point compensated transmission line, so, it should be reliable and secure. In this chapter, a novel fault section identification algorithm is proposed for all types of mid-point compensated transmission line and the algorithm is tested at voltage level of 230 kV and 400 kV, respectively. The proposed algorithm independently works for the line parameters and the mode of operation of compensator. A HPF is installed at the PCC, which filter out all the high frequency components (above 1 kHz), generated during fault in transmission line. DWT-MRA is found to be a powerful tool which breaks fault current into different frequency bands. RBFNN/SVM analyzes the different frequency bands to take decision whether the fault occurred in section-I or II. The technique has the advantage of cascade filtering at different stages and benefit of adaptive learning which reduce the error. The proposed algorithm is tested for wide variation in power system parameters, fault locations, fault types and different compensation levels of series (TCSC) and shunt compensators (SVC/STATCOM). The combined WT-SVM/RBFNN techniques successfully classify the fault section with 99.9 % accuracy.

In this chapter fault section has been successfully identified for mid-point compensated transmission line. After the identification of fault section, next task is the protection of line and the estimation of fault location which has been discussed in next chapters. Chapter-3 discuss about the adaptive protection of mid-point series compensated transmission line.

CHAPTER 3

SERIES COMPENSATED TRANSMISSION NETWORK PROTECTION

Development of accurate and secure protection algorithm for transmission line having thyristor controlled series compensator (TCSC) is a challenging task for protection engineer. This chapter presents an advance compensated Mho relay for the protection of the transmission line having TCSC. The main advantage of the scheme is that TCSC impedance is calculated for the entire operating range of thyristor firing angle in capacitive and inductive mode of operation that make it a versatile algorithm. Protective MOV/ spark gap impedance is modeled in terms of relay current separately. Finally, combined impedance of TCSC and its transmission line protection system is calculated at the relay bus that is used to calculate actual fault impedance. Extensive simulation studies indicate that the proposed relay does not exhibit any mal-operation so it is reliable, accurate and secure under capacitive and inductive modes of operations.

3.1 Introduction

FACTS technology opens up new opportunity for controlling power and enhancing the usable capacity of existing and upgraded lines [1], [3]. FACTS device comprises of power electronic devices like Thyristor, GTO (Gate turn-off Thyristor) and IGBT (Integrated Gate Bipolar Transistor). One of the main thyristor controlled FACTS device is TCSC, which can control power flow by controlling its impedance. TCSC is a combination of Thyristor Controlled Reactor (TCR) connected across a series capacitor. In modern power system, TCSC transmission lines are employed to enhance power transmission capability of transmission line, improvement in system stability, reduction in transmission losses and more power flow control. However, the presence of TCSC in transmission line introduces reaching problems (distance measurements) and that affect Mho relay functionality. The overhead transmission lines are more prone to shunt fault. Mho distance relays are widely used for the protection of uncompensated and compensated transmission lines. TCSC badly affects accuracy, selectivity and reliability of Mho relay, which leads to an unsecure power system [14]. It is responsible for mal-operation of Mho relays, particularly the reaching characteristic of the relay. In TCSC transmission line, reach measurement by distance relay depends upon the status of the TCSC impedance which is varying in nature. The varying nature of impedance inserted by TCSC in

the line creates under-reaching and over-reaching at the relay point in inductive and capacitive modes respectively and that is a challenge to the protection engineer[22].

Recently a lot of work has been done on methods to overcome the adversities that arise in the protection of transmission lines due to the presence of TCSC. In literature, Artificial Intelligence (AI) based techniques like Artificial Neural Network (ANN) and Fuzzy are suggested for protection of TCSC transmission line. Composite technique like wavelet-fuzzy approach is advantageous in terms of feature extraction from current signal [103], [104]. In these techniques, separate AI based relays are used to detect healthy or faulty conditions for each phase and ground conductor. ANN based relay has some limitations in classification accuracy such as multiple optimum solutions, dependability on input space and it follows heuristic path [69], [73], [78]. To improve accuracy, SVM is used for fault detection and classification in series compensated transmission line [93], [94]. The Wavelet Transform (WT) based techniques have some advantageous such as simultaneous localization in time and frequency domain, computationally very fast and ability to separate the fine details in a signal but they are affected by noise content present in the signal [98], [99]. Adaptive compensation based relay are successful for the purpose as they calculate on-line the voltage across series compensated device and compensate it at relay location when the faults occurs [108]. An expensive differential current protection method (DCPM) is found to be an alternate way to protect compensated lines [176], [160]. Some other adaptive protection schemes have also been proposed in literature, but they are true only for some fixed degree of compensation so the accuracy and reliability of these relays is not satisfactory [111], [113], [126]. To overcome all the above mentioned difficulties an adaptive Mho relay algorithm is proposed in this chapter which protects the mid-point series compensated line in all possible operating conditions.

3.2 Test System

A typical 230 kV, 50 Hz, power transmission line having TCSC is considered to develop and test the capability of the proposed compensated Mho relay protection algorithm. Test system is shown in Fig. 3.1, it consists of two sources connected through a 320 km transmission line. Parameters of the source have been given in Appendix-A. Per km sequence impedances of transmission line in ohms are as: $Z1$ = 0.035+j0.507, $Z2$ = 0.035+j0.507 and $Z0$ = 0.363+j1.32. TCSC is placed at 160 km from the sending end generator, which compensate the transmission line in between 0- 50 % [158], [167]. Zone-1 impedance setting of the Mho

relay is 85 % of transmission line impedance, i.e. Z_{set} = 138.227 Ω. Distance relay monitors phase voltage and line current through a Coupled Capacitor Voltage Transformer (CCVT) and Current Transformer (CT) respectively [134], [177]. Parameters of the CCVT and CT are given in Appendix-B.

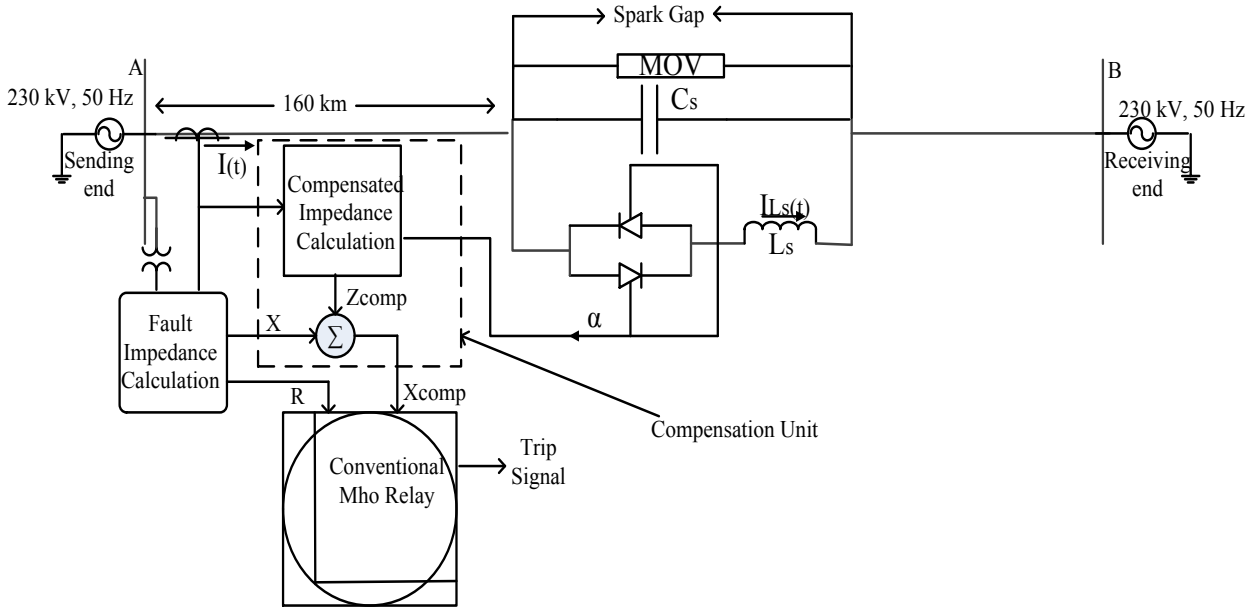

Fig. 3.1 Typical single line diagram of test system

During line fault condition, MOV protects TCSC from high current; again, a spark gap protects MOV from excessive energy conditions if the fault last longer. A fast and reliable communication channel exist between bus 'A' and TCSC point to transmit the thyristor firing angle (α) from TCSC substation to the Mho relay compensation unit at bus 'A'. CT measured current is another input to compensation unit, which is used to measure MOV/spark-gap resistance. In compensation unit, equivalent impedance inserted by the TCSC in the transmission line is calculated and subtracted from the measured impedance (Z). TCSC compensates the transmission line in both healthy and faulty conditions by this compensated impedance (Z_{comp}). Individual modeling of MOV/spark-gap and TCSC is as follows:

3.2.1 MOV Modeling

MOV is set to protect TCSC from high current faults like fault near TCSC or three phase faults with less fault resistance. MOV is connected across TCSC (Fig. 3.2(a)) and it bypasses the excessive energy when it reaches above a pre-set value. MOV is a non-linear

resistance that shows high resistance for low current and low resistance for high current. MOV used to protect TCSC, is modeled according to maximum current rating of thyristor and set to follow the impedance curve as shown in Fig. 3.2(b).

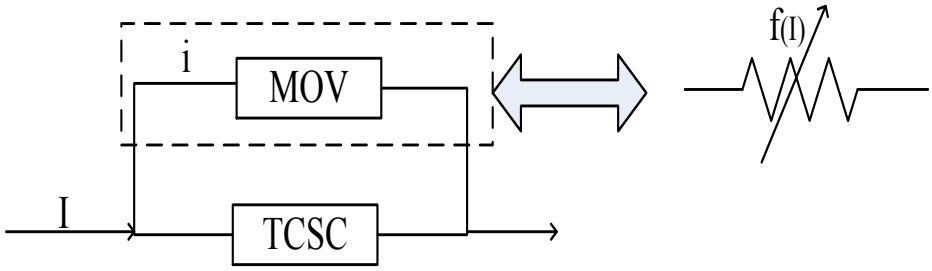

(a)

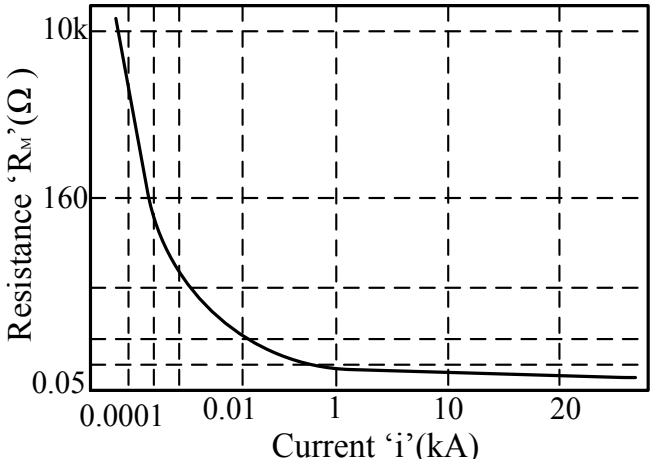

(b)

Fig. 3.2 (a) MOV symbolic model (b) Impedance curve of MOV

In literature, the work related to the impedance modeling of TCSC give a combined picture of TCSC and protective MOV, which is not suitable for complete possible firing angle range of thyristor. Extensive simulation attempts taken to find out the relation between MOV resistance and current measured at CT terminals. Different voltages greater than the rated (one per-unit) voltage (V_M) is applied across MOV in transmission line and corresponding MOV current (i) and CT current (I) are measured. V_M and i calculate impedance trajectory of MOV, and finally a relation given by equation (3.1) has been developed in between MOV resistance (R_M) and CT current (I) by using MATLAB curve fitting tool. Under normal operating conditions or below rated current, MOV does not operate and behaves like open circuit and above the rated current or in fault condition, its resistance can be given by equation (3.1).

$$R_M(I) = a * I^b \tag{3.1}$$

Where, coefficients of MOV in equation (3.1) are:

$a = 1.036*10^8$

$b = -3.315$

3.2.2 TCSC Modeling

An elementary single-phase TCSC is shown in Fig. 3.3(a). It consists of a fixed capacitor (C_S), shunted through Thyristor Controlled Reactor (TCR). Current in TCR can be controlled from maximum to zero by the method of firing angle delay control.

TCSC is generally operated in four different modes which are as follows: [1-2]

(i) Capacitive Boost Mode *($\alpha_{Clim} < \alpha < \pi / 2$)*

(ii) Inductive Boost Mode *($0 < \alpha < \alpha_{Llim}$)*

(iii) Bypass Mode *($\alpha = 0$)*

(iv) Blocking Mode *($\alpha = \pi/2$)*

Complete range of α for capacitive and inductive compensation is shown in Fig. 3.3(b). When the gating of the valve is delayed by an angle *α ($0 \leq \alpha \leq 90$)* with respect to the peak of driving line voltage *V(t)* which can be expressed as:

$$V(t) = V_m \cos(\omega t) \tag{3.2}$$

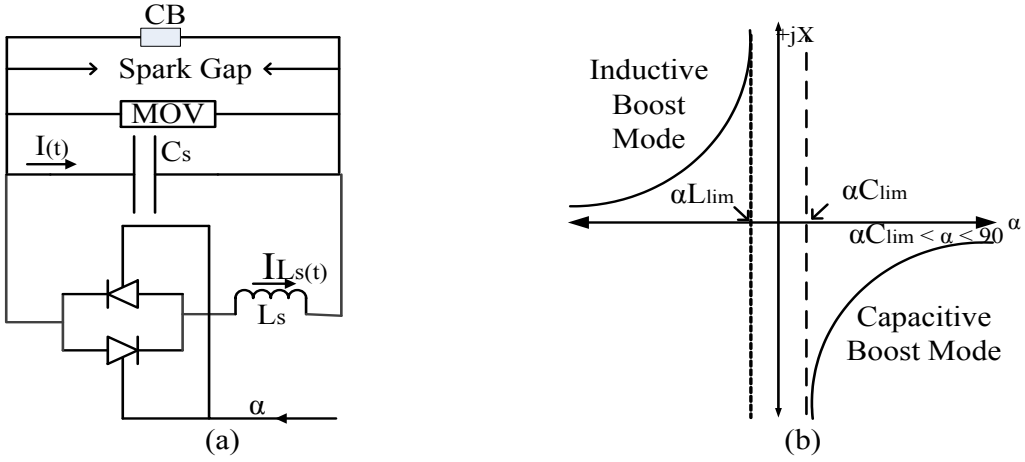

Fig. 3.3 TCSC (a) model (b) Operating characteristic [1-3]

Current I_{Ls} *(t)* in the reactor depends on angle α and expressed by equation (3.3) as:

$$I_{Ls}(t) = \frac{V_m}{\omega L_s} \int_{\alpha}^{\omega t} \cos(\omega t)\ \mathrm{d}(\omega t) \tag{3.3}$$

Fundamental component of the reactor current is given by equation (3.4) and equation (3.5):

$$I_F = \frac{2}{\pi} \int_{\alpha}^{\pi-\alpha} I_{Ls}(t) sin(\omega t) d(\omega t) \tag{3.4}$$

$$I_F = \frac{V_m}{\omega L_s} \left[\frac{\pi - 2\alpha - \sin(2\alpha)}{\pi} \right] \tag{3.5}$$

Equivalent reactance of inductor and a series connected bidirectional switch is a function of α and can be calculated from equation (3.6) as:

$$X_L(\alpha) = \frac{V_m}{I_F} = X_{Ls} \left[\frac{\pi}{\pi - 2\alpha - sin(2\alpha)} \right] \tag{3.6}$$

Where, $X_L = \omega L_s$

Steady-state impedance (X_{TCSC}) of the TCSC is that of the parallel LC circuit, consisting of a fixed capacitor having reactance X_{Cs}, and a variable inductance having reactance $X_L(\alpha)$. Impedance inserted by TCSC is equivalent to compensated impedance (X_{comp}) which is given by equation (3.7):

$$X_{comp}(\alpha) = \frac{X_{Cs} * X_L(\alpha)}{X_L(\alpha) - X_{Cs}} \tag{3.7}$$

Where, $X_{Cs} = \frac{1}{\omega C_s}$

Therefore, from equations (3.1) and (3.7) resultant compensated impedance (Z_{comp}) of TCSC and its protective circuit can be defined under following discrete equation (3.8).

$$Z_{comp} = \begin{Bmatrix} X_{comp}(\alpha), \textit{ for low current faults, } I < 1.1(pu) \\ R_M(I) \parallel X_{comp}(\alpha), \textit{for high current faults, } I > 1.1\ (pu) \\ \sim\ 0, \textit{ for spark gap flashover} \\ 0, \textit{ for breaker bypass} \end{Bmatrix} \quad (3.8)$$

Similarly, the compensated impedance of fixed series capacitor protected through MOV can be given by equation (3.9):

$$Z_{comp} = \begin{Bmatrix} X_{CS}, \textit{ for low current faults, } I < 1.1(pu) \\ R_M(I) \parallel X_{CS}, \textit{for high current faults, } I > 1.1\ (pu) \\ \sim\ 0, \textit{ for spark gap flashover} \\ 0, \textit{ for breaker bypass} \end{Bmatrix} \quad (3.9)$$

Z_{comp} is a complex number, which real portion indicates the resistance inserted by TCSC into the line. Imaginary portion of Z_{comp} shows the compensated reactance of TCSC that is positive for inductive mode and negative for capacitive mode of TCSC.

3.3 Compensated Mho Relay

Adaptive relay algorithm is achieved by calculating the error inserted by TCSC/ ASC into the fault impedance and compensated it from the gross fault impedance. Such algorithm is modification of Mho relay by adding a compensation unit in it. Following are the steps for constructing a compensated Mho relay algorithm.

3.3.1 Apparent Impedance Calculations

In conventional Mho relay algorithm the equivalent fault impedance at bus 'A' can be calculated by equation (3.10) [11]:

$$Z = \begin{Bmatrix} \dfrac{V}{I + \mathrm{k}\, I_0}, \text{ For LL fault} \\ \dfrac{V_{1s} - V_{2s}}{I_{1s} - I_{2s}}, \text{ For LL fault} \end{Bmatrix} \quad (3.10)$$

Where, $k = \dfrac{Z_0 - Z_1}{Z_1}$

V and I are the phase voltage and current, respectively.

Z_0 and Z_1 are the zero and positive sequence impedances, respectively.

V_{1s} and V_{2s} are positive and negative sequence voltage respectively.

I_{1s} and I_{2s} are positive and negative sequence current respectively.

I_0 is zero sequence component of fault current.

Fig. 3.4 shows the sequence diagram of TCSC transmission line for LG fault at '*n*' per unit length from the bus 'A'. It is assumed that fault occurred at right side of the TCSC (section-II).

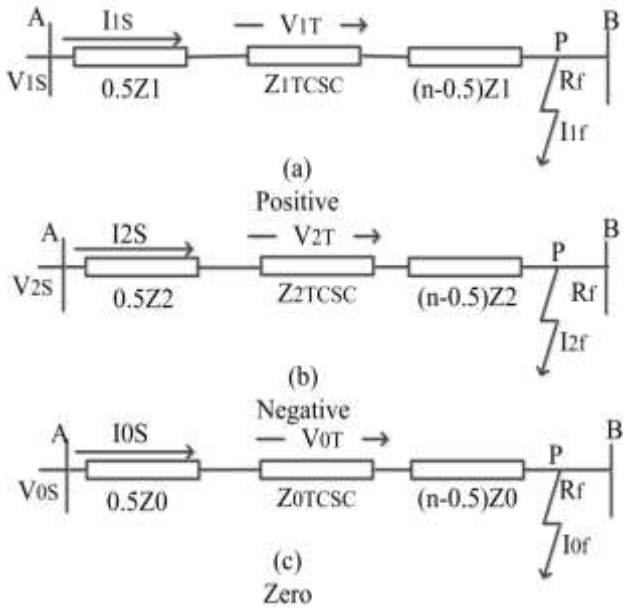

Fig. 3.4 Sequence network of the system during LG fault (a) Positive (b) Negative (c) Zero

Where,

I_{1s}, I_{2s} and I_{0s} are the sequence currents during fault.

V_{1T}, V_{2T} and V_{0T} are the sequence voltages across TCSC during fault.

I_{1f}, I_{2f} and I_{0f} are fault currents through fault resistance R_f.

The sequence voltages at the relay point can be expressed as equation (3.11) to equation (3.13) respectively.

$$V_{1s} = 0.5\, I_{1s}\, Z_1 + V_{1T} + I_{1s}\,(n - 0.5)\, Z_1 + I_{1f} R_{1f} \tag{3.11}$$

$$V_{2s} = 0.5\, I_{2s}\, Z_2 + V_{2T} + I_{2s}\,(n - 0.5)\, Z_2 + I_{2f} R_{2f} \tag{3.12}$$

$$V_{0s} = 0.5\, I_{0s}\, Z_0 + V_{0T} + I_{0s}\,(n - 0.5)\, Z_0 + I_{0f} R_{0f} \tag{3.13}$$

Total voltage at the relay point can be calculated by equation (3.14):

$$V_s = V_{1s} + V_{2s} + V_{0s} \tag{3.14}$$

Therefore, from equation (3.11) to (3.14) relay bus voltage and current can be given by equation (3.15) and (3.16), respectively:

$$V_s = nI_sZ_1 + nI_{0s}\left(Z_0 - Z_1\right) + V_T + R_fI_f \tag{3.15}$$

$$I_{\text{relay}} = I_{\text{s}} + \frac{Z_0 - Z_1}{Z_1} I_{0\text{s}} \tag{3.16}$$

Therefore, apparent equivalent impedance (Z_{eq}) at relay point can be calculated as given by equation (3.17):

$$Z_{eq} = \frac{V_s}{I_{\text{relay}}} = (\text{n}\, Z_1) + \left(\frac{V_T}{I_{\text{relay}}}\right) + \left(\frac{R_f I_f}{I_{\text{relay}}}\right) \tag{3.17}$$

Similarly, for LL (line-to-line) fault, the compensated impedance can be calculated from Fig. 3.5 as:

From equation (3.11) and (3.12) relaying voltage can be obtained as:

$$V_{1s} - V_{2s} = 0.5\,(I_{1s} - I_{2s})\,Z_1 + (V_{1T} - V_{2T}) + (n - 0.5)\,Z_1 (I_{1s} - I_{2s}) + (I_{1f} - I_{2f})\,R_{1f} \tag{3.18}$$

After dividing equation (3.18) by ($I_{1s} - I_{2s}$), equivalent apparent impedance during LL fault can be found as given by equation (3.19) [11]:

$$Z_{\text{eqLL}} = \frac{V_{1\text{s}} - V_{2\text{s}}}{I_{1\text{s}} - I_{2\text{s}}} = (n\, Z_1) + \left(\frac{V_{1\text{T}} - V_{2\text{T}}}{I_{1\text{s}} - I_{2\text{s}}}\right) + \left(\frac{I_{1\text{f}} - I_{2\text{f}}}{I_{1\text{s}} - I_{2\text{s}}} R_{1f}\right) \tag{3.19}$$

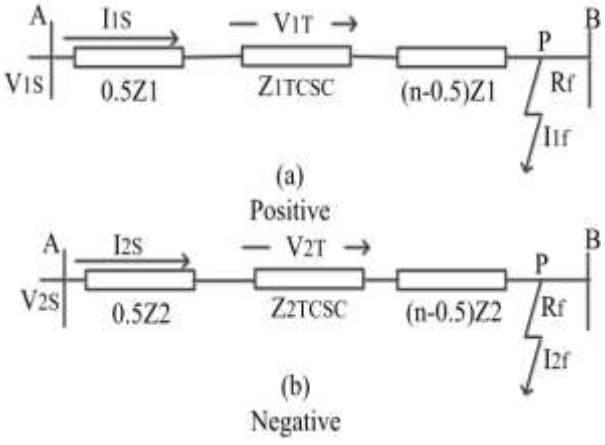

Fig. 3.5 Sequence network of the system during LL faults (a) Positive (b) Negative

From equation (3.17) and (3.19), it is clear that the apparent equivalent impedance seen by the conventional relay has three parts. First portion is the positive sequence impedance from relay point to fault point. Second portion is the impedance inserted by the TCSC; this impedance can be termed as compensated impedance (Z_{comp}) which creates error in impedance measurement and third portion is the impedance due to fault resistance.

3.3.2 Proposed Mho Relay Algorithm

Synchronized measurement of voltage and current based on accurate and synchronized time reference takes place in between bus 'A' and TCSC sub-station. Fig. 3.6 describes the algorithm of the proposed Mho relay. In this algorithm, the conventional Mho relay is altered by adding a compensation unit. This unit computes the compensated impedance (Z_{comp}) introduced by TCSC in fault loop. At bus 'A', mho relay takes voltage and current signal through CCVT and CT, respectively. Fault impedance Z (R and X) is calculated by conventional method at the relay point using fundamental and sequence components of fault voltage and current signal. Fast Fourier Transform (FFT) decomposes the transient voltage and current into the fundamental quantity and sequence filter gives the positive and zero sequence value of current.

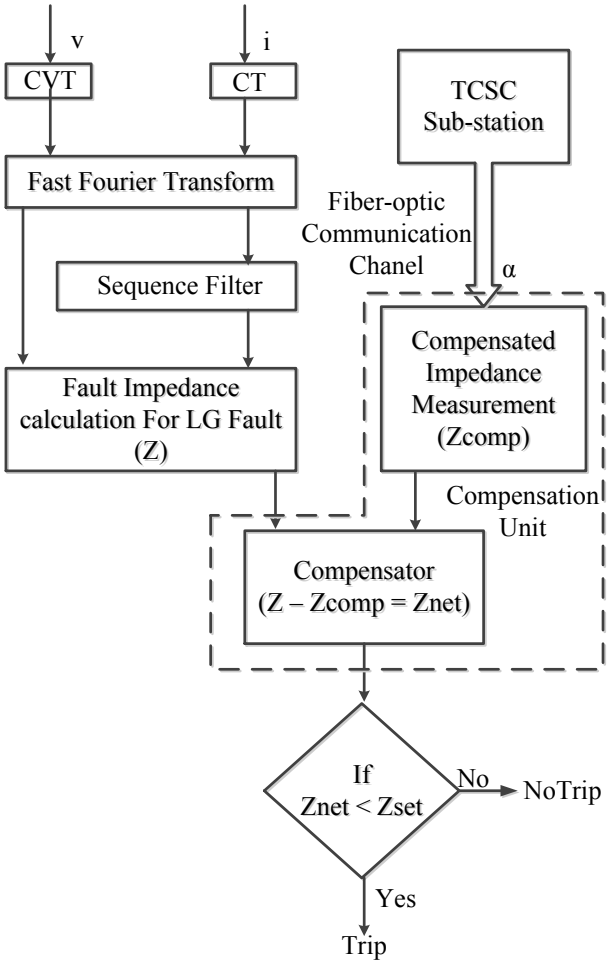

Fig. 3.6 Proposed compensated Mho relay algorithm

Proposed Mho relay compensation unit on-line calculates the compensated impedance (Z_{comp}) of TCSC and simultaneously compensate it form the measured impedance (Z) at relay point. Finally, net line fault impedance ($Z_{net} = Z - Z_{comp}$) is calculated at relay bus 'A'. If Z_{net} is less than the $Z_{set,}$ it indicates line fault condition otherwise healthy condition.

3.3.3 Communication Channel

The proposed Mho relay requires a reliable and high speed communication channel in between TCSC substation to the relay location. TCSC control circuit generates synchronized firing pulses, which fire thyristors at the firing angle. Communication channel transmits firing angle to the relay location to calculate compensated impedance. Reliability of the proposed relay depends on the reliability and fastness of the communication channel. It is assumed that the communication channel is reliable and fast enough to send measured angle from TCSC point to relay bus 'A' for any fault in between TCSC point and bus 'B'. If there is any fault in between bus 'A' and TCSC point, communication channel breaks and does not send any signal, in this case, relay behaves normally as a conventional relay. The newly built EHV/UHV transmission lines in are all equipped with dedicated fiber-optics channels or Global Positioning System (GPS) through which the signals can be transmitted from one end of the transmission line to the other [156], [178].

3.4 Results and Discussion

Extensive simulations are carries out to evaluate the performance of proposed adaptive Mho relay algorithm. A 230 kV and 320 km long series compensated transmission line is used to test the capability of the proposed adaptive protection algorithm for midpoint series compensated line. The first zone of the Mho relay is set to protect 85 % (272 km) of the transmission line, the second zone is set to protect rest of the line and an assumes extended section which may stretch in next adjacent line (not shown in the test diagram) up-to 384 km from relay bus A. Results are discussed for capacitive and inductive mode of operations under different operating conditions as follows:

3.4.1 Capacitive Mode

In capacitive mode of operation, TCSC inserts capacitive reactance into the transmission line and hence reduces the impedance of transmission line. In this operation, net line impedance trajectory shifts towards the origin in R-X plane and relay over-reaches.

Adaptive compensated Mho relay calculates the shift and again places the impedance trajectory at actual position. Following are the different cases taken for validation of the working of adaptive relay.

3.4.1.1 Single Line-to-Ground Fault

Proposed adaptive relay is tested under different line fault conditions. Separate Mho distance relays were placed at relay bus to detect fault in transmission line to ground (LG) fault. To detect LG fault in three phases line, three similar Mho relays are placed for each phase. Operation of proposed and conventional relay for LG fault condition is discussed as follows:

Case: 1 Low Current Fault Condition

Generally low current fault occur in transmission line if fault is at the far end of transmission line. If the fault resistance is very high, it can cause a low current fault. In this case, TCSC remains in the system and inserts its complete capacitive reactance in to the system. For low current fault, TCSC impedance is given by equation (3.7) as "$Z_{comp} = X_{comp}(\alpha)$". Forcefully, low current faults are created by taking assumed conditions to test the accuracy of adaptive relay for various compensation levels from 7.5 % to 50 %. Following are the supportive results for different cases.

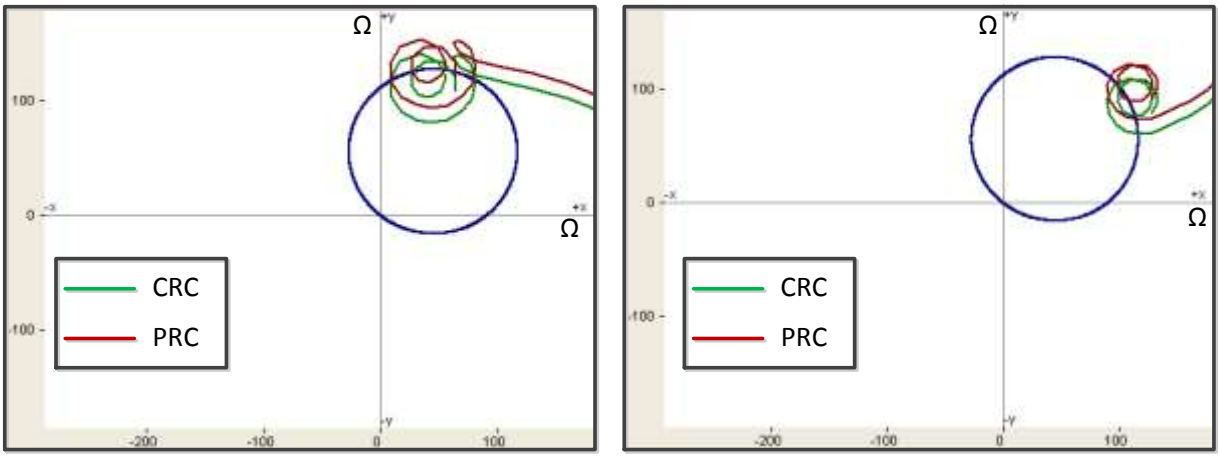

(a) (b)

Fig. 3.7 Comparative performance at 7.5 % compensation with fault resistance (a) 5 Ω (b) 40Ω

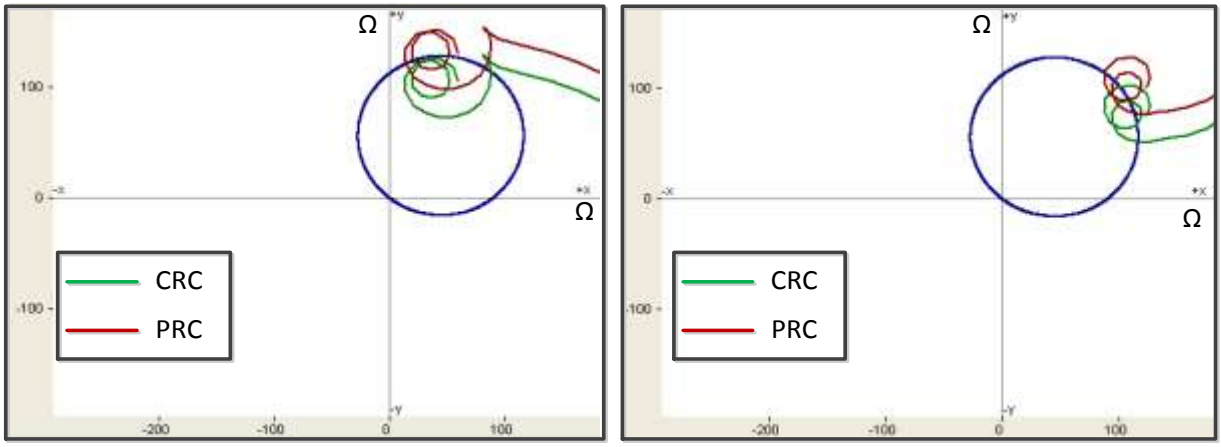

(a) (b)

Fig. 3.8 Comparative performance at 15 % compensation with fault resistance (a) 5 Ω (b) 40 Ω

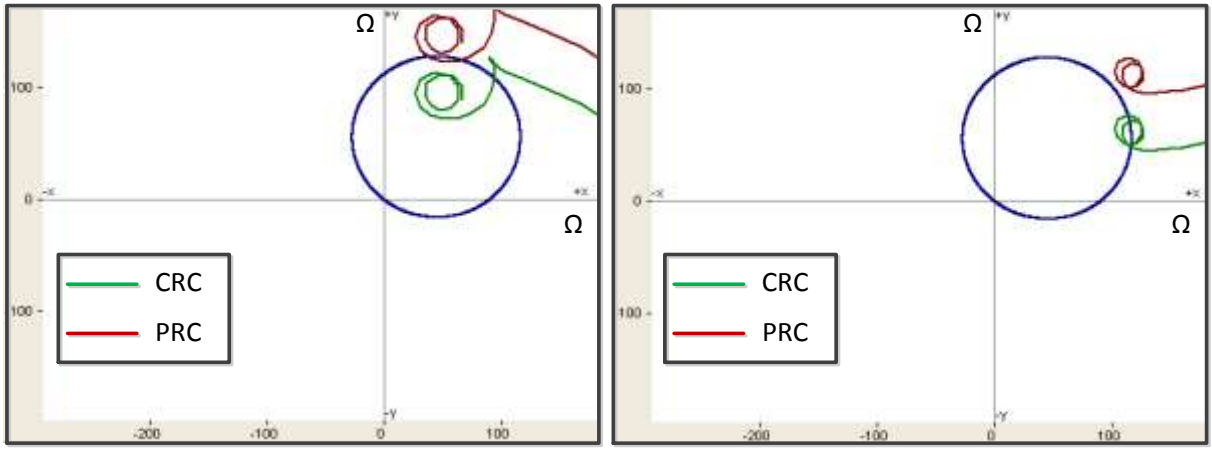

(a) (b)

Fig. 3.9 Comparative performance at 30 % compensation with fault resistance (a) 5 Ω (b) 40 Ω

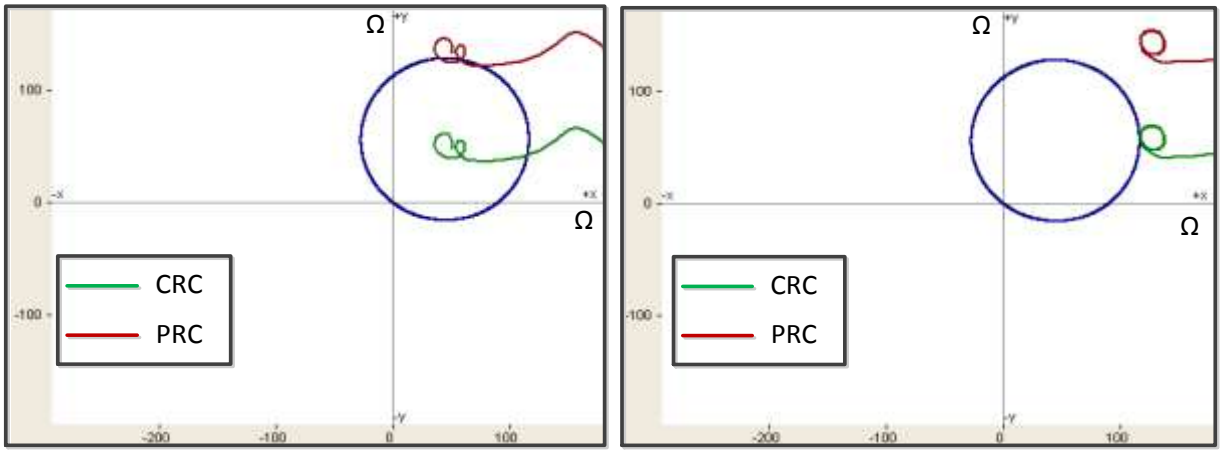

(a) (b)

Fig. 3.10 Comparative performance at 50% compensation with fault resistance (a) 5 Ω (b) 40 Ω

Far end single line to ground faults are created with taking a permissible limit of fault resistance from 5 Ω to 40 Ω with loading angle of 30°. As the faults are created at the zonal boundary of Mho relay, the impedance curve must be settle down at the boundary location. Conventional Relay Curve (CRC) shown by green line over-reaches due to capacitive compensation by TCSC. Proposed Relay Curve (PRC) takes adaptive action and sort-out the error at relay end to settle at correct location. Varying level of TCSC compensation affects the performance of the conventional relay; as the level of compensation increases, it shows more overreaching affects as shown in Fig. 3.7 to Fig. 3.10. As the fault was created at same location therefore curve trajectory must not shift considerably for variation in compensation level which is validated for proposed relay. Fault resistance creates a considerable shift in CRC as well in PRC trajectory. As fault was created at the boundary location, so characteristics are highly affected due to fault resistance and show error for higher side value of fault resistance.

Case: 2 High Current Faults Condition

In case of high current fault, excessive energy generated across TCSC and MOV protects the TCSC from high current by way of bypassing it. In this condition, TCSC has been bypassed from the line and equivalent impedance of TCSC and MOV comes into the line which is given by equation (3.7) as: "$Z_{comp} = X_{comp}\ (\alpha) || R_M(I)$". In this state, value of Z_{comp} is slightly less, hence error introduced is less. High current fault generally happens if fault occurs near the TCSC installation with having less value of fault resistance.

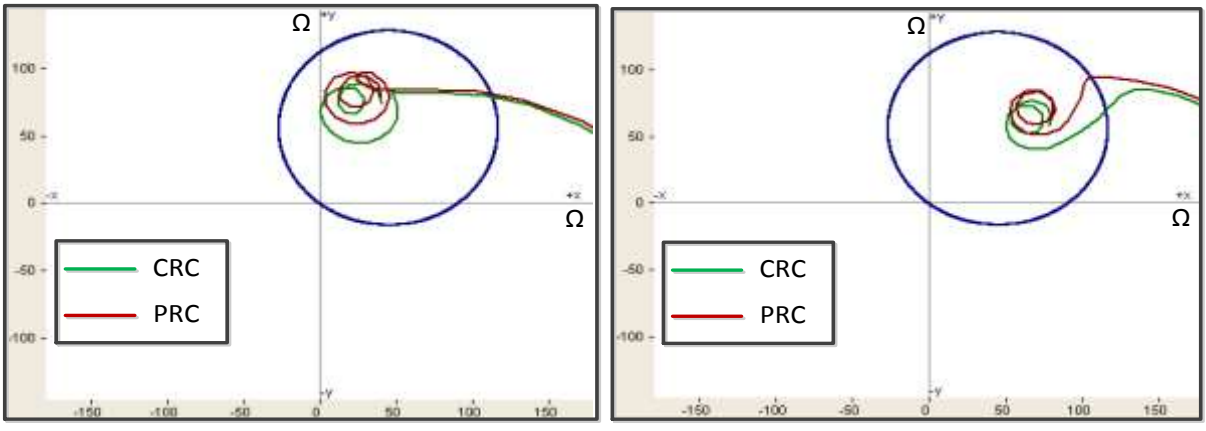

(a) (b)

Fig. 3.11 Comparative performance at 7.5 % compensation with fault resistance of (a) 5 Ω (b) 40 Ω

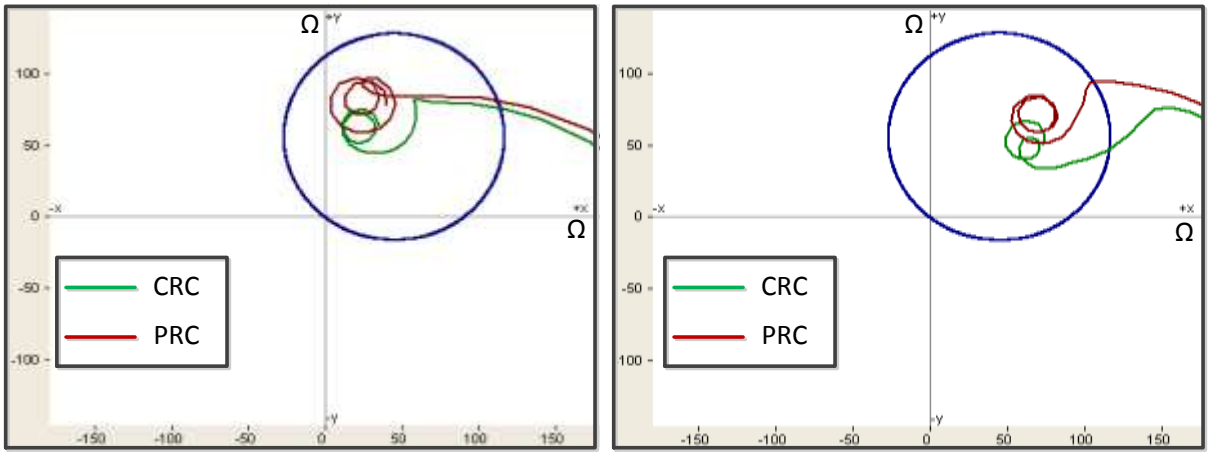

(a) (b)

Fig. 3.12 Comparative performance at 15 % compensation with fault resistance of (a) 5 Ω (b) 40 Ω

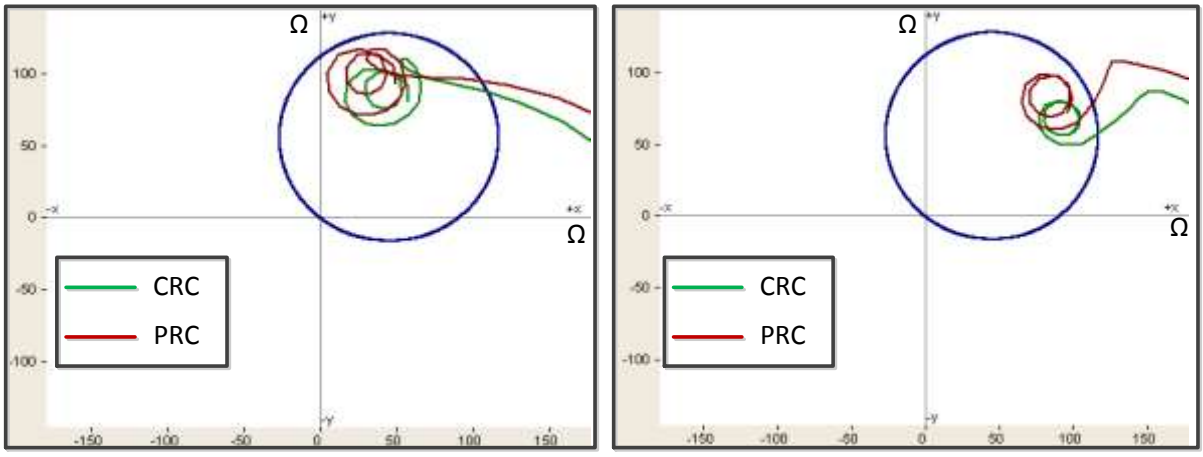

(a) (b)

Fig. 3.13 Comparative performance at 30 % compensation with fault resistance of (a) 5 Ω (b) 40 Ω

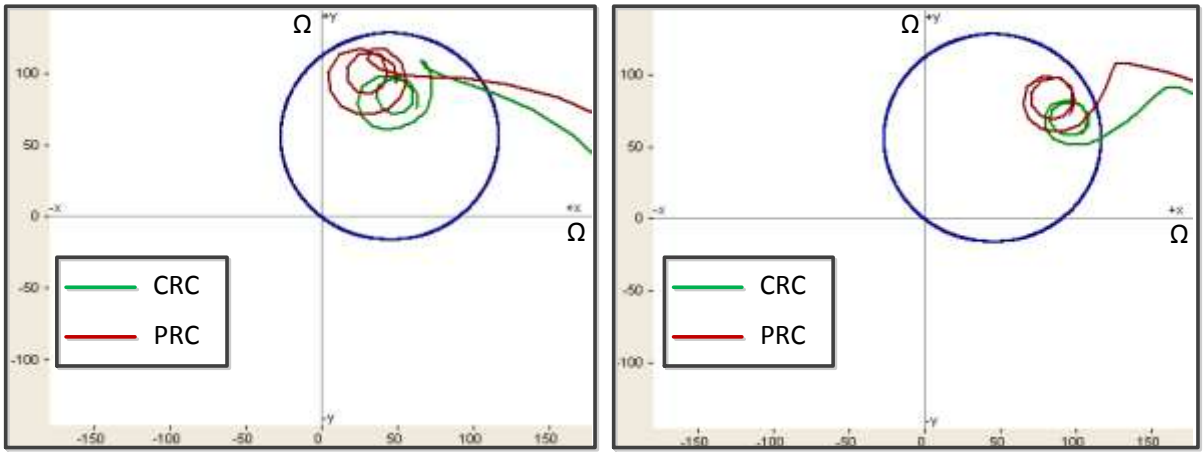

(a) (b)

Fig. 3.14 Comparative performance at 50 % compensation with fault resistance of (a) 5 Ω (b) 40 Ω

Forcefully, the high current fault are created in one phase to ground to validate the accuracy of proposed relay under various compensation level of TCSC and permissible limit of fault resistance was taken between 5 Ω to 40 Ω and results are taken for various conditions. It has been observed from Fig. 3.11 to Fig. 3.14 that PRC curve trajectory slightly shifted from CRC trajectory. Irrespective of the compensation level both the curves settle at considerably similar position. Adaptive relay compensates the error similarly in high fault condition and settle at actual fault location slightly different from conventional relay. It is clear from the results that both relay curves show more tolerance for fault resistance and exhibits right operation for taken fault resistance range.

3.4.1.2 Line-to-Line Fault

Proposed relay has been also tested for LL faults in three phase line and compared with conventional relay. Relay bus consist of three similar LL fault detection relay to detect fault between three phases. Operation of proposed and conventional relay for low and high fault condition has been discussed as follows:

Case 1: Low Current Faults Condition

Similarly as in LG fault condition, forcefully low current faults are created at the boundary of Mho relay zone with varying the fault resistance between 5 Ω to 40 Ω. Results are taken for various level of compensation from 7.5 % to 50 % as follows:

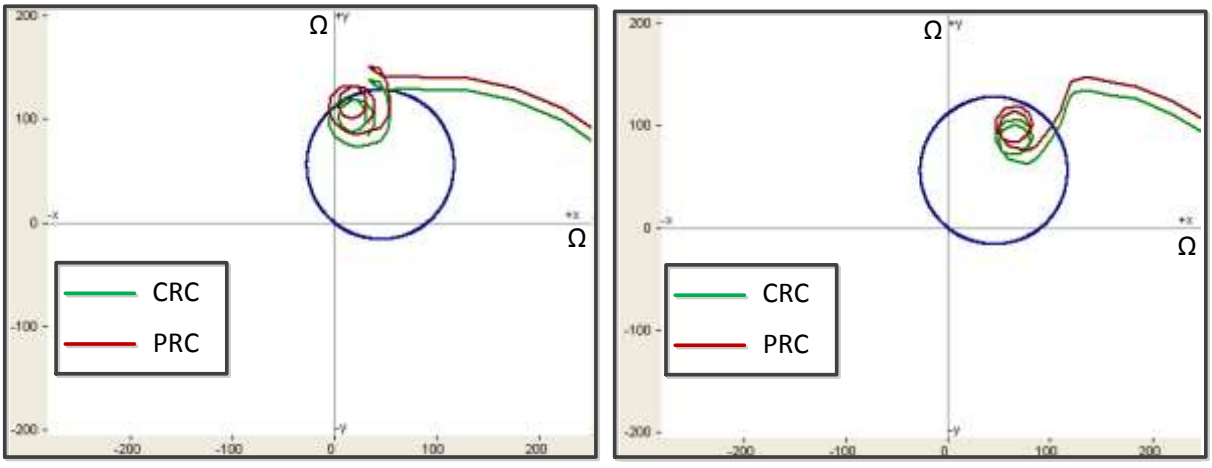

(a) (b)

Fig. 3.15 Comparative performance at 7.5 % compensation with fault resistance of (a) 5 Ω (b) 40 Ω

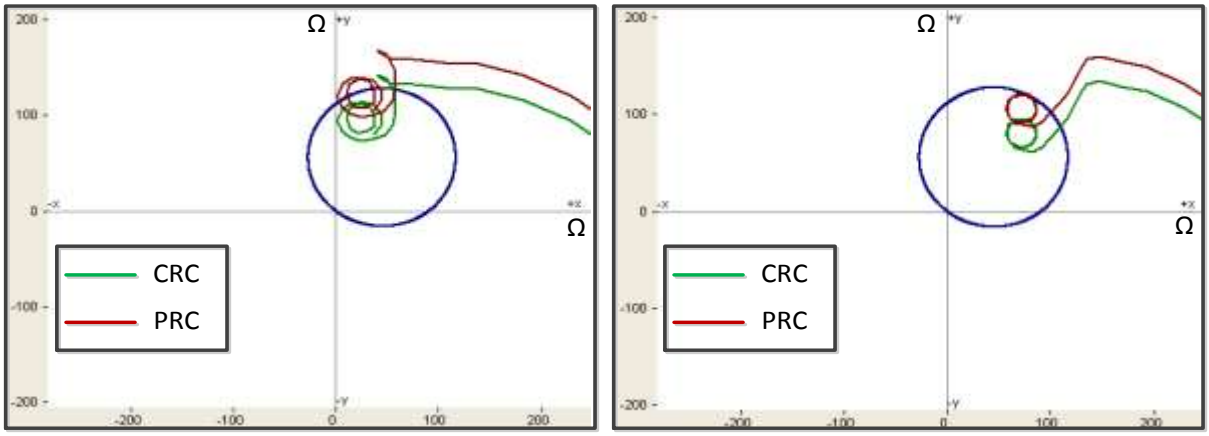

(a) (b)

Fig. 3.16 Comparative performance at 15 % compensation with fault resistance of (a) 5 Ω (b) 40 Ω

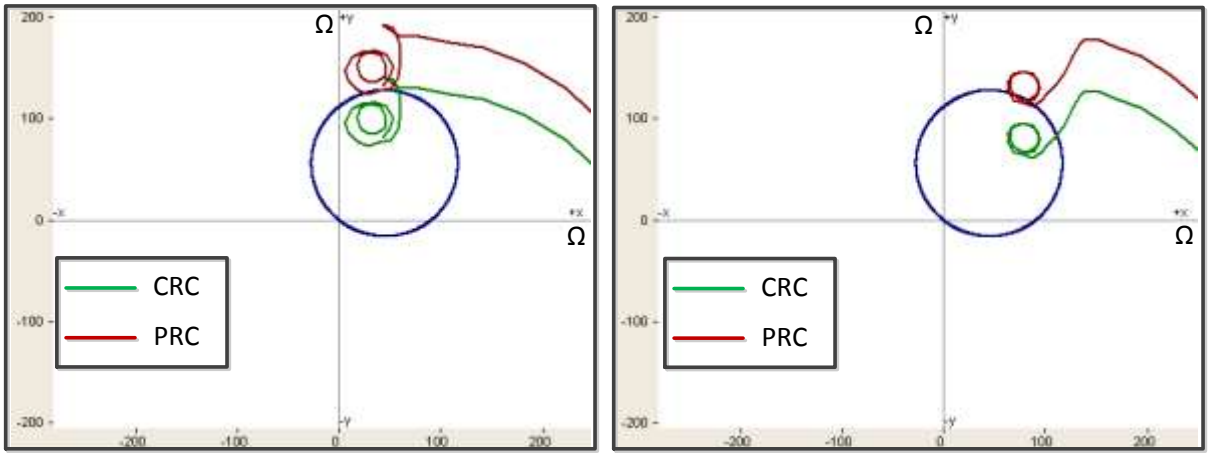

(a) (b)

Fig. 3.17 Comparative performance at 30 % compensation with fault resistance of (a) 5 Ω (b) 40 Ω

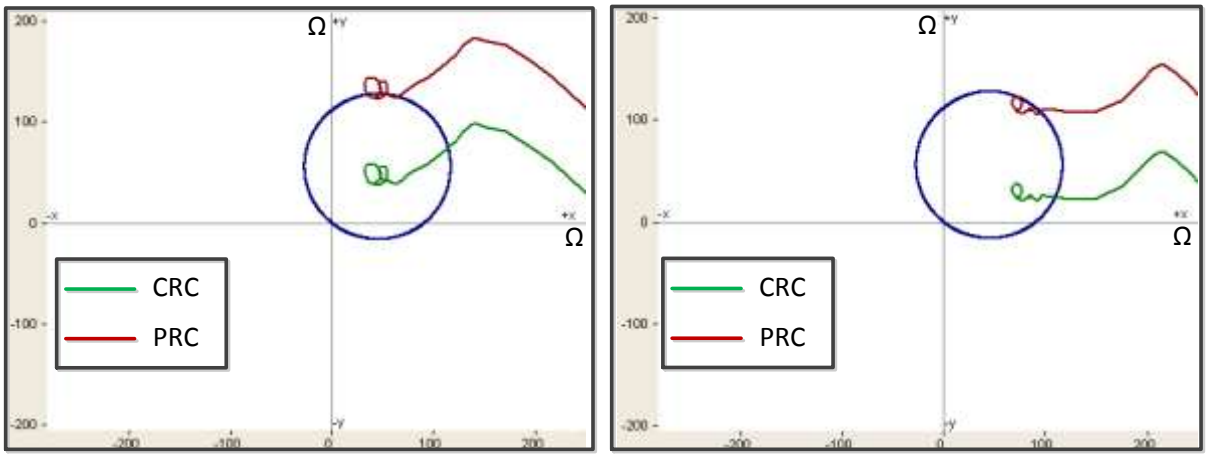

(a) (b)

Fig. 3.18 Comparative performance at 50 % compensation with fault resistance of (a) 5 Ω (b) 40 Ω

It has been depicted from Fig. 3.15 to Fig. 3.18 that adaptive relay is equally effective for low current LL fault in TCSC line. Proposed relay removes the error introduced by TCSC for every level of compensation and shows correct operation in contrast to conventional relay. It is also observed from the results that CRC and PRC trajectory shows more tolerance for fault resistance in LL fault condition than LG fault condition.

Case 2: High Current Faults Condition

High current faults near the TCSC installation point are created to test the accuracy of proposed relay under LL fault condition. Again in high fault condition, equivalent TCSC and MOV impedance comes into picture and adaptive relay computes the error to take adequate action. Following are the comparative results which justified the operation of proposed Mho relay.

LL faults are created with varying fault resistance and level of compensation. In this case, CRC trajectory show a little over-reaching and proposed relay takes adaptive action and PRC trajectory shifts marginally upward with no reaching mal-operation as shown in Fig. 3.19 to Fig. 3.22.

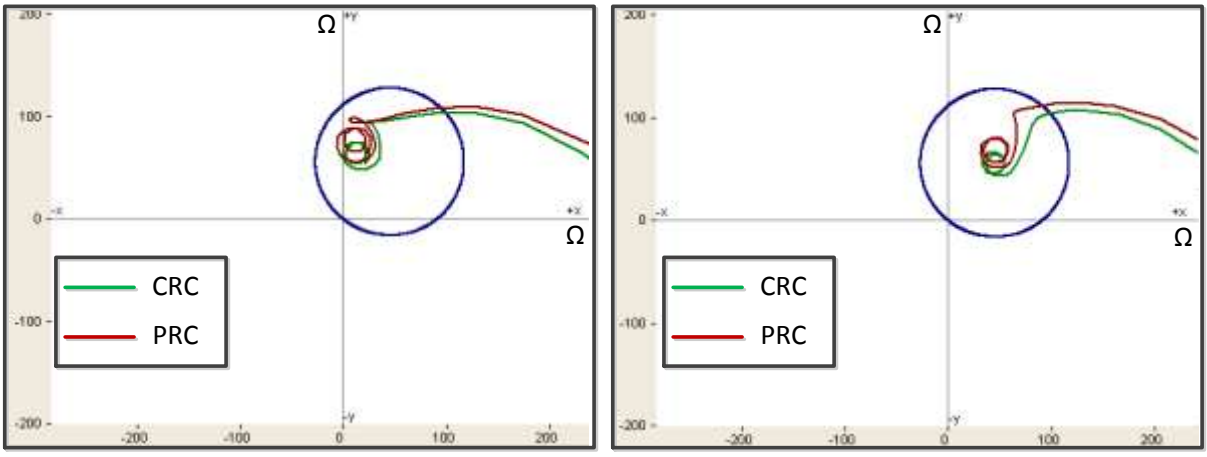

(a) (b)

Fig. 3.19 Comparative performance at 7.5 % compensation with fault resistance of (a) 5 Ω (b) 40 Ω

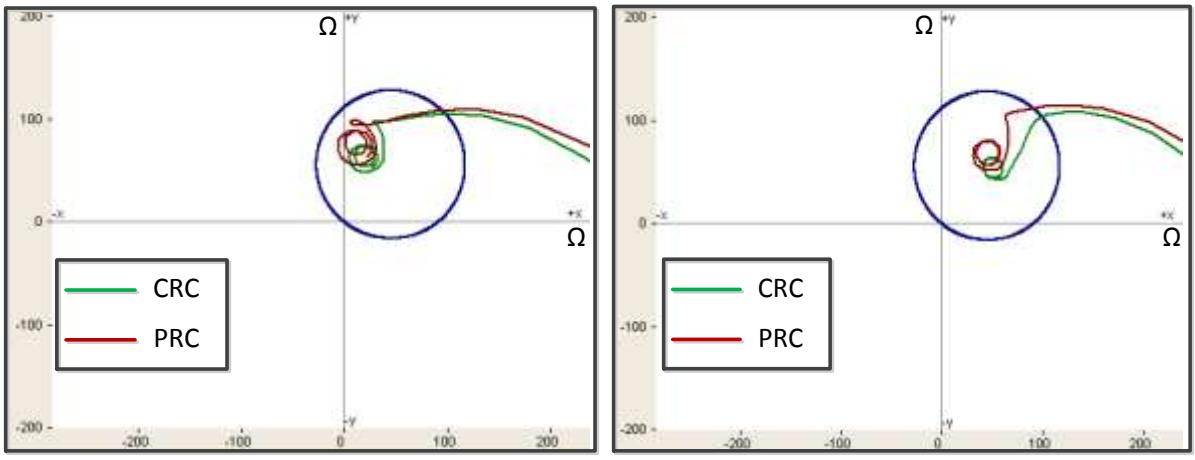

(a) (b)

Fig. 3.20 Comparative performance at 15 % compensation with fault resistance of (a) 5 Ω (b) 40 Ω

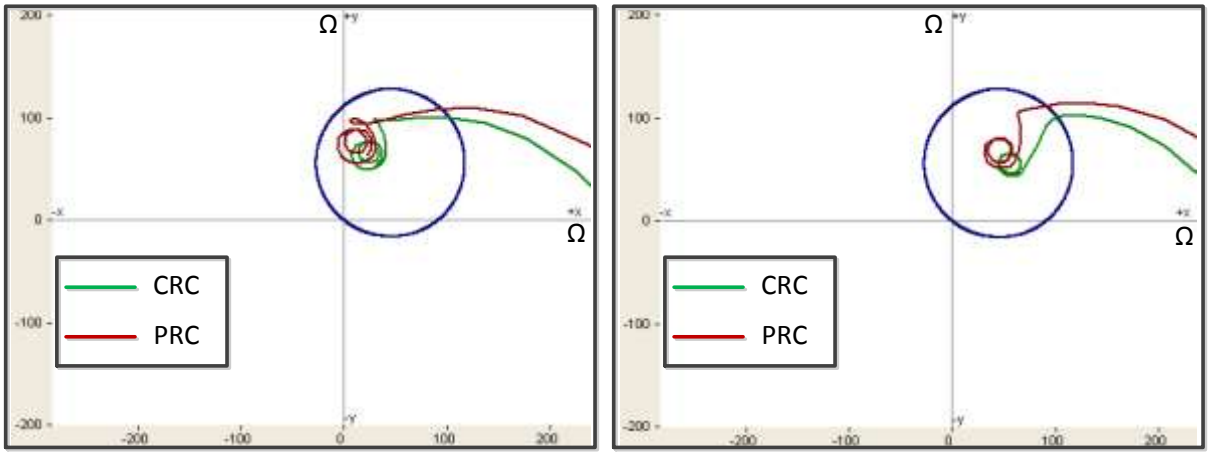

(a) (b)

Fig. 3.21 Comparative performance at 30 % compensation with fault resistance of (a) 5 Ω (b) 40 Ω

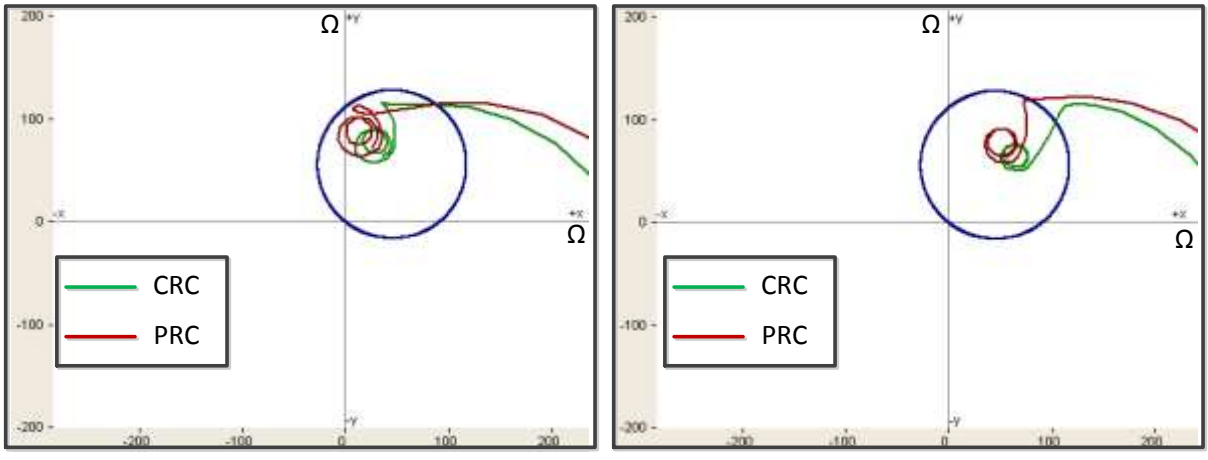

(a) (b)

Fig. 3.22 Comparative performance at 50 % compensation with fault resistance of (a) 5 Ω (b) 40 Ω

3.4.2 Inductive Mode

TCSC works in inductive mode of operation in case of light loading to control voltage under permissible limit. In this state TCSC inserts inductive reactance into the transmission line and hence increases the impedance of line. Therefore, if any line fault occurs in this situation, Mho relay shows under-reaching mal-operation at relay bus. To sort-out this error, proposed adaptive relay calculates the TCSC impedance equally well in inductive mode of operation and take correct decision. Following are the different line fault conditions which validate the operation of adaptive Mho relay.

3.4.2.1 Single Line to Ground Faults

Performance of proposed and conventional relay under LG fault condition when fault occur at different location is observed as follows:

Case: 1 Low Current Fault Condition

In case of low current fault, protective MOV does not bypass the current from itself and complete inductive reactance comes into fault loop. It is observed from Fig. 3.23 that inductive reactance shifted the CRC trajectory beyond the fault point and hence shows under-reaching problem and adaptive relay takes corrective action and subtract the error introduced by inductive reactance to settle at correct location.

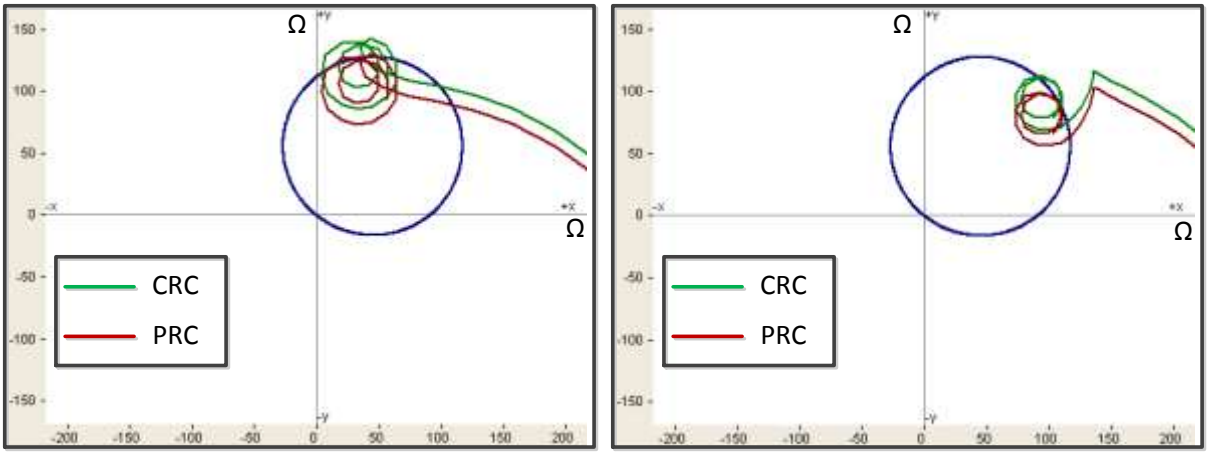

(a) (b)

Fig. 3.23 Inductive mode fault resistance (a) 5 Ω (b) 40 Ω

Low current faults are created at the far end of transmission line by taking variation in fault resistance from 5 Ω to 40 Ω as shown in Fig. 3.23(a) and (b). Both the relays also show good tolerance for higher value of fault resistance.

Case 2: High Current Fault Condition

Similarly, in inductive mode, protective MOV bypasses the series inductor and equivalent impedance of inductor and MOV comes into picture. In this state, both the relays shows almost similar characteristics as shown in Fig. 3.24. It is clear from Fig. 3.24 that proposed relay correctly measures the error and illustrate suitable results for low and high value of fault resistance.

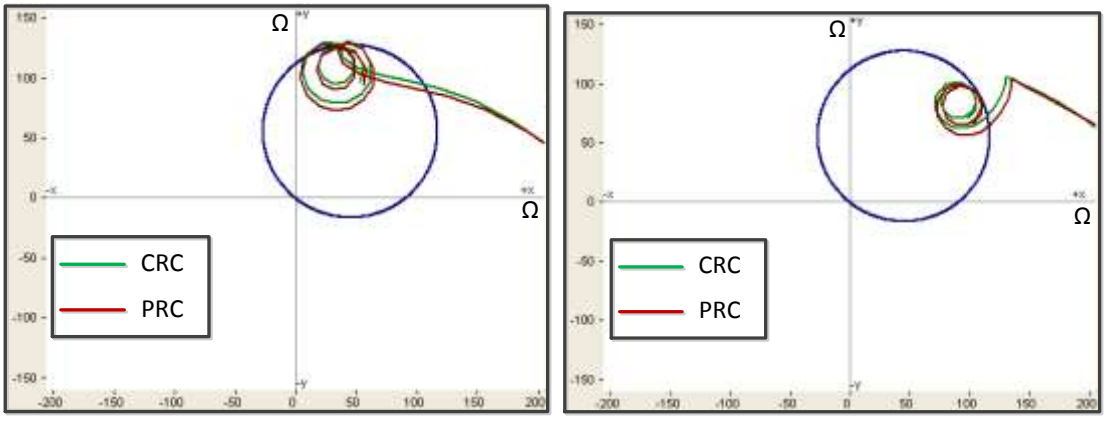

(a) (b)

Fig. 3.24 Inductive mode fault resistance (a) 5 Ω (b) 40 Ω

3.4.2.2 Line-to-Line Faults

Proposed relay also tested for LL fault condition in low and high fault current condition within normal range of fault resistance and it is found that the relay behaves properly while conventional relay has some limitations to find the actual fault location.

Case: 1 Low Current Fault Condition

Fig. 3.25 and Fig. 3.26 show the impedance trajectory for CRC and PRC. Both the relays show good tolerance for fault resistance but proposed relay shows better characteristics with respect to inductive compensation.

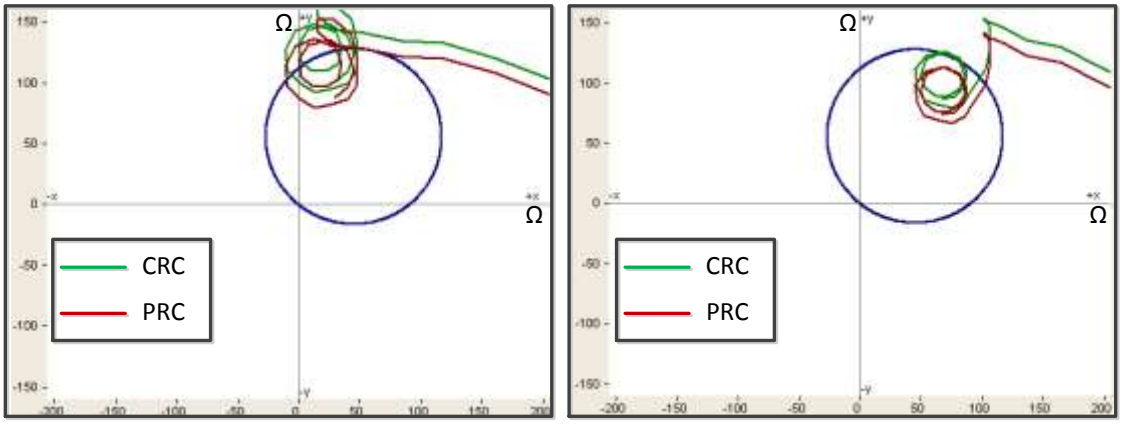

(a) (b)

Fig. 3.25 Inductive mode fault resistance (a) 5 Ω (b) 40 Ω

Case 2: High Current Fault Condition

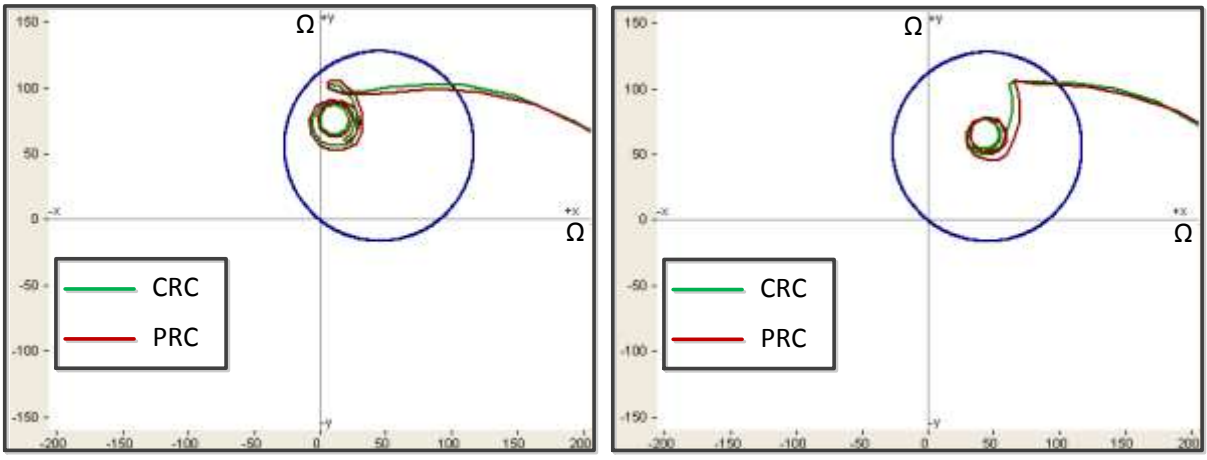

(a) (b)

Fig. 3.26 Inductive mode fault resistance (a) 5 Ω (b) 40 Ω

From the above results, it is clear that the performance of the proposed Mho relay algorithm is far better than the conventional Mho relay. However, the proposed Mho relay has a few limitations, under certain operating conditions of large fault resistance, if the fault is at the boundary of zone. Nevertheless, it is found that the proposed Mho relay is highly accurate under normal loading conditions (load angle in between 10° to 45°) and fault resistance in between 5 Ω to 40 Ω for both LG and LL fault conditions and various operating modes of TCSC line.

3.4.3 Fault Location Estimation

Fault location has been estimated by the proposed adaptive distance protection algorithm. To check the effect of induced adaptive compensation, it is assumed that the effect of fault resistance is negligible which is kept as 0.01 Ω for the whole analysis. Fault location is estimated by computing the inductive reactance of transmission line during fault which is affected by the TCSC compensation and independent of line resistance. Sampling frequency is chosen as 40 samples/ cycle and the fault reactance is measured by taking the average of all the reactance value for one quarter cycle i.e. 10 samples from a moving window. Percentage fault location accuracy is calculated by equation (3.19).

$$\% \text{ fault location accuracy} = \frac{\text{Measured reactance}}{\text{Actual line reactance}} * 100 \qquad (3.19)$$

Where, Actual line reactance is the gross reactance of fault location in the transmission line which is calculated by multiplying the per km line reactance to the created fault distance from the relay bus.

3.4.3.1 Fault Location Estimation Accuracy in Low Fault Current

Table 3.1 Fault location accuracy in low fault current at 50 % compensation

S. N.	Fault at location (km)	Actual positive sequence fault reactance (X) in Ω	Measured reactance with conventional Algorithm (Ω)	Measured reactance with proposed algorithm (Ω)	Fault location accuracy with conventional Algorithm (%)	Fault location accuracy with proposed Algorithm (%)
1	170	86.19	6.08	83.99	7.05	97.44
2	200	101.4	22.143	99.25	21.83	97.87
3	225	114.075	34.26	111.85	30.03	98.04
4	250	126.75	46.63	124.61	36.78	98.31
5	272	137.90	56.668	135.42	41.09	98.20
6	300	152.1	72.11	149.9	47.40	98.55
7	325	164.775	84.90	161.79	51.52	98.18
8	350	177.45	95.78	174.89	53.97	98.55
9	384	194.668	110.60	191.82	56.81	98.53

Table 3.2 Fault location accuracy in low fault current at 30 % compensation

S. N.	Fault at location (km)	Actual positive sequence fault reactance (X) in Ω	Measured reactance (Ω) with conventional algorithm	Measured reactance (Ω) with proposed algorithm	Fault location accuracy with conventional Algorithm (%)	Fault location accuracy with proposed Algorithm (%)
1	170	86.19	38.381	84.08	44.53	97.55
2	200	101.4	53.653	99.44	52.91	98.06
3	225	114.075	66.119	112.21	57.96	98.36
4	250	126.75	78.93	124.51	62.27	98.23
5	272	137.90	90.38	135.95	65.54	98.58
6	300	152.1	105.04	150.03	69.05	98.63
7	325	164.775	117.27	163.0	71.16	98.92
8	350	177.45	130.01	175.22	73.26	98.74
9	384	194.668	147.73	192.35	75.88	98.80

Table 3.3 Fault location accuracy in low fault current at 15 % compensation

S. N.	Fault at location (km)	Actual positive sequence fault reactance (X) in Ω	Measured reactance with conventional algorithm	Measured reactance with proposed algorithm	Fault location accuracy with conventional Algorithm (%)	Fault location accuracy with proposed Algorithm (%)
1	170	86.19	62.64	84.50	72.67	98.03
2	200	101.4	78.17	100.44	77.09	99.05
3	225	114.075	91.31	112.68	80.04	98.77
4	250	126.75	103.75	124.95	81.85	98.57
5	272	137.90	114.26	136.25	82.85	98.80
6	300	152.1	129.13	150.85	84.89	99.17
7	325	164.775	141.35	162.14	85.78	98.40
8	350	177.45	155.09	175.97	87.39	99.16
9	384	194.668	172.63	192.72	88.67	98.99

Accuracy of the conventional and proposed Mho relay scheme has been compared for the estimation of fault location in terms of line reactance. Line-to-ground fault has been created forcefully at several predefined locations in section-II of the mid-point series compensated transmission line. In low fault current conditions, the effect of MOV has been removed and only the effect of TCSC has been included in the fault reactance computation. Comparative performance of the conventional and the proposed algorithm for different maximum compensation levels of 50%, 30% and 15% has been given in following Table 3.1, Table 3.2, and Table 3.3, respectively.

3.4.3.2 Fault Location Estimation Accuracy in High Current Fault

Accuracy of the conventional and proposed Mho relay scheme has been compared in high fault current condition for the estimation of fault location in terms of line reactance. Line-to-ground fault has been created forcefully at several predefined locations in section-II of the mid-point series compensated transmission line. In high fault current conditions, the effect of MOV and TCSC has been included in the fault impedance computation. Comparative performance of the conventional and the proposed algorithm for different maximum compensation levels of 50%, 30% and 15% has been given in following Table 3.4, Table 3.5 and Table 3.6, respectively.

Table 3.4 Fault location accuracy in high fault current at 50 % compensation

S. N.	Fault at location (km)	Actual positive sequence fault reactance (X) in Ω	Measured reactance with conventional Algorithm (Ω)	Measured reactance with proposed algorithm (Ω)	Fault location accuracy with conventional Algorithm (%)	Fault location accuracy with proposed Algorithm (%)
1	170	86.19	66.5	81.52	77.15	94.58
2	200	101.4	80.4	98.27	79.28	96.91
3	225	114.075	92.2	109.88	80.82	96.32
4	250	126.75	106.75	123.21	84.22	97.20
5	272	137.90	117.83	134.89	85.44	97.81
6	300	152.1	133.3	147.19	87.63	96.77
7	325	164.775	145.9	158.45	88.54	96.16
8	350	177.45	155.25	171.24	87.48	96.50
9	384	194.668	171.03	189.75	87.85	97.47

Table 3.5 Fault location accuracy in high fault current at 30 % compensation

S. N.	Fault at location (km)	Actual positive sequence fault reactance (X) in Ω	Measured reactance (Ω) with conventional algorithm	Measured reactance (Ω) with proposed algorithm	Fault location accuracy with conventional Algorithm (%)	Fault location accuracy with proposed Algorithm (%)
1	170	86.19	68.48	81.84	79.45	94.95
2	200	101.4	82.90	98.77	81.75	97.40
3	225	114.075	93.56	110.05	82.01	96.47
4	250	126.75	107.90	123.62	85.12	97.53
5	272	137.90	119.12	134.95	86.38	97.86
6	300	152.1	134.35	147.50	88.33	96.97
7	325	164.775	146.98	158.95	89.20	96.46
8	350	177.45	156.45	171.87	88.16	96.85
9	384	194.668	172.03	190.45	88.37	97.83

Table 3.6 Fault location accuracy in high fault current at 15 % compensation

S. N.	Fault at location (km)	Actual positive sequence fault reactance (X) in Ω	Measured reactance with conventional algorithm	Measured reactance with proposed algorithm	Fault location accuracy with conventional Algorithm (%)	Fault location accuracy with proposed Algorithm (%)
1	170	86.19	69.68	82.35	80.84	95.54
2	200	101.4	83.67	99.53	82.51	98.15
3	225	114.075	94.69	110.86	83.00	97.18
4	250	126.75	109.10	123.95	86.07	97.79
5	272	137.90	120.12	135.33	87.10	98.13
6	300	152.1	134.35	147.92	88.33	97.25
7	325	164.775	147.30	159.05	89.39	96.52
8	350	177.45	157.68	173.02	88.85	97.50
9	384	194.668	173.54	191.23	89.14	98.23

Table 3.1 to Table 3.6 summarizes the results obtained for the fault location estimation accuracy in all possible conditions of mid-point series compensated transmission line. As can be seen, in both the cases, the fault location accuracy was found to be better for the proposed algorithm as compared to the conventional algorithm.

3.4.4 Effect of Source Impedance Ratio (SIR) on Proposed Relay Fault Location Estimation Accuracy

Fault Location estimation in transmission line depends on source impedance ratio which is given by the ratio of source impedance to transmission line impedance. Protection scheme for transmission line is determined by the length of the line. Length of the line is determined by corporeal length, impedance or SIR level of the system. Length of the line based upon the SIR level can be classified as:

1. Short Line (SIR > 4)
2. Medium Line (0.5 < SIR < 4)
3. Long Line (SIR < 0.5)

Over-reaching accuracy of the impedance relay depends upon the SIR level of the transmission system. In the proposed work effect of SIR level on the fault location accuracy has been analyzed. SIR of the system is changed by varying the source impedance and then the percent accuracy is calculated. Table 3.7 indicates the effect of varying SIR on fault location accuracy and it is observed that accuracy decreases as the SIR level increases.

Table 3.7 Effect of SIR at zone-1 boundary (272 km)

S. No.	SIR	Accuracy (%)
1	0.272	97.81
2	1.366	96.61
3	2.730	94.91
4	4.091	93.22
5	5.440	90.96

Table 3.8 Effect of SIR in zone-2 (350 km)

S. No.	SIR	Accuracy (%)
1	0.272	96.80
2	1.366	96.32
3	2.730	95.64
4	4.091	94.3
5	5.440	92.0

Table 3.8 shows the fault location accuracy in zone-2 at 350 km and similar variation in accuracy observed at different SIR. In the proposed algorithm, SIR of the system is kept fixed at 0.272 which is adequate for long transmission line.

3.5 Case Study: Application of Proposed Relay on Double Circuit Line

Proposed compensated Mho relay algorithm has been tested on a simple two bus double circuit transmission line. Proposed Mho relay set to protect the in which TCSC placed at mid-point.

3.5.1 Test System

A typical 230 kV, 50 Hz, parallel transmission lines having TCSC in one line is considered to develop and test the capability of the proposed adaptive Mho relay algorithm. Test system is shown in Fig. 3.27; it consists of two sources connected through a 320 km transmission line. Per km sequence impedances of both the line in ohms are as: *Z1* = 0.034+j0.42, *Z2* = 0.034+j0.42 and *Z0* = 0.363+j1.32. TCSC is placed at 160 km from the sending end generator, which compensate the transmission line up-to 50 %. MOV is connected across TCSC and it bypasses the excessive energy when it reaches above a pre-set value.

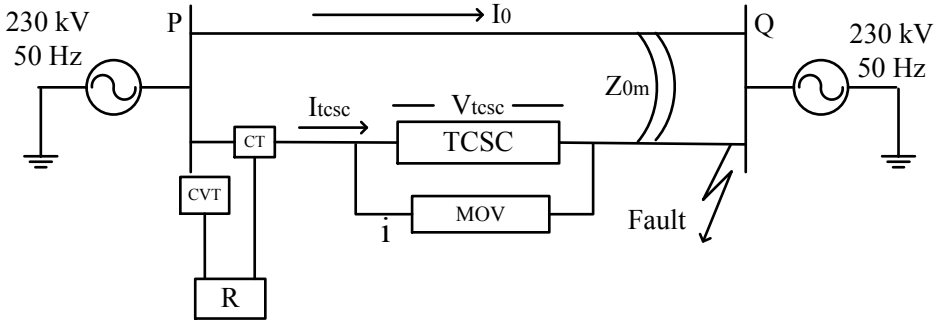

Fig. 3.27 Double circuit test system

3.5.2 Results

Same results are taken for the double circuit transmission line for the validation of the proposed algorithm as follows:

3.5.2.1 Capacitive mode

Case 1: Low Current Fault Condition

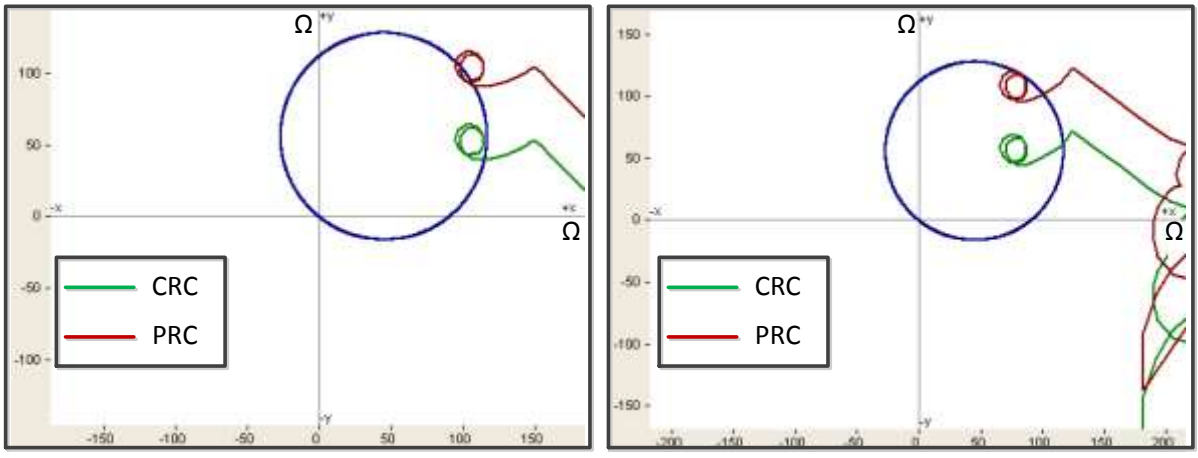

(a) (b)

Fig. 3.28 Far end fault with low fault resistance (a) LG (b) LL fault

Case 2: High Current Fault Condition

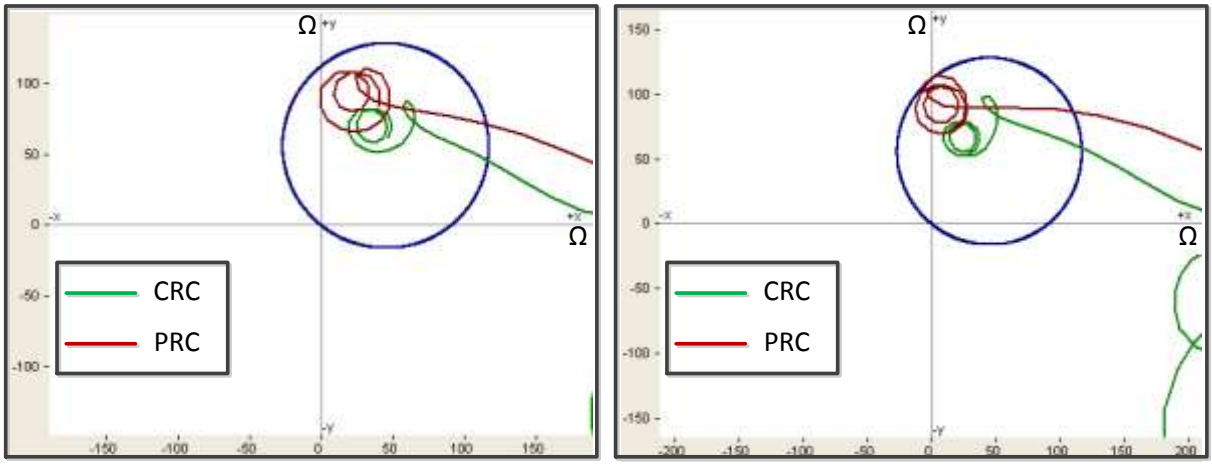

(a) (b)

Fig. 3.29 Fault near TCSC with high fault resistance (a) LG (b) LL fault

3.5.2.2 Inductive mode

Case 1: Low Current Fault Condition

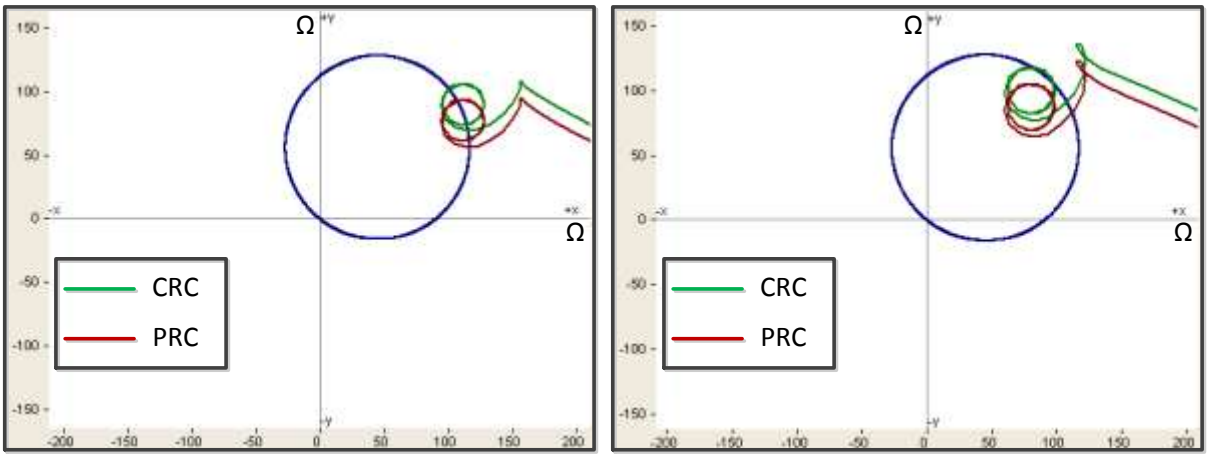

(a) (b)

Fig. 3.30 Far end fault with low fault resistance (a) LG (b) LL fault

Case 2: High Current Fault Condition

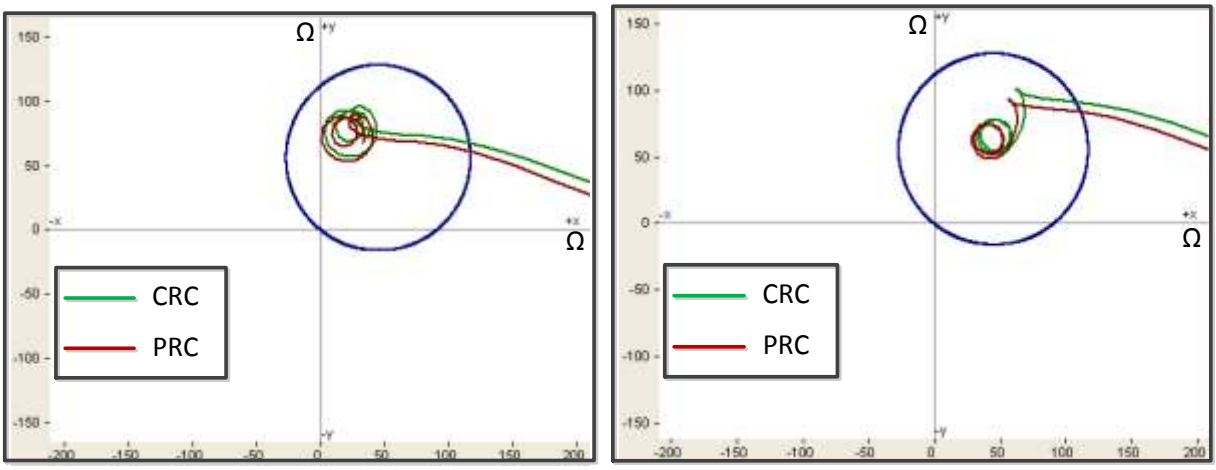

(a) (b)

Fig. 3.31 Fault near TCSC with high fault resistance (a) LG (b) LL fault

It has been observed from the above results that proposed compensated Mho relay has identical performance for the double circuit line for all possible conditions taken previously.

3.6 Summary

This chapter describes an adaptive Mho relay algorithm for series compensated transmission line having TCSC. This technique employs addition of a compensation unit in conventional Mho relay. Compensation unit compensates the impedance inserted by the TCSC in fault loop and Mho relay calculates the actual impedance coordinates of fault point. TCSC and its protective circuit (MOV/ spark gap) are modeled separately to calculate the equivalent series compensated impedance. The main advantage of proposed relay is its adaptability to work in capacitive as well as inductive mode of operation.

Proposed adaptive Mho relay algorithm is constrained by the high value of fault resistance (> 50 Ω) and high loading conditions. Hence, in the next chapter, AI based algorithms have been developed to overcome these constrains.

CHAPTER 4
ZONE SETTING OF SERIES COMPENSATED TRANSMISSION NETWORK

This chapter introduces a novel approach for zone identification in transmission line employing TCSC at mid-point. The technique depends on the modified apparent impedance seen by the impedance relay for all possible operating conditions. In this technique the impedance patters are generated for different faults in zone-1 and zone-2 and AI techniques like RBFNN and SVM are used for discriminating faulty zone (zone-1 or zone-2) in mid-point series compensated line. In addition, an optimization technique viz. Genetic Algorithm (GA) is used to optimize SVM parameters. A typical 230 kV system is simulated in PSCAD/ EMTP software and the results show that the proposed scheme is secure, accurate and reliable under the wide variation in power system parameters like load angle, fault resistance, fault location, inception angle and compensation level.

4.1 Introduction

In distance protection of transmission line, assessment of faulty zone, in which the fault occurs, is an important task. Zone setting of transmission line is adversely affected due to presence of TCSC in transmission and that, in turn, affects Mho relay functionality. As the power system needed, TCSC inserts equivalent amount of capacitive or inductive reactance into the line depending upon the mode of operation viz. capacitive or inductive mode, respectively. In case of fault at the boundary of zone-1 and zone-2, it is difficult for protection engineer to decide which zone relay should trip. Further, the presence of fault resistance and loading conditions majorly decides the fault zone in transmission line. Therefore, zone setting in mid-point compensated transmission line is constrained by the factors such as TCSC, fault resistance and loading level.

A few reports have suggested for overcoming the adversities that arise due to the presence of TCSC in the zone setting of transmission lines. An advance interphase distance relaying technique is proposed in ref. [120], which is useful in term of its undependability on series capacitor parameter. Adaptive zonal setting in distance relaying technique via suitable communication channel is presented in ref. [179]. SVM is used as a pattern classifier for

obtaining zonal setting of transmission line in which apparent line impedance is used as training pattern [180], [181]. Series compensator inserts nonlinear impedance into the transmission line which creates error in reach measurement of distance protection. A deterministic method to calculate the value of nonlinear impedance has been proposed by Damier Novosel *et al.* and a FFNN had been implemented to calculate the nonlinear voltage across the series capacitor in terms of line current. Proposed techniques allowed online adjustment to reach measurement of distance relay and fault location in series compensated line, however, the method was simple but constrained by accuracy [24]. Travelling wave was helpful in fault location estimation technique in which fault distance from measurement point was measured by time taken by travelling wave generated during fault. Fast Fourier Transform (FFT) detects the harmonic content present in fault and correspondingly removes the error [97]. Application of Phasor Measurement Unit (PMU) in series compensated transmission line can be important in locating faults without need of line parameters and series capacitor (SC) specifications [102]. Ali H. Al-Mohammed and M. A. Abido proposed a similar PMU based technique which measures pre-fault voltage and current at both the terminals of SC and line terminals to estimate exact fault location [103]. Proposed algorithm overcomes the difficulty arise in fault zone setting in mid-point series compensated transmission line. Actual impedance parameters of line fault are calculated after removing the error introduce by TCSC into the line impedance. Further, the fault impedance parameters are train with adaptive learning techniques like RBFNN and SVM to classify the faulty zone which able to achieve better accuracy.

4.2 Analysis of Test System

A typical 230 kV, 50 Hz, doubly fed power transmission line having TCSC at mid-point, is considered to develop and test the capability of the proposed optimal SVM and RBFNN based zonal classifier of Mho relay. Test system is shown in Fig. 4.1. Mho relay is placed at sending bus, which is set to protect transmission line in between bus A and B, which is 320 km long. CT and CCVT measure the line current and voltage respectively. Parameters of CT and CCVT are given in Appendix-B. Mho relay zone-1 is set at 85 % of line i.e. at 272 km from bus A. Zone-2 is set above 20 % of section A-B i.e. at 384 km as shown in Fig. 4.1. TCSC is placed at 160 km from the sending end generator which compensate the transmission line 0- 50 %.

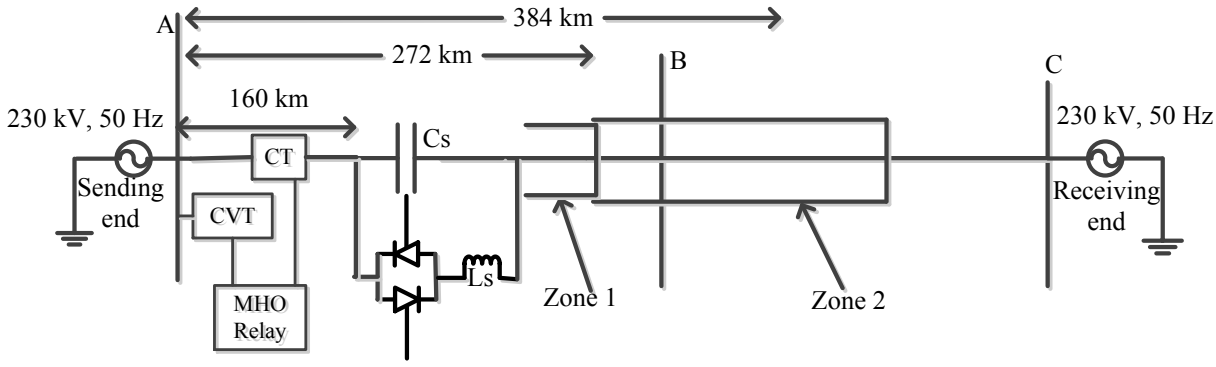

Fig. 4.1 Typical single line diagram of test system

4.2.1 Problem Associated with Conventional Distance Protection

In TCSC transmission line, reach measurement by distance relay depends upon the status of the TCSC impedance which is varying in nature. The varying nature of impedance inserted by TCSC in the line creates under-reaching and over-reaching at the relay point in inductive and capacitive compensation respectively and that is a challenge to the protection engineer. Due to this variable impedance, there is no clear boundary between zone-1 and zone-2, hence, overlapping area exists at the boundary as shown in Fig. 4.2. Due to this overlapping area, fault in zone-1 can extend up to zone-2 while zone-2 faults may fall within zone-1, according to the mode of operation of TCSC. Fault resistance also play important role in deciding the correct fault zone. Fault resistance can vary in a wide range between 0.01 Ω to above 200 Ω. Therefore it is required to make protection algorithm adaptive with series compensation level and fault Resistance to decide correct fault zone.

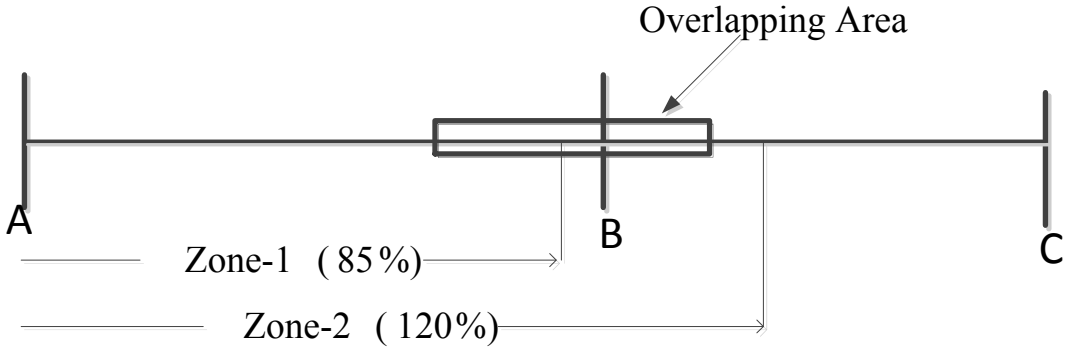

Fig. 4.2 Overlapping area between zone-1 and zone-2

This creates severe problem of zone identification in case of fault in transmission line having TCSC. Several other factors are there which can influence the zonal setting of distance

protection viz. loading, inception angle and fault location. Conventional distance protection fails to operate several time or mal-operate in case of boundary fault or very high fault resistance or high loading conditions. AI has the ability to adapt the conditions which are not possible to classify linearly. Proposed AI classifier for zonal setting of distance protection is established under various operating conditions as given in Table 4.1.

Table 4.1 Parameter range for classifier

S. No.	Parameters	Range
1	Load Angle	5 to 50°
2	Fault Resistance	0.01– 200 Ω
3	Fault inception angle	0 to 180°.
4	Fault Location	1 to 384 km in step of 40 km
5	Compensation Level	In Capacitive Mode -7.5, 15, 30 and 50 % In Inductive Mode – Up to 14 %

4.3 Proposed Adaptive Zone Setting Algorithm

As discussed earlier, the algorithm based on conventional impedance parameters measured by Mho relay cannot predict the faulty zone accurately and reliably in series compensated transmission line. Therefore, it is required to calculate the impedance parameters in such a way which are adaptive to series compensation and exhibits some realistic situation. Modified impedance parameters at least avoid the overlapping in imaginary axis and increases the accuracy of AI based classifier. Fig. 4.3 describes the algorithm of the proposed zonal classifier. Power system is simulated for various fault conditions considering all possible value of parameters and the system is forcefully taken to extreme and boundary conditions. For all taken conditions, three phase voltage and current are measured at relay bus through CCVT and CT, respectively, which was further processed for impedance calculation. In proposed algorithm, the conventional impedance calculation process is reformed by adding a compensation impedance calculation unit. This unit takes two inputs, one from CT output the relaying current and another from TCSC substation which is firing angle of thyristor. This unit computes the compensated impedance (Z_{comp}) introduced by TCSC in fault loop. CT current is used to calculate the resistance of protective MOV and firing angle (Alfa, α) calculates the reactance of TCSC given by equation (4.1) and (4.2), respectively. Z_{comp} is the parallel combination of MOV and TCSC given by equation (4.3). Fault impedance Z (R and X) is

calculated by the conventional method at the relay point using fundamental and sequence components of fault voltage and current signal. Fast Fourier Transform (FFT) decomposes the transient voltage and current into the fundamental quantity and sequence filter gives the positive and zero sequence value of current.

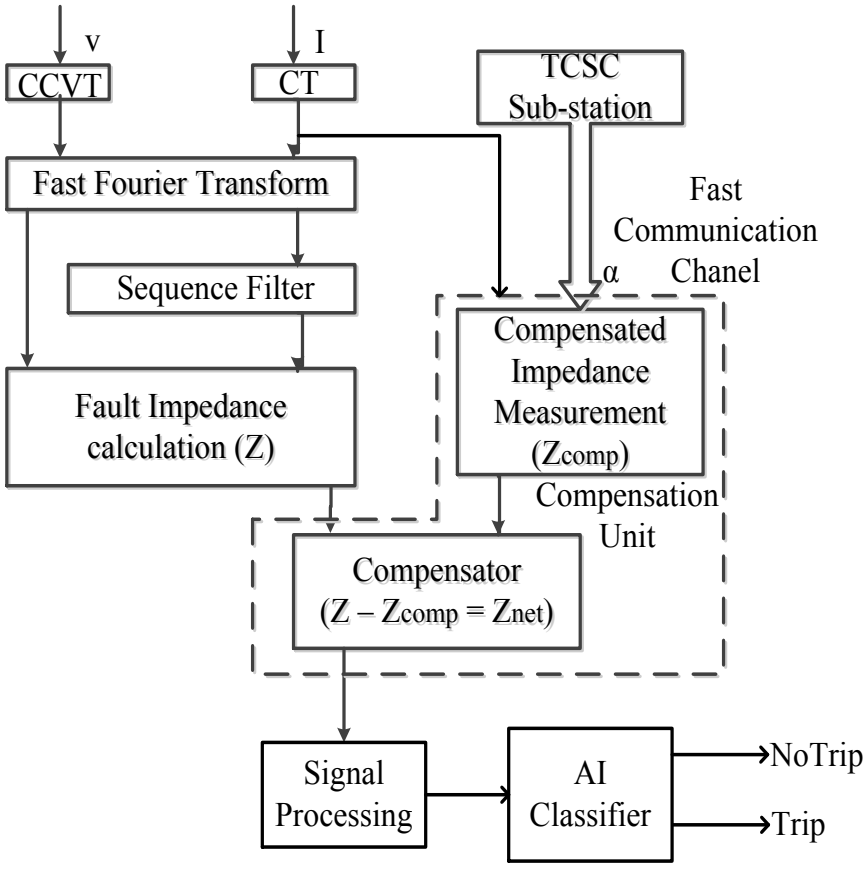

Fig. 4.3 Proposed compensated Mho relay algorithm

From previous chapter section-3.2, non-linear resistance of the protective MOV can be given by equation (4.1) as:

$$R_M(I) = a * I^b \tag{4.1}$$

Similarly the impedance of TCSC in terms of thyristor firing angle (α) can be given by equation (4.2):

$$X_{comp}(\alpha) = \frac{X_{Cs} * X_L(\alpha)}{X_L(\alpha) - X_{Cs}} \tag{4.2}$$

Therefore, the combined equivalent impedance which is the compensated impedance of MOV and TCSC is given by equation (4.3):

$$Z_{comp} = \begin{Bmatrix} X_{comp}(\alpha), \textit{for low current faults}, I < 1.1(pu) \\ R_M(I) \parallel X_{comp}(\alpha), \textit{for high current faults}, I > 1.1\,(pu) \\ \sim\ 0, \textit{for spark gap flashover} \\ 0, \textit{for breaker bypass} \end{Bmatrix} \quad (4.3)$$

Equivalent fault impedance at bus 'A' for LG fault is calculated by the conventional distance protection algorithm as given by equation (4.4):

$$Z = V/(I + k\,I_0), \quad (4.4)$$

Where, $k = (Z_0 - Z_1)/Z_1$,

V and I are the phase voltage and current, respectively.

Z_0, Z_1 are the zero and positive sequence impedances, respectively and

I_0 is zero sequence component of fault current.

Equivalent fault impedance at bus 'A' for LL fault is calculated by conventional distance protection algorithm as given by equation (4.5):

$$Z_{LL} = \frac{V_{1s} - V_{2s}}{I_{1s} - I_{2s}} \quad (4.5)$$

V_{1s}, V_{2s} are positive and negative sequence voltages, respectively, and

I_{1s}, I_{2s} are positive and negative sequence voltages, respectively

Finally, net line fault impedance ($Z_m = Z - Z_{comp}$) is calculated at relay bus 'A', which is then fed to AI classifier to decide whether the fault is in zone-1 or zone-2. Proposed Mho relay compensation unit on-line calculates the compensated impedance (Z_{comp}) of TCSC and simultaneously compensate it form the measured impedance (Z) at relay point. Modified impedance parameters (R_m, X_m) are used to avoid overreaching and under-reaching operation under the influence of TCSC. The feature vectors for AI classifier are R_m and X_m of several fault instances as shown in Fig. 4.4. In line fault conditions, Mho relay observe impedance characteristic in R-X plane and if the impedance characteristic enters in particular zone then corresponding Mho relay trips according to time dial setting. Let any fault occurs in a stable transmission system at time t_1 and the conventional distance relay algorithm detects the fault at time t_2. The time lapse $T=t_2-t_1$ (relay operating time) consist of the impedance seen during fault.

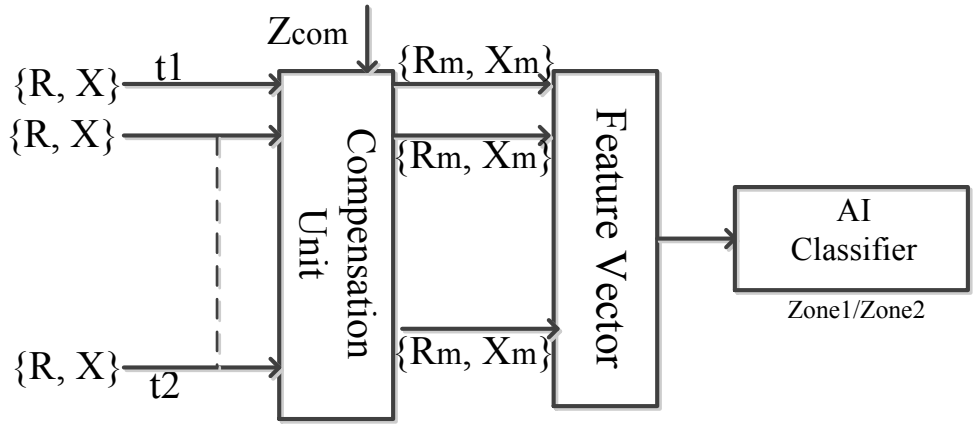

Fig. 4.4 General block diagram of AI based classifier for zonal discrimination

So the feature vector consists of the modified impedance parameters seen during time '*T*' by the relay located at the bus 'A'.

4.4 Training Features for AI Learning

Input feature for AI based classifier is the fault impedance trajectory for different fault conditions. Faults are created throughout the line and impedance trajectories are stored for offline training of AI classifier. In PSCAD/EMTDC simulation faults are created in steady state at 1.0 s with fault duration kept as 0.5 s. Fault data of 0.05 s is stored for AI training. With taking 800 Hz as sampling frequency 40 samples of fault impedance are taken as input for AI classifier. Discussion of taken training patters is as follows.

4.4.1 Locus of Fault Impedance at Boundary Conditions

Some critical fault impedance trajectories taken at boundary locations with extreme fault resistance are shown in the Fig. 4.5 to Fig. 4.7. Fig. 4.5(a) and Fig. 4.5(b) show the impedance pattern if fault created near the relay bus at 1 km with fault resistance 0.01 Ω and 100 Ω, respectively.

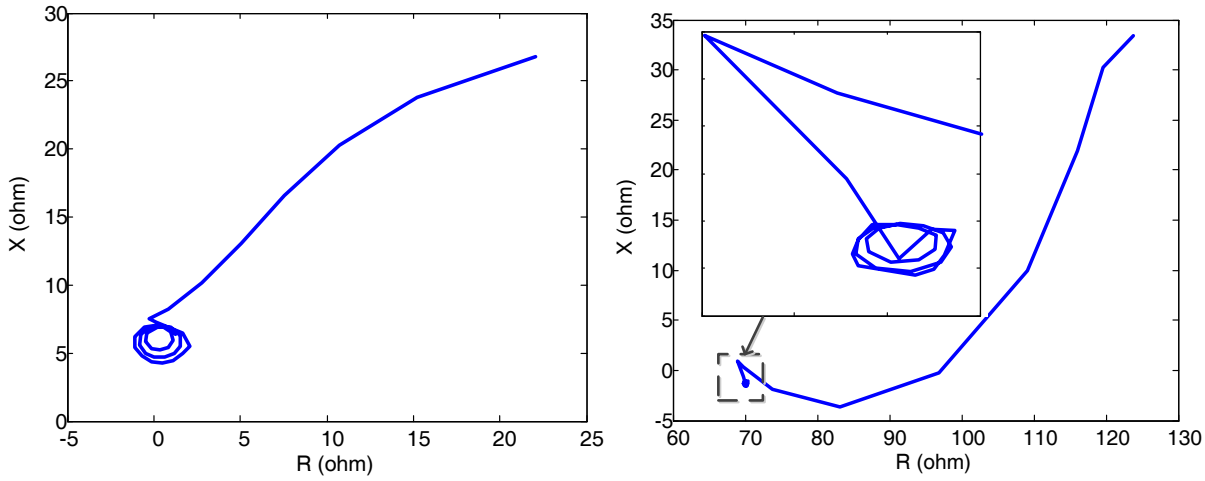

(a) (b)

Fig. 4.5 Impedance trajectory for fault at sending end with fault resistance (a) 0.01 Ω (b) 100 Ω

Fig. 4.6 shows the impedance trajectory for a fault occurred near TCSC substation which is a high current fault. Two plots are taken for extreme value of fault resistance.

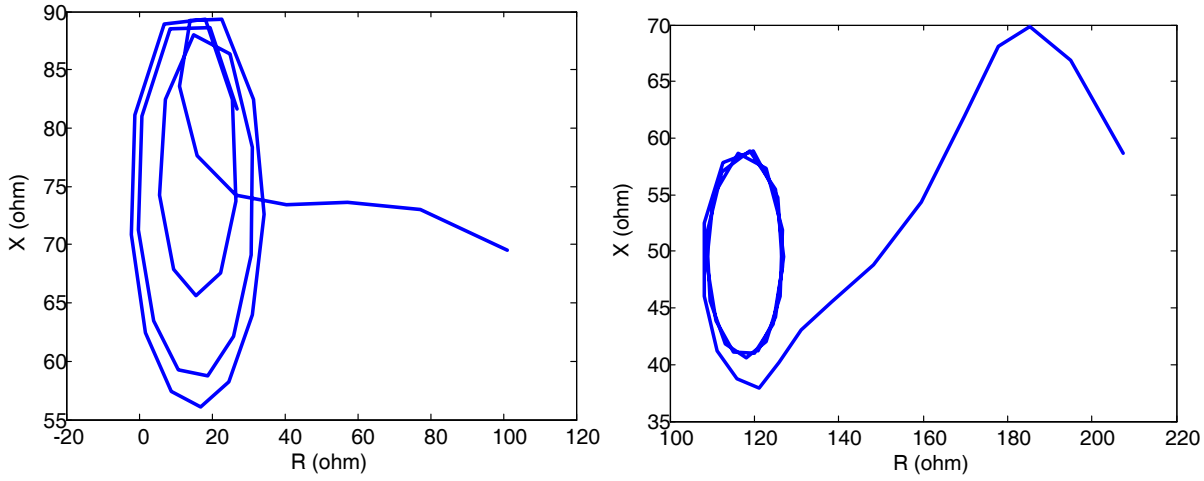

(a) (b)

Fig. 4.6 Impedance trajectory for fault at TCSC point with fault resistance (a) 0.01 Ω (b) 100 Ω

Some critical fault impedance patterns at the far boundary of line for fault resistance 0.01 Ω and 100 Ω is shown in Fig. 4.7(a) and Fig. 4.7(b), respectively.

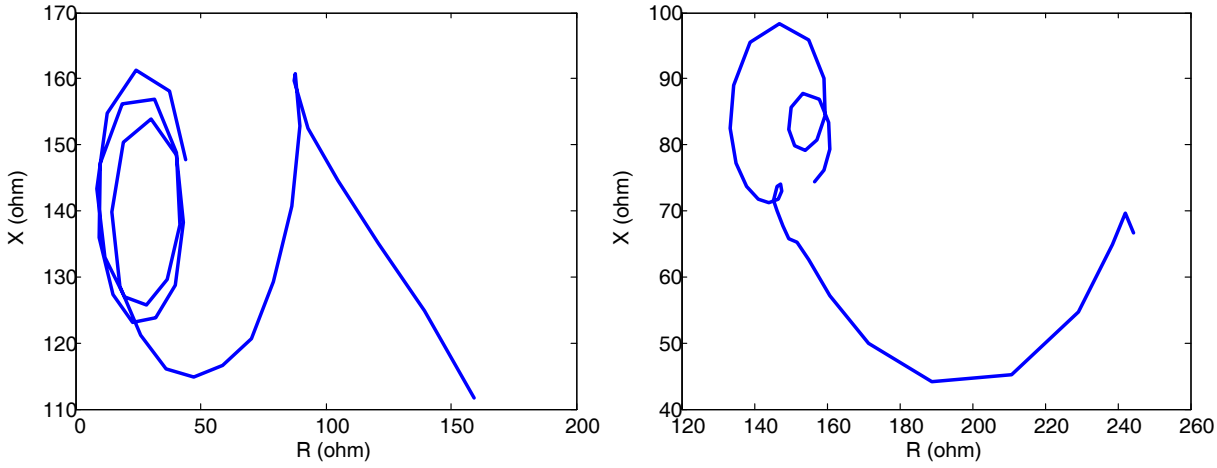

(a) (b)

Fig. 4.7 Impedance trajectory for fault at receiving end & fault resistance (a) 0.01 Ω (b) 100 Ω

Visualization of the impedance patterns have been expressed in the above figures from Fig. 4.5 to Fig. 4.7. It can be concluded from the patterns that impedance trajectory linearly vary with the fault resistance and fault distance from the relay bus. Each fault pattern has two axis, hence, each point in impedance trajectory has two values. Real axis shows the value of effective resistance and imaginary axis shows resultant value of reactance. Therefore, the effective number of input samples for each pattern for AI classifier is to be 80 samples.

Zone setting algorithm is tested with the features generated with the conventional impedance calculation method as well as modified impedance calculation method. Comparative results are discussed based upon the feature selections of generated patterns. Discussion of the training patterns selected for both the techniques is given as follows:

4.4.2 Training Patterns Generated with the Conventional Algorithm

As it has been discussed earlier that conventional impedance measurement algorithm has a lot of limitations when deciding the faulty zone. Here is the discussion of some critical patterns which describes the limits of conventional method for LG and LL fault conditions.

(A) Generated Patterns in LG Fault

To analyze the different training patterns, LG faults are created at the boundary of zone-1 and zone-2 as shown in Fig. 4.8(a). Impedance patterns for fault in zone-1 are shown by green lines and for fault in zone-2 are shown by red lines. LG faults are created throughout the line in zone-1 and zone-2. Due to TCSC compensation, zone-2 patterns fall in zone-2 and create complete overlapping if the compensation is above 30 %. The overlapping patterns cannot be

discriminated easily and create error. Similarly, the overlapping can be seen at the mid-point where TCSC is installed in Fig. 4.8(b).

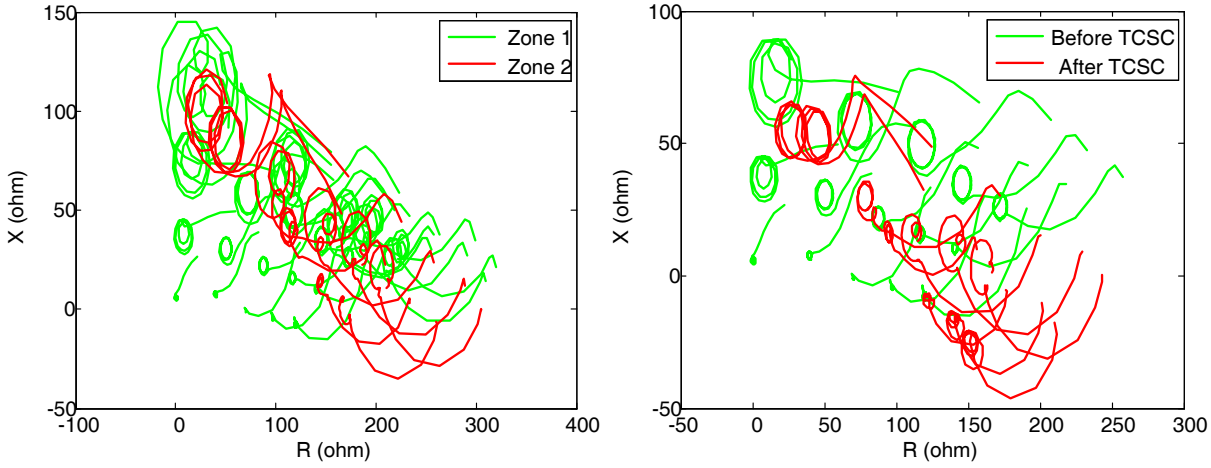

(a) (b)

Fig. 4.8 Overlapping of impedance patterns at (a) zone-1 boundary (b) mid-point location

(B) Generated Patterns in LL Fault

Same as in case of LG fault, effect of TCSC compensation on conventional method can be seen on LL fault at the boundary of zones and at the point of TCSC installation. Fig. 4.9(a) shows that patterns are overlapping at the boundary locations and difficult to discriminate linearly. Also, at mid-point, far distance patterns fall before the pre location fault as shown in Fig. 4.9(b) and can create miss-classification.

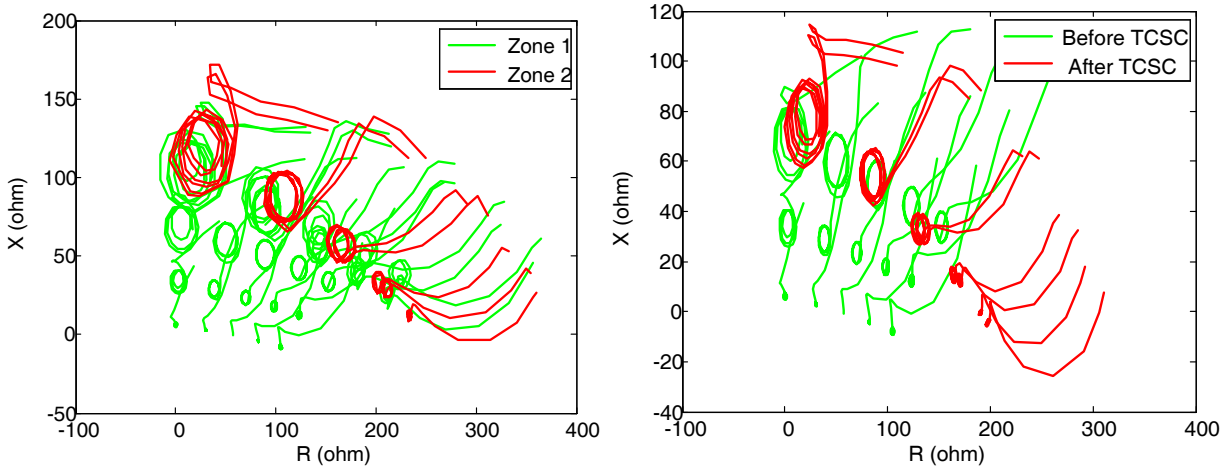

(a) (b)

Fig. 4.9 Overlapping of impedance patterns at (a) zone boundary location. (b) Mid-point

4.4.3 Training Patterns Generated with the Proposed Algorithm

Proposed algorithm calculates the modified impedance parameters after removing the error inserted by TCSC. Proposed method settle the impedance patterns on the proper location and removes the chances of similarity of different locations, hence, increases the accuracy. Following are some taken cases which discuss about the ability of modified impedance parameters to avoid the overlapping of different sections.

(A) Generated Patterns in LG Fault

Modified impedance patterns are generated for LG fault at different locations viz. 1, 80, 160, 220, 272, 320, 350 and 384 km from the sending bus by taking wide range of possible fault resistance such as: 0.01, 50, 100, 150 and 200 ohms. Patterns are produced for different compensation level viz. 7.5, 15, 30 and 50 % as shown in Fig. 4.10 (a) to (d), respectively.

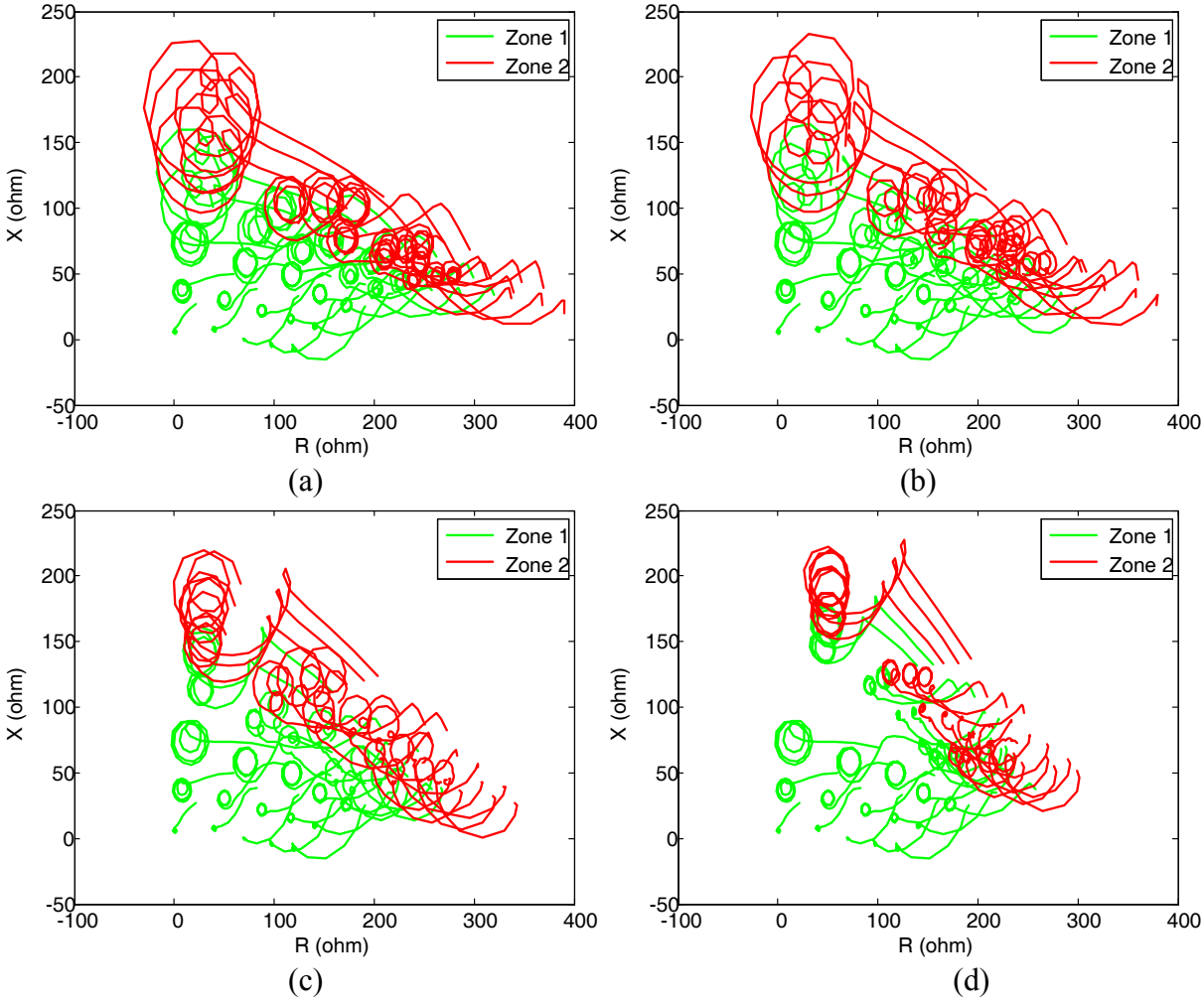

Fig. 4.10 Impedance patterns with power angle 30° and % compensation (a) 7.5 (b) 15 (c) 30 (d) 50

It is clear from Fig. 4.10, that, use of modified impedance patterns avoid the overlapping to a large extend and a boundary can be visualized between zone-1 and zone-2.

(B) Generated Patterns in LL Fault

Similar results for LL faults are generated to validate that, modified impedance parameters improves the input feature vector for AI classifier. LL faults are created between any two phases and wide range of input features are generated which classify the zone boundaries. Again, the proposed method tried to settle the impedance curve at proper locations and minimizes the probability of overlapping as shown in Fig. 4.11.

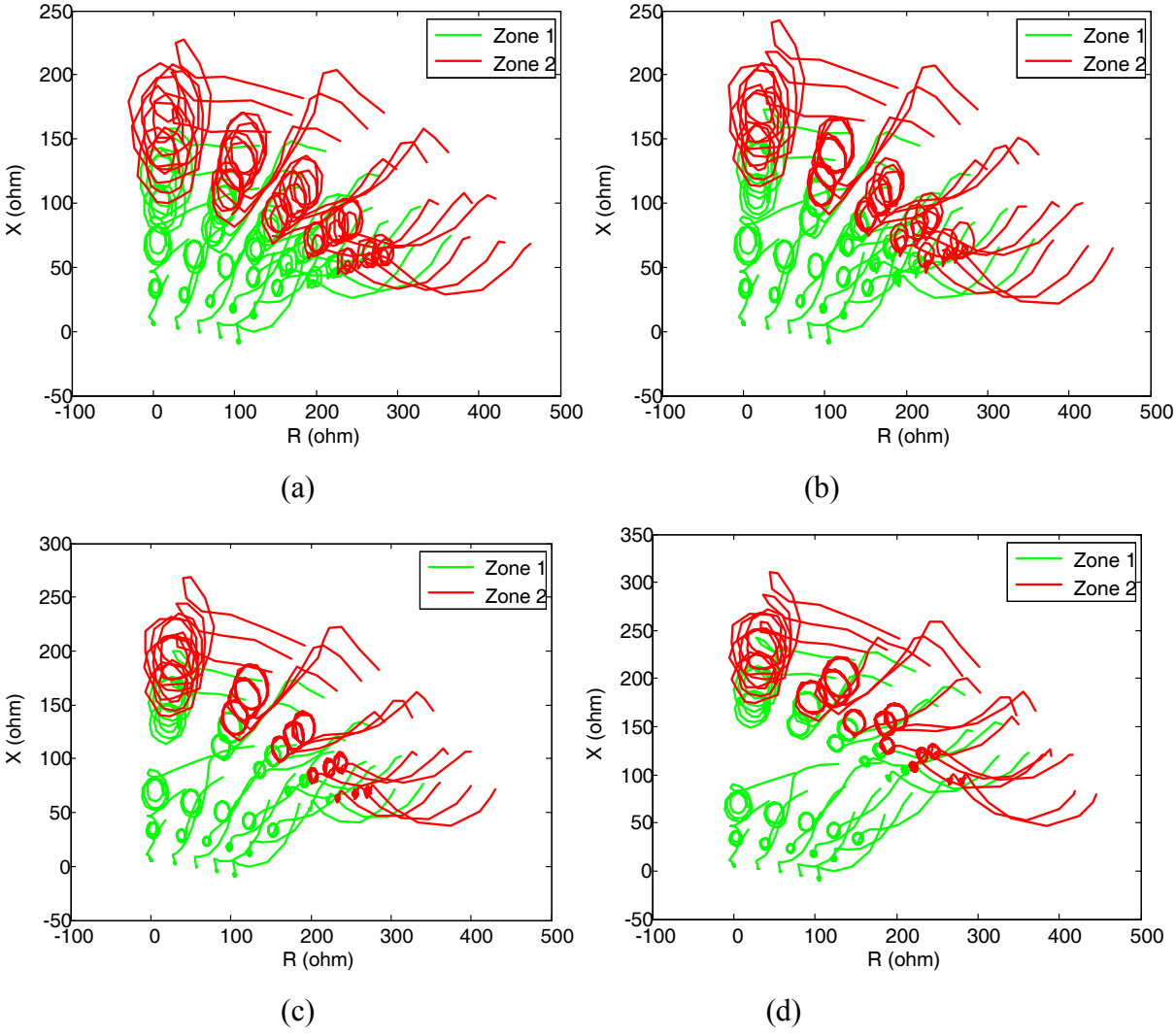

Fig. 4.11 Impedance patterns with power angle 30° and % compensation (a) 7.5 (b) 15 (c) 30 (d) 50

It is clear from analysis of features, that, patterns generated with conventional method for zone-1 are not easy to separate from zone-2 due to similarity and overlapping, while, patterns generated with proposed method is quite clear and separable. AI has the ability to separate the two different types of patterns adaptively and an attempt has been taken to discriminate zone-1 and zone-2 using different AI techniques.

4.5 Signal Processing Tool

Different AI algorithms are used to analyze input patterns and classify the zone-1 and zone-2 faults in series compensated transmission line. A brief summary of all the used techniques has been point out as follows:

4.5.1 Artificial Neural Network

ANN has the ability to classify the high dimension non-linear features of different classes. For zone setting of series compensated line, ANN has been used for classifying the impedance patterns of different zones. Following are some NN structures which have been used for the zone classification purpose in mid-point series compensated network.

4.5.1.1 Back Propagation Neural Network

To solve highly non-linear problem neurons are modeled in multilayer perceptron (MLP), this model has an input layer and a hidden layer. For the perceptron at the input layer, a linear transfer function has been used and for the perceptron in the hidden and output layer sigmoidal function is used. BP is a general method for iteratively solving for a multilayer perceptron's weight and biases. It uses a steepest decent technique which is very stable when a small learning rate is used, but has slow convergence properties. A typical three layer network is shown in Fig. 4.12 in which '*I*' is the input and '*O*' is the output of MLP.

The input output mapping of a three layer perceptron is given by equation (4.6):

$$O = P_3[P_2[P_1[I]]] \tag{4.6}$$

Where P_1, P_2 and P_3 represent nonlinear mapping provided by input, hidden, and output layer, respectively. In FFBPNN, error transmits from output layer towards input layer. If the output of the network is O and target output is T, error norm in the output is given by equation (4.7).

$$E = \frac{1}{2}(T - O)^2 \tag{4.7}$$

In the proposed scheme, total numbers of inputs are 80 (40 each for resistive and inductive portion of impedance), therefore the numbers of neurons in input layer are fixed which is 80 neurons.

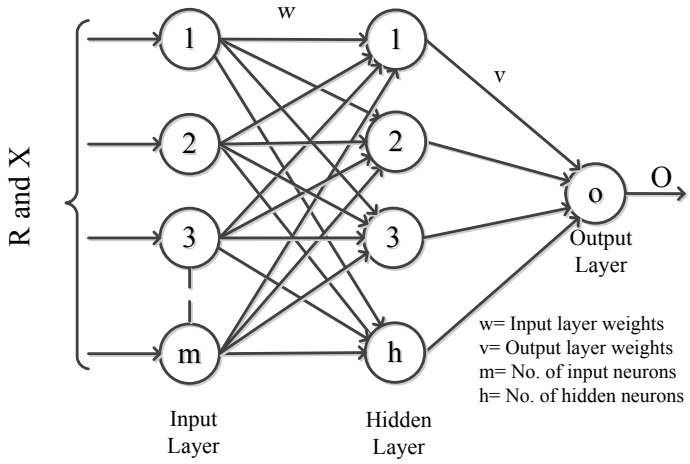

Fig. 4.12 A typical MLP-BPNN structure

4.5.1.2 Radial Basis Function Neural Network

Implementation of RBFNN has been done as discussed in chapter 2, section 2.3.2. In this arrangement, the numbers of input neurons are taken as 80 and hidden layer neurons are optimized for minimization of mean square error which is obtained as 45 neurons. Radial basis kernel function is used as activation function at hidden layer and linear function at input and output layers. Selected structure of RBFNN network is shown in Fig. 4.13.

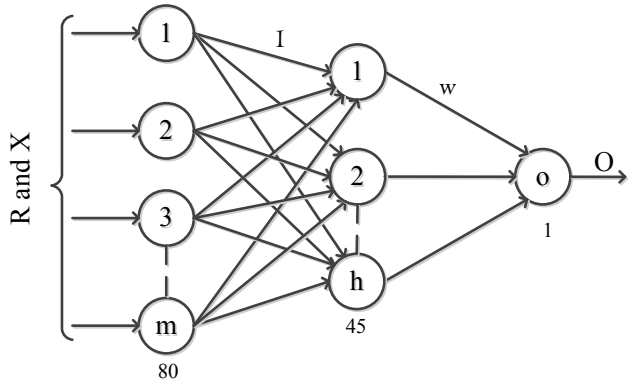

Fig. 4.13 Selected RBFNN structure for zone classification

4.5.2 Support Vector Machine

SVM linearly classifies the non-linear data by mapping it into a high dimensional feature space. Mapping is accomplished by using kernel functions which creates high dimensional feature space. Selection of kernel function is important phase for implementation of SVM for classification. Accuracy of the SVM is tested with different types of kernel functions and it is found that Gaussian radial basis function is best suited for the classification problem. Implementation, objective function and other parameters of SVM are similar as given in chapter-2 section-2.3.3. Different classifier functions like linear, polynomial, Gaussian radial basis and sigmoidal functions can be used as kernel function. These kernel functions based optimal SVM is applied to classify the zones of SVC transmission line. In the proposed algorithm, Radial Basis Function (RBF) has been considered as kernel function because it is advantageous in non-separable classification problem due to its ability of nonlinear input mapping. Performance of different kernel function based upon testing accuracy at data set of different location is shown in Fig. 4.14 which suggests that RBF kernel is best suited for the required classification. RBF kernel required only one parameter, γ ($\gamma = 1/2\sigma^2$, σ is kernel width), to adjust.

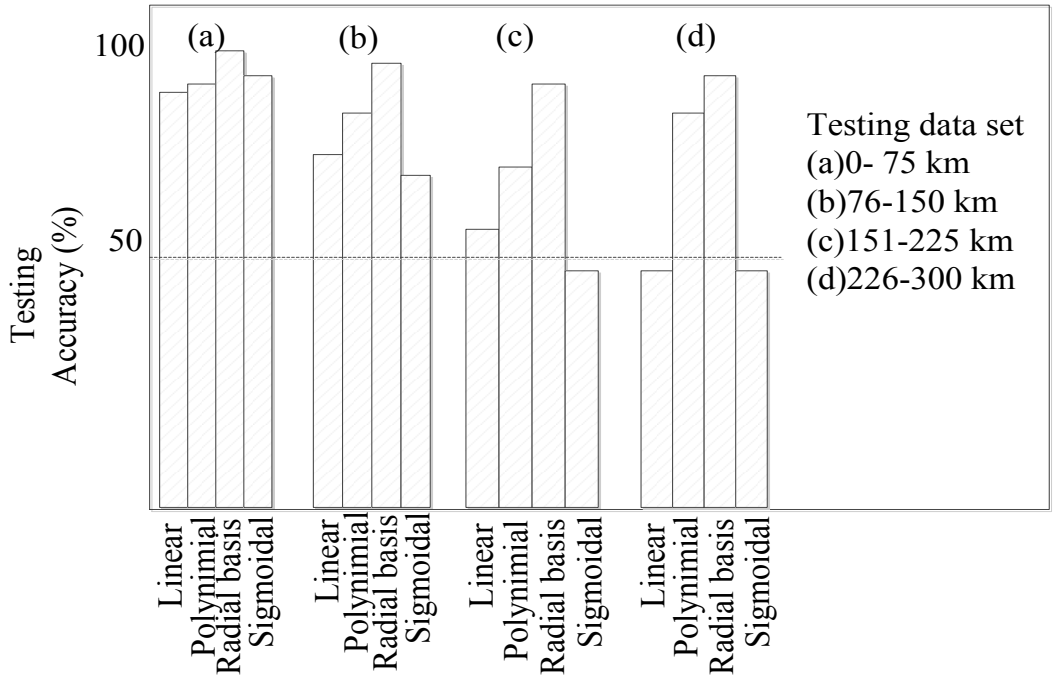

Fig. 4.14 Testing accuracy of different kernel function

4.6 Results and Discussions

Extensive simulations are carried out to evaluate the performance of proposed optimal AI based zone identification techniques. A 230 kV and 320 km long series compensated transmission line is used to test the capability of the proposed algorithm for the zonal setting of Mho relay. To provide the required training and testing data sets, various faults are created at several locations throughout the complete length of transmission line. The details of all the training combination are as follows:

(a) Fault resistance 0.1, 50, 100, 150 and 200 Ω.

(b) Fault inception angle 0, 30, 45, 60, 90, 135 and 180°.

(c) Load angle 1, 10, 20, 30, 40 and 50°.

(d) Fault type AG, BG, CG, AB, BC, CA, ABG, BCG, CAG, ABC and ABCG.

(e) Fault Location 1, 40, 80, 120, 140, 160, 200, 240, 280, 320, 360, 384 km.

Thus, total training data points generated at each location are 5*7*6*11= 2310 and total numbers of locations taken for data generation are 12 so total numbers of training data patterns are 2310*12 = 27720. The first zone of the Mho relay is set to protect 85 % (272 km) of the transmission line, the second zone is set to protect rest of the line and assumes extended section which may stretch in next adjacent line (not shown in the test diagram) up-to 384 km from relay bus 'A'.

The details of testing patterns for evaluating the classifier performance are given below.

(a) Fault resistance 0, 60, 120 and 180 Ω.

(b) Inception angle 10, 50, 100 and 150°.

(c) Load angel 15, 35 and 45°.

(d) Fault type AG, AB, ABG, ABC and ABCG.

(e) Fault Location 20, 100, 180, 260, 340, 380

Total number of testing patterns at a particular location is 4*4*3*5*6 = 1440. After randomize the testing patterns they are randomly selected for the testing of AI zone classifiers. For comparison purpose two sets of training and testing data stored each for conventional and modified AI classifier.

4.6.1 Performance of ANN Classifiers

Performance of FFBPNN and RBFNN is compared for fault zone classification of mid-point series compensated transmission network. Both the classifiers are analyzed with same

number of training and testing patterns. RBFNN has less number of parameters to be tuned than FFBPNN, therefore, it takes less time for training. Testing accuracy of both types of classifier for the conventional and proposed algorithm is given in Table 4.2. It has been observed from Table 4.2 that the accuracy of both classifiers is less in case of the conventional type of algorithm which is due to overlapping of patterns. Accuracy of the classifiers increases with the proposed algorithm because modified impedance parameters are taken as input which reduces the chance of overlapping. Also, it has been detected from the Table 4.2 that the performance of RBFNN is better than FFBPNN algorithm. Overall, it can be concluded from Table 4.2 that use of modified impedance patterns with RBFNN classifier is the best combination which can be used for classification.

Table 4.2 Accuracy of different ANN classifier

S. No	Algorithm Type	Type of ANN	Training Patterns	Testing Patterns	Correctly Classified	Testing Accuracy (%)
1	**Conventional**	**BPNN**	27720	1000	671	67.1
		RBFNN	27720	1000	704	70.4
2	**Proposed**	**BPNN**	27720	1000	877	87.7
		RBFN	27720	1000	935	93.5

Maximum classification accuracy obtained with the ANN classifier is 93.5 % with the proposed algorithm. There is a further need to improve the zone classification accuracy. Therefore, the work has been extended towards the application of SVM for classification which has better classification ability with less number of parameters to be tuned.

4.6.2 Application of SVM for Zone Classification

Different zone patterns are analyzed with SVM classifier to test the accuracy of classification. Performance of SVM classifier is tested at different value of parameters. Maximum accuracy of classification is obtained at C= 128 and $\gamma = 1$ from the selected value as shown in Table 4.3.

Table 4.3 Cross validation accuracy of SVM at different parameters

C	γ	% Accuracy
1	0.125	92.1
8	0.250	93.5
32	0.500	93.9
128	1	96.3
512	2	94.8
4096	8	92.0
32768	32	88.2

Table 4.4 indicates the comparative performance of RBFNN and SVM for same classification feature. SVM acquires maximum classification accuracy 96.3 % with modified impedance patterns as input as shown in Table 4.4.

Table 4.4 Comparative performance of SVM and RBFNN classifier

S. No.	AI Type	Training time taken (sec)		Testing accuracy (%)	
		Conventional	Modified	Conventional	Modified
1	**RBFNN**	124	131	69.9	93.1
2	**SVM**	45	34	71.2	96.3

It has been concluded from the Table 4.4 that, SVM classifier is best suited for the zone classification in mid-point series compensated transmission line. Further, the parameters of SVM classifier have been optimized to obtain maximum possible zone classification accuracy. For classification purpose genetic optimization tool has been used in Matlab-2013.

4.6.3 Optimization of SVM Parameters: Genetic Algorithm

A Genetic Algorithm (GA) is a search algorithm based on the mechanism of natural selection and natural genetics motivated from biological genetic evolution. Its fundamental principle is that the fittest member of a population has highest probability for survival. A GA operates in a population of current approximations, the individuals, initially drawn in a random order, from which improvement is sought. Individuals are encoded as strings, the chromosomes,

so that their values represent a possible solution for a given optimization problem. It starts with guessing initial population in the feasible region, then, value of fitness function is evaluated for individuals of this population and from this population the next generation is produced on the basis of some criteria. This process is continued for next generations until some stopping criterion is not met. Best individuals are passed from one generation to next generation on the principle of survival of the fittest. It can be anticipated that solution will improve with coming generations. Best individual obtained after last generation represents the global optimal solution.

SVM has cost function (C) and parameters related to kernel function parameters. Different classifier functions like linear, polynomial, Gaussian radial basis and sigmoidal functions can be used as kernel function. These kernel functions based optimal SVM is applied to classify the zones of SVC transmission line. In the proposed work, Radial Basis Function (RBF) has been considered as kernel function. RBF kernel required only one parameter γ ($\gamma = 1/2\sigma^2$, σ is kernel width) to adjust. SVM classifier has two parameters (C, γ) and finding optimal value of these parameters is necessary for efficient performance of SVM. In present work, these values are estimated using Genetic-Algorithm (GA) [15-16].

SVM training and testing is performed using libsvm-mat-2.91-1 and GA is applied from MATLAB's Global Optimization Toolbox to search the best value of SVM-parameters (C, γ) based on fitness function of maximizing the Cross Validation (CV) accuracy. The range of C chosen for training is $\{2^0$ to $2^{15}\}$ and γ ranges from $\{2^{-3}$ to $2^5\}$.

The fitness function of GA to maximize classification accuracy obtained using 5-fold cross-validation is defined as:

max $f(C, \gamma)$ = max (*CV-accuracy*),

Where,

CV-accuracy= (Correctly classified patterns*100)/ (Total number of patterns)

Properties of GA to find the optimal value of "C" and "γ" are as follows:

Population size = 20

Stopping Criteria: Fitness Limit =0.002 and Stall generation limit = 5

With the obtained training parameters (C, γ) of SVM by using GA optimization the obtained testing accuracy at different location is shown in Table 4.5.

Table 4.5 Classification accuracy of the proposed optimal SVM classifier at different locations

S. No.	Testing data at location (in km from bus A)	Total number of samples	Correctly classified samples	Percentage testing accuracy
1.	40	500	486	97.2
2.	80	500	485	97.0
3.	120	500	485	97.0
4.	160	500	481	96.2
5.	200	500	480	96.0
6.	240	500	488	97.6
7.	280	500	487	97.4
8.	320	500	489	97.8
9.	360	500	490	98.0

From the above observations, it is clear that the trained SVM classifier is robust under different operating conditions and well suited for zone discrimination scheme in distance protection of mid-point series compensated transmission line.

4.7 Summary

Fault zone in mid-point series compensated transmission line has been classified successfully in this chapter. Classification accuracy is checked with different AI classifiers with modified and conventional impedance parameters. It is concluded that classification accuracy is best with modified impedance parameters as input along with SVM as classifier. Classification accuracy of the SVM classifier increases slightly when the parameters of classifiers are optimized with genetic algorithm.

In the next chapter adaptive Mho relay algorithm has been developed for the protection of shunt compensated transmission line.

CHAPTER 5
SHUNT COMPENSATED TRANSMISSION NETWORK PROTECTION

This chapter presents a compensated Mho relay algorithm for a transmission system having shunt FACTS devices at the mid-point of line. The proposed Mho relay is a combination of the conventional Mho relay with an additional compensation unit. Shunt FACTS device inserts additional equivalent impedance in the fault loop which depends on the current injected by the particular FACTS device. The impedance by which the shunt device compensates the fault impedance is calculated online at relay point. Calculated compensated impedance creates error in actual impedance measurement, finally the error can be eliminated at the relay point with the help of a compensation unit. This improves security, accuracy and reliability of the Mho relay for protection of the transmission line having shunt FACTS device.

5.1 Introduction

All the FACTS devices affect steady state and transient response of voltage and current during normal and fault condition. FACTS devices affect distance protection scheme during faulty/ transient condition because it is based on the voltage and current response at the relay point. SVC and STATCOM are important shunt FACTS devices and widely used all over the world. They maintain constant line voltage at the point of connection in transmission line and preferably connected in the middle of the line because voltage sag is maximum in middle. Both the devices inject current at the point of connection to the line. SVC is a parallel combination of Thyristor Controlled Reactor (TCR) and Thyristor Switch Capacitor (TSC). STATCOM is a Voltage Source Convertor (VSC) based device so it has better control and can supply a constant current over the complete voltage profile.

Shunt FACTS devices supply or absorb current into the connecting bus [1]–[3]. According to the direction of current injection into the transmission line, distance relay shows under-reaching or over-reaching effects [182]. The goal of distance protection is to calculate the impedance between relay and fault point. If FACTS device is located in between relay and fault point, it inserts equivalent impedance in fault loop and the relay therefore is not able to calculate the correct fault impedance which leads to accuracy, security and reliability problems.

In literature, research has been done on the impact of shunt and combined series–shunt device like UPFC (Unified Power Flow Controller) on distance protection of transmission line.

SVC and STATCOM affect the performance of distance protection relays when applied to protect transmission network. It was found that mid-point FACTS compensation can affect the distance relays with regard to impedance measurement, phase selection and operating times leading to under-reaching and over-reaching [53], [64]. The action of the STATCOM, even at a reduced small rating, increases the resistance to reactance ratio of the line that results in under-reaching phenomena of the impedance relay is discussed in [18] but suitable remedial measures for the protection are not deliberated.

Zone protection of transmission network which employ STATCOM is presented in [159] and new setting principles for different protection zones are proposed but the strategy would be different with SVC that works as variable current source. Authors in [182] presented the effects of UPFC on the measured impedance at the relaying point. In addition to UPFC controlling parameters, its installation point also affects the measured impedance [20], [183]–[185]. Due to variation in UPFC controlling parameters tripping characteristics of relay changes hence an adaptive quadrilateral characteristic is proposed in [147]. An expensive differential current protection scheme for the protection of transmission line having shunt FACTS device is presented in [160].

Apparent impedance calculations for a transmission line operating with UPFC are presented and it is suggested that an Artificial Intelligent (AI) approach for on-line calculation of boundaries during a distance relay operation is convenient [186]. ANN based adaptive relaying scheme computes on-line control parameters of the UPFC based on synchronized phasor measurements from Phasor Measurement Units (PMU) installed at line terminals [187]. Work in [188] concludes useful contribution about the apparent impedance calculation for distance protection in case of transmission line having series devices viz. UPFC , TCPST and TCSC however it does not include the impact and apparent impedance calculation in case of transmission line having shunt FACTS devices like SVC and STATCOM.

A lot of effort has been taken to analyze the impact of SVC and STATCOM on transmission network. However a robust and adaptive protection algorithm is needed to protection mid-point shunt compensated transmission line which takes care of all operating modes of the device. In the proposed work a compensated Mho relay algorithm is proposed which compensates the inaccuracy due to device into the fault impedance measurement and removes it at relay end. Description of the impact of shunt FACTS devices on distance protection based upon the V-I characteristics has been explained as follow.

5.2 Shunt FACTS Device and Impact on Distance Relay

There are mainly two types of shunt FACTS device (i) SVC and (ii) STATCOM. Both the devices affect the distance relay performance according to their V-I characteristics. SVC and STATCOM regulate voltage at the connecting bus by injecting a current in quadrature to the driving line voltage and in phase with line current. Current injected by SVC into the connecting bus linearly vary with the line voltage at that point i. e. it works as a variable current source over the operating characteristic as shown in Fig. 5.1(a).

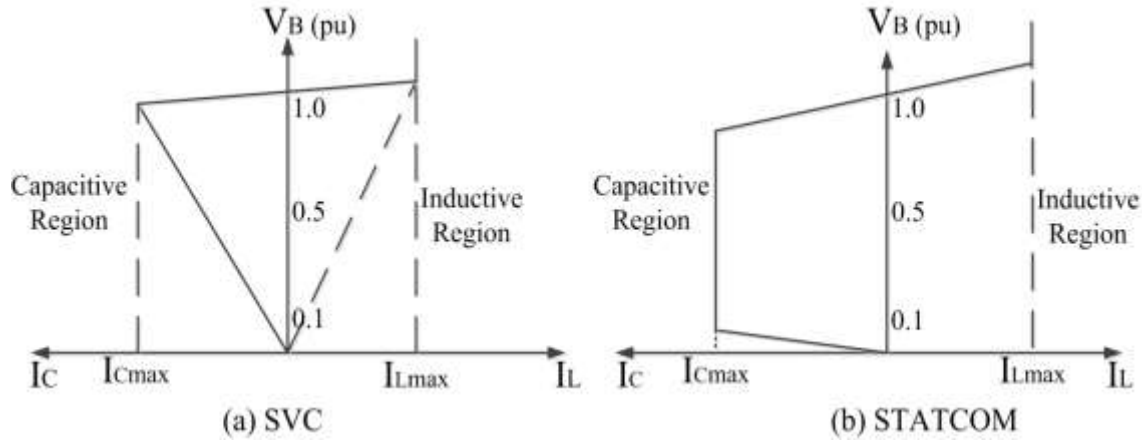

Fig. 5.1 Operating V-I characteristic of shunt FACTS devices [1-3]

STATCOM injects a constant current into the line so it acts as a constant current source over the operating characteristic as shown in Fig. 5.1(b). It has been observed from Fig. 5.1 that STATCOM has larger impact on the V-I characteristics and hence larger impact than SVC on the distance protection of line. Both the devices work in two modes of operation viz. (i) Capacitive mode, and (ii) Inductive mode. In case of heavy loads, line voltage drops below reference value or permissible value and the shunt FACTS device works in capacitive mode and supply current into the bus and hence injects reactive power to the system. In this case, net impedance of transmission line increases, therefore, distance relay shows under-reaching effects. Whereas, in case of light load or capacitive load condition, line voltage increases due to Ferranti effect and shunt FACTS device works in inductive mode and takes current from the system and absorb reactive power from the system. So, in inductive mode, net line impedance reduces and relay shows over-reaching effects. The amount of impedance added or subtracted by the shunt FACTS devices in capacitive or inductive mode, respectively, is a function of current injected by the device [1], [3]. Based upon the analysis of V-I characteristics of shunt

FACTS devices, an adaptive distance protection algorithm can be developed which is adaptive w.r.t. the action of shunt FACTS device. System modeling and descriptive steps of proposed algorithms are given in next sections.

5.3 System Modeling

Fig. 5.2 shows the single line diagram of SVC and STATCOM in a doubly fed transmission test system simulated in PSCAD/EMTDC software. SVC and STATCOM connections at bus 'C' are separately shown in Fig. 5.2(a) and (b), respectively. Fig. 5.2(a) shows transmission line with equivalent SVC of capacitive rating 167 MVA and inductive rating 100 MVA and Fig. 5.2(b) illustrates the transmission line with equivalent circuit of STATCOM of power rating ± 100MVA [158], [167].

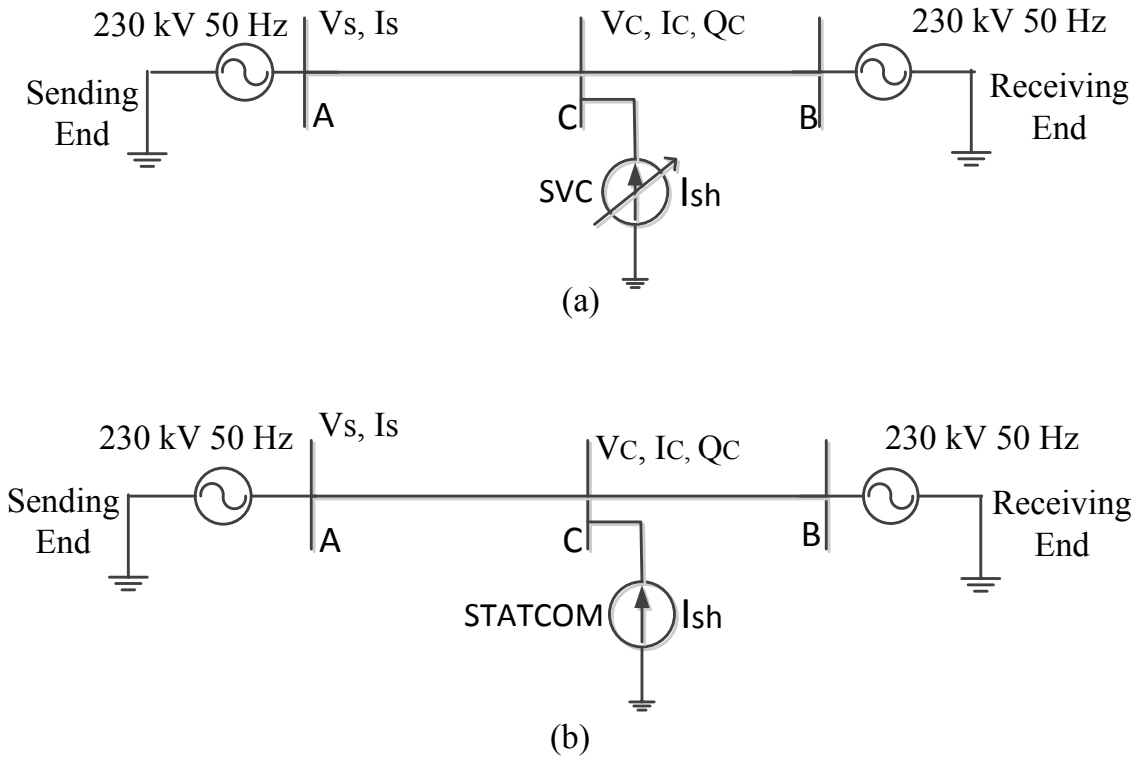

Fig. 5.2 Typical single line diagram of test system for (a) SVC and (b) STATCOM

The proposed Mho relay is used for protection of a typical 230 kV, 50 Hz, 320 km long power transmission network. A doubly fed transmission line is connected between bus 'A' and 'B'. Parameters of the source have been given in Appendix-A. Per km sequence impedances of transmission line in ohms are: $Z1$ = 0.0362 + j0.508, $Z2$ = 0.0362 + j0.508 and $Z0$ = 0.365 +

j1.33. Mho relay is set to protect 85 % of transmission line and placed at sending end of bus 'A'. The distance relay (Mho relay) at bus 'A' monitors phase voltage (V_s) and line current (I_s) through a Coupled Capacitor Voltage Transformer (CCVT) and Current Transformer (CT) respectively [177]. Parameters of the CCVT and CT are given in Appendix-B. Zone-1 impedance setting of the Mho relay is 85 % of transmission line impedance, i.e. Z_{set} = 138.227 Ω. Shunt FACTS device is placed at 160 km from the sending end generator at coupling bus 'C'. The Bus Voltage V_C, current I_C, reactive power Q_C and current injected by shunt FACTS device I_{sh} are measured at coupling bus. SVC and STATCOM are thyristor based devices hence they need a firing angle control logic to fire the thyristors. Fig. 5.4 elaborates the control logic of SVC for generation of Alfa order to thyristors. Voltage is measured at the coupling bus with 3 % droop. Reference voltage is 1.0 p.u. and minimum voltage to be regulated is 0.08 p.u. of the system voltage. A Proportional plus Integral (PI) controller provides the susceptance of the SVC and with the help of SVC susceptance (B_{svc}) characteristic, susceptance of TCR (B_{tcr}) is calculated which provides the Alfa order of thyristors.

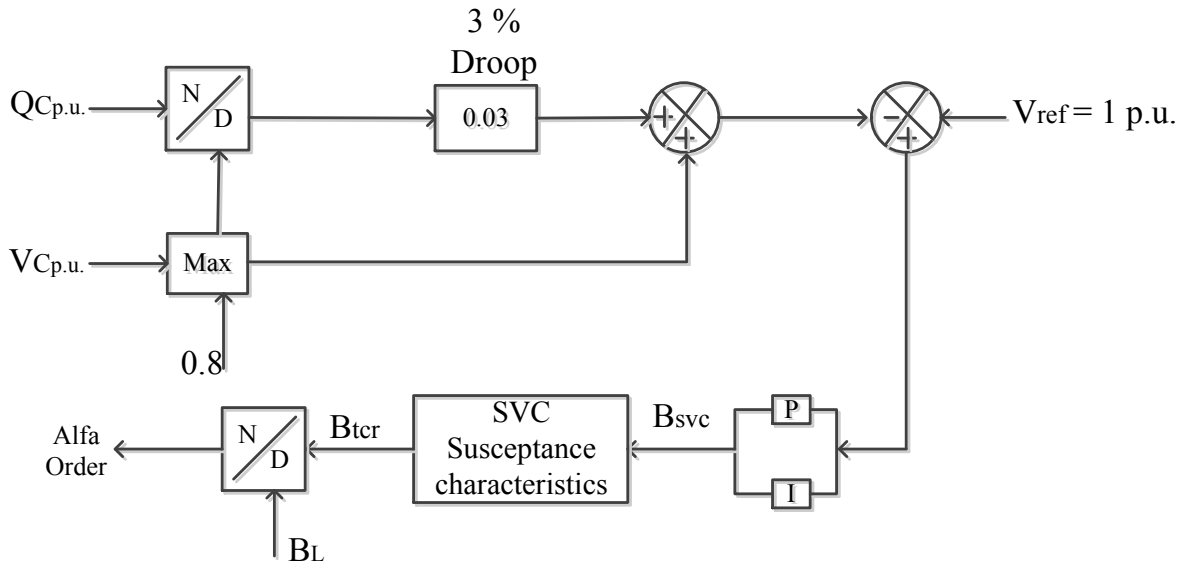

Fig. 5.3 Alfa order generation for SVC

Similarly the Alfa order of thyristors for STATCOM has been generated according to Fig. 5.4. STACOM can supply the needed reactive power even at the voltage of 0.1 p.u., which is used to calculate the measured input voltage for PI controller. A lead-lag controller has been added before the PI controller to limit the Alfa order within the limit. In the proposed work, 6-

pulse STATCOM with Pulse Width Modulation (PWM) control is used to boost voltage level at mid-point. PWM frequency is selected 33 times higher than the base frequency which reduces all dominating harmonics.

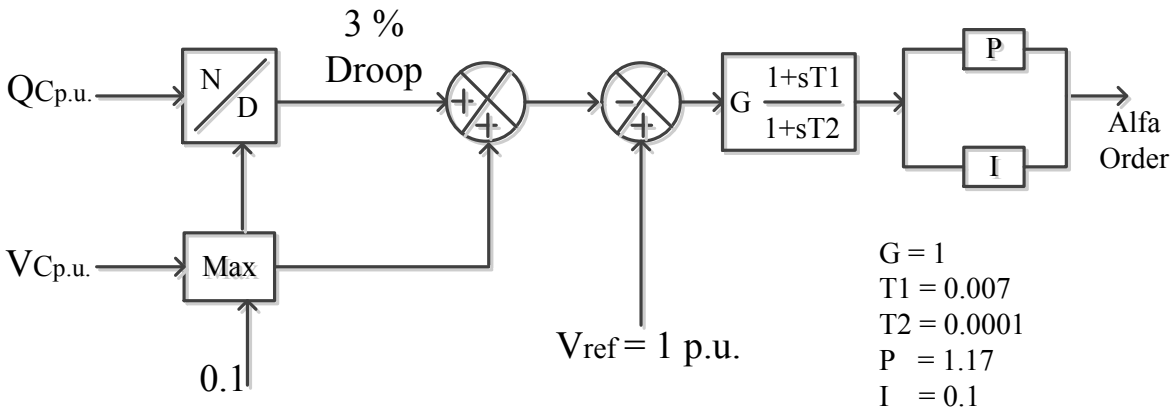

Fig. 5.4 Alfa order generation for STATCOM

All the measurements (voltages and currents) at bus 'C' are transmitted through a fiber-optic communication channel to bus 'A' and fed to the Mho relay compensation unit. In compensation unit, equivalent impedance inserted by the shunt FACTS device in the transmission line is calculated, which is a function of Current (I_{sh}) injected by FACTS device. This is the impedance by which shunt FACTS device compensates the transmission line in healthy and faulty conditions. In PSCAD/ EMTDC software fibre optic communication channel is simulated by using transmitter /receiver tools by taking data signal as global variable assuming that relaying signal is perfectly transmitted in a fibre-optic channel.

5.4 Proposed Compensated Mho Relay Algorithm

Synchronized measurement of voltage and current based on accurate time reference takes place in between bus 'A' and 'B' as shown in Fig. 5.5 [189]. Fig. 5.5 describes the proposed Mho relay algorithm for the protection of transmission line with shunt FACTS devices. In this algorithm, the conventional Mho relay algorithm is modified by adding a fault impedance compensation unit. The compensation unit computes the compensated impedance (Z_{comp}) introduced by shunt FACTS device in fault loop which is a function of shunt injected current I_{sh}, coming from bus 'B' via a fast communication channel. Relay at bus 'A' takes voltage and current signal through CCVT and CT, respectively. Fault impedance Z (R and X) is

calculated by conventional method at the relay point using fundamental and sequence components of fault voltage and current signal, respectively [177].

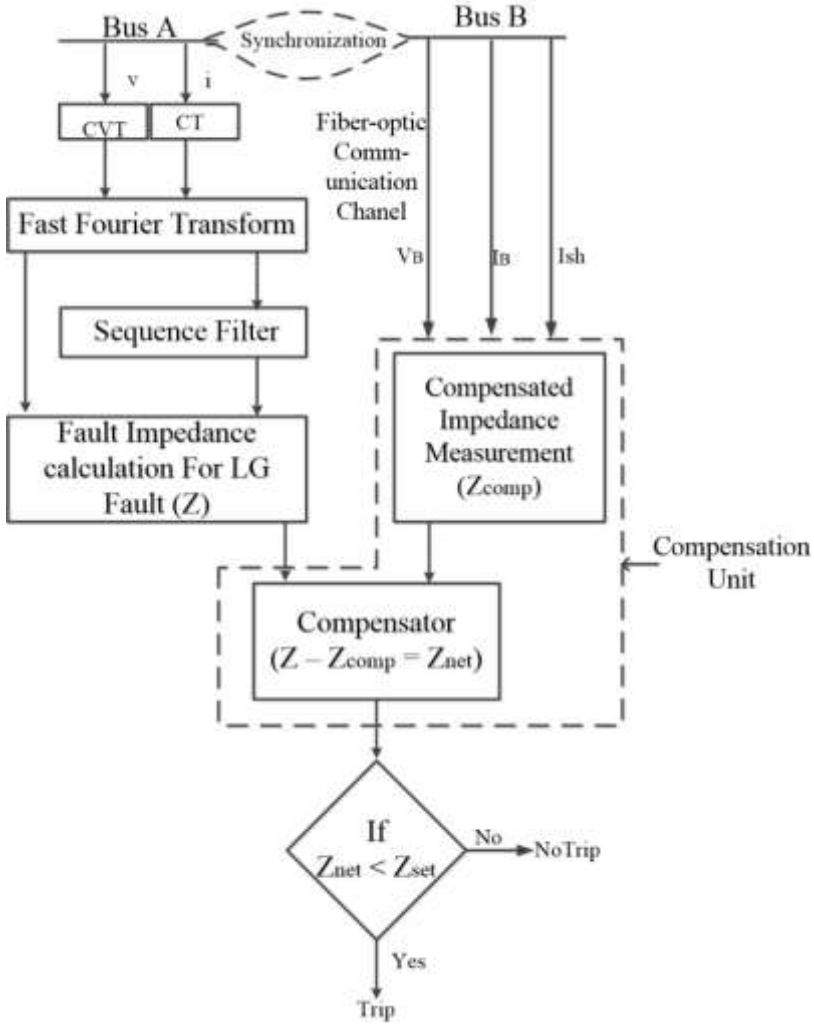

Fig. 5.5 Proposed Mho relay algorithm

Fast Fourier Transform decomposes the transient voltage and current into the fundamental quantity and sequence filter gives the positive and zero sequence value of current. In conventional Mho relay algorithm the equivalent fault impedance at bus A can be calculated by equation (5.1) [11]:

$$Z = \begin{Bmatrix} \dfrac{V}{I + \mathrm{k}\, I_0}, \text{ For LL fault} \\ \dfrac{V_{1s} - V_{2s}}{I_{1s} - I_{2s}}, \text{ For LL fault} \end{Bmatrix} \tag{5.1}$$

Where, $k = \dfrac{Z_0 - Z_1}{Z_1}$

V and I are the phase voltage and current, respectively.

Z_0 and Z_1 are the zero and positive sequence impedances, respectively.

V_{1s} and V_{2s} are positive and negative sequence voltage respectively.

I_{1s} and I_{2s} are positive and negative sequence current respectively.

I_0 is zero sequence component of fault current.

Finally, net line fault impedance (Z_{net} = Z- Z_{comp}) is calculated by compensator which is then fed to conventional Mho relay to decide whether the fault is within the reach (Z_{set}) or not. Proposed Mho relay compensation unit instantaneously calculates the compensated impedance (Z_{comp}) of shunt FACTS device and simultaneously compensate it form the measured impedance (Z) at relay point.

5.4.1 Compensate Impedance Calculation

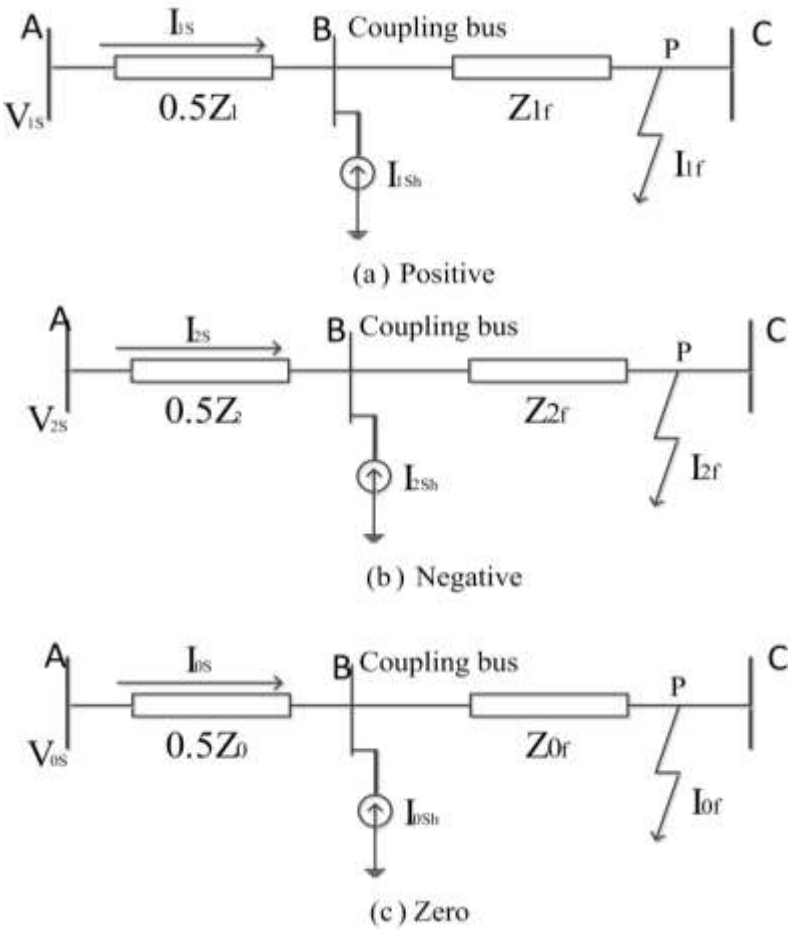

Fig. 5.6 Sequence network for LG fault at point P

Equivalent sequence network for phase-to-ground (L-G) fault at point 'P' is shown in Fig. 5.6. It is assumed that shunt device is connected at 50 % of the total transmission line length and a solid (fault resistance $R_f = 0$) L-G fault occurred at right side of the shunt FACTS device. From Fig. 5.6, the sequence voltages at relay point (bus 'A') can be obtained by applying Kirchhoff Voltage Law (KVL) [20].

In Fig. 5.6(a), the resultant current flowing through the impedance Z_{1f} is $(I_{1s} + I_{1sh})$. By applying KVL in positive sequence circuit of Fig. 5.6(a), voltage equation (5.2) is given by:

$$V_{1s} = I_{1s}\,(0.5)\,Z_1 + (I_{1s} + I_{1sh})\,Z_{1f} \tag{5.2}$$

Similarly, the KVL equations can be written for the negative and zero sequence circuit as equation (5.3) and (5.4), respectively.

$$V_{2s} = I_{2s}\,(0.5)\,Z_2 + (I_{2s} + I_{2sh})\,Z_{2f} \tag{5.3}$$

$$V_{0s} = I_{0s}\,(0.5)\,Z_0 + (I_{0s} + I_{0sh})\,Z_{0f} \tag{5.4}$$

Where,

V_{1s}, $V_{2s}$and V_{0s} are the sequence voltages at sending end (relay point).

Z_0, $Z_1$and Z_2 are zero, positive and negative sequence impedance of transmission line, respectively.

Z_{0f}, $Z_{1f}$and Z_{2f} are zero, positive and negative sequence impedance of transmission line from mid-point to fault point 'P', respectively.

I_{1s}, $I_{2s}$and I_{0s} are the sequence currents at sending end.

I_{1sh}, $I_{2sh}$and I_{0sh} are the sequence currents injected by FACTS device at bus 'B'.

Total voltage at the relay point can be calculated by equation (5.5):

$$V_s = V_{1s} + V_{2s} + V_{0s} \tag{5.5}$$

Using equation (5.2) to (5.5), relay bus voltage can be written by equation (5.6):

$$V_s = (0.5\,Z_1 + Z_{1f})\,(I_s) + I_{0s}\,(Z_0 - 0.5\,Z_1) + Z_{1f}\,(I_{sh}) + (Z_{0f} - Z_{1f})\,I_{0s} + (Z_{0f} - Z_{1f})\,I_{0sh} \tag{5.6}$$

For single phase to ground fault, apparent equivalent impedance (Z_{eq}) of distance relay at bus 'A' can be calculated using equation (5.7):

$$Z_{eq} = \frac{V_s}{I_{relay}} = \frac{V_s}{I_s + \frac{Z_0 - Z_1}{Z_1} I_{0s}} = \left(0.5\, Z_1 + Z_{1f}\right) + \frac{I_{sh}}{I_{relay}} Z_{1f} \quad (5.7)$$

First portion ($0.5\, Z_1 + Z_{1f}$) of the equation (5.7) is the actual fault impedance which includes the positive sequence impedance of fault point to relay point and arc resistance. Second portion ($\frac{I_{sh}}{I_{relay}} Z_{1f}$) of the equivalent impedance is directly proportional to the current (I_{sh}) injected by the shunt FACTS device into the coupling bus and this is the impedance inserted by shunt compensator in transmission line, can be termed as compensated impedance (Z_{comp}) given by equation (5.8).

$$Z_{comp} = \frac{I_{sh}}{I_{relay}} Z_{1f} \quad (5.8)$$

This impedance creates error and is responsible for mal-operation of Mho relay. If shunt FACTS device is SVC, then I_{sh} is in between 0 to I_{Cmax} in capacitive mode and 0 to I_{Lmax} in inductive mode. I_{sh} depends on the terminal voltage V_B as shown in Fig. 5.1(a). In case of STATCOM, I_{sh} is independent of terminal voltage and inject a fix current I_{Cmax} or I_{Lmax} in capacitive mode or inductive mode, respectively as shown in Fig. 5.1(b). The compensated impedance depend upon current injected by compensator (I_{sh}), relay current (I_{relay}) at bus 'A' and positive sequence impedance (Z_{1f}) transmission line from midpoint to fault point which can be calculated by taking voltage and current measurement at coupling bus 'B'.

5.4.2 Requirement of Communication Channel

The proposed Mho relay requires a reliable and high speed communication channel in between coupling bus 'B' to the Mho relay location. Three phase Voltages and currents are measured at bus 'B'. Communication channel transmits these measured signals to the relay location to calculate compensated impedance. In this work, reliability of the proposed protection algorithm depends on the reliability and fastness of the communication channel. It is assumed that the communication channel is reliable and fast enough to send measured current and voltage signal from coupling bus 'B' to relay bus A for any fault in between bus 'B' and 'C'. If there is any fault in between bus 'A' and 'B', communication channel breaks and does not send any signal, in this case I_{sh}=0, i.e. relay behaves normally as a conventional relay. The newly built EHV/UHV transmission lines are equipped with dedicated fiber-optics channels

through which the signals are transmitted from one end of the transmission line to the other [156], [178][190]. In PSCAD/EMTDC signals are transmitted between the buses through the transmitter and receiver arrangement which insets no delay in communication between the buses.

5.5 Results and Discussion

Proposed Mho relay protection algorithm has been tested on a 230 kV, 50 Hz, 320 km long, mid-point shunt compensated transmission line. The Mho relay is set to protect up to 85% of the line (272 km) for zone-1. Experiment has been carried out on the typical test system to check the accuracy, reliability and security of the proposed Mho relay. To check the over-reach and under-reach effects, L-G faults are created at different locations within zone-1 and beyond zone-1, under various load angles (10° to 50°) and wide range of fault resistance (0.01 to 50 ohms). It is observed that the proposed relay senses the fault within 0.01 second (less than half cycle), after the occurrence of fault. Following various cases have been taken to verify the capability of proposed Mho relay algorithm.

5.5.1 Relay Performance with SVC

Case 1: Test to check Under-Reaching effect (Capacitive Mode)

In capacitive mode, net impedance of transmission line increases. So, if there is fault within zone-1, the conventional relay realizes the fault outside the zone-1 and cannot sense the fault, on contrary, the proposed relay compensates the error caused by SVC in impedance measurement and trip for any fault within zone-1.

Comparative performance of conventional and proposed Mho relay is shown in Fig. 5.7. To check the performance, LG faults are created at boundary location of zone-1 i.e. at 265 km from the sending end, with taking variations in load angle from 10° to 50°. Proposed relay is also tested for wide variation in fault resistance (0.01 Ω to 50 Ω). Fig. 5.7 suggests that the proposed relay trips for fault within the zone-1 while the conventional relay mal-operates. It is also observed from the results that the proposed Mho relay shows more tolerance than the conventional Mho relay for fault resistance if the fault is at the boundary of zone-1.

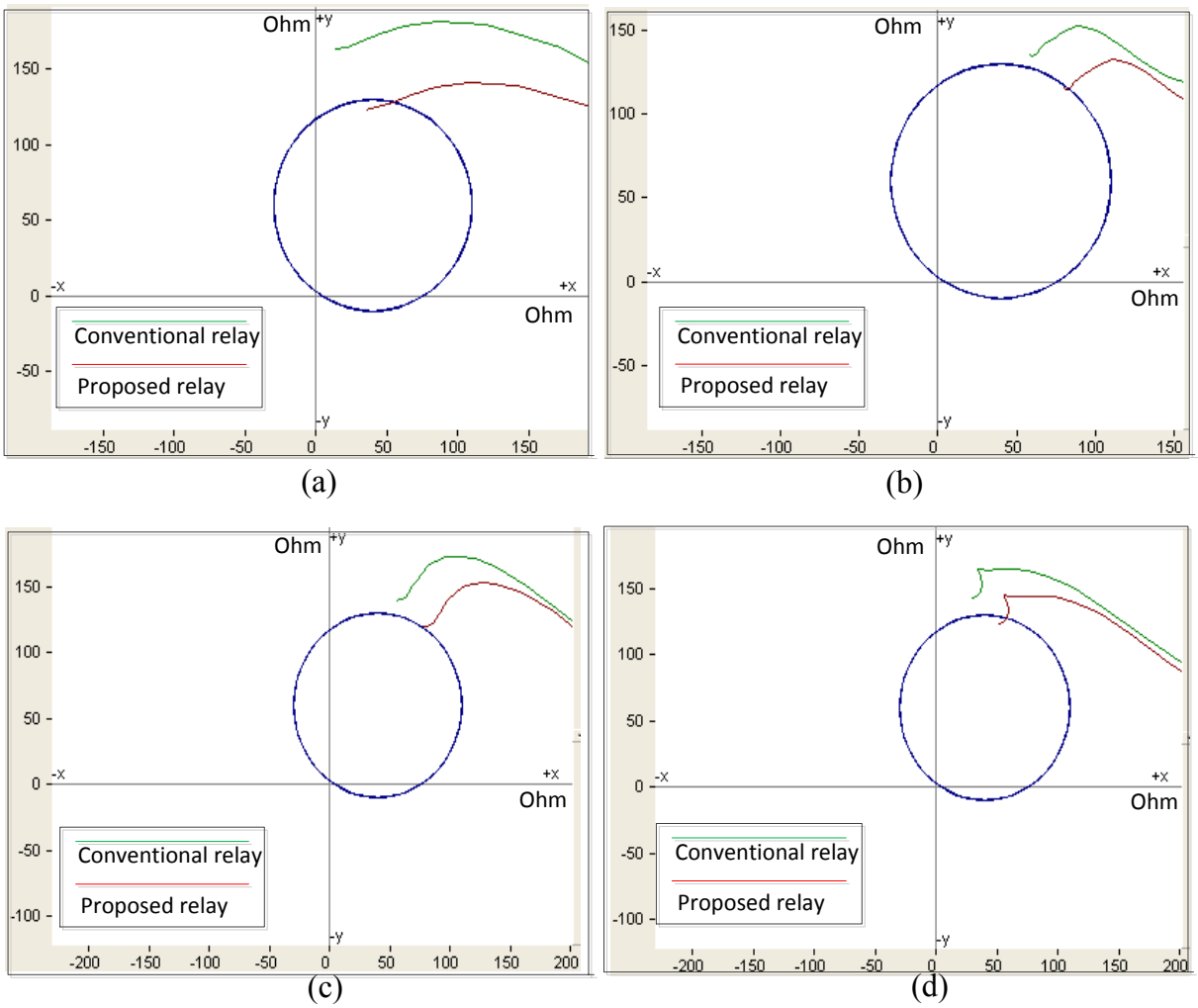

Fig. 5.7 Operating characteristics of proposed and conventional Mho relay during L-G fault at 265 km for: (a) Load angle 10° and fault resistance 0.01 Ω. (b) Load angle 30° and fault resistance 50 Ω. (c) Load angle 40° and fault resistance 50 Ω. (d) Load angle 50° and fault resistance 0.01 Ω.

Case 2: Test to check Over-Reaching effect (Inductive Mode)

In inductive mode, net impedance of transmission line reduces, so, if fault is outside the zone, conventional relay realizes it as inside the zone and mal-operates. Proposed relay again compensates the effect of SVC and does not trip for any fault outside the zone as shown in Fig. 5.8 for L-G fault at 280 km.

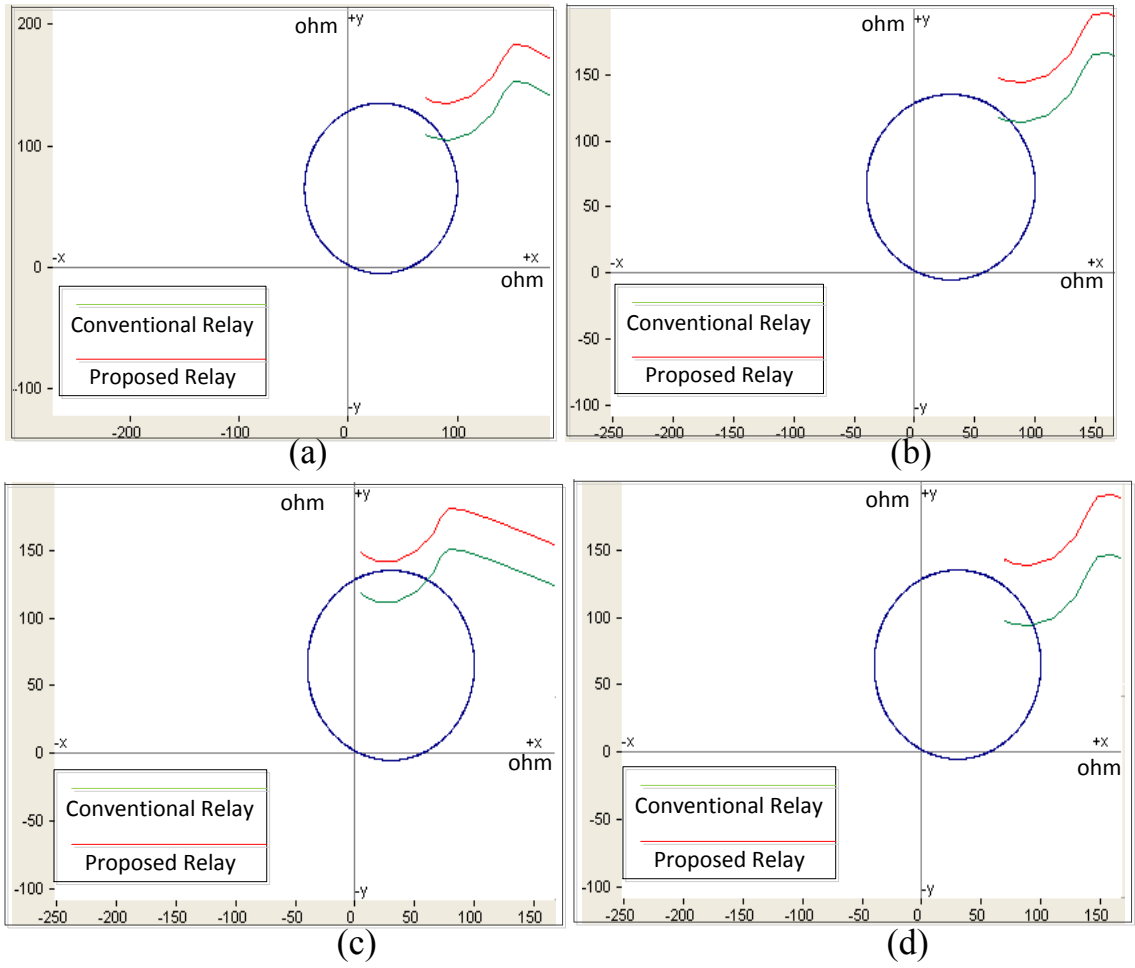

Fig. 5.8 Operating characteristic of proposed and conventional Mho relay during L-G fault at 280 km for: (a) Load angle 10° and fault resistance 50 Ω. (b) Load angle 30° and fault resistance 50 Ω. (c) Load angle 40° and fault resistance 30 Ω. (d) Load angle 50° and fault resistance 60 Ω.

5.5.2 Relay Performance with STATCOM

STATCOM injects constant current at the point of connection even in the fault condition, so it's having larger impact on distance protection than SVC in both the modes of

operation. Proposed Mho relay correspondingly remove the error generated by STATCOM in fault impedance measurement during fault condition. Following cases have been taken to justify the accuracy, security and reliability of the proposed scheme.

Case 1- Test to check Under-reaching Effect (Capacitive Mode)

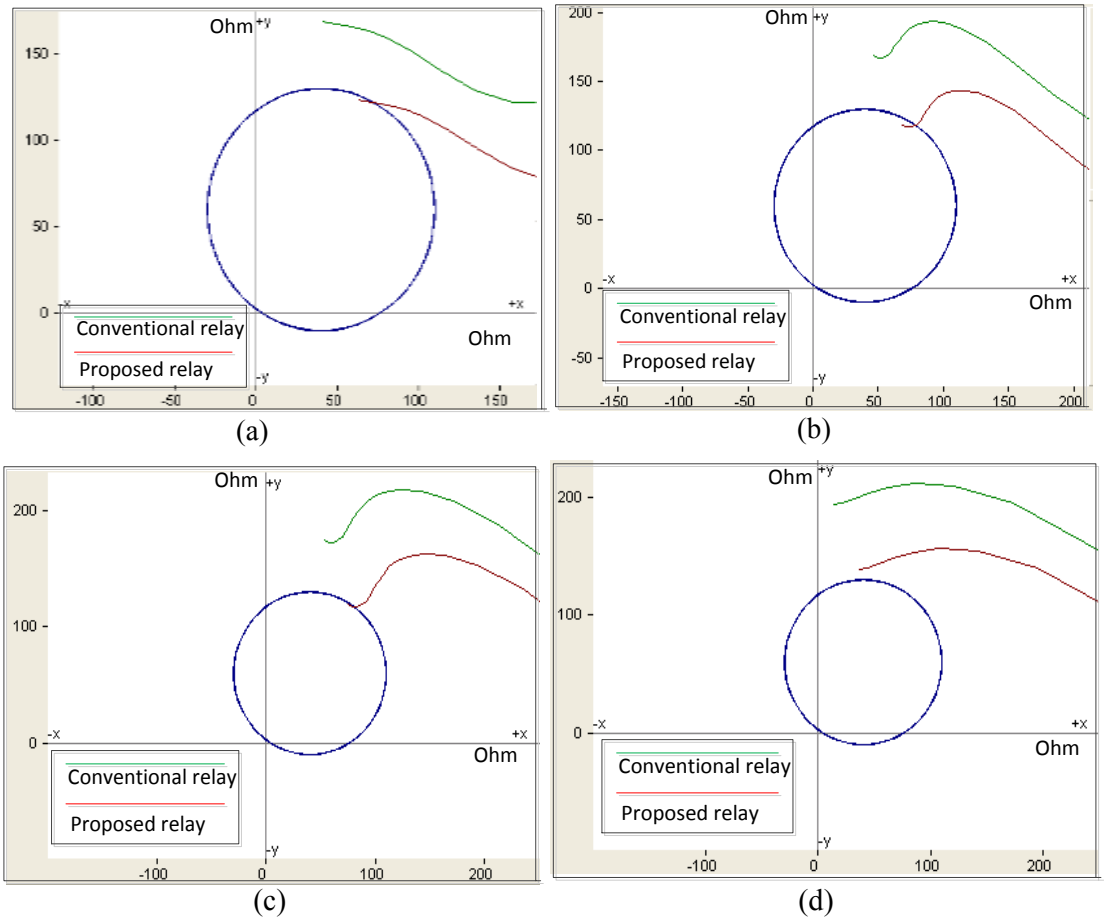

Fig. 5.9 Operating characteristic of proposed and conventional Mho relay during L-G fault at 265 km for: (a) Load angle 10° and fault resistance 20 Ω. (b) Load angle 30° and fault resistance 50 Ω. (c) Load angle 40° and fault resistance 50 Ω. (d) Load angle 50° and fault resistance 0.01 Ω

In capacitive mode, net impedance of transmission line increases. If fault occur near the boundary of zone-1 (272 km) conventional relay mal-operate and does not trip. Proposed Mho relay compensate the error caused by STATCOM and operate for any fault inside the zone. Operation of the conventional and the proposed relay at typical boundary location at 265 km is shown in Fig. 5.9.

Case 2- Test to check Over-reaching Effect (Inductive Mode)

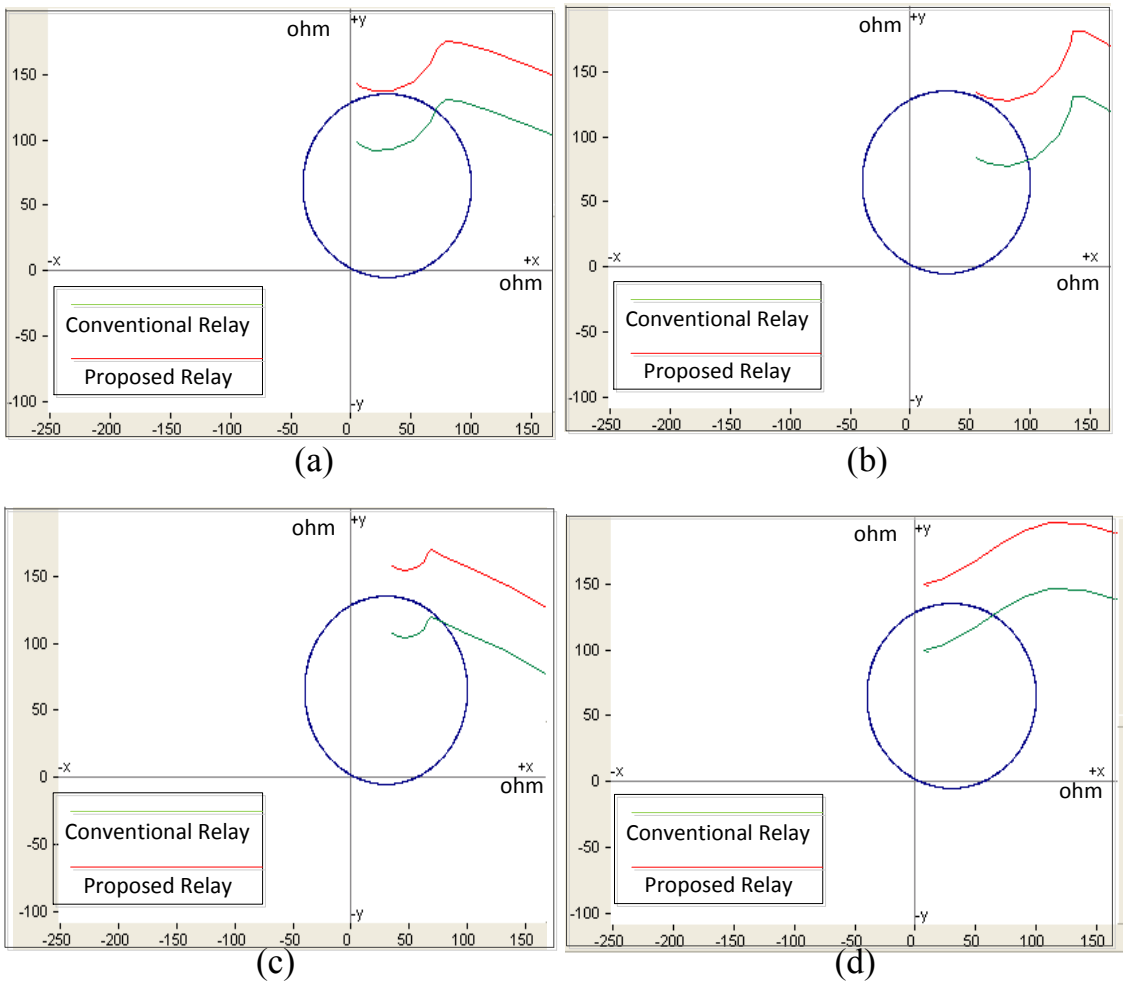

Fig. 5.10 Operating characteristic of proposed and conventional Mho relay during L-G fault at 280 km for: (a) Load angle 10° and fault resistance 0.01 Ω. (b) Load angle 30° and fault resistance 50 Ω. (c) Load angle 40° and fault resistance 50 Ω. (d) Load angle 50° and fault resistance 0.01 Ω.

In capacitive mode of STATCOM, net impedance of transmission line reduces so conventional relay over-reach but proposed Mho relay again correct the error caused by STATCOM and does not operate for any fault outside the zone-1 as shown in Fig. 5.10.

It is clear from the simulation results that the performance of the proposed Mho relay algorithm is far better than the conventional Mho relay. Although the proposed Mho relay has limitations: if the fault is at the boundary of zone-1, under certain operating conditions such as high loading angle and large fault resistance. It is found that the proposed Mho relay is highly

accurate under normal loading conditions (load angle in between 20° to 40°) and fault resistance in between 0.01 Ω to 50 Ω.

5.5.3 Effect of CT Saturation

In case of CT saturation, CT is not able to produce the secondary current in proportionate to the primary current. In such case, magnetic saturation takes place in the core of the CT. CT saturation happens if primary current is very high (above limit), high burden at CT secondary, unfitting CT transformation ratio or an open circuit in secondary is present. Boundary limit of the CT saturation voltage is specified by knee voltage (V_K) and given by equation (5.9). CT secondary voltage should always be less than the knee voltage to avoid saturation in CT.

$$V_K = I_{FSE} * (R_{CT} + R_L + R_R) \tag{5.9}$$

Where,

I_{FSE} = Fault current of secondary side CT

R_{CT} =Resistance of CT secondary

R_L =Lead resistance

R_R = Relay resistance

In the proposed work, CT turn ratio is 1200:5 which is best suited for the application and does not allow saturation even in the case of maximum fault current in the primary windings. So, it can be claimed that the proposed Mho relay is not prone to CT saturation and quite reliable w.r.t. CT functionality. Although, if due to some cause, such as very high remnant flux or if secondary burden is very high or an open circuit (in extreme conditions) occurs in the secondary, then, CT saturation occurs. In this situation, proposed Mho relay algorithm affects similar to the conventional Mho relay. Fig. 5.11 shows the ratio current and actual secondary current in case of saturation. It is observed that secondary current is not the replica of primary current and a loss of current is there with large distortion. In such condition, RMS value of the secondary current is much less than the actual ratio current and depends upon the CT burden, therefore, the proposed Mho relay mal-operates and shows under-reaching conditions. CT can be avoided to saturation by re-sizing the CT core such that to keep flux density below the knee point (V_K) hence equation (5.9) can be modified as equation (5.10).

$$V_K = I_{FSE} * (1 + \frac{X}{R}) (R_{CT} + R_L + R_R) \tag{5.10}$$

Where $(1+\frac{X}{R})$ is over-sizing factor and for the taken transmission line value of the factor is (1+14 = 15) '15'.

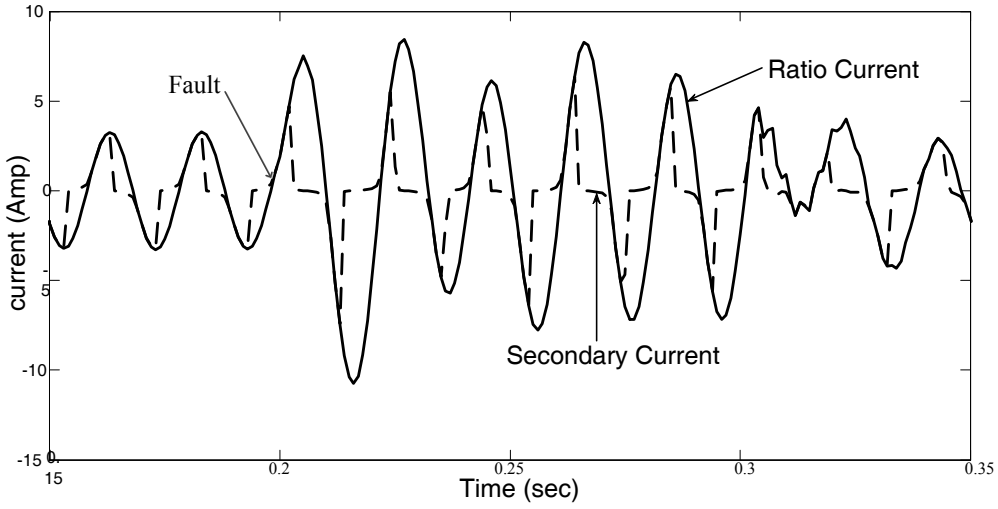

Fig. 5.11 CT saturation in compensated transmission line

5.5.4 Fault Location Estimation Accuracy in Shunt compensated Line

Fault location has been estimated by the proposed adaptive distance protection algorithm for shunt compensated transmission line. Fault location is estimated by computing the inductive reactance of transmission line during fault which is affected by the shunt compensation and independent of line resistance. It is assumed that the effect of fault resistance is negligible which is kept as 0.01 Ω for the whole analysis. Sampling frequency is chosen as 40 samples/cycle and the fault reactance is measured by taking the average of all the reactance value for one quarter cycle i.e. 10 samples from a moving window. Percentage fault location accuracy is calculated by equation (5.11) and (5.12).

$$\text{Percent fault location accuracy} = \frac{\text{Calculated line reactance}}{\text{Actual line reactance}} * 100 \qquad (5.11)$$

$$\text{Percent fault location accuracy} = 1 - \frac{\text{Error}}{\text{Actual line reactance}} * 100 \qquad (5.12)$$

Table 5.1 Fault estimation accuracy in inductive mode

S. N.	Fault at location (km)	Actual positive sequence fault reactance (X) in Ω	Measured reactance with conventional Algorithm (Ω)	Measured reactance with proposed algorithm (Ω)	Fault location accuracy with conventional Algorithm (%)	Fault location accuracy with proposed Algorithm (%)
1	170	86.19	83.21	83.78	96.54	97.30
2	200	101.4	93.10	100.02	91.81	98.63
3	225	114.075	97.48	112.84	85.45	98.91
4	250	126.75	103.82	125.34	81.90	98.88
5	272	137.90	109.91	136.12	79.70	98.70
6	300	152.1	118.34	149.78	77.80	98.47
7	325	164.775	124.38	161.26	75.48	97.86
8	350	177.45	130.88	174.97	73.75	98.60
9	384	194.668	139.70	190.73	71.76	97.97

Table 5.2 Fault estimation accuracy in capacitive mode

S. N.	Fault at location (km)	Actual positive sequence fault reactance (X) in Ω	Measured reactance (Ω) with conventional algorithm	Measured reactance (Ω) with proposed algorithm	Fault location accuracy with conventional Algorithm (%)	Fault location accuracy with proposed Algorithm (%)
1	170	86.19	88.52	87.26	97.29	98.75
2	200	101.4	110.94	103.13	90.59	98.29
3	225	114.075	131.25	116.45	84.94	97.91
4	250	126.75	149.96	129.05	81.68	98.18
5	272	137.90	166.99	140.10	78.90	98.40
6	300	152.1	186.87	156.24	77.14	97.27
7	325	164.775	206.98	168.51	74.38	97.73
8	350	177.45	224.91	182.05	73.25	97.40
9	384	194.668	250.86	199.20	71.13	97.67

Where, Actual line reactance is the gross reactance of fault location in the shunt compensated transmission line which is calculated by multiplying the per km line reactance to the created fault distance from the relay bus and error is the deviation of calculated fault reactance from actual fault resistance of fault point. Table 5.1 and Table 5.2 summarize the results obtained for the fault location estimation accuracy in inductive and capacitive mode, respectively. As can be seen, in both the cases, the fault location accuracy was found to be better for the proposed algorithm as compared to the conventional algorithm.

5.5.5 Effect of Source Impedance Ratio (SIR) on Proposed Relay Fault Location Estimation Accuracy

Fault Location estimation in transmission line depends on source impedance ratio which is given by the ratio of source impedance to transmission line impedance. Protection scheme for transmission line is determined by the length of the line. Length of the line is determined by corporeal length, impedance or SIR level of the system. Length of the line based upon the SIR level can be classified as:

1. Short Line (SIR > 4)
2. Medium Line (0.5 < SIR < 4)
3. Long Line (SIR < 0.5)

Over-reaching accuracy of the impedance relay depends upon the SIR level of the transmission system. Effect of SIR level on the fault location accuracy in mid-point shunt compensated line has been analyzed. SIR of the system is changes by varying the source impedance and percent fault location accuracy have been calculated. Table 5.3 indicates the effect of varying SIR on fault location accuracy in capacitive mode of operation and it is observed that accuracy decreases as the SIR level increases.

Table 5.3 Effect of SIR at zone-1 boundary (272 km)

S. No.	SIR	Accuracy (%)
1	0.272	98.40
2	1.366	96.42
3	2.730	93.45
4	4.091	90.92
5	5.440	88.55

Table 5.4 Effect of SIR in zone-2 (350 km)

S. No.	SIR	Accuracy (%)
1	0.272	97.40
2	1.366	94.85
3	2.730	92.32
4	4.091	91.69
5	5.440	89.68

Table 5.4 shows the fault location accuracy in zone-2 at 350 km and similar variation is observed at the location. In the proposed work SIR of the system is kept fixed at 0.272 which is adequate for long transmission line.

5.6 Summary

An advanced compensated Mho relay algorithm is developed for the protection of transmission line having shunt FACTS devices and its comparative performance with the conventional Mho relay are presented. Detailed analysis of protection algorithm is carried out with the help of PSCAD/EMTDC simulation package. Relay is set to protect 85% of the transmission line for zone-1 and it is tested under wide range of load angle and fault resistance. Results show that in inductive mode of shunt FACTS device, for any fault beyond zone-1 the conventional relay trips due to reduction in impedance hence it overreaches whereas the proposed Mho relay does not operate for any fault beyond its zone because it compensates the error through compensation unit. In capacitive mode, net impedance of transmission line increases therefore the conventional relay does not trip for the fault just inside the boundary of zone-1, hence, it under-reaches. However, the proposed Mho relay operates for the faults inside zone-1 at all locations.

Proposed adaptive Mho relay algorithm is constrained by the high value of fault resistance (> 50 Ω) and high loading conditions. Hence, in the next chapter, AI based algorithms have been developed to overcome these constrains.

CHAPTER 6
ZONE SETTING OF SHUNT COMPENSATED TRANSMISSION NETWORK

This chapter presents a modified AI based algorithm to identify the zone of distance relay for a transmission network having shunt compensator at middle of the line. Modified apparent impedance parameters are calculated as training patterns for AI zone classifier. Shunt FACTS device inserts additional equivalent impedance in the fault loop which depends on the current injected by the particular FACTS device. The impedance by which shunt device compensates the fault impedance is calculated on line at relay point. Calculated compensated impedance creates error in actual impedance measurement, finally the error can be sorted out at the relay point to acquire the modified impedance parameters.

6.1 Introduction

Fault zone identification is an important task for protection engineer in the protection of compensated/uncompensated transmission line. SVC and STATCOM affect the zone setting of distance protection relays in compensated transmission lines. It was found that mid-point FACTS compensation affect the distance relay concerning impedance measurement (zone setting), phase selection and operating times leading to under-reaching and over-reaching [64]. The action of the STATCOM, even at a reduced small rating, increases the resistance to reactance ratio of the line that results in under-reaching phenomena of the impedance relay[18], but suitable remedial measures for the protection are not discussed. Zone protection of transmission network that employ STATCOM is presented in [159] and new setting principles for different protection zones are proposed but the strategy would be different with SVC that works as variable current source. An adaptive protection scheme has been proposed for transmission line having SVC/STATCOM at the middle of transmission line which successfully removes the error inserted by shunt devices but the scheme is constrained by wide variations in fault resistance and loading [156], [158]. An expensive differential current protection scheme for the protection of transmission line having shunt FACTS device is presented in [160]. An integrated impedance based pilot relay protection scheme has been proposed for detecting internal fault for line having SVC at mid-point but has limitations in identifying zonal boundary [190]. Artificial Neural Network (ANN) has an application in

protection of transmission line for protection of mid-point shunt compensated line having STATCOM which successfully detect the faulty phase but does not clear about zone boundary [73]. In the proposed work zone setting is achieved by training an AI classifier with the modified impedance parameters. Modified impedance parameters are the actual fault parameters and calculated by removing the impedance inserted by shunt FACTS device in fault loop. Use of modified impedance parameters avoid the uncertainty in the fault zone classification and give the correct solution.

6.2 Shunt FACTS Device and Impact on Distance Relay Zone Setting

Shunt FACTS devices taken for this study are, (i) SVC and (ii) STATCOM; both devices affect the zone setting of distance relay according to their *V-I* characteristic. Shunt FACTS devices regulates voltage at the connecting bus by injecting a current in quadrature to the driving line voltage and in phase to line current [1]. Current injected by SVC into the connecting bus linearly vary with the line voltage at that point i. e. it works as a variable current source over the operating characteristic as shown in Fig. 6.1(a). STATCOM is a voltage source invertor (VSI) based device and capable of injecting a constant current even at the reduced system voltage (> 0.1pu) and act as a constant current source as shown in Fig. 6.1 (b).

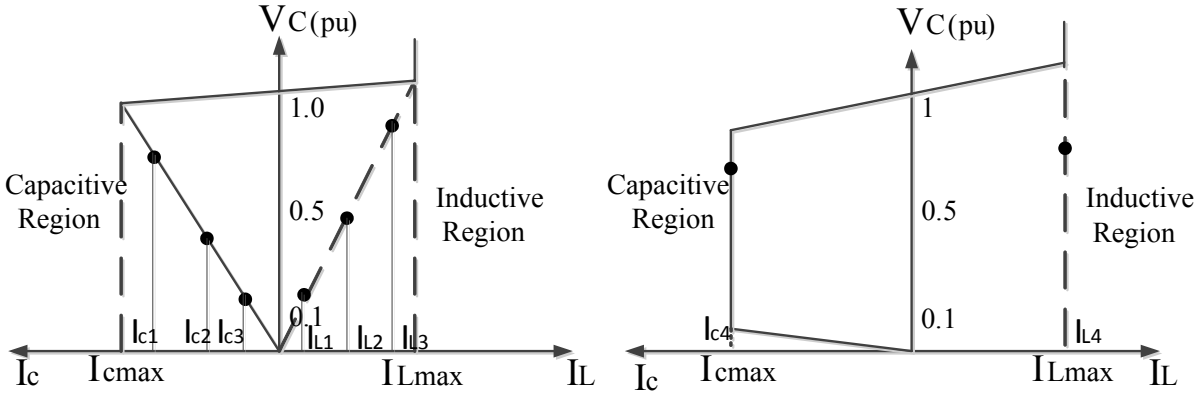

(a) (b)

Fig. 6.1 Operating V-I characteristic of shunt FACTS device (a) SVC (b) STATCOM

Shunt devices operate in two modes of operation, (i) Capacitive mode and (ii) Inductive mode. In case of heavy loads, line voltage drops below the reference value and they work in capacitive mode of operation. It supplies current into the connecting bus hence injects reactive power into the system. In this case net impedance of transmission line increases hence distance relay shows under-reaching effects. In case of light loads, line voltage increases and they work

in inductive mode of operation. It takes current from the connecting bus hence absorbs reactive power from the system. In inductive mode, net line impedance reduces hence relay show over-reaching effects. The change in transmission line impedance by the devices in both operating modes is a function of current injected by the device. This variable impedance is termed as compensated impedance (Z_{comp}). Due to this compensated impedance, there is no clear boundary between zone-1 and zone-2 hence, an overlapping area exists at the boundary as shown in Fig. 6.2.

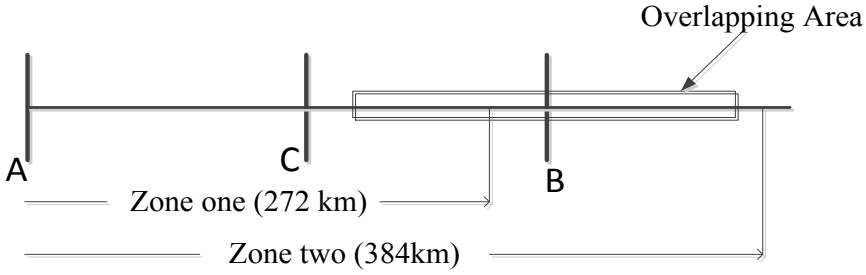

Fig. 6.2 Overlapping area between zone-1 and zone-2

Due to this overlapping area, fault in zone-1 can extend up to zone-2 while zone-2 faults may fall within zone-1 according to the mode of operation. This creates severe reaching problem of zone identification in case of fault in transmission line.

6.3 System Descriptions and Impedance Calculation

6.3.1 System Modeling

Equivalent circuit of shunt FACTS devices in a double fed transmission test system with source power rating of 250MVA is simulated in PSCAD/EMTDC software, which is illustrated in Fig. 6.3. Fig. 6.3 shows transmission system with variable current source equivalent of shunt device having reactive power rating of ±150 MVAr. A typical 230kV, 50 Hz, 320 km long power transmission system is used for testing the capabilities of proposed Mho relay zonal setting algorithm. Transmission line is connected between bus 'A' and 'B'. Per km sequence impedances of transmission line in ohms are: $Z1$ = 0.0362 + j0.508, $Z2$ = 0.0362 + j0.508 and $Z0$ = 0.365 + j1.33.

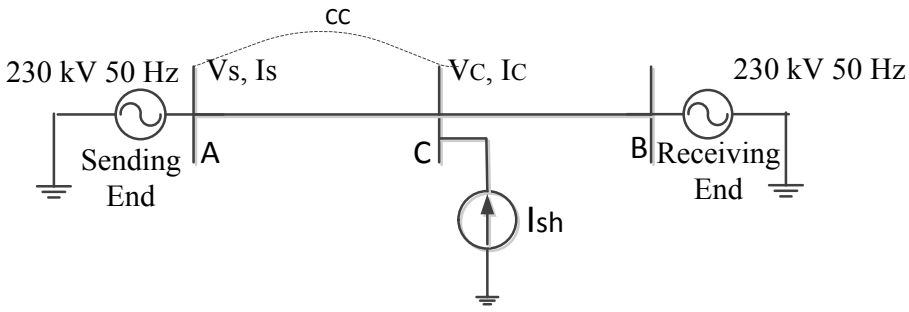

Fig. 6.3 Typical single line diagram of transmission system with shunt device

Distance relay zone-1 is set to protect 85 % of transmission line and zone-2 is set complete line between bus A and B and assumed 20 % in next section which is extended to 384 km not shown in Fig. 6.3. The distance relay at bus 'A' monitors phase voltage (V_s) and line current (I_s) through a coupled capacitor voltage transformer (CCVT) and current transformer (CT) respectively. Shunt device is placed at 160 km from the sending end generator at coupling bus 'C'. Bus Voltage V_C current I_C and current injected by shunt FACTS device I_{sh} is measured at coupling bus.

It is assumed that all the measurements (voltage and current) at bus 'C' transmitted through a fiber-optic communication channel (CC) to bus 'A' and fed to the distance relay compensation unit. In compensation unit equivalent impedance inserted by the shunt FACTS device in the transmission line is calculated, which is a function of Current (I_{sh}) injected by shunt FACTS device. This is the impedance by which shunt FACTS device compensates the transmission line in healthy and faulty conditions.

6.3.2 Compensated Impedance Calculation

Equivalent sequence network for phase to ground (L-G) fault at point 'P' is shown in Fig. 6.4. It is assumed that shunt device is connected at 50 % (160 km) of the total transmission line length and an L-G fault occurs at right side of the shunt FACTS device. Z_{lf} is the equivalent fault impedance calculated at coupling bus which includes fault resistance.

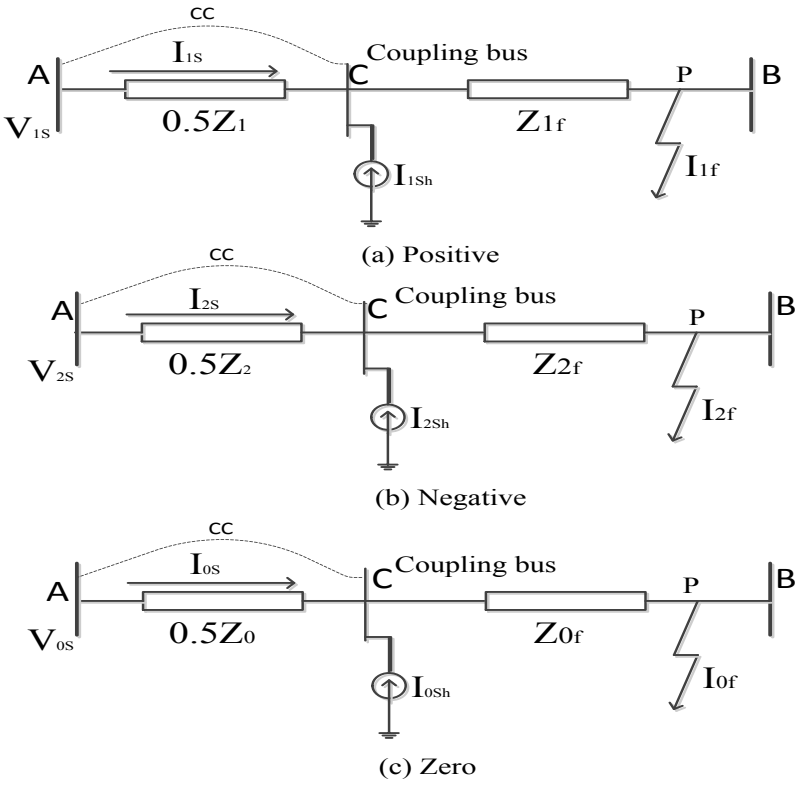

Fig. 6.4 Sequence network of shunt compensated line for LG fault at point P

Resultant current flowing through the impedance Z_{1f} is (I_{1s}+ I_{1sh}). By applying Kirchhoff voltage law (KVL) in positive sequence circuit of Fig. 6.4, voltage equation can be written similar to chapter-5 section 5.4.1 as [158]:

$$V_{1s} = 0.5\, I_{1s}\, Z_1 + (I_{1s} + I_{1sh})\, Z_{1f} \quad (6.1)$$

Similarly, the KVL equations can be written for the negative and zero sequence circuit as (6.2) and (6.3) respectively.

$$V_{2s} = 0.5\, I_{2s}\, Z_2 + (I_{2s} + I_{2sh})\, Z_{2f} \quad (6.2)$$

$$V_{0s} = 0.5\, I_{0s}\, Z_0 + (I_{0s} + I_{0sh})\, Z_{0f} \quad (6.3)$$

Where,

V_{1s}, V_{2s} and V_{0s} are the sequence voltages at sending end (relay point).

Z_0, Z_1 and Z_2 are zero, positive and negative sequence impedance of transmission line respectively.

Z_{0f}, Z_{1f} and Z_{2f} are zero, positive and negative sequence impedance of transmission line from mid-point to fault point 'P' respectively.

I_{1s}, I_{2s} and I_{0s} are the sequence currents at sending end.

I_{1sh}, I_{2sh} and I_{0sh} are the sequence currents injected by shunt FACTS device at bus 'C'.

Total voltage at the relay point can be calculated as:

$$V_s = V_{1s} + V_{2s} + V_{0s} \tag{6.4}$$

So from equation (6.1) to (6.4), bus voltage

$$V_s = (0.5\,Z_1 + Z_{1f})\,(I_s) + I_{0s}\,(Z_0 - 0.5\,Z_1) + Z_{1f}\,(I_{sh}) + (Z_{0f} - Z_{1f})\,I_{0s} + (Z_{0f} - Z_{1f})\,I_0 \tag{6.5}$$

For single phase to ground fault, apparent impedance of distance relay at bus 'A' can be calculated using equation below:

$$Z = \frac{V_s}{I_s + \frac{Z_0 - Z_1}{Z_1} I_{0s}} = \frac{V_s}{I_{relay}} = \left(0.5\,Z_1 + Z_{1f}\right) + \frac{I_{sh}}{I_{relay}} Z_{1f} \tag{6.6}$$

First portion of the equation (6.6) is the actual fault impedance which includes the positive sequence impedance of fault point to relay point and arc resistance. Second portion of the equivalent impedance is directly proportional to the current (I_{sh}) injected by the shunt FACTS device into the coupling bus and this is the impedance inserted by shunt compensator in transmission line, can be termed as compensated impedance (Z_{comp}).

$$Z_{comp} = \frac{I_{sh}}{I_{relay}} Z_{1f} \tag{6.7}$$

Similarly for LL fault the compensated impedance can be calculated from Fig. 6.5 as:

From (6.1) and (6.2)

$$V_{1s} - V_{2s} = 0.5\left(I_{1s} - I_{2s}\right)Z_1 + [(I_{1s} - I_{2s}) + (I_{1sh} - I_{2sh})]\,Z_{1f} \tag{6.8}$$

Equivalent fault impedance (Z_{eqLL}) during LL fault can be found by dividing (6.8) by ($I_{1s} - I_{2s}$)

$$Z_{eqLL} = \frac{V_{1s} - V_{2s}}{I_{1s} - I_{2s}} = \left(0.5 Z_1 + Z_{1f}\right) + \frac{I_{1sh} - I_{2sh}}{I_{1s} - I_{2s}} Z_{1f} \tag{6.9}$$

Again from (6.9) the first portion $\left(0.5\,Z_1 + Z_{1f}\right)$ is the actual fault impedance and the second portion ($\frac{I_{1sh} - I_{2sh}}{I_{1s} - I_{2s}} Z_{1f}$) is compensated impedance, can be termed as:

$$\left(Z_{comp}\right)_{LL} = \left(\frac{I_{1sh} - I_{2sh}}{I_{1s} - I_{2s}} Z_{1f}\right) \tag{6.10}$$

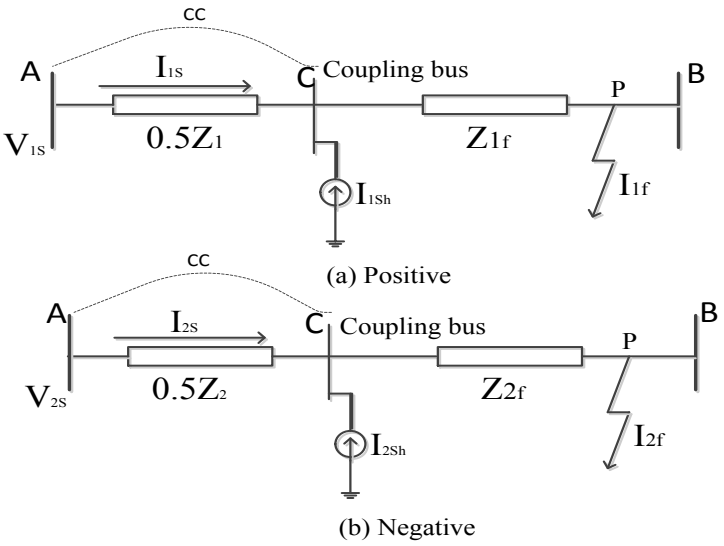

Fig. 6.5 Sequence network for LL fault at point P

This impedance (Z_{comp}) creates error and responsible for mal-operation of Mho relay in any type of fault. STATCOM current is I_{Cmax} or I_{Lmax} in capacitive or inductive mode of operation respectively; therefore it compensates the line by constant impedance. For SVC, I_{sh} is in between 0 to I_{Cmax} in capacitive mode and in between 0 to I_{Lmax} in inductive mode depends on the terminal voltage V_C as shown in Fig. 6.1 (a). Z_{comp} depend upon current inject by shunt compensator (I_{sh}), relay current (I_{relay}) at bus A and positive sequence impedance (Z_{1f}) transmission line from midpoint to fault point which can be calculated by taking voltage and current measurement at coupling bus 'C'.

6.4 Generated Training Features

Feature extraction is the important expect of the AI based classification. In the proposed work input training feature for AI based zonal classifier is the modified impedance trajectory generated by removing the error due to shunt compensation from measured impedance. To make the AI classifier robust and universal modified impedance patterns are generated for wide variations in fault resistance from 0.01 Ω to 200 Ω, all possible loading angles from 1^o to 50^o and all possible operating current points as shown in Fig. 6.1 (a) for SVC (C1 to C3 and L1 to L3) and Fig. 6.1 (b) for STATCOM (C4 and L4). Description of input training features generated with different operating modes is as follows:

6.4.1 Shunt Device as Reactive Power Supplier

In capacitive mode shunt device supply reactive power and exhibits under-reaching characteristics. In this condition zone-2 impedance features penetrates into zone-1 and creates error. Comparison of different patterns generated with proposed and conventional relay is as follows.

6.4.1.1 Generated Features with Proposed Method

Proposed relay removed the error produced by shunt fact device and minimizes the zone-2 patterns penetration into zone-1. To check the patterns of generated impedance feature with proposed relay in presence of shunt device, line to ground (LG) and line to line (LL) faults are created at different locations throughout the line. Modified impedance patterns are generated at critical locations such as sending end, near mid-point, near the boundary of zones and at the far end of zone-2. At each location fault resistance varied as 0.01, 50, 100, 150 and 200 ohms. Patterns for different operating conditions are generated for SVC and STATCOM described as follows:

A. Generated Features with STATCOM

STATCOM supplies maximum current at any possible system voltage hence creates maximum under-reaching at all possible operating points. Proposed measured impedance method removes the error simultaneously and tries to separate out zone-1 and zone-2 impedance patterns and minimizes the possibility of overlapping as shown in Fig. 6.6. Proposed technique is fully applicable with LG and LL fault conditions as visualize in Fig. 6.6(a) and Fig. 6.6(b) simultaneously.

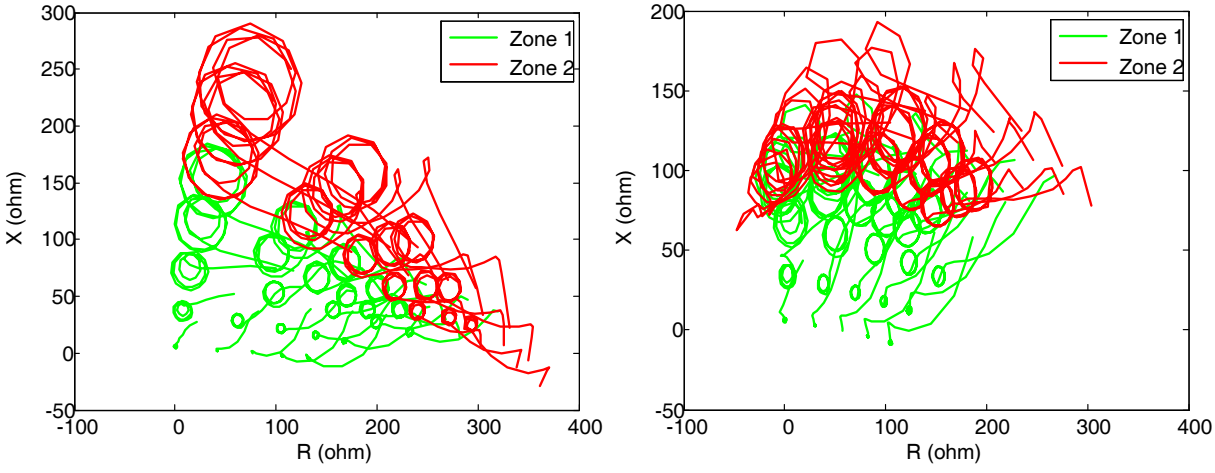

(a) (b)

Fig. 6.6 Proposed relay generated impedance patterns with STATCOM (a) LG (b) LL

B. Generated Features with SVC

SVC supplies reactive current depending upon the system operating condition as shown in Fig. 6.1(a) by black dots. Patterns are generated for LG and LL fault conditions at different operating points as shown in Fig. 6.7 and Fig. 6.8 respectively. After analyzing the generated features it is clear that proposed method minimizes the error and reduces the possibility of overlapping.

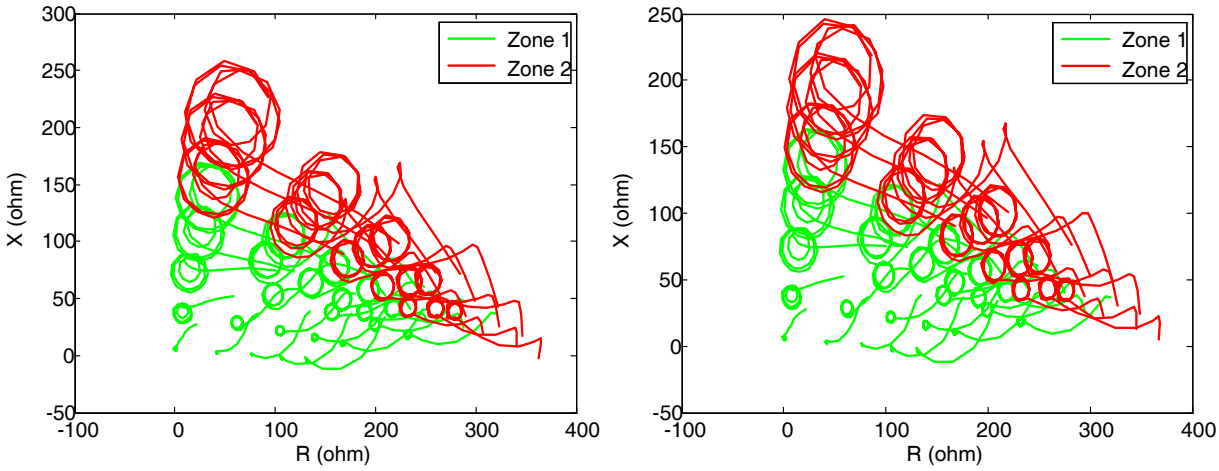

(a) (b)

Fig. 6.7 Proposed relay generated LG fault patterns with SVC for operating point (a) C1 (b) C2

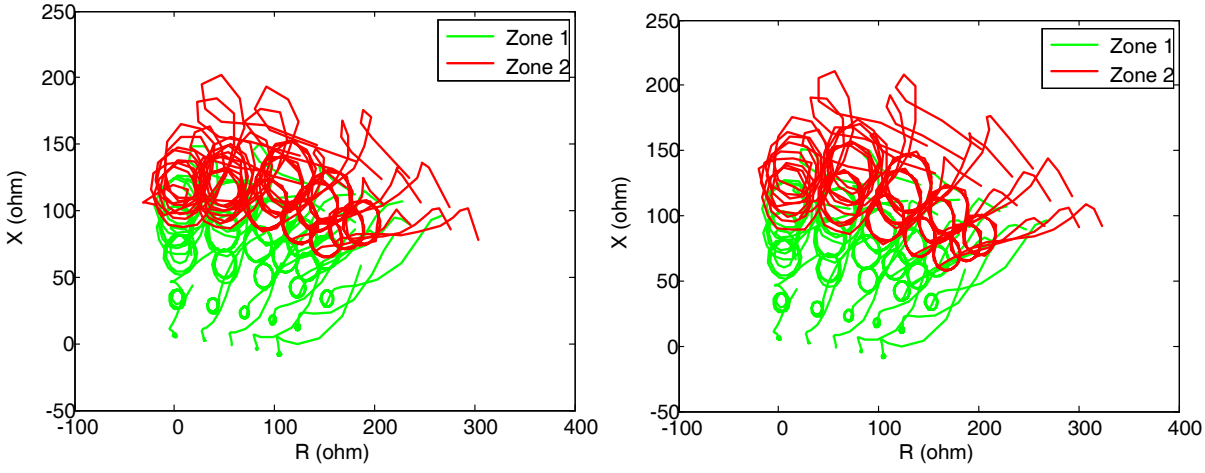

(a) (b)

Fig. 6.8 Proposed relay generated LL fault patterns with SVC for operating point (a) C1 (b) C2

6.4.1.2 Generated Features with Conventional Impedance Calculation Method

A brief analysis of generated patterns with conventional method has been done. Impedance patterns are generated at different locations in zone-1 and zone-2 with keeping all the operating conditions identical. Patterns are generated for both LG and LL faults throughout

the length of line as shown in Fig. 6.9(a) and Fig. 6.9(b) respectively. It is clear from Fig. 6.9 that in case of conventional strategy zone-1 and zone-2 patterns are overlapping and cannot be discriminated easily.

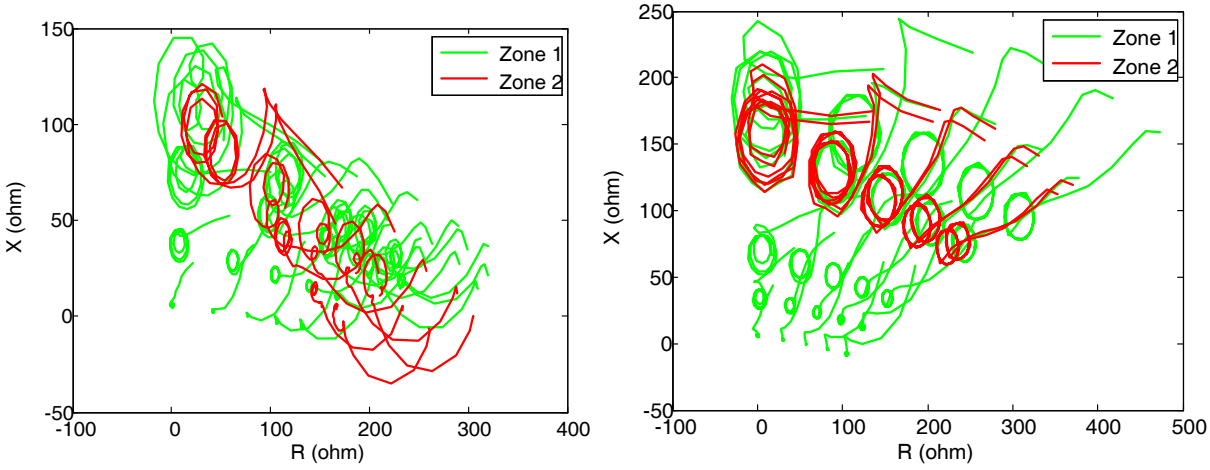

(a) (b)

Fig. 6.9 Conventional relay generated impedance patterns for (a) LG (b) LL fault

6.4.2 Shunt Device as Reactive Power Absorber

Shunt FACTS device absorbs the reactive power in light load condition and operates in inductive mode of operation. In this conditions net line impedance decreases and distance relay exhibits over-reaching characteristic. In absorber mode zone-1 impedance curves penetrate into zone-2 and create an overlapping area near the boundary of zones. Different zone curves for proposed and conventional relay have been explored as follows:

6.4.2.1 Generated Patterns with Proposed Method

In proposed methodology the error inserted by shunt device in impedance measurement is calculated and simultaneously removed. Impedance curves strains to settle at proper fault location. Analysis of different zone impedance patterns for STATCOM and SVC is as follows:

A. Generated Features with STATCOM

STATCOM supplies negative reactive power in case of inductive mode and absorbs maximum current from the system at any system voltage. In this case penetration of zone-1 curves into zone-2 is maximum but proposed modified technique tries to avoid overlapping by removing the error as shown in Fig. 6.10. Patterns are generated for LG and LL fault cases as

shown in Fig. 6.10(a) and Fig. 6.10(b) and it is clear that proposed technique separate out different zone features.

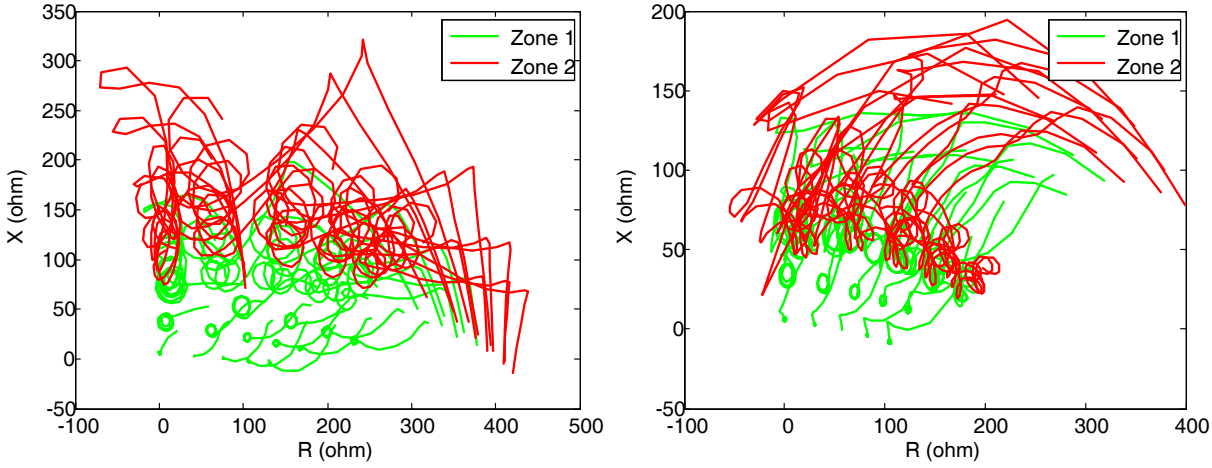

(a) (b)

Fig. 6.10 Proposed relay generated impedance patterns with STATCOM for (a) LG (b) LL

B. Generated Features with SVC

In inductive mode SVC also work as variable current source and absorbs reactive power from the system. Penetration of zone-1 curves into zone-2 depends upon the current supplied by SVC into the system. Proposed impedance calculation scheme eliminate the effect of SVC in fault impedance calculation at any operating point shown in Fig. 6.1(a). Different zone patterns for LG and LL fault are visualize in Fig. 6.11 and Fig. 6.12 respectively. It is clear from the Figs. that proposed relay takes the action to avoid the possibility of overlapping.

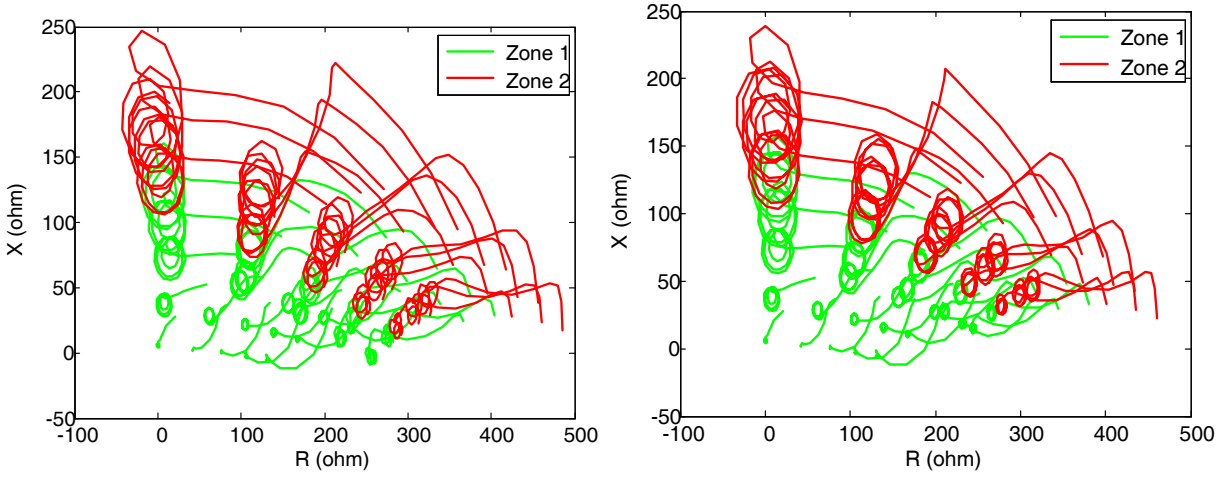

(a) (b)

Fig. 6.11 Proposed relay generated impedance patterns for LG fault (a) L2 (b) L3

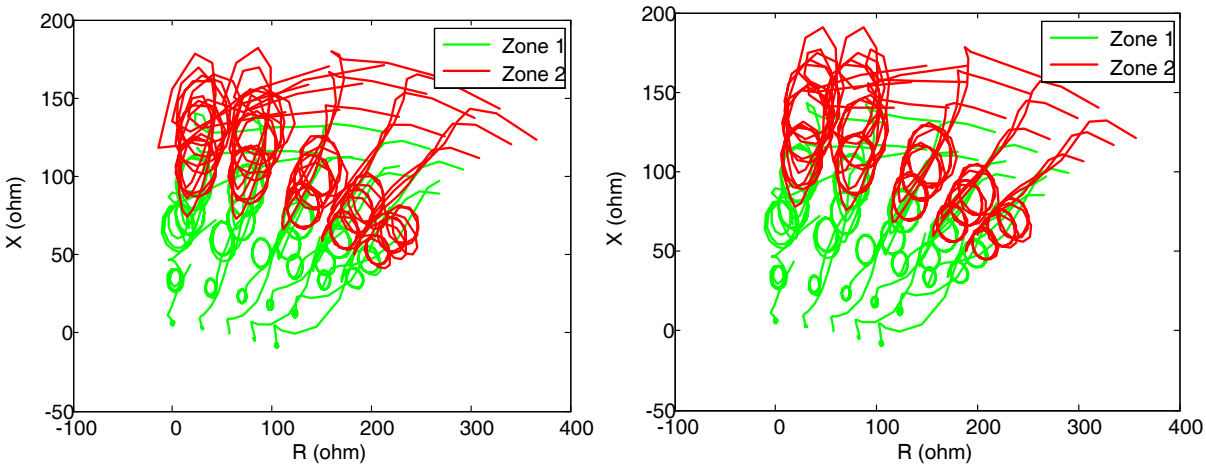

(a) (b)

Fig. 6.12 Proposed relay generated impedance patterns for LL fault (a) L2 (b) L3

6.4.2.2 Generated Patterns with Conventional Impedance Calculation Method

Conventional relay has the limitations and it calculates the fault impedance irrespective of the compensation introduce by shunt FACTS device into line. Therefore it generates similar patterns for faults at different locations due to this several zone-1 fault seems in zone-2 and vice versa. A few such types of patterns are generated for LG and LL faults as shown in Fig. 6.13(a) and Fig. 6.13(b) respectively. It is visualize from Fig. 6.13 that zone-2 patterns fall before zone-1 and the patterns are similar so cannot be discriminated easily even by a non-linear classifier and creates error.

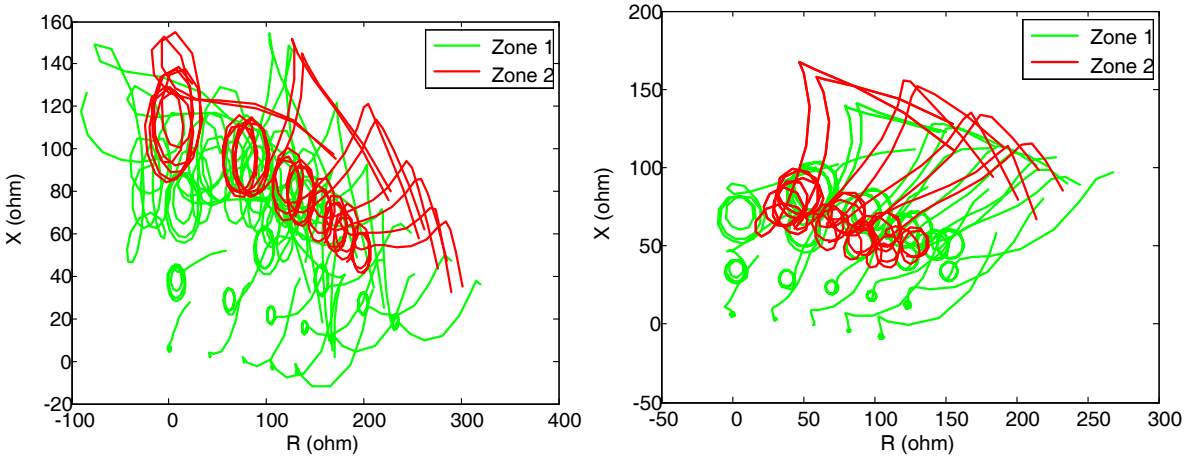

(a) (b)

Fig. 6.13 Conventional relay generated impedance patterns for (a) LG (b) LL fault

In the proposed work data is sampled at the sampling frequency of 800 samples/ second. With the power cycle length of 20 milliseconds, the zone classifier is set to classify the zone within the quarter cycle which is 5 milliseconds which is also the operating time of classifier. In this operating time the classifier observes the 40 samples of modified impedance parameters to take decision. Therefore the arrangement of total number of training patterns has been arranged as follows:

$$\begin{bmatrix} R_{m11} & X_{m11} & \cdots & \cdots & R_{m140} & X_{m140} \\ R_{m21} & X_{m21} & \cdots & \cdots & R_{m240} & X_{m240} \\ \vdots & \vdots & & & \vdots & \vdots \\ R_{mx1} & X_{mx1} & \cdots & \cdots & R_{mx40} & X_{mx40} \\ \vdots & \vdots & \cdots & \cdots & \vdots & \vdots \\ R_{mn1} & X_{mn1} & \cdots & \cdots & R_{mn40} & X_{mn40} \end{bmatrix}_{n*80}$$

Where 'n' the total numbers of training patterns, 'x' denotes an arbitrary intermediate pattern. In zone classification the arranged data is row wise fed to the AI classifier i.e. the numbers of inputs of classifier are 80. Proposed zone classification algorithm for mid-point shunt compensated transmission line is elaborated as follows:

6.5 Proposed Zone Classification Algorithm

Complete sequence of proposed AI based fault zone classifier algorithm for line having SVC or STATCOM at mid-point is shown in Fig. 6.14. Synchronized measurement of voltage and current based on accurate time reference takes place in between bus 'A' and 'C'. Relay at bus 'A' takes voltage and current signal through CCVT and CT respectively.

Fault impedance Z (R and X) calculated by conventional method at the relay point using fundamental and sequence components of fault voltage and current signal. For LG fault condition equivalent fault impedance at bus A is calculated as [11].

$$Z_{LG} = \frac{V}{I + k I_0} \tag{6.11}$$

Where, $k = \frac{Z_0 - Z_1}{Z_1}$,

V and I are the phase voltage and current respectively.

Z_0, Z_1 are the zero and positive sequence impedances respectively and

I_0 is zero sequence component of fault current.

For LL fault,

$$Z_{LL} = \frac{V_{1s}-V_{2s}}{I_{1s}-I_{2s}} \tag{6.12}$$

Where, V_{1s} and V_{2s} are positive and negative sequence voltages respectively and I_{1s} and I_{2s} are positive and negative sequence voltages respectively.

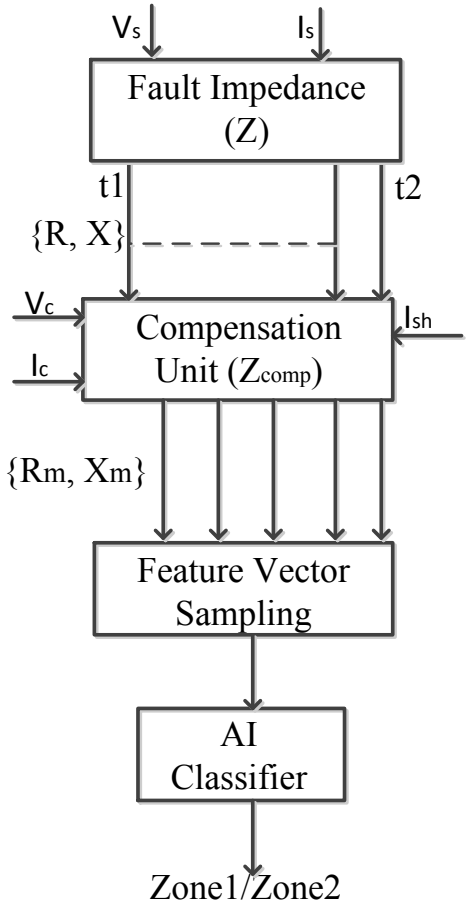

Fig. 6.14 AI classifier for zonal discrimination

Error introduced by SVC or STATCOM into the fault impedance calculation of transmission line for LG and LL fault condition can be given by eq. (6.7) and (6.10) respectively. Finally, net line fault impedance (Z_m = Z- Z_{comp}) is calculated at relay bus A, which is then fed to AI classifier to decide whether the fault is in zone-1 or zone-2. Proposed Mho relay compensation unit on-line calculates the compensated impedance (Z_{comp}) of shunt FACTS device and simultaneously compensate it form the measured impedance (Z) at relay point. Modified impedance parameters (R_m, X_m) are used to avoid overreaching and under-

reaching operation under the influence of shunt FACTS device. AI has the ability to classify the non-linear patterns accurately. The feature vectors for AI classifier are R_m and X_m of several fault instances as shown in Fig. 6.14. Let any fault occurs in a stable transmission system at time t_1 and conventional distance relay algorithm detects the fault at time t_2. The time lapse $T=t_2-t_1$ (relay operating time) consist of the impedance seen during fault. So the feature vector consists of the modified impedance parameters seen during time T by the relay located at the bus 'A'. In this work fault simulation time is taken up to 1.05 s, fault occur at 1.0 s and fault data is generated for 0.05 s which is used to form the modified impedance patterns. During this time total 40 samples of modified fault impedance are used as feature vector input to AI classifier.

6.5.1 Requirement of Communication Channel

The proposed Mho relay zone identification technique requires a reliable and high speed communication channel in between coupling bus 'C' to the Mho relay location. Voltage and currents are measured at bus 'C'. Communication channel transmits these measured signals to the relay location to calculate compensated impedance. In this work reliability of the proposed algorithm depends on the reliability and fastness of the communication channel. It is assumed that the communication channel is reliable and fast enough to send measured current and voltage signal from coupling bus 'C' to relay bus 'A' for any fault in between bus 'C' and 'B'. If there is any fault in between bus 'A' and 'C' communication channel breaks and does not send any signal in this case I_{sh}=0, i.e. relay behaves normally as a conventional relay. The newly built EHV/UHV transmission lines are equipped with dedicated fiber-optics channels through which the signals can be transmitted from one end of the transmission line to the other [190][156], [178].

6.6 AI Based Zone Classifier Testing Results

Extensive simulations are carries out to evaluate the performance of proposed AI based zone identification technique. A 230- kV and 320 km long shunt compensated transmission line is used for to test the capability of the proposed algorithm for the zonal setting of Mho relay. To provide the required training and testing data sets, various faults are created at several locations throughout the complete length of transmission line. The details of all the training combination are as follows.

(a) Fault resistance 0.1, 10, 50, 100, 150 and 200 Ω.

(b) Fault inception angle 0, 30, 45, 60, 90, 135 and 180°.

(c) Load angle 5, 10, 20, 30, 40 and 50°.

(d) Fault type AG, BG, CG, AB, BC, CA, ABG, BCG, CAG, ABC and ABCG. And

(e) Capacitive mode (C1, C2, C3 and C4) and inductive mode (L1, L2, L3 and L4).

(f) Fault Location 1, 80, 160, 220, 272, 320, 350 and 384 km.

Thus, total training data points generated at each location are 6*7*6*11*8= 22176 and total numbers of locations taken for data generation are 8 so total numbers of training data patterns are 22176*8=177408. All conditions are taken for both SVC and STATCOM and AI classifier trained with all the generated patterns. The first zone of the Mho relay is set to protect 85 % (272 km) of the transmission line, the second zone is set to protect rest of the line and an assumes extended section which may stretch in next adjacent line up-to 384 km from relay bus 'A'.

The details of testing patterns for evaluating the classifier performance are given below.

(a) Fault resistance 0, 25, 75, 135 and 175 Ω.

(b) Inception angle 20, 50, 80, 120 and 150°.

(c) Load angel 15, 25, 35 and 45°.

(d) Fault type AG, AB, ABG, ABC and ABCG.

(e) Capacitive mode (C1, C4) and inductive mode (L2, L4).

Total number of testing patterns at a particular location is 5*5*4*5*4 = 2000. After randomize the testing patterns randomly 1000 patterns are selected for the testing of AI zone classifier.

6.6.1 Performance Comparison of RBFNN and SVM

With the obtained training patterns of modified impedance, obtained testing accuracy of RBFNN and SVM is shown in Table 6.1. Performance comparison of classifiers is also obtained with conventional impedance parameters. Testing data is taken from several critical locations from zone-1 and zone-2. Accuracy of AI classifiers with zone-1 data before mid-point is found to be accurate and it is around 99.0 %. Accuracy issue arises if the fault occurs after mid-point in zone-1 and zone-2. Testing accuracy with conventional impedance patterns is found very less in both type of AI classifier. With the conventional impedance patterns, overlapping takes place and redundant data is generates at several locations which cost for accuracy. Testing accuracy with modified impedance patterns as input increases sharply and with the high number of testing

patterns it fails in a few cases. As discussed before, modified impedance parameters reduce the chance of overlapping and redundancy and increase the accuracy.

Table 6.1 Testing accuracy of AI classifier for zone classification

S. No.	AI Type	Taken testing data locations (km)	Fault Zone	Testing accuracy (%) of	
				Conventional impedance patterns	Modified impedance patterns
1	RBFNN	85	One	99.8	99.8
		170		76.0	96.9
		275	Two	71.6	91.3
		350		77.6	97.5
2	SVM	85	One	99.8	**99.8**
		170		74.5	**98.2**
		275	Two	76.2	**97.8**
		350		77.9	**99.0**

It is also observed from Table 6.1 that classification accuracy reduces slightly in all the cases if the testing data location is at the boundary of zones. Table 6.1 also gives the performance comparison of RBFNN and SVM. It is realized from the results that percentage accuracy of both the classifiers for the testing patterns taken at location before compensator (mid-point) is almost same and they classify the faulty zone with almost 99% accuracy. For testing patterns taken after mid-point the accuracy of both the classifiers decreases and SVM shows slightly better performance due to its better classification features. It is concluded from the Table 6.1 that SVM classifier with modified impedance parameter is the best choice for fault zone classification in mid-point shunt compensated transmission line.

6.7 Summary

AI based scheme for fault zonal identification in shunt compensated transmission line having SVC or STATCOM is addressed in this chapter. A novel technique presented which depends on the modified apparent impedance seen by impedance relay for all possible operating conditions of shunt compensated transmission line. Modified fault impedance patterns are generated for SVC and STATCOM in LG and LL fault conditions. Performance of

RBFNN and SVM based classifier is discussed with modified and conventional impedance parameters. It is clear from the testing result that in all cases, classification accuracy of AI classifiers is far better in cases of modified impedance patterns as input. In the comparative results of RBFNN and SVM, it is concluded that SVM is useful for zonal discrimination in shunt compensated transmission line and use of modified impedance parameter disregards the possibility of misclassification while the conventional relay mal-operates. Therefore, the proposed method is reliable under the wide variation in power system parameters like load angle, fault resistance, fault location, inception angle and compensation level.

CHAPTER 7
VALIDATION OF PROPOSED PROTECTION ALGORITHM IN RTDS/RSCAD

In this chapter, validation of various adaptive distance protection algorithms presented in previous chapters for protection of series/ shunt compensated transmission line has been performed in RTDS/RSCAD environment. Models of series compensators and shunt compensators are discussed in brief along with the discussion of transmission system components. Adaptive compensation technique has been applied on the series/shunt transmission systems and similar results are produced for various faults which validate the various adaptive protection algorithms.

7.1 Introduction

Proposed adaptive Mho relay algorithms for mid-point series and shunt compensated transmission line are needed to be implemented in the real time environment. Due to several limitations, it is not possible to implement real time hardware of the proposed algorithms. For real time hardware implementation of the proposed algorithm EHV transmission line, FACTS stations and several other high power devices are needed which is not possible at laboratory level. At present level, only the real-time software simulations of the proposed algorithms can be performed. The Real Time Digital Simulator (RTDS/RSCAD) is a special purpose, Digital Signal Processor (DSP) based computer to study electromagnetic transient phenomena in real-time. Digital simulators compute the state of the power system model in discrete time instants. These time instances are called simulation time step. Thousands of calculations must be performed during each time−step in order to compute the state of the power system at that instant. RTDS/RSCAD maintains the continuous real time operation by using reduced instruction set and utilizing advanced parallel processing techniques. RTDS/ RSCAD includes all the basic power system elements which designed based on Dommel's solution algorithms [191]. Dommel formulated the complex power network into the integration of distributed and lumped parameter and proposed a nodal admittance based solution.

7.2 Hardware Structure

RTDS/ RSCAD hardware consists of two similar racks which can execute two different tasks at the same time. To perform a function, RTDS/ RSCAD rack has four different types of cards. To achieve high simulation speed of real time step (50 μs to 60 μs), RTDS/ RSCAD uses two parallel high speed processor cards described below:

(1) The Triple Processor Card (3PC)

The 3PC card contains three ADSP21064 processors and fibre-optic channels which are used as communication medium.

(2) The Risc Processor Card (RPC)

The RPC card contains two power PC750CXe processors and a local high speed ring bus is used for communication. RTDS/ RSCAD rack primarily uses this card for network solution.

In addition to processor cards a RTDS/ RSCAD rack contains a workstation interface card and an inter-rack communication card:

(1) Workstation Interface Card (WIF)

It performs following four main functions:

i. Rack diagnostics
ii. RTDS to computer workstation communication
iii. Multi-rack case synchronization
iv. Backplane communication

(2) Inter Rack Communication Card (IRC)

The main function of this card is to perform communication between interconnected racks.

7.3 Power System Modeling in RTDS/ RSCAD

7.3.1 Source Model

In RTDS/RSCAD, the source model is selected as same which has been used in PSCAD/EMTDC simulations, as shown in Fig. 7.1. The R//L source's positive sequence impedance may be specified either in absolute terms by entering the actual R_p and L_p parameters, or by entering the source impedance magnitude and damping angle.

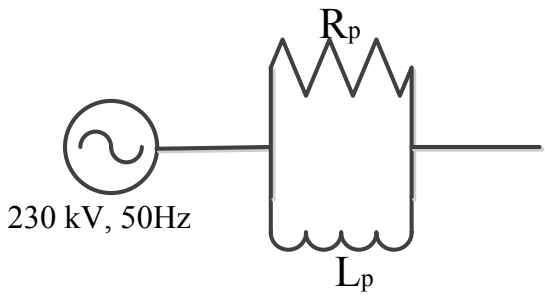

Fig. 7.1 Source model in RTDS/ RSCAD

Given a system impedance $|Z_p|\angle\theta$

Where,

$|Z_p|$ is the equivalent system short circuit impedance magnitude.

'θ' is the system damping angle at fundamental frequency.

'R_p' is parallel resistance.

'L_p' is parallel inductance.

Then the R//L parameters may be calculated as follows –

$$\frac{R_P * jX_P}{R_P + jX_P} = |Z_P| \angle\theta \tag{7.1}$$

R_p and X_p are solved for using this expression, and then

$$L_p = X_p / (2\pi f) \tag{7.2}$$

Where, '*f*' is the base system frequency.

7.3.2 Transmission Line Model

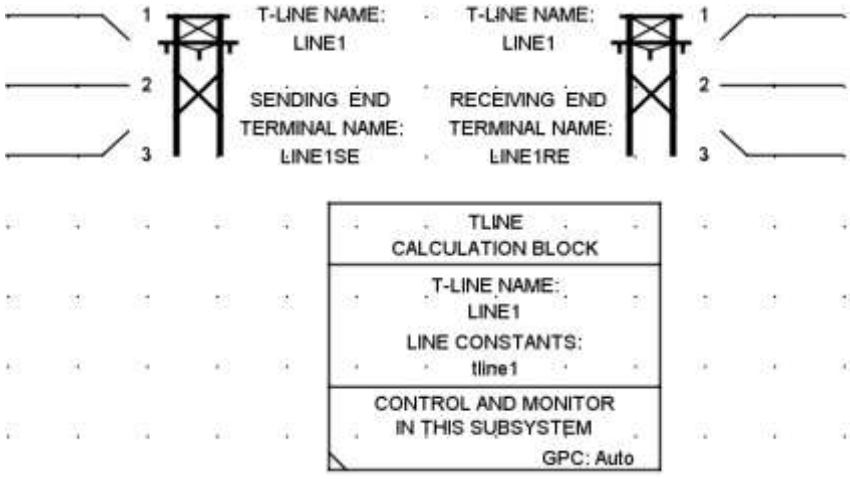

Fig. 7.2 Transmission line model in RTDS/ RSCAD

Travelling wave and pi section transmission line models are available in RSCAD/RTDS. For long line, travelling wave model is used because it represents the distributed parameters of transmission line. Unified T-line having a calculation block associated with two set of draft icon are used to represent a line as shown in Fig. 7.2.

7.3.3 MOV Protected Fixed Series Capacitor (FSC) Model

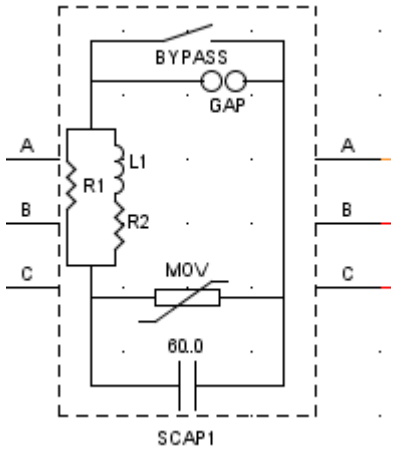

(a)

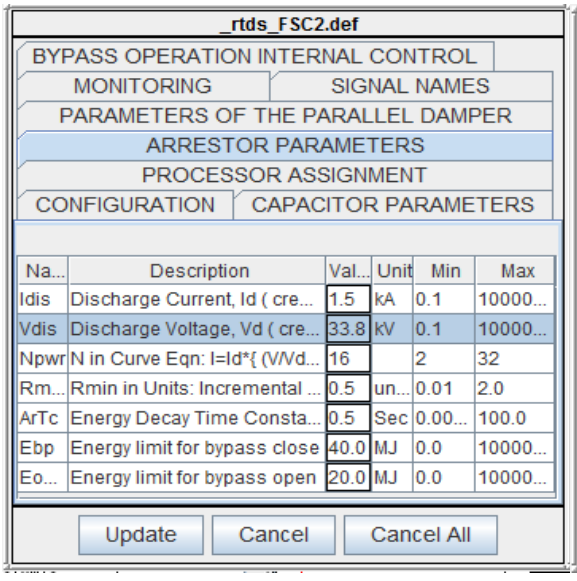

(b)

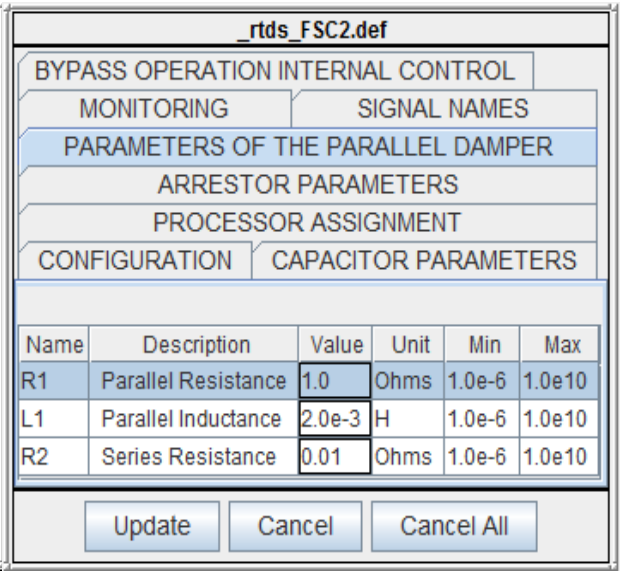

(c)

Fig. 7.3 MOV protected series capacitor in RTDS/ RSCAD (a) Model (b) Arrester parameters (c) Damper parameters

A three phase fixed series capacitor is shown in Fig. 7.3 as modeled in RTDS/ RSCAD software. MOV is placed in parallel with the fixed series capacitor compensation to protect it against over-voltages. It is a non−linear device which appears as an open circuit to the line current when the voltage across the capacitor is low. At higher voltages, it begins to conduct more current, therefore preventing a large voltage from being developed across the series capacitor. In such case, equivalent impedance of MOV and fixed series capacitor affects the protection scheme. The MOV itself is protected by a parallel by−pass switch as shown in Fig. 7.3(a), which can be closed when the energy absorbed by the MOV exceeds some predetermined threshold limit. The energy absorbed by the MOV is a function of the voltage across, and the current through the MOV. During high current fault conditions, the energy build up in the MOV is very fast. In order to protect it against permanent damage, it has to be removed from the circuit by closing its parallel by−pass switch. When this happens, the series capacitor compensation is also removed from the circuit and in such case series compensation does not affect the line protection. Parameters of the FSC have been indicated in Fig. 7.3(b-c). A device name must be specified with the μF rating of capacitor. Several other parameters like discharge voltage of MOV, power of normalize voltage on which MOV current depends have to be given as input. MOV energy limit to operate bypass switch has to be specified.

7.3.4 Thyristor Controlled Series Compensator Model

The Thyristor Controlled Series Compensation (TCSC) model was developed to bring advanced testing of TCSC control systems to the RTDS/ RSCAD simulator. Model used for the validation algorithm is shown in Fig. 7.4(a). D1 and D2 are the unconnected nodes at these nodes TCSC can be connected in series with the transmission line through breaker. FLT1 and FLT2 are two fault switches included in the model. The Sharc TCSC model consists of a thyristor controlled reactor (TCR) with snubber circuit. A protective MOV is connected across the series capacitor for over voltage protection. MOV current can be measure and scaled with using two separate measurements A1 and A2. Similarly two measurements of main capacitor current can be done in capacitor branch. MOV energy can be calculated and it can be kept in ‘ON’ and ‘OFF’ position as required in high and low fault current condition. The Main Gap (GAP) includes a damping circuit which damps current oscillations when the GAP is fired. The main by-pass circuit connected across the whole TCSC includes a damping circuit which damps current oscillations when the gap is fired. Block diagram of the firing angle generation

for anti-parallel thyristors of TCR is shown in Fig. 7.4(b). PLL generates a reference angle (θ) corresponding to 3-phase input voltage and firing pulse generator produce 180^o shifted firing pulses for anti-parallel thyristors with respect to firing angle Alfa.

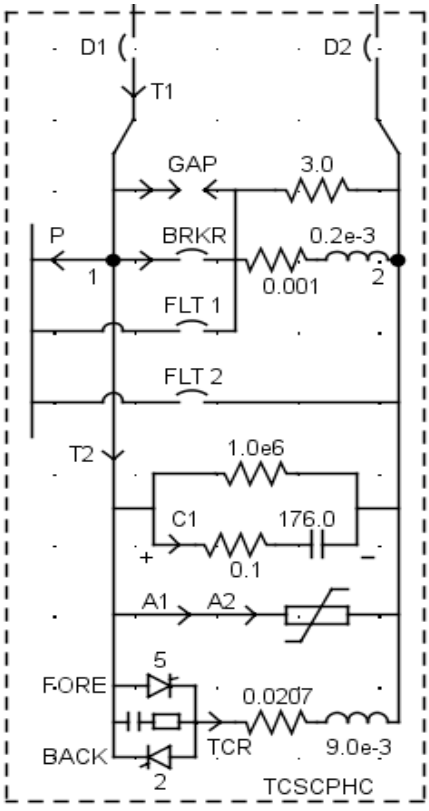

(a)

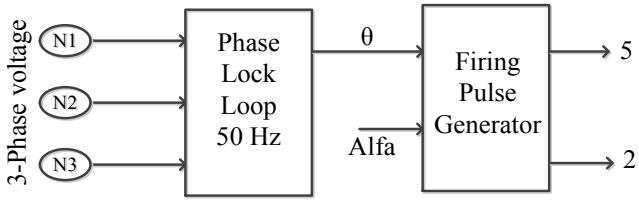

(b)

Fig. 7.4 MOV protected TCSC (a) Model in RTDS/ RSCAD (b) TCR firing pulse control

7.3.5 SVC Model

A three phase SVC model given in RTDS/ RSCAD is shown in Fig. 7.5(a). This model is configured either as a TCR bank or a TSC bank. At one time maximum of two banks can be used of TCR or TSC configuration. Three parallel branches of TSC consist of an antiparallel thyristor switch, snubber circuit and series inductor having some resistance. Firing pulse

generator produces firing pulses synchronized to three phase voltage with the help of PLL. Card configuration and parameters of TSC have been shown in Fig. 7.5(b) and Fig. 7.5(c) respectively.

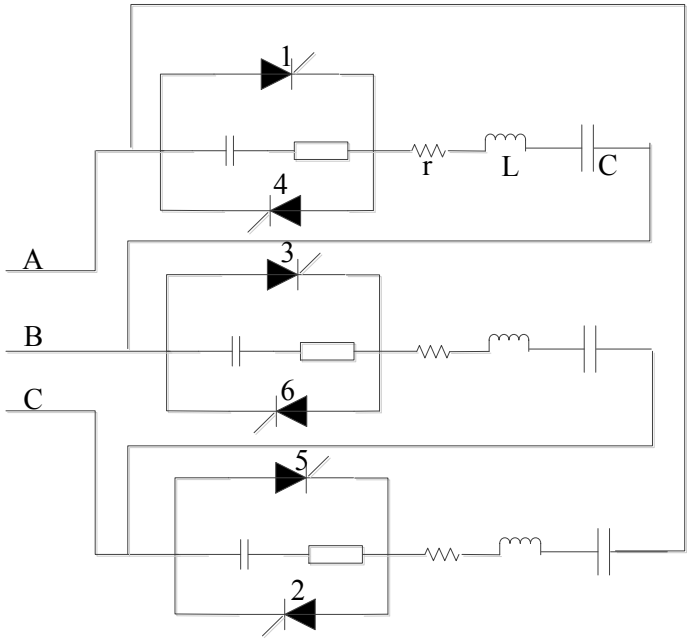

(a)

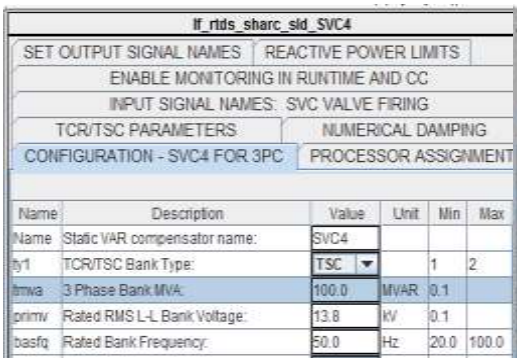

(b)

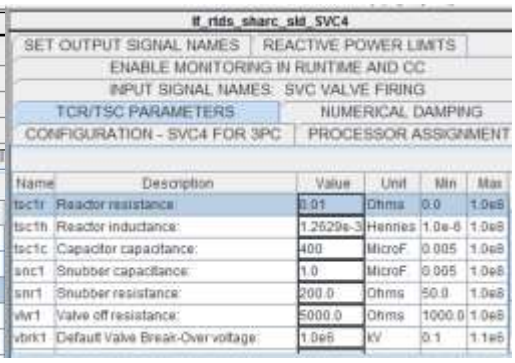

(c)

Fig. 7.5 SVC (a) Model in RTDS/ RSCAD (b) Card configuration (c) TCR parameters

7.4 Validation of Proposed Algorithm with Compensated Transmission Network

Validation of the adaptive distance algorithm is tested with the series and shunt compensated transmission network. For protection of series compensated line the algorithm proposed in chapter- 3 (section-3.3.2) has been validated and for protection of shunt compensated transmission line the algorithm proposed in chapter-5 (section 5.4) has been

validated respectively. An identical network has been designed in RTDS/ RSCAD for the justification of the suggested protection algorithms. A 320 km long doubly fed transmission system having FSC at mid-point has been taken for the validation of the proposed algorithm. FSC is connected at 160 km with fixed series compensation equal to 30 % of the line. Parameters of the CT, CCVT, power source and transmission line are similar to PSCAD/EMTDC model given in appendix-A and B. Line fault (L-G) has been created at 272 km in the segment after the FSC at zone-1 boundary. Fault has been created at 0.3 s and the duration of fault is 0.3 s. To check the adaptive behavior of the proposed Mho relay algorithm to compensate the error introduced by the FACTS compensation, effect of fault resistance is kept negligible which does not affect the fault location estimation. Performance of the proposed adaptive distance algorithms for series and shunt compensated network is discussed as follows:

7.4.1 With Fixed Series Capacitor

Arrangement of the FSC transmission network is shown in Fig. 7.6. The transmission network consists of two segments of the transmission line, both having same impedance parameters. Comparative results of the conventional and the proposed algorithm for a boundary fault at 272 km with 30° loading angle, fault resistance 0.01 Ω is shown in Fig. 7.7. Black curve specifies the conventional relay impedance trajectory, red curve directs the proposed relay impedance trajectory respectively. Z_{set} is the impedance of the 85 % of the transmission line which is calculated as 138.227 Ω. L-G Fault is created at 272 km with 15 % fixed compensation of the line, it is observed from the result in Fig. 7.7 that the conventional relay impedance curve is widely shifted from the actual fault location and shows larger error, on the other side proposed relay curve compensates the error and shows negligible error. For the comparison of the both the relay performance and to find the percentage fault location accuracy, generated data points has been plotted in Matlab.

Error in fault location can be calculated by equation (7.3) as:

$$\% \text{ fault location accuracy} = \frac{\text{measured impedance}}{\text{Actual line impedance}} * 100 \qquad (7.3)$$

% fault location accuracy with conventional algorithm = 90.07 %

% fault location accuracy with proposed algorithm = 99.11 %

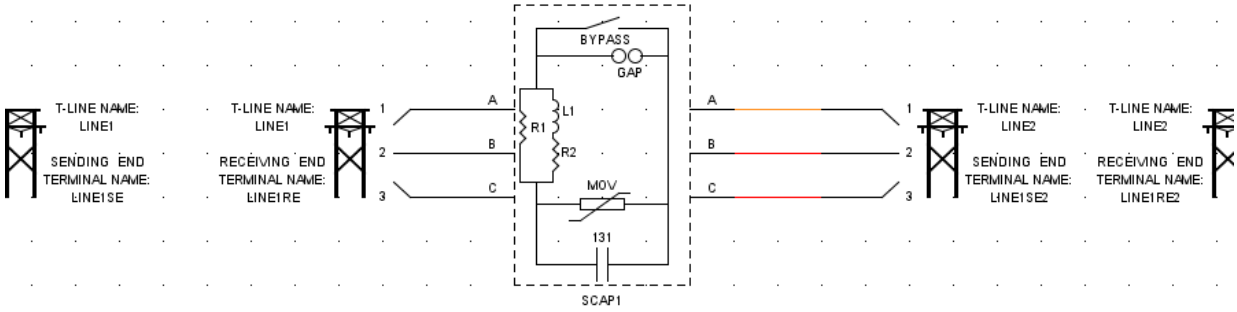

Fig. 7.6 Transmission network with FSC/MOV

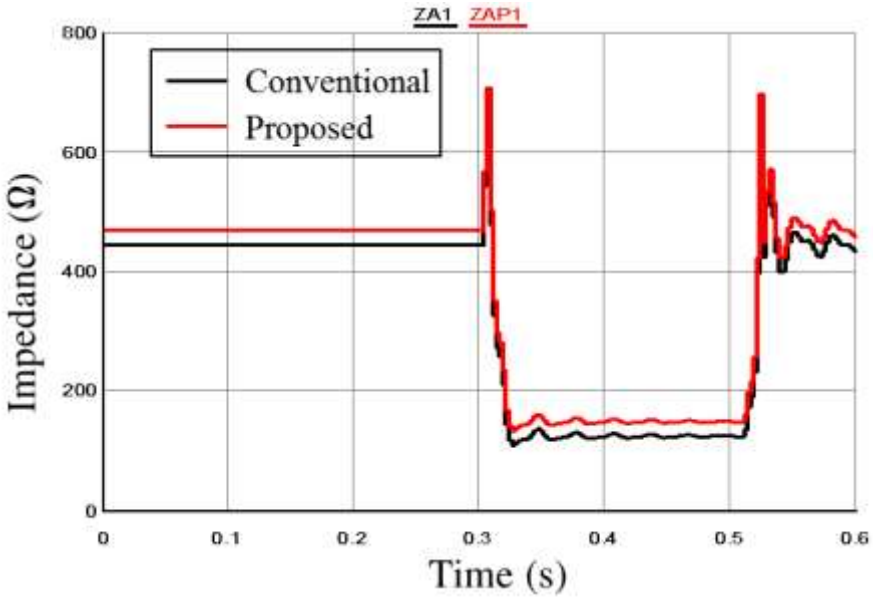

Fig. 7.7 Comparative result with 15% FSC

Similar results have been identified with the mid-point compensated transmission line having TCSC and SVC at mid-point.

7.4.2 With TCSC

Arrangement of the mid-point series compensated transmission line having TCSC at mid-point has been shown in Fig. 7.8. Proposed and the conventional relay algorithm for mid-point TCSC compensated line has been analyzed for low and high fault current conditions. Comparative result in low fault current condition for the conventional and the proposed algorithm for a boundary fault at 272 km with 30° loading angle, fault resistance 0.01 Ω is shown in Fig. 7.9(a).

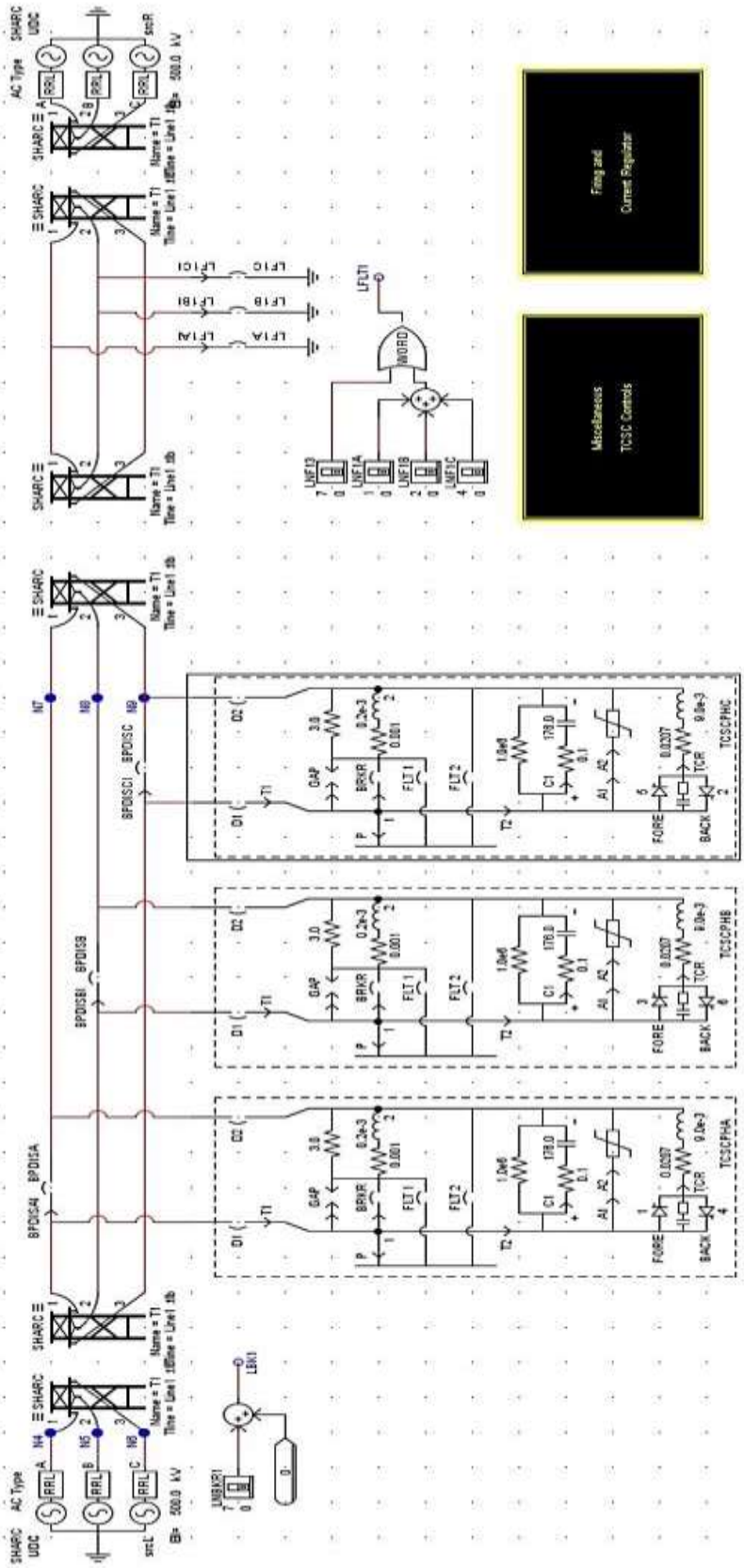

Fig. 7. 8 Transmission system with TCSC

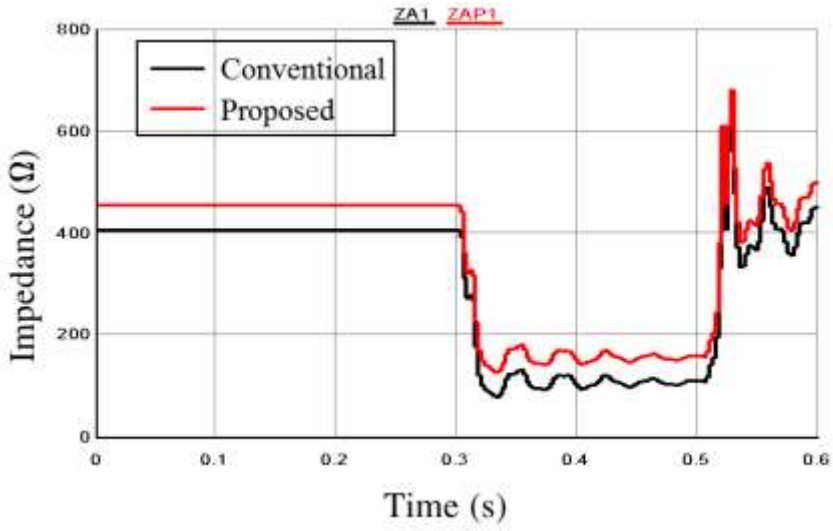

(a)

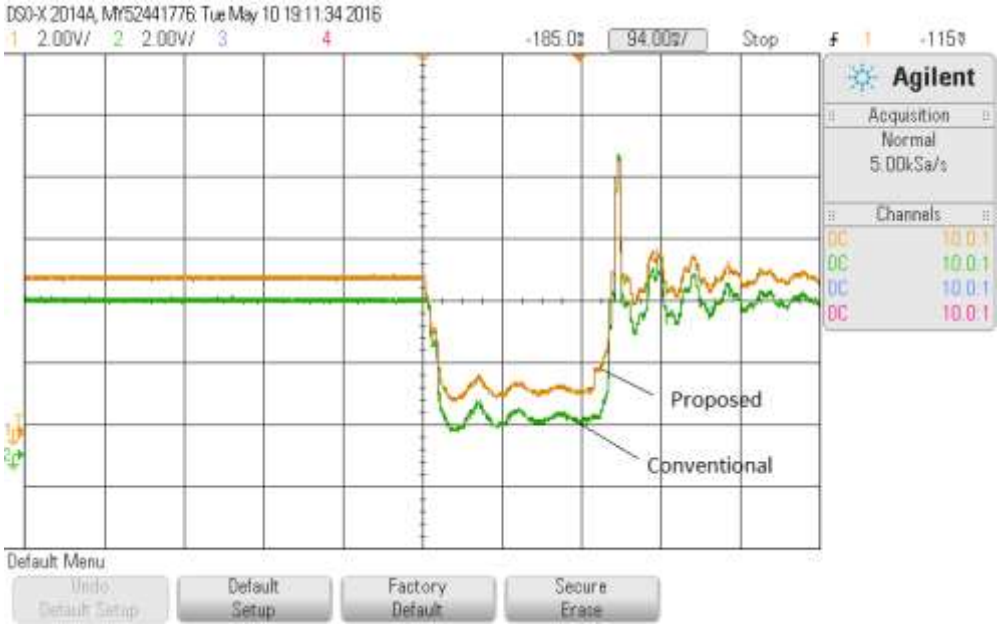

(b)

Fig. 7.9 Comparative result with 30 % compensation and fault at 272 km low fault current (a) RSCAD output (b) DSO output

Black curve specifies the conventional relay impedance trajectory, red curve directs the proposed relay impedance trajectory, respectively. The results have been verified using a Digital storage oscilloscope (DSO) as shown in Fig. 7.9(b). The low fault current condition has been created forcefully to avoid the action of MOV to bypass TCSC from the line. In such condition TCSC inserts the maximum error in the fault impedance calculation which is calculated as 59.42 % in case of conventional relay algorithm. Proposed relay algorithm

compensates the error introduced by the TCSC into the line and accurately detect the fault location with 97.82 % accuracy. Fault location accuracy is calculated by importing impedance data points in a Matlab program. From Fig. 7.9, fault location accuracy for different algorithms was calculated via a Matlab program as:

% fault location accuracy with conventional algorithm = 59.42 %
% fault location accuracy with proposed algorithm = 97.82 %

Similarly, the comparative result of the proposed and the convention Mho relay algorithm are taken for high fault current condition and shown in Fig. 7.10. In high fault current condition, MOV bypass line fault current and protect TCSC from the high voltage. In such condition error impedance is the parallel combination of MOV and TCSC. Fig. 7.10 indicates the performance of different algorithms and the accuracy is calculated as:
% fault location accuracy with conventional algorithm = 87.68 %
% fault location accuracy with proposed algorithm = 98.18 %

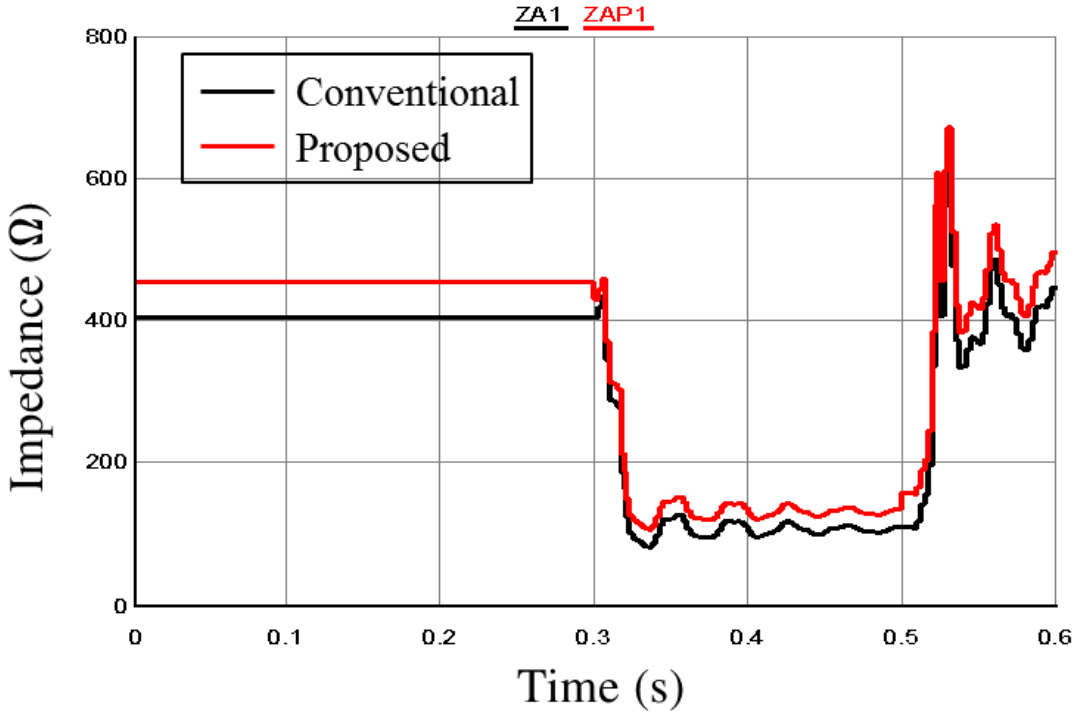

Fig. 7.10 30 % compensation and fault at 272 km high fault current

7.4.3 With SVC

Arrangement of the mid-point shunt compensated transmission line having SVC at mid-point has been shown in Fig. 7.11. Proposed and the conventional relay algorithm for mid-point

SVC compensated line has been analyzed for different modes of operations. Comparative result in inductive mode of operation for conventional and the proposed algorithm for a boundary fault at 272 km with 30° loading angle, fault resistance 0.01 Ω is shown in Fig. 7.12 (a). Black curve specifies the conventional relay impedance trajectory, red curve directs the proposed relay impedance trajectory, respectively. The results have been verified using a Digital storage oscilloscope (DSO) as shown in Fig. 7.12(b). Fig. 7.12 indicates the performance of different algorithms and the accuracy is calculated through a Matlab program as:

% fault location accuracy with conventional algorithm = 96.36 %

% fault location accuracy with proposed algorithm = 69.56 %

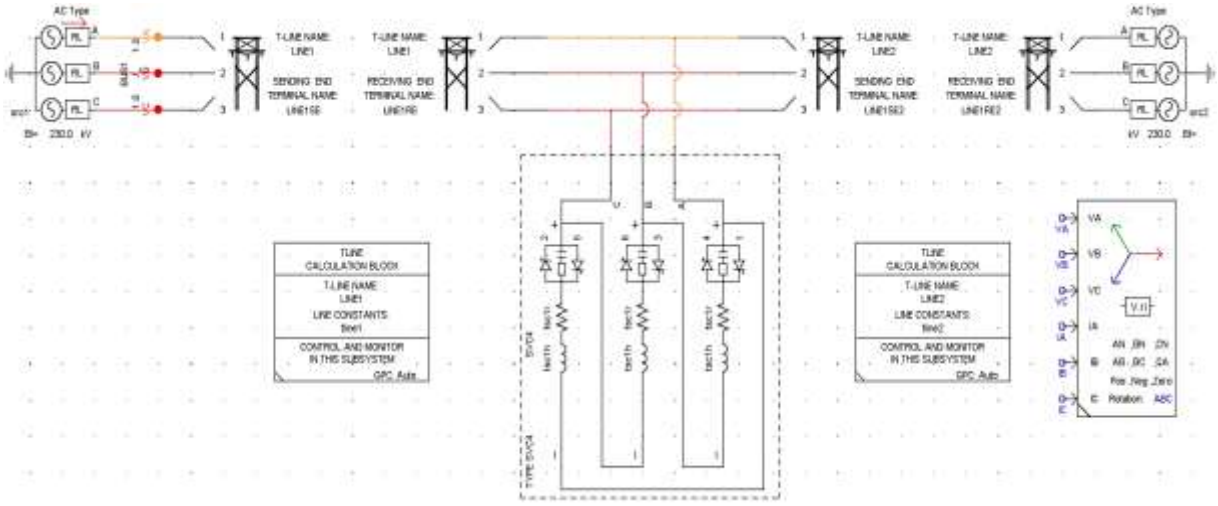

Fig. 7.11 Transmission system with SVC

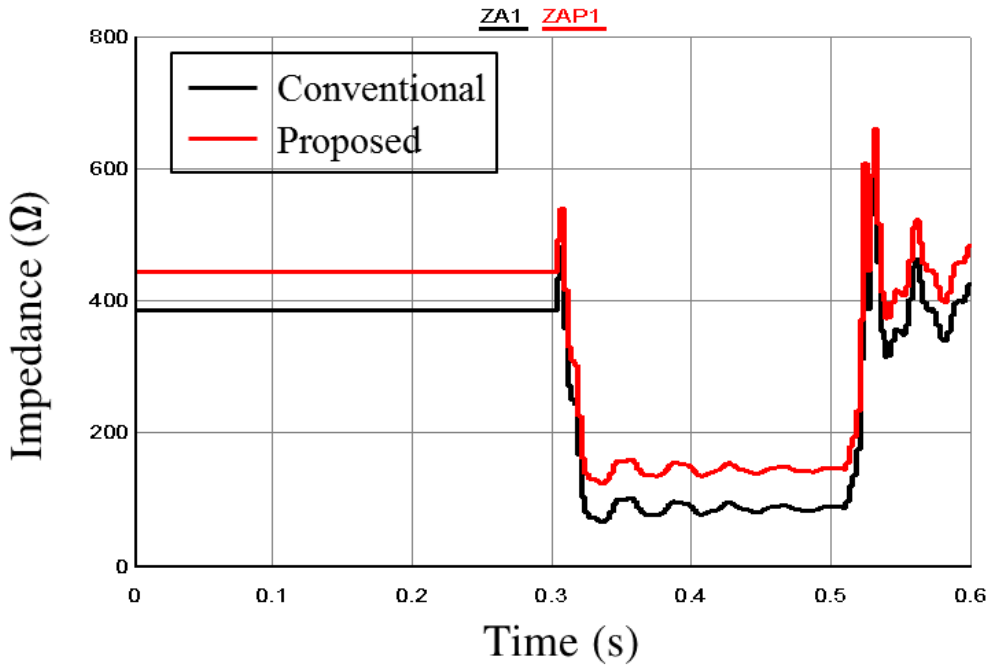

(a)

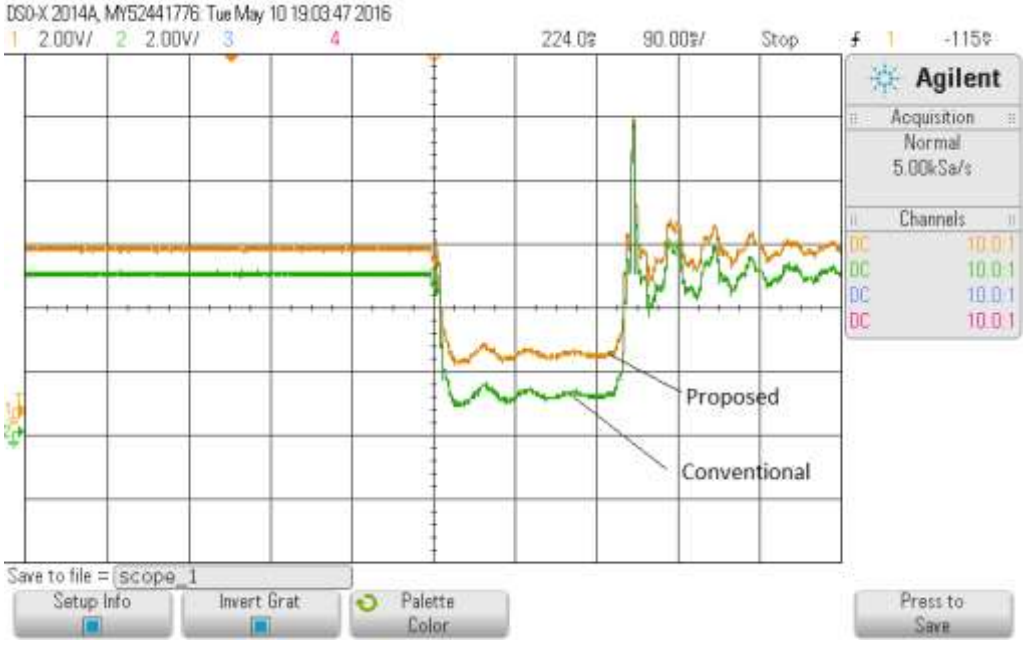

(b)

Fig. 7.12 SVC in inductive mode (a) RSCAD output (b) DSO output

Fig. 7.13 shows the performance of different algorithms in capacitive mode of operation. Far a boundary fault condition conventional relay shows under-reaching effect and proposed relay removes the error and tries to settle at boundary location. Fault location accuracy with both the algorithms is calculated with the help of Matlab program as:

% fault location accuracy with conventional algorithm = 75.6 %

% fault location accuracy with proposed algorithm = 98.56 %

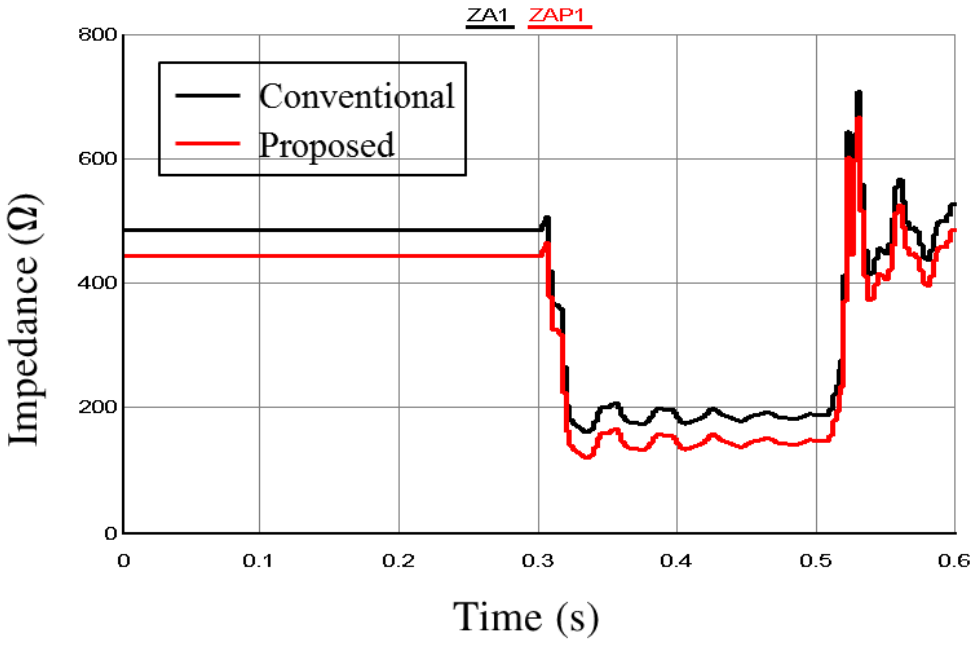

Fig. 7.13 SVC in capacitive mode

7.5 Summary

Series and shunt compensated transmission network have been designed in RTDS/ RSCAD to validate the adaptive distance protection algorithm. Adaptive protection algorithm is tested on transmission system having one of the FACTS compensator among FSC, TCSC and SVC at mid-point. Parameters of the transmission system and FACTS compensators are taken to be same as used in PSCAD/EMTDC simulation. A few cases have been analyzed to validate the adaptive protection algorithm in RTDS/ RSCAD environment. It has been observed from the validation results that the adaptive distance protection algorithm equally works in RTDS/ RSCAD environment. Maximum accuracy of the fault location estimation was found to be 99.11 % in FSC line, 98.18 % in TCSC line and 98.56 % in SVC line respectively.

CHAPTER 8
CONCLUSION AND FUTURE SCOPE

8.1 Conclusion

This thesis presents a complete study of the protection of mid-point series as well shunt compensated transmission network. Work on fault section identification, adaptive distance protection and zone setting of mid-point compensated transmission network has been carried out in the chapters. Both the series and the shunt type of compensators are used for mid-point compensated transmission line protection schemes. All the work has been carried out in PSCAD/EMTDC and MATLAB background and adaptive distance protection algorithms are also validated in real time Real Time Digital Simulator (RTDS). The work carried out in this thesis has been summarized and concluded chapter vise as following.

In chapter-1, a brief introduction about the advantages of FACTS devices on transmission network has been given. A detailed description of the impact of different FACTS devices on transmission line protection has been addressed. A comprehensive review of all the techniques presented in literature regarding the protection of series and shunt compensated line has been discussed. It has been concluded that FACTS compensators are very popular in power transmission network due to several advantages. However, it adversely affects the transmission line protection system, mainly the distance protection of transmission line. Further, in literature, several remedial methods are suggested which overcome the problems associated with FACTS compensator w.r.t. the protection of transmission network.

In chapter-2, problem regarding the fault section identification in mid-point compensated transmission network, which is the primary requirement for protection, has been considered. A HPF is applied at the separation point of two sections of mid-point compensated line. Main advantage of application of HPF at separation point is its ability to clearly differentiate the fault patterns generated in both the sections. The HPF filters high frequency transient signal generated during fault in section after separation point. High frequency transient fault signals are present in a fault before the separation point. DWT-MRA decomposes the relaying current signal at relay bus at the receiving end. WT has the ability of fast time-frequency localization of a signal. WT-MRA decomposition of fault current shows that the magnitude of high frequency signals present in the faults of section-II is very less or

negligible and comparatively very high in faults of section-I. Effect of worst possible noise on DWT-MRA is analyzed with the insertion of the maximum possible noise in the current signal. It is shown that noise does not affect the DWT-MRA decomposition considerably. Analysis of DWT-MRA frequency patterns have been performed with different AI techniques. Fault patterns are generated for all possible power system operating conditions for series as well shunt compensated transmission line for two transmission voltage level i.e. 230kV and 400kV. Accuracy of the section identification algorithm is very satisfactory with the proposed method. In this chapter, fault section was identified for series as well shunt compensated transmission line. After identifying the fault section next task was to protect the transmission network if fault loop consist of FACTS device i.e. fault in section-II, which were discussed in the subsequent chapters.

In chapter-3, an adaptive distance relay protection for mid-point series compensated transmission line having TCSC at mid-point is presented. TCSC induces variable impedance into the transmission line according to mode of operation. TCSC affects the distance protection of transmission line if it falls in fault loop or if fault occurs in section-II. A compensated Mho relay is developed for such protection which is fully adaptive with the changes of TCSC impedance. Impedance inserted by TCSC in the impedance loop is calculated in terms of relay current and firing angle of TCSC. Protective MOV impedance is calculated in terms of line current and TCSC impedance is calculated by firing angle of thyristor. Equivalent impedance of MOV and TCSC is calculated, which is the resultant impedance inserted by TCSC in fault loop. Adaptive Mho relay satisfactorily removes the error inserted by TCSC in fault loop and protect transmission network. Proposed relay adaptively protects the transmission line's capacitive and inductive mode of TCSC. Relay is also tested with wide range of loading and fault resistance at several locations. The results obtained show that the proposed adaptive relay successfully mitigates the reaching problem associated with TCSC. It is also shown in the work that proposed relay also positively work in double circuit transmission line.

In chapter-4, protection of series compensated line is extended towards the zone setting of transmission network. Proposed adaptive Mho relay is constrained by the very high variation in fault resistance and loading conditions. Therefore, an adaptive zone setting is achieved which is fully compatible of TCSC compensation, high fault resistance and wide loading conditions. Adaptive impedance patterns are generated at different location in zone-1 and zone-2 by taking wide variations in load angle, fault resistance and several other power system

parameters. It is found that adaptive impedance patterns have clear advantage over conventional impedance patterns in term of overlapping. In conventional impedance patterns, a large overlapping area is observed while adaptive impedance patterns have light overlapping area. AI classifier viz. SVM and RBFNN discriminates the zone-1 and zone-2 in series compensated line. Comparative results suggest that classification accuracy with adaptive patterns is much better than the conventional method and the SVM classifier has slightly better accuracy than the RBFNN based classifier.

In chapter-5, an adaptive Mho relay for mid-point shunt compensated transmission line having SVC/ STATCOM has been presented. Shunt FACTS device inject a current into the line at the point of connection and affect the line protection if fault occurs after that point. Equivalent impedance inserted by shunt device in the fault loop is calculated in terms of the current which the particular device injects into the line. Adaptive relay calculates the inserted impedance in both capacitive and inductive modes of operation and simultaneously subtracts it from the total fault impedance. Net output impedance decides whether the relay should trip or not. Adaptive relay is tested with the complete operating characteristics of SVC and STATCOM and results suggest that adaptive relay successfully mitigates the problem which arises due to shunt device. Performance of the proposed adaptive relay has been compared with the conventional relay. It is concluded from the comparative results, that the conventional Mho relay fails at several locations and shows under-reaching or over-reaching while proposed relay doesn't show any reaching problems.

In chapter-6, work on protection of shunt compensated line is stretched towards the zone setting of transmission network. Proposed adaptive Mho relay for mid-point shunt compensated line is constrained by the excessive variation in fault resistance and load angle. Therefore, an adaptive zone setting is achieved, which is fully compatible of shunt device characteristics, high fault resistance and wide loading conditions. Adaptive impedance patterns are generated at different location in zone-1 and zone-2by taking wide variations in load angle, fault resistance, SVC/ STATCOM characteristics and several other power system parameters. It is found that adaptive impedance patterns have clear advantage over conventional impedance patterns in term of overlapping. In the conventional impedance patterns, a large overlapping area is observed while adaptive impedance patterns have a reduced amount of overlapping area. AI classifier viz. SVM and RBFNN discriminates the zone-1 and zone-2 in shunt compensated line. Comparative results suggest that classification accuracy with adaptive patterns is much

better than conventional patterns and SVM classifier has slightly better accuracy than the RBFNN based classifier.

In seventh chapter, adaptive distance algorithms presented for protection of series and shunt compensated transmission network has been tested and validated in RTDS/RSCAD real time simulator. Similar systems have been designed in the RSCAD environment to check the accuracy of adaptive Mho relay algorithm for protection of mid-point compensated transmission line. It is clear from the validation results that adaptive relay performs equally well in RTDS/RSCAD environment.

8.2 Future Scope

In the present research work, protection of mid-point series as well shunt compensated transmission line has been presented. Adaptive distance protection based and AI technique based algorithms are developed for the protection. The following suggestions are made for future work:

1. Adaptive protection algorithms can be developed for mid-point compensated transmission line having UPFC and SSSC at mid-point.
2. A microcontroller/microprocessor based hardware implementation of digital relay can be designed for protection of mid-point compensated transmission line on the basis of proposed algorithms in this thesis.
3. Multiple sections transmission lines are popular in present time. Protection schemes can be developed for multiple FACTS devices installed in the transmission line at different locations.
4. Behavior of the adaptive protection schemes in larger bus system having mid-point compensators can be analyzed.

REFERENCES

[1] N. G. Hingorani and L. Gyugyi, *Understanding FACTS concepts and technology of flexible ac transmission systems*. Institute of Electrical and Electronics Engineers, IEEE Press, 2000.

[2] R. Mathur and R. Varma, *Thyristor-based FACTS controllers for electrical transmission systems*. Wiley-IEEE Press, 2002.

[3] K. Padiyar, *FACTS controllers in power transmission and distribution*. New Age International Publisher, 2007.

[4] S. N. Singh, "Present and Future of Flexible AC Transmission Systems (FACTS) Controllers in the Power Systems," *International Journal of Energy Technology and Policy (IJETP)*, vol. 4, no. 3/4, pp. 229–235, 2006.

[5] T. J. Hammons and S. K. Lim, "Flexible Ac Transmission Systems (Facts)," *Electric Machines & Power Systems*, vol. 25, no. 1, pp. 73–85, Jan. 1997.

[6] D. J. Gotham and G. T. Heydt, "Power Flow Control in Systems With Facts Devices," *Electric Machines & Power Systems*, vol. 26, no. 9, pp. 951–962, Nov. 1998.

[7] Y. Xiao, Y. H. Song, C. Liu, and Y. Z. Sun, "Available Transfer Capability Enhancement Using FACTS Devices," *IEEE Transactions on Power Systems*, vol. 18, no. 1, pp. 305–312, 2003.

[8] B. K. Kumar, S. N. Singh, and S. C. Srivastava, "Placement of SVC, TCSC and UPFC using Controllability Index Method to Damp Out Inter-Area Oscillations," *IEE Proc. Generation, Transmission & Distribution*, vol. 1, no. 2, pp. 209–217, 2007.

[9] J. G. Singh, S. N. Singh, and S. C. Srivastava, "An Approach for Optimal Placement of Static VAr Compensators Based on Reactive Power Spot Price," *Power Systems, IEEE Transactions on*, vol. 22, no. 4, pp. 2021–2029, 2007.

[10] C. Mason, "The art and science of protective relaying," *General Electric Company*, 1956.

[11] S. Horowitz and A. Phadke, *Power system relaying*, Third Edit. Wiley, 2013.

[12] A. Phadke and J. Thorp, *Computer relaying for power systems*, Second Edi. Wiley, 2009.

[13] G. D. Breuer, H. M. Rustebakke, R. A. Gibley, and H. O. Simmons, "The Use of Series Capacitors to Obtain Maximum EHV Transmission Capability," *IEEE Transactions on Power Apparatus and Systems*, vol. 83, no. 11, pp. 1090 – 1102, 1964.

[14] M. Khederzadeh and T. S. Sidhu, "Impact of TCSC on the protection of transmission lines," *IEEE Transactions on Power Delivery*, vol. 21, no. 1, pp. 80–87, 2006.

[15] Z. Xiang, J. Lin, L. Ban, and B. Zheng, "Investigation of TRV across circuit-breaker of series compensated double-circuit UHV transmission lines," in *Power System Technology conf.*, 2010, pp. 1–5.

[16] S. Jamali, A. Kazemi, and H. Shateri, "Voltage Inversion Due To Presence of TCSC on Adjacent Lines and Distance Relay Mal-Operation," in *Universities Power Engineering Conference*, 2008, pp. 1–5.

[17] M. Khederzadeh, A. Ghorbani, and A. Salemnia, "Impact of SSSC on the digital distance relaying," *IEEE Power & Energy Society General Meeting*, pp. 1–8, Jul. 2009.

[18] K. El-Arroudi, G. Joos, and D. McGillis, "Operation of impedance protection relays with the STATCOM," *IEEE Transactions on Power Delivery*, vol. 17, no. 2, pp. 381–387, 2002.

[19] F. Albasri, T. Sidhu, and R. Varma, "Performance comparison of distance protection schemes for shunt-FACTS compensated transmission lines," *IEEE Transactions on Power Delivery*, vol. 22, no. 4, pp. 2116–2125, 2007.

[20] X. Zhou, H. Wang, R. K. Aggarwal, and P. Beaumont, "Performance evaluation of a distance relay as applied to a transmission system with UPFC," *IEEE Transactions on Power Delivery*, vol. 21, no. 3, pp. 1137–1147, 2006.

[21] M. Zellagui and A. Chaghi, "Impact of series compensation (SC) on the MHO distance Relay in Algerian 220kV Transmission Line'," *Canadian journal on Electrical and Electronics*, vol. 2, no. 6, pp. 181–189, 2011.

[22] T. S. Sidhu and M. Khederzadeh, "TCSC impact on communication-aided distance-

protection schemes and its mitigation," *IEE Proceedings - Generation Transmission and Distribution*, vol. 152, no. 5, pp. 714–728, 2005.

[23] D. Novosel, A. Phadke, M. M. Saha, and S. Lindahl, "Problems and Solutions for Microprocessor Protection of Series Compensated Line," *Sixth International Conference on Developments in power system protection*, no. 434, pp. 18–23, 1997.

[24] D. Novosel, B. Bachmann, D. Hart, Y. Hu, and M. M. Saha, "Algorithms for Locating Faults on Series Compensated Lines using Neural Network and Deterministic Methods," *IEEE Transactions on Power Delivery*, vol. 11, no. 4, pp. 1728–1736, 1996.

[25] A. Nekoubin, "Simulation of Series Compensated Transmission Lines Protected with Mov," *World Academy of Science Engineering and Technology*, pp. 1002–1006, 2011.

[26] D. L. Goldsworthy, "A Linearized Model for MOV-Protected Series Capacitors," *IEEE Transactions on Power Delivery*, vol. PWRS-2, no. 4, pp. 953–957, 1987.

[27] A. K. Pradhan, M. Biswal, and B. B. Pati, "Directional relaying for double circuit line with series compensation," *IET Generation Transmission & Distribution*, vol. 7, no. 4, pp. 405–413, Apr. 2013.

[28] P. Jena and A. K. Pradhan, "Directional Relaying in the Presence of a Thyristor-Controlled Series Capacitor," *IEEE Transactions on Power Delivery*, vol. 28, no. 2, pp. 628–636, 2013.

[29] R. A. Castro and H. A. Pineda, "Protection system considerations for 400 kV series compensated transmission lines of the central Western network in Venezuela," in *2006 IEEE PES Transmission and Distribution Conference and Exposition: Latin America, TDC'06*, 2006, pp. 1–5.

[30] H. J. Altuve, J. B. Mooney, and G. E. Alexander, "Advances in series-compensated line protection," in *2009 62nd Annual Conference for Protective Relay Engineers*, 2009, pp. 263–275.

[31] S. O. Faried and S. Aboreshaid, "Stochastic evaluation of transient recovery voltages across circuit breakers of series capacitor compensated transmission lines," *IEEE Transactions on Power Delivery*, vol. 16, no. 1, pp. 33–37, 2001.

[32] H. García, J. Segundo, and M. Madrigal, “Harmonic analysis of power systems including thyristor-controlled series capacitor (TCSC) and its interaction with the transmission line,” *Electric Power Systems Research*, vol. 106, pp. 151–159, Jan. 2014.

[33] D. D. Wilson, “Series Compensated Line Voltages Across Circuit Breakers and Terminals Caused by Switching,” in *IEEE PES summer meeting San Francisco*, 1972, pp. 1050–1056.

[34] A. Parvizi, M. Rostami, and A. M. Ghadiri, “Sensitivity analysis of TRV in TCSC compensated transmission lines during fault clearing by line CB,” in *Power and Energy Society General Meeting*, 2008, no. PECon 08, pp. 1345–1349.

[35] R. Grunbaum, K. Wikstrom, and G. Stromberg, “On series compensation impact on line protection and TRV,” in *North American Power Symposium (NAPS),* 2009, pp. 1–5.

[36] R. Balasubramanian, B. Ram, and S. Tripathy, “Temporary overvoltages due to load rejection on a series-compensated transmission line,” *IEE Proceedings - Generation Transmission and Distribution*, vol. 130, no. 1, pp. 8–15, 1983.

[37] V. Madzarevic, F. K. Tseng, D. H. Woo, W. D. Niebhur, and R. G. Rocamora, “Overvoltage on EHV Transmission Line Due to Faults and Subsequent Bypassing of Series Capacitors,” *IEEE Transactions on Power Apparatus and Systems*, vol. PAS-96, no. 6, pp. 1847–1855, 1977.

[38] F. Iliceto, F. M. Gatta, E. Cinieri, and G. Asan, “TRVs across circuit breakers of series compensated lines: status with present technology and analysis for the Turkish 420 kV grid,” *IEEE Transactions on Power Delivery*, vol. 7, no. 2, pp. 757–766, 1992.

[39] S. Jamali, A. Kazemi, and H. Shateri, “Effects of voltage transformers connection point on measured impedance at relaying point for inter phase faults in presence of TCSC,” in *PECon 2008 - 2008 IEEE 2nd International Power and Energy Conference*, 2008, pp. 553–558.

[40] H. Abdollahzadeh, B. Mozafari, A. Tavighi, and J. Marti, “Impact of Shunt Capacitance of a SSSC-Compensated Transmission line on Performance of Distance Relays,” in *Power and Energy Society General Meeting (PES) IEEE*, 2013, pp. 1–5.

[41] A. Kazemi, S. Jamali, and H. Shateri, “Effects of SSSC on Distance Relay Tripping

Characteristic," *IEEE International Symposium on Industrial Electronics*, pp. 1899–1904, Jul. 2006.

[42] A. Kazemi, S. Jamali, and H. Shateri, "Effects of SMES equipped SSSC on distance relay tripping characteristic," *EEE/PES Transmission and Distribution Conference and Exposition*, pp. 1–6, Apr. 2008.

[43] A. Kazemi, S. Jamali, and H. Shateri, "Effects of Instrument Transformers Connection Point on Measured Impedance by Distance Relay in Presence of SSSC," *Power System Technology*, pp. 7–12, 2006.

[44] S. Jamali, A. Kazemi, and H. Shateri, "Voltage inversion due to presence of SSSC on adjacent lines and distance relay mal-operation," in *IEEE International Conference on Industrial Technology*, 2008, pp. 1–6.

[45] S. Jamali, A. Kazemi, and H. Shateri, "Distance relay over-reaching due to SSSC presence on second circuit of double circuit line," in *3rd IEEE Conference on Industrial Electronics and Applications*, 2008, pp. 918–923.

[46] A. Kazemi, S. Jamali, and H. Shateri, "Distance Relay Mal-Operation due to Presence of SSSC on Adjacent Lines in Inter Phase Faults," in *IEEE Region 5 Conference*, 2008, pp. 1–6.

[47] A. Kazemi, S. Jamali, and H. Shateri, "Comparing impacts of SSSC and STATCOM on measured impedance at relaying point," *IEEE Power & Energy Society General Meeting*, pp. 1–7, Jul. 2009.

[48] A. L. Courts, N. G. Hingorani, and G. E. Stemler, "A new Series capacitor Protection Scheme using Nonlinear Resistors," *IEEE Transactions on Power Apparatus and Systems*, vol. PAS-97, no. 4, pp. 1042–1052, 1978.

[49] J. R. Hamann, S. A. Miske, I. B. Johnson, and A. L. Courts, "A Zinc Oxide Varistor Protective System for Series capacitor," *IEEE Transactions on Power Apparatus and Systems*, vol. PAS-100, no. 3, pp. 929–937, 1981.

[50] R. J. Marttila, "Performance of distance relay mho elements on MOV-proteced series-compensated transmission," *IEEE Transactions on Power Delivery*, vol. 7, no. 3, pp. 1167–1178, 1992.

[51] J. Bapiraju and J. Shenoy, “Implementation of DSP based relaying with particular reference to effect of STATCOM on transmission line protection,” *Power System Technology PowerCon*, vol. 2, pp. 1381 – 1385, 2004.

[52] X. Zhou and H. Wang, “The impact of STATCOM on distance relay- Modeling and Simulation using PSCAD/EMTDC,” *Electrical Electronics and Computer Science (SCEECS)*, pp. 1–6, 2005.

[53] T. Sidhu and R. Varma, “Performance of distance relays on shunt-FACTS compensated transmission lines,” *IEEE Transactions on Power Delivery*, vol. 20, no. 3, pp. 1837–1845, 2005.

[54] S. Jamali, A. Kazemi, and H. Shateri, “Measured impedance by distance relay for inter phase faults in presence of STATCOM,” in *Power and Energy Society General Meeting*, 2008, pp. 1–6.

[55] S. Jamali, A. Kazemi, and H. Shateri, “Comparing effects of SVC and STATCOM on distance relay tripping characteristic,” in *Industrial Electronics ISIE*, 2008, pp. 1568–1573.

[56] S. Jamali and H. Shateri, “Effects of SMES Equipped STATCOM on distance relay ideal tripping characteristic,” in *Transmission & Distribution Conference and Exposition:IEEE/PES*, 2008, pp. 1–6.

[57] A. Kazemi, S. Jamali, and H. Shateri, “Impact of STATCOM modeling on its effect on distance relay tripping characteristic,” in *Industrial Electronics and Applications, ICIEA 3rd IEEE Conference on*, 2008, pp. 1746–1751.

[58] A. Kazemi, S. Jamali, and H. Shateri, “Measured impedance by distance relay for inter phase faults in presence of SVC,” in *Power System Technology*, 2010, pp. 1–6.

[59] S. Maturu and U. Shenoy, “Performance issues of distance relays for shunt FACTS compensated transmission lines,” in *Power System Technology*, 2010, pp. 1–6.

[60] S. ZhiJian and J. Jing, “Influence of SVC on fault component directional protection and its improvement approach,” *Advanced Power System Automation and Protection (APAP)*, vol. 3, pp. 1845–1850, 2011.

[61] M. Zellagui and A. Chaghi, “Effects of Shunt FACTS Devices on MHO Distance Protection Setting in 400 kV Transmission Line,” *Electrical and Electronic Engineering*, vol. 2, no. 3, pp. 164–169, Aug. 2012.

[62] M. Khederzadeh and A. Ghorbani, “Impact of VSC-based multiline FACTS controllers on distance protection of transmission lines,” *IEEE Transactions on Power Delivery*, vol. 27, no. 1, pp. 32–39, 2012.

[63] D. Hemasundar, M. Thakre, and V. Kale, “Impact of STATCOM on distance relay-Modeling and simulation using PSCAD/EMTDC,” in *Electrical Electronics and Computer Science (SCEECS)*, 2014, pp. 1–6.

[64] F. A. Albasri, T. S. Sidhu, and R. K. Varma, “Impact of Shunt-FACTS on Distance Protection of Transmission Lines,” in *Power Systems Conference: Advanced Metering, Protection, Control, Communication, and Distributed Resources*, 2006, pp. 249–256.

[65] A. Kazemi, S. Jamali, and H. Shateri, “Measured Impedance by Distance Relay in Presence of SVC on Transmission Line,” in *IEEE Industrial Electronics*, 2006, pp. 2214–2219.

[66] M. Elsamahy, S. O. Faried, and T. Sidhu, “Impact of Midpoint STATCOM on Generator Loss of Excitation Protection,” *Power Delivery, IEEE Transactions on*, vol. 29, no. 2, pp. 724–732, 2014.

[67] F. Albasri, T. Sidhu, and R. Varma, “Mitigation of adverse effects of midpoint shunt-FACTS compensated transmission lines on distance protection schemes,” in *Power Engineering Society*, 2007, pp. 1–8.

[68] Z. Moravej, D. N. Vishwakarma, and S. P. Singh, “Protection and Conditions Monitoring of Power Transformer Using ANN,” *Electric Power Components and Systems*, vol. 30, no. 3, pp. 217–231, 2002.

[69] A. Y. Abdelaziz, A. M. Ibrahim, M. M. Mansour, and H. E. Talaat, “Modern approaches for protection of series compensated transmission lines,” *Electric Power Systems Research*, vol. 75, no. 1, pp. 85–98, Jul. 2005.

[70] B. Bachmann, D. Novosel, and D. Hart, “Application of artificial neural networks for series compensated line protection,” in *Applications to PowerIntelligent Systems*

Applications to Power Systems, 1996, pp. 68–73.

[71] P. K. Dash, A. K. Pradhan, and G. Panda, "Application of Artificial Intelligence Techniques for Classification and Location of Faults on Thyristor-Controlled Series-Compensated Line," *Electric Power Components and Systems*, vol. 31, no. 3, pp. 241–260, Mar. 2010.

[72] A. Hosny and M. Safiuddin, "ANN-based protection system for controllable series-compensated transmission lines," *Power Systems Conference and Exposition*, pp. 1–6, 2009.

[73] A. M. Ibrahim, M. I. Marei, S. F. Mekhamer, and M. M. Mansour, "An Artificial Neural Network Based Protection Approach Using Total Least Square Estimation of Signal Parameters via the Rotational Invariance Technique for Flexible AC Transmission System Compensated Transmission Lines," *Electric Power Components and Systems*, vol. 39, no. 1, pp. 64–79, Jan. 2011.

[74] A. Solat and A. Deihimi, "A novel scheme for distance protection of series compensated transmission lines with TCSC using artificial neural networks," *20th Iranial Conf. on Electrical Engineering (ICEE)*, pp. 517–522, 2012.

[75] Y. H. Song, A. T. Johns, and Q. Y. Xuan, "Artificial Neural Network based Protection Scheme for Controllable Series compensated EHV Transmission line," *IEE Proceedings - Generation Transmission and Distribution Transmission and Distribution*, vol. 143, no. 6, pp. 535–540, 1996.

[76] Y. H. Song, A. T. Johns, Q. Y. Xuan, and R. K. Aggarwal, "Integrated Adaptive Protection and Control for Controllable Series Compensated Transmission System using Neural Network," in *AC and DC Power Transmission*, 1996, pp. 335–339.

[77] Y. H. Song, Q. Y. Xuan, and A. T. Johns, "Protection Scheme for Ehv Transmission Systems With Thyristor Controlled Series Compensation Using Radial Basis Function Neural Networks," *Electric Machines & Power Systems*, vol. 25, no. 5, pp. 553–565, May 1997.

[78] B. Vyas, R. P. Maheshwari, and B. Das, "Investigation for Improved Artificial Intelligence Techniques for Thyristor-controlled Series-compensated Transmission Line

Fault Classification with Discrete Wavelet Packet Entropy Measures," *Electric Power Components and Systems*, vol. 42, no. 6, pp. 554–566, Apr. 2014.

[79] H. Wang and W. W. L. Keerthipala, "Fuzzy-neuro Approach to Fault Classification for Transmission Line Protection," *IEEE Transactions on Power Delivery*, vol. 13, no. 4, pp. 1093–1104, 1998.

[80] Q. Xuan, A. Johns, and Y. Song, "Adaptive protection technique for controllable series compensated EHV transmission systems using neural networks," *Advances in Power System Control Operation and Management*, vol. 2, pp. 621–625, 1993.

[81] Z. Moravej, D. N. Vishwakarma, and S. P. Singh, "ANN-Based Protection Scheme for Power Transformer," *Electric Machines & Power Systems*, vol. 28, no. 9, pp. 875–884, 2000.

[82] Z. Moravej, D. N. Vishwakarma, and S. P. Singh, "Radial Basis Function Neural Network Model For Protection of Power Transformer," *Electric Power Components and Systems*, vol. 29, no. 4, pp. 307–320, 2001.

[83] M. Tripathy, R. P. Maheshwari, and H. K. Verma, "Advances in Transformer Protection: A Review," *Electric Power Components and Systems*, vol. 33, no. 11, pp. 1203–1209, 2005.

[84] M. Tripathy, R. P. Maheshwari, and H. K. Verma, "Radial basis probabilistic neural network for differential protection of power transformer," *Generation, Transmission & Distribution, IET*, vol. 2, no. 1, pp. 43–52, 2008.

[85] M. Tripathy, R. P. Maheshwari, and H. K. Verma, "Power Transformer Differential Protection Based On Optimal Probabilistic Neural Network," *IEEE Transactions on Power Delivery*, vol. 25, no. 1, pp. 102–112, 2010.

[86] B. Vyas, B. Das, and R. P. Maheshwari, "An improved scheme for identifying fault zone in a series compensated transmission line using undecimated wavelet transform and Chebyshev Neural Network," *International Journal of Electrical Power & Energy Systems*, vol. 63, pp. 760–768, Dec. 2014.

[87] E. Mohagheghi, A. Bagherian, W. A. Ashiru, and A. Esmaeilian, "A new fault location method based on adaptive neuro fuzzy in presence of SSSC on transmission line," in

Environment and Electrical Engineering (EEEIC),11th International Conference on, 2012, pp. 2–5.

[88] P. Ray, K. Panigrahi, and N. Senroy, "An AI approach for fault distance estimation in series compensated transmission line," *Energy Automation and Signal (ICEAS)*, pp. 1–6, 2011.

[89] Z. Moravej, M. Khederzadeh, and M. Pazoki, "New Combined Method for Fault Detection, Classification, and Location in Series-compensated Transmission Line," *Electric Power Components and Systems*, vol. 40, no. 9, pp. 1050–1071, Jun. 2012.

[90] U. B. Parikh, B. Das, and R. P. Maheshwari, "Combined wavelet-SVM technique for fault zone detection in a series compensated transmission line," *IEEE Transactions on Power Delivery*, vol. 23, no. 4, pp. 1789–1794, 2008.

[91] B. Vyas, R. Maheshwari, and B. Das, "Fault analysis of controllable series compensated transmission line with Wavelet Transform and Support Vector Machine," *International Conference on Engineering (NUiCONE) Nirma University*, pp. 1–5, 2012.

[92] P. Tripathi, G. Pillai, and H. Gupta, "New method for fault classification in TCSC compensated transmission line using GA tuned SVM," *Power System Technology conf.*, pp. 1–6, 2012.

[93] P. K. Dash, S. R. Samantaray, and G. Panda, "Fault Classification and Section Identification of an Advanced Series Compensated Transmission Line Using Support Vector Machine," *IEEE Transactions on Power Delivery*, vol. 22, no. 1, pp. 67–73, 2007.

[94] U. B. Parikh, B. Das, and R. Maheshwari, "Fault classification technique for series compensated transmission line using support vector machine," *International Journal of Electrical Power & Energy Systems*, vol. 32, no. 6, pp. 629–636, Jul. 2010.

[95] S. F. Mekhamer, A. Y. Abdelaziz, A. M. Ibrahim, and M. Ramadan, "Fault Classification of Series-Compensated Transmission Lines Using Support Vector Machine," *selected works*, pp. 1–7, 2011.

[96] P. K. Dash and S. R. Samantray, "Phase selection and fault section identification in thyristor controlled series compensated line using discrete wavelet transform,"

International Journal of Electrical Power & Energy Systems, vol. 26, no. 9, pp. 725–732, Nov. 2004.

[97] Z. Chen, X. Lin, and Z. Q. Bo, "Wavelet Transform Based Boundary Protection Scheme for Series Compensated Line," *Eighth IEE International Conference on Developments in Power System Protection*, vol. 1, pp. 56–59, 2004.

[98] A. I. Megahed, A. M. Moussa, and A. E. Bayoumy, "Usage of Wavelet Transform in the Protection of Series Compensated Transmission Line," *IEEE Transactions on Power Delivery*, vol. 21, no. 3, pp. 1213–1221, 2006.

[99] V. J. Pandya and S. A. Kanitkar, "A novel unit protection scheme for protection of series compensated transmission line using wavelet transform," *Power Engineering Conference AUPEC AUPEC*, pp. 1–5, 2007.

[100] E. Eldin and D. Ibrahim, "High impedance fault detection in EHV series compensated lines using the wavelet transform," *Power Systems Conference and Exposition, PSCE '09. IEEE/PES*, pp. 1–10, 2009.

[101] H. Dubeya, S. Mohanty, N. Kishor, and P. Ray, "Fault detection in a series compensated transmission line using discrete wavelet transform and independent component analysis: A comparative study," *Power Engineering and Optimization Conference (PEOCO) 5th International*, pp. 22–26, 2011.

[102] U. B. Parikh, B. R. Bhalja, R. P. Maheshwari, and B. Das, "Decision Tree Based Fault Classification Scheme for Protection of Series Compensated Transmission Lines," *International Journal of Emerging Electric Power Systems*, vol. 8, no. 6, pp. 1–12, Jan. 2007.

[103] A. K. Pradhan, A. Routray, and B. Biswal, "Higher Order Statistics-Fuzzy Integrated Scheme for Fault Classification of a Series-Compensated Transmission Line," *IEEE Transactions on Power Delivery*, vol. 19, no. 2, pp. 2003–2005, 2004.

[104] A. K. Pradhan, A. Routray, S. Pati, and D. K. Pradhan, "Wavelet Fuzzy Combined Approach for Fault Classification of a Series-Compensated Transmission Line," *IEEE Transactions on Power Delivery*, vol. 19, no. 4, pp. 1612–1618, 2004.

[105] S. R. Samantaray, P. K. Dash, G. Panda, and B. K. Panigrahi, "Distance Protection of

Compensated Transmission Line using Computational Intelligence," *computer science*, vol. 3801, pp. 163–169, 2005.

[106] S. Dambhare;, N. Kinhekar;, S. A. Soman;, and M. C. Chandorkar, "ATP-EMTP Analysis of Series Compensated Lines for Distance Protection Schemes," in *International Conference on Power System Protection, Bangalore, India*, 2007, pp. 1–5.

[107] P. Balcerek and M. Fulczyk, "Optimization of distance protection algorithm for double-circuit series-compensated transmission line," in *Advanced Power System Automation and Protection (APAP),* 2011, pp. 3–8.

[108] M. M. Saha, B. Kasztenny, E. Rosolowski, and J. Izykowski, "First Zone Algorithm for Series Compensated Lines," *IEEE Transactions on Power Delivery*, vol. 16, no. 2, pp. 200–207, 2001.

[109] E. Rosolowski and J. Izykowski, "High voltage series-compensated transmission line-evaluation of new distance protection," *High Voltage Engineering and Application (ICHVE)*, no. 1, pp. 513–516, 2010.

[110] E. Rosolowki and J. Izykowski, "Optimization of distance protection algorithm for series-compensated transmission line," *PowerTech IEEE Trondheim*, pp. 1–7, 2011.

[111] R. Dutra, L. Fabiano, W. Oliveira, M. M. Saha, and S. Lidstrom, "Adaptive distance protection for series compensated transmission lines," *Transmission and Distribution Conference and Exposition: Latin America IEEE/PES*, pp. 1–6, 2004.

[112] A. Shah, V. Sood, O. Saad, and V. Ramachandran, "Mho relay for protection of series compensated line," *Science and Technology for Humanity*, pp. 648–651, 2009.

[113] S. Srivani and K. Vittal, "Adaptive distance relaying scheme in series compensated transmission lines," *Power Electronics Drives and Energy Systems (PEDES)*, pp. 1–7, 2010.

[114] R. K. Gajbhiye, B. Gopi, P. Kulkarni, and S. A. Soman, "Computationally efficient methodology for analysis of faulted power systems with series-compensated transmission lines: A phase coordinate approach," *IEEE Transactions on Power Delivery*, vol. 23, no. 2, pp. 873–880, 2008.

[115] P. K. Dash, A. K. Pradhan, and G. Panda, “Apparent Impedance Calculations for Distance- Protected Transmission Lines Employing Series-Connected FACTS Devices,” *Electric Power Components and Systems*, vol. 29, no. 7, pp. 37–41, 2001.

[116] V. H. Makwana and B. R. Bhalja, “A New Adaptive Distance Relaying Scheme for Mutually Coupled Series-Compensated Parallel Transmission Lines During Intercircuit Faults,” *IEEE Transactions on Power Delivery*, vol. 26, no. 4, pp. 2726–2734, 2011.

[117] V. Makwana and B. Bhalja, “New digital distance relaying scheme for phase faults on doubly fed transmission lines,” *IET generation transmission & distribution*, vol. 6, no. 3, pp. 265–273, 2012.

[118] H. Shien, S. JaLe, and K. Xiaoning, “Fault component integrated impedance-based pilot protection scheme for the TCSC compensated EHV/UHV transmission line,” *Advanced Power System Automation and Protection (APAP)*, vol. 1, pp. 517–523, 2011.

[119] S. He, J. Suonan, and Z. Q. Bo, “Integrated Impedance-Based Pilot Protection Scheme for the TCSC-Compensated EHV/UHV Transmission line,” *IEEE Transactions on Power Delivery*, vol. 28, no. 2, pp. 835–844, 2013.

[120] Z. Xu, J. Zhang, Z. Su, X. Zhang, M. J. Iqbal, A. Wen, and Q. Yang, “A New Distance Relaying Algorithm for Single-phase-to-ground Faults on Series-compensated Parallel Lines without the Parameter Requirement of Mutual Coupling and Series Capacitor Device,” *Electric Power Components and Systems*, vol. 42, no. 6, pp. 650–657, Apr. 2014.

[121] Z. Xu, Z. Su, J. Zhang, A. Wen, and Q. Yang, “An Interphase Distance Relaying Algorithm for Series-Compensated Transmission Lines,” *IEEE Transactions on Power Delivery*, vol. 29, no. 2, pp. 834–841, 2014.

[122] S. Wilkinson, “Series Compensated Line Protection Issues,” *GE Power Management*, pp. 1–22, 1999.

[123] P. Jena and A. Pradhan, “A positive-sequence directional relaying algorithm for series-compensated line,” *IEEE Transactions on Power Delivery*, vol. 25, no. 4, pp. 2288–2298, 2010.

[124] M. Biswal, B. B. Pati, and a. K. Pradhan, “Directional Relaying of Series-compensated

Line Using an Integrated Approach," *Electric Power Components and Systems*, vol. 40, no. 7, pp. 691–710, 2012.

[125] M. M. Saha, J. Izykowski, E. Rosolowski, and B. Kasztenny, "A new accurate fault locating algorithm for series compensated lines," *IEEE Transactions on Power Delivery*, vol. 14, no. 3, pp. 789–795, 1999.

[126] A. A. Girgis, A. A. Sallam, and A. K. El-din, "An adaptive protection scheme for advanced series compensated (ASC) transmission line," *IEEE Transactions on Power Delivery*, vol. 13, no. 2, pp. 414–420, 1998.

[127] C.-S. YU, C.-W. Liu, and J.-A. Jiang, "A New Fault Location Algorithm for Series Compensated Lines Using Synchronized Phasor Measurements," *Power Engineering Society Summer Meeting, 2000. IEEE*, pp. 1350–1354, 2000.

[128] W. Cheong and R. Aggarwal, "Accurate fault location in high voltage transmission systems comprising an improved thyristor controlled series capacitor model using wavelet transforms and neural network," *Transmission and Distribution Conference*, vol. 2, pp. 840–845, 2002.

[129] W. J. Cheong and R. K. Aggarwal, "A Novel Fault Location Technique Based on Current Signals only for Thyristor Controlled Series compensated Transmission Line using Wavelet Analysis and Self Organising Map Neural Networks," *Developments in Power System Protection IEE*, vol. 1, pp. 224–227, 2004.

[130] P. Ray, B. K. Panigrahi, and N. Senroy, "Extreme Learning Machine based Fault Classification in a Series Compensated Transmission Line," *IEEE International Conference on Power Electronics, Drives and Energy Systems*, pp. 1–6, 2012.

[131] P. Ray, "Fast and Accurate Fault Location by Extreme Learning Machine in a Series Compensated Transmission Line," no. Pestse, 2014.

[132] S. Dambhare, S. A. Soman, and M. C. Chandorkar, "Adaptive current differential protection schemes for transmission-line protection," *IEEE Transactions on Power Delivery*, vol. 24, no. 4, pp. 1832–1841, 2009.

[133] M. M. Saha, J. Izykowski, and E. Rosolowski, "A Fault Location Method for Application With Current Differntial Protective Relays of Series-Compensated

Transmission Line," *10th IET International Conference on Developments in Power System Protection (DPSP). Managing the Change*, pp. 1–5, 2010.

[134] M. S. Mamis and M. Arkan, "FFT Based Fault Location Algorithm for Transmission Lines," in *7th International Conference on Electrical and Electronics Engineering (ELECO)*, 2011, p. I 71–I 75.

[135] M. G. Ahsaee and J. Sadeh, "A novel fault-location algorithm for long transmission lines compensated by series FACTS devices," *IEEE Transactions on Power Delivery*, vol. 26, no. 4, pp. 2299–2308, 2011.

[136] J. Izykowski and E. Rosolowski, "Fault location on double-circuit series-compensated lines using two-end unsynchronized measurements," *IEEE Transactions on Power Delivery*, vol. 26, no. 4, pp. 2072–2080, 2011.

[137] M. M. Saha, P. Balcerek, P. Pierz, E. Rosolowski, and J. Izykowski, "A New and Fast Method of Determining the Faulted Circuit in the Parallel Lines with use of One-end Current Measurements," *12th IET International Conference on Developments in Power System Protection (DPSP),* pp. 1–6, 2014.

[138] N. Kang, J. Chen, Y. Liao, and S. Member, "A Fault-Location Algorithm for Series-Compensated Double-Circuit Transmission Lines Using the Distributed Parameter Line Model," *IEEE Transactions on Power Delivery*, vol. 30, no. 1, pp. 360–367, 2015.

[139] C. S. Yu, C. W. Liu, S. L. Yu, and J. A. Jiang, "A new PMU-based fault location algorithm for series compensated lines," *IEEE Transactions on Power Delivery*, vol. 17, no. 1, pp. 33–46, 2002.

[140] A. H. Al-mohammed and M. A. Abido, "A Fully Adaptive PMU-Based Fault Location Algorithm for Series-Compensated Lines," *IEEE Transactions on Power Delivery*, vol. 29, no. 5, pp. 2129–2137, 2014.

[141] A. Y. Abdelaziz, S. F. Mekhamer, and M. Ezzat, "Fault Location of Uncompensated/Series-compensated Lines Using Two-end Synchronized Measurements," *Electric Power Components and Systems*, vol. 41, no. 7, pp. 693–715, May 2013.

[142] T. Maekawa, Y. Obata, M. Yamaura, Y. Kurosawa, and H. Takani, "Fault Location for

Series Compensated Parallel Lines," *Transmission and Distribution Conference and Exhibition, Asia Pacific*, vol. 2, pp. 824–829, 2002.

[143] R. Rubeena, M. R. D. Zadeh, and T. P. S. Bains, "An accurate offline phasor estimation for fault location in series-compensated lines," *IEEE Transactions on Power Delivery*, vol. 29, no. 2, pp. 876–883, 2014.

[144] B. Vyas, R. P. Maheshwari, and B. Das, "Protection of series compensated transmission line: Issues and state of art," *Electric Power Systems Research*, vol. 107, pp. 93–108, Feb. 2014.

[145] A. Kazemi, S. Jamali, and H. Shateri, "Distance Relay Ideal Tripping Characteristic for Inter Phase Faults in Presence of SSSC on Next Line," *Electrical and Computer Engineering, (ICECE)*, no. December, pp. 337–342, 2008.

[146] S. Jamali, A. Kazemi, and H. Shateri, "Measured Impedance by Distance Relay for Inter Phase Faults in Presence of SSSC," *Power Systems Conference and Exposition PSCE '09 IEEE/PES*, pp. 1–6, 2009.

[147] S. Jamali, A. Kazemi, and H. Shateri, "Modified distance protection in presence of UPFC on a transmission line," *Power & Energy Society*, pp. 1–8, 2009.

[148] S. Jamali, A. Kazemi, and H. Shateri, "Adaptive Distance Protection in Presence of SSSC on a Transmission Line," *Power System Technology (POWERCON)*, pp. 1–7, 2010.

[149] H. Rastegar and A. Khansaryan, "A New Method for Adaptive Distance Relay Setting in the Presence of SSSC using Neural Networks," *IEEE Conference on Industrial Electronics and Applications*, pp. 1–8, May 2006.

[150] X. Y. Zhou, H. F. Wang, R. K. Aggarwal, and P. Beaumont, "The Impact of STATCOM on Distance Relay," in *15th PSCC*, 2005, pp. 22–26.

[151] Z. Shen, J. Jin, X. Xiong, and J. Ouyang, "Influence of SVC on fault component directional protection and its improvement approach," in *APAP 2011 - Proceedings: 2011 International Conference on Advanced Power System Automation and Protection*, 2011, vol. 3, pp. 1845–1850.

[152] S. Bhattacharya and Z. Xi, “A practical operation strategy for STATCOM under single line to ground faults in the power system,” in *Power Systems Conference and Exposition*, 2006, pp. 877–883.

[153] S. Jamali, A. Kazemi, and H. Shateri, “Modified distance protection due to presence of STATCOM on a transmission line,” in *PowerTech IEEE*, 2009, pp. 1–6.

[154] A. Kazemi, S. Jamali, and H. Shateri, “Adaptive distance protection in presence of STATCOM on a transmission line,” in *Transmission and Distribution Conference*, 2010, pp. 1–6.

[155] M. Sham, K. Chethan, and K. Vittal, “Development of adaptive distance relay for STATCOM connected transmission line,” in *Innovative Smart Grid Technologies India (ISGT India)/ IEEE PES*, 2011, pp. 248 – 253.

[156] A. R. Singh, A. Ahmed, and S. Dambhare, “Robust distance protection of mid-point shunt compensated transmission line,” in *Power India Conference*, 2012, pp. 1–5.

[157] L. Qing, W. Zeng-ping, and Z. Yuan, “Study on a novel method of distance protection in transmission line with STATCOM,” in *Power and Energy Engineering conf.*, 2010, pp. 1–5.

[158] A. Manori, M. Tripathy, and H. O. Gupta, “Advance Compensated Mho Relay Algorithm for a Transmission System with Shunt Flexible AC Transmission System Device,” *Electric Power Components and Systems*, vol. 42, no. 16, pp. 1802–1810, Nov. 2014.

[159] W. H. Zhang, S. J. Lee, and M. S. Choi, “Setting Considerations of Distance Relay for Transmission Line with STATCOM,” *Journal of Electrical Engineering and Technology*, vol. 5, no. 4, pp. 522–529, Nov. 2010.

[160] J. Lim and J. N. Jiang, “A Refined Differential Current protection Method in the FACTS-compensated Line,” in *Power and Energy Society General Meeting (PES) IEEE*, 2008, pp. 1–6.

[161] Z. Xi, B. Parkhideh, and S. Bhattacharya, “Instantaneous Phase-Locked Loop for performance improvement of power system with STATCOM under single-line to ground fault,” in *Energy Conversion Congress and Exposition (ECCE) IEEE*, 2011, pp. 3750–

3757.

[162] P. Dash and A. Pradhan, “Digital protection of power transmission lines in the presence of series connected FACTS devices,” *Power Engineering Society Winter Meeting, IEEE*, vol. 3, pp. 1967–1972, 2000.

[163] M. Ghazizadeh-Ahsaee and J. Sadeh, “Accurate fault location algorithm for transmission lines in the presence of shunt-connected flexible AC transmission system devices,” *IET Generation Transmission & Distribution*, vol. 6, no. 3, pp. 247–255, 2012.

[164] D. Novosel, B. Bachmann, D. Hart, Y. Hu, and M. M. Saha, “Algorithms for Locating Faults on Series Compensated Lines Using Neural Network,” *IEEE Transactions on Power Delivery*, vol. 11, no. 4, pp. 1728–1736, 1996.

[165] Z. Moravej, M. Pazoki, and A. Akbar, “A new approach for fault classification and section detection in compensated transmission line with TCSC,” *European Transactions on Electrical Power*, vol. 21, pp. 997–1014, 2011.

[166] D. Thukaram, H. P. Khincha, and B. Ravikumar, “An intelligent approach using support vector machines for monitoring and identification of faults on transmission systems,” in *2006 IEEE Power India Conference, Vols 1 and 2*, 2006, pp. 307–313.

[167] A. Manori, M. Tripathy, and H. O. Gupta, “SVM based zonal setting of Mho relay for shunt compensated transmission line,” *International Journal of Electrical Power and Energy Systems*, vol. 78, no. 2016, pp. 422–428, 2016.

[168] P. Jafarian and M. Sanaye-pasand, “High-Frequency Transients-Based Protection of Multiterminal Transmission Lines Using the SVM Technique,” *IEEE Transactions on Power Delivery*, vol. 28, no. 1, pp. 188–196, 2013.

[169] I. Daubechies, “Where do wavelets Come From? - A personal Point of View,” *Proceedings of the IEEE*, vol. 84, no. 4, pp. 510–513, 1996.

[170] C.-L. Liu, “A Tutorial of the Wavelet Transform,” pp. 1–72, 2010.

[171] R. N. Mahanty and P. B. D. Gupta, “Application of RBF neural network to fault classification and location in transmission lines,” *IEE Proceedings-Generation, Transmission and ...*, vol. 151, no. 2, pp. 201–212, 2004.

[172] S. R. Samantaray, P. K. Dash, and G. Panda, “Distance relaying for transmission line using support vector machine and radial basis function neural network,” *International Journal of Electrical Power & Energy Systems*, vol. 29, pp. 551–556, 2007.

[173] A. K. Pradhan, P. K. Dash, and G. Panda, “A fast and accurate distance relaying scheme using an efficient radial basis function neural network,” *Electric Power Systems Research*, vol. 60, pp. 1–8, 2001.

[174] K. R. Müller, S. Mika, G. Rätsch, K. Tsuda, and B. Schölkopf, “An introduction to kernel-based learning algorithms.,” *IEEE transactions on neural networks*, vol. 12, no. 2, pp. 181–201, Jan. 2001.

[175] C. Chang and C. Lin, “LIBSVM : A Library for Support Vector Machines,” *ACM Transactions on Intelligent Systems and Technology*, vol. 2, no. 3, pp. 27:1–27:27, 2011.

[176] T. S. Sidhu and M. Khederzadeh, “Series Compensated Line Protection Enhancement by Modified Pilot Relaying Schemes,” vol. 21, no. 3, pp. 1191–1198, 2006.

[177] J. Lambert, A. Phadke, and M. D. Nabb, “Accurate voltage phasor measurement in a series-compensated network,” *IEEE Transactions on Power Delivery*, vol. 9, no. 1, pp. 501–509, 1994.

[178] H. Kirkham, A. R. Johnston, and G. D. Allen, “Design Consederations for a Fiber Optic Communications Network for Power Systems,” *IEEE Transactions on Power Delivery*, vol. 9, no. 1, pp. 510–518, 1994.

[179] V. Gohari Sadr and S. M. Kouhsari, “An adaptive distance relaying strategy based on global network simulation,” *European Transaction on Electric Power*, vol. 20, pp. 845–861, 2009.

[180] B. Ravikumar, D. Thukaram, and H. P. Khincha, “An Approach Using Support Vector Machines for Distance Relay Coordination in Transmission System,” *IEEE Transactions on Power Delivery*, vol. 24, no. 1, pp. 79–88, 2009.

[181] B. Ravikumar, D. Thukaram, and H. P. Khincha, “Comparison of multiclass SVM classification methods to use in a supportive system for distance relay coordination,” *IEEE Transactions on Power Delivery*, vol. 25, no. 3, pp. 1296–1305, 2010.

[182] C. Chaoying, C. Yong, D. Xuefei, and C. Liyi, "Study of Protective Relay's Behaviors in Unified Power Flow Controller of FACTS," *Advances in Power System Control, Operation and Management APSCOM*, vol. 2, pp. 632–637, 1997.

[183] S. Jamali, A. Kazemi, and H. Shateri, "Distance Relay Tripping Characteristic in Presence of UPFC," *Power Electronics Drives and Energy Systems PEDES*, pp. 1–6, 2006.

[184] M. Khederzadeh, "UPFC operating characteristics impact on transmission line distance protection," *Power and Energy Society General Meeting*, pp. 1–6, 2008.

[185] T. Manokaran and V. Karpagam, "Performance of distance relay estimation in transmission line with UPFC," *International Journal of Computer and Electrical Engg.*, vol. 2, no. 1, pp. 158–161, 2010.

[186] P. K. Dash, A. K. Pradhan, G. Panda, and A. C. Liew, "Adaptive relay setting for flexible AC transmission systems (FACTS)," *IEEE Transactions on Power Delivery*, vol. 15, no. 1, pp. 38–43, 2000.

[187] K. Seethalekshmi, S. N. Singh, and S. C. Srivastava, "Adaptive distance relaying scheme in presence of UPFC using WAMS," *Power Systems Conference and Exposition IEEE/PES*, pp. 1–6, 2009.

[188] P. K. Dash, A. K. Pradhan, G. Panda, "Apparent Impedance Calculations for Distance-Protected Transmission Lines Employing Series-Connected FACTS Devices," *Electric Power Components and Systems*, vol. 29, no. 7, pp. 577–595, 2001.

[189] A. Y. Abdelaziz, S. F. Mekhamer, and M. Ezzat, "Fault Location of Uncompensated/Series-compensated Lines Using Two-end Synchronized Measurements," *Electric Power Components and Systems*, vol. 41, no. 7, pp. 693–715, 2013.

[190] O. H. Gupta and M. Tripathy, "An Innovative Pilot Relaying Scheme for shunt compensated line," *IEEE Transactions on Power Delivery*, vol. 30, no. 3, pp. 1439–1448, 2015.

[191] H. W. Dommel, "Digital computer solution of electromagnetic transients in single and multiphase," *Networks IEEE*, vol. 88, no. 4, pp. 388–399, 1969.

PUBLICATIONS FROM THE WORK

Journals:

1. A. Manori, M. Tripathy, and H. O. Gupta, "Advance Compensated Mho Relay Algorithm for a Transmission System with Shunt Flexible AC Transmission System Device," *Electr. Power Components Syst.*, vol. 42, no. 16, pp. 1802–1810, Nov. 2014.
2. A. Manori, M. Tripathy, and H. O. Gupta, "SVM based Zonal Setting of Mho Relay for Shunt Compensated Transmission Line" Electric Power and Energy Systems, Vol. 78, pp. 422-428, Jan 2016.
3. A. Manori, M. Tripathy, and H. O. Gupta, "A Universal Fault Section Identification Algorithm for Mid-point Compensated Transmission Line" International Transaction on Electrical Energy and Systems, March 2015. **(Third review)**
4. A. Manori, M. Tripathy, and H. O. Gupta, "An Advanced SVM based Mho Relay for Zonal Setting of Transmission Line Having TCSC" IETE, April. 2014. **(Communicated)**

Conferences:

1. A. Manori, M. Tripathy, and H. O. Gupta, "An advance compensated mho relay for protection of TCSC transmission line" Proc. IEEE Power India conf. (PIICON 2014), New Delhi, pp. 1-5 Dec. 5-7 2014.
2. A. Manori, M. Tripathy, and H. O. Gupta, "SVM based zonal setting of mho relay for transmission line having TCSC" Proc. IEEE Power India conf. (PIICON 2014), New Delhi, pp. 1-5, Dec. 5-7 2014.
3. A. Manori, M. Tripathy, and H. O. Gupta, "Investigation of an advanced compensated Mho relay on double circuit series compensated transmission line" TENCON 2015, Macau, pp. 1-5, Nov. 1-4, 2015

RTDS/RSCAD and DSO Setup

APPENDIX-A

Source Data

Table A. 1 Source data

S. No.	Parameters	Value
1	Source impedance type	R/L
2	Voltage control	External
3	Phase angle control	External
4	R	6.186 [Ω]
5	L	0.138 [H]
6	Voltage ramp up time	0.05 [s]

APPENDIX-B

Current Transformer and Coupled Capacitive Voltage Transformer Data

B.1 CT Parameters Range

Table B.1 Parameters of CT

S. No.	Parameter	Value
1	Primary Turns	5
2	Secondary Turns	1200
3	Secondary resistance	0.5 [Ω]
4	Secondary reactance	0.8×10^{-3}[H]
5	Area	6.5×10^{-3}[m^2]
6	Path length	0.5 [m]
7	Frequency	50 [Hz]
8	Remnant flux density	0.0 [T]
9	Initial Current in core	0.0 [A]

B.1.1 CT Burden

Resistance = 0.5 Ω

Inductance = 0.8×10^{-3} H

B.2 CCVT Parameters

The schematic of the CCVT circuit model is shown in Fig. B.1:

Where,

V_p is primary input voltage in (kV).

V_s is secondary measured voltage in (V).

C_1, C_2 are primary coupled capacitors.

L_{comp} is compensating inductance.

L_p, R_p primary inductance and resistance respectively.

L_s, R_s secondary inductance and resistance respectively.

R_{bur}, L_{bur} are resistance and inductance of series burden respectively

R_{pbur} is resistance of parallel burden, and

R_{f1}, L_{f1}, C_{f2}, L_{f2}, R_{f2} and R_{f3} are the parameters of Ferro-Resonance filter

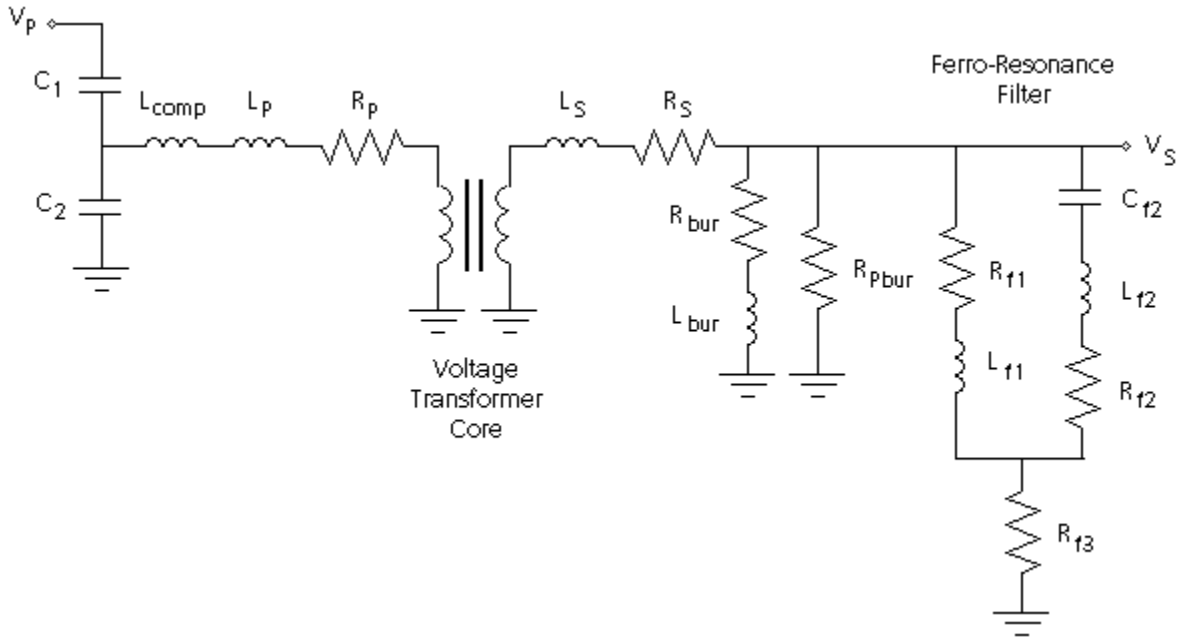

Fig. B.1 Schematic diagram of the CCVT

Parameters range for CCVT is given in Table-B.2

Table B.2 Parameters of CCVT

S. No.	Parameter	Value
1	C_1	2920.0 [pF]
2	C_2	134852 [pF]
3	L_{comp}	42.0 [pF]
4	V_s	115 [V]
5	L_p	0.47×10^{-3} [H]
6	R_p	0.05 [Ω]
7	L_s	0.47×10^{-3} [H]
8	R_s	0.18 [Ω]
9	Initial remnance	0.0 [T]
10	R_{bur}	301.0 [Ω]
11	L_{bur}	2.4 [H]
12	R_{pbur}	785.0 [Ω]
13	R_{f1}	5.5 [Ω]
14	L_{f1}	0.01 [H]
15	C_{f2}	8.0 [μF]
16	L_{f2}	0.394 [H]
17	R_{f2}	3.9 [Ω]
18	R_{f3}	40 [Ω]